Vascular dysfunction in rheumatoid arthritis

Sophie L. Reynolds

This thesis is dedicated to the memory of my father, Justin Reynolds.

DECLARATION

This work has not previously been accepted in substance for any degree and is not being currently submitted in candidature for any degree.

Signed.....S. Reynolds.....(candidate)

Date.....12-01-2011.....

Statement 1

This Thesis is the result of my own independent work/investigations, except where otherwise stated. Other sources are acknowledged by footnotes giving explicit references.

Signed.....S. Reynolds.....(candidate)

Date.....12-01-2011.....

Statement 2

I hereby give consent for my Thesis, if accepted, to be available for photocopying and for inter-library loan, and for the title and summary to be made available to outside organisations.

Signed.....S. Reynolds.....(candidate)

Date.....12-01-2011.....

Statements endorsed by:

Supervisor.....(Dr Derek Lang)

Date.....Jan 12th 2011.....

Supervisor.....(Dr Anwen S Williams)

DATE.....12th Jan 2011.....

DISCLAIMER

The work described in this thesis was planned and carried out by the candidate with the exception of a minority of the MMP-9 incubation work, which was assisted by Hayden Stephenson.

PUBLICATIONS ARISING

'Vascular Dysfunction in Inflammatory Arthritis: A Role for MMP-9?'

Sophie L Reynolds, Hayden Stephenson, Nick Amos, Anwen S Williams, Derek Lang

Arthritis & Rheumatism 2010 (Submitted)

Prizes, Presentations and Posters

The Jonathan Boulter Memorial Prize: awarded for best student presentation.

Presented at the **Annual Infection, Inflammation and Immunity Meeting**, September 2008, Cardiff University, Gregynog Hall, Powys, Wales.

'Matrix Metalloproteinase-9 May Contribute to Vascular Dysfunction in Rheumatoid Arthritis'

Sophie L. Reynolds, Anwen S. Williams, Derek Lang

First Prize Poster Presentation

The **Cardiff University Annual Postgraduate Meeting**, November 2007, Cardiff University, Cardiff, Wales.

'Vascular Dysfunction in Rheumatoid Arthritis'

Sophie L. Reynolds, Anwen S. Williams, Derek Lang

Presented work at **The British Pharmacological Meeting,** December 2008, Brighton, UK

'Vascular Dysfunction in Rheumatoid Arthritis: a Possible Role for Matrix Metalloproteinase-9'

Sophie L. Reynolds, Anwen S. Williams, Derek Lang

The Inflammation, Cardiovascular Risk and Connective Tissue Disease Meeting, Poster Presentation, May 2009, New York, USA

'Matrix Metalloproteinase-9 May Contribute to Vascular Dysfunction in Rheumatoid Arthritis'

Sophie L. Reynolds, Hayden Stephenson, Nick Amos, Anwen S. Williams, Derek Lang

ABSTRACT

Rheumatoid arthritis (RA) is a severely debilitating disease that affects 1% of the Western population. In addition to suffering pain and deformation of joints, patients are also at a higher risk of developing cardiovascular co-morbidities and experience a lower life expectancy as a result. Evidence for a link between RA and cardiovascular disease (CVD) is overwhelming and the large RA-associated inflammatory burden is thought to be responsible for the development of such distal pathologies; inflammatory mediators characteristic of RA cause injury to the endothelium ultimately resulting in endothelial dysfunction, a precursor to CVD. Therefore the main aim of this thesis was to characterise the vascular phenotype of a murine model of RA. Secondary aims were to relate changes in vascular function to the extent of experimental arthritis and to explore causative mechanisms therein.

The well described collagen-induced murine (mCIA) model of human RA was used in all experiments. Subsequently paw and aortic tissue and blood were collected from both arthritic and non-immunised aged-matched controls. The severity of arthritis was confirmed by clinical arthritic scoring and histological assessment of the paws. Isometric tension studies were used to investigate vascular function in the isolated tissues in the absence and presence of various pharmacological inhibitors, the latter depending on the particular system under investigation. Lastly a role for matrix metalloproteinase-9 (MMP-9) was investigated. To this end levels were quantified in paw and aortic homogenates and plasma by ELISA, and cellular sources of this gelatinase explored using immunohistochemistry.

Aortae taken from arthritic animals displayed increasing contractile dysfunction (evidenced by a reduced capability to constrict to specific mediators K+ and the agonist 5-hydroxytryptamine compared to normal control vessels) with increasing severity of experimental arthritis. Interestingly, and in contrast to many studies in the literature, endothelial function appeared unchanged throughout disease. Subsequent investigations

ruled out a role for increased production of nitric oxide and prostacyclin in this pathology. Conversely aortic (and also paw and plasma) levels of MMP-9 were shown to associate with increasing contractile dysfunction and indeed that contractile function was compromised following exposure of control aortic tissues to exogenous MMP-9. A role for neutrophils and macrophages in MMP-9 production and arthritis progression was confirmed by their concomitant presence in paws.

These findings suggest that systemic and vascular wall levels of MMP-9, related to inflammation at the joint site, may play a prominent role in the development of vascular dysfunction in this experimental model. As such this thesis goes someway to elucidating the potential mechanisms of vascular dysfunction in RA. Importantly identification of the earliest changes in vascular function following the initial onset of RA, and the pathological mechanisms therein, may result in a re-evaluation of current treatments or indeed the development of new therapies.

CONTENTS

LISTS OF TABLES/FIGURES

ABBREVIATIONS

AA Aortic Aneurysm

AC Adenylate Cyclase

ACE Angiotensin Converting Enzyme

ACh Acetylcholine

AChE Acetylcholinesterase

AdA Adjuvant-induced arthritis

Ang Angiotensin

ANOVA Analysis of Variance

APC Adenomatosis Polyposis Coli APC,

APC Antigen Presenting Cell

AUC Area Under Curve

BH_4 Tetrahydrobiopterin

BSA Bovine Serum Albumin

Ca^{2+} /CaM Calcium/Calmodulin Complex

Ca^{2+} Calcium

Ca2+/CaM Calcium/Calmodulin Complex

CAIA Collagen antibody-induced arthritis

CC Carbachol

CCC Cytoplasmic Cell Adhesion Complex

CFA Complete Freunds Adjuvant

cGMP Cyclic Guanosine Monopohsphate

CII Type II Collagen

CO_2 Carbon Dioxide

COX Cyclooxygenase

COXIBS Specific COX-2 Inhibitors

CVD Cardiovascular Disease

DAG Diacylglycerol

DC Dendritic Cell

DMARDS Disease Modifying Anti-Rheumatic Drugs

DMEM Dulbecco's Modified Eagle Medium

DNA Deoxyribonucleic Acid

EC50 Half Maximal Effective Concentration

ECM Extra-cellular Matrix

EDRF Endothelial Derived Relaxing Factor

EDTA Ethylenediaminetetraacetic acid

EGF Endothelial Growth Factor

ELISA Enzymel-linked immunosorbent assay

eNOS Endothelial Nitric Oxide Synthase

EPC Endothelial Progenitor Cells

ET Endothelin

FAD Flavin Adenine Dinucleotide

FC Foam Cell

FCS Foetal Calf Serum

Fe Haem Centre

FMD Flavin Mononucleotide

Fz Frizzled

GAPDH Glyceraldehyde 3-phosphate dehydrogenase

GDP Guanosine Diphosphate

GEF Guanin Exchange Factors

GPCR G-Protein Coupled Receptor

GSK3β Glycogen Synthase Kinase-3β

GTP Guanosine Triphosphate

H & E Haematoxylin and Eosin

HA hyaluronic acid

Hb Haemoglobin

HB-EGF Heparin binding epidermal-like growth factor

HCl Hydrochloric Acid

HDL High Density Lipoprotein

HLA Human Leukocyte Antigen

HUVECs Human umbilical vein endothelial cells

hv photon

ID Intradermal

IFNγ Inteferon-γ

IHC Immunohistochemistry

IL Interleukin

iNOS Inducible Nitric Oxide Synthase

IP Prostacyclin Receptor

IP3 Inositol phosphate – 3

JMD Juxtamembrane domain

K^+ Potassium

KI Potassium Iodide

KO Knock out

LDL Low Density Lipoprotein

L-NAME N^{G}-nitro-L-arginine methyl ester

LRP low-density-lipoprotein-receptor-related proteins

mCIA Murine Collagen Induced Arthritis

MHC Major Histocompatibility Complex

MLC Myosin Light Chain

MLCK Myosin Light Chain Kinase

MLCP Myosin Light Chain Phosphatase

MMP Matrix Metalloproteinase

mN Milinewtons

MTX Methotrexate

MYPT1 The Regulatory Sub-unit of Myosin Light Chain Phosphatase

N_2 Nitrogen

NA Noradrenaline

NaCl Sodium Chloride

NADPH Nicotinamide adenine dinucleotide phosphate

NaOH Sodium Hydroxide

NBSF Neutral Buffered Saline Formalin

nNOS Neuronal Nitric Oxide Synthase

NO Nitric Oxide

NO_2^- Nitrite

NO_3^- Nitrate

NOA Nitric Oxide Analyser

NOS Nitric Oxide Synthase

NO_x Total NO

NSAIDS Non-Steroidal Anti-inflammatory Drug

O_2 Oxygen

OCT Optimal Cutting Temperature (embedding media)

O-cuff Occlusion Cuff

ODu Optical Density Units

ONOO- Peroxynitrite

OPG Osteoprotegerin

OPN Osteopontin

Ox-LDL Oxidised low density lipoprotein

PAI Plasminogen Activator Inhibitor

PBS Phosphate Buffered Saline

PDGF Platelet Derived Growth Factor

PDGF-BB platelet derived growth factor-BB

PE Phenylepherine

PG Prostaglandin

PGE_2 Prostaglandin E_2

PGI_2 Prostacyclin

PIP2 phosphatidylinositol 4,5 bisphosphate

PKA Protein Kinase A

PKG Protein Kinase G

PLC Phospholipase C

RA Rheumatoid Arthritis

RANKL Receptor Activator for Nuclear Factor κappa B Ligand

RBC Red Blood Cell

RIPA Radioimmunoprecipitation assay buffer

ROCK Rho Kinase

ROS Reactive Oxygen Species

SDS Sodium Dodecyl Sulphate.

SEM Standard Error of the Mean

SF Synovial Fibroblast

sGC Soluble Guanylate Cyclase

SHR Spontaneously hypertensive rat

SNP Sodium Nitroprusside

SR Sarcoplasmic Reticulum

TBS Tris Buffered Saline

TCF/LEF T-cell enhancer factor/lymphoid enhancer factor

TGFβ Transforming Growth Factor Beta

TIMP Tissue Inhibitor of Matrix Metalloproteinase

TM4SF Tetraspanin Family

TNFα Tumour Necrosis Factor Alpha

TXA_1 Thromboxane A1

v/v Volume/volume Percentage Solution

VEGF Vascular Endothelial Growth Factor

VSMC Vascular Smooth Muscle Cell

$\bullet O_2$ Superoxide

1400W N-(3-(Aminomethyl)benzyl)acetamidine.

5HT 5 Hydroxytryptamine

ACKNOWLEDGEMENTS

The work described in this thesis was carried out in the Wales Heart Research Institute at the Cardiff University School of Medicine between October 2006 and September 2009 and was funded by the British Heart Foundation.

My thanks go to my supervisors Derek Lang and Anwen Williams for the opportunity to pursue this project, and for their continual support, guidance and encouragement over the last three years. Thanks for putting up with me! Additionally I'd like to thank Nick Amos, and Sarah Taylor for their assistance and expertise on anything antibody related, it's been a pleasure to pick your brains!

I am additionally grateful for the opportunity to work in various departments at Cardiff University - Pharmacology, Biomedical Services, Rheumatology, Tenovus and the Henry Welcome building; together your help and guidance made working and learning at this great establishment a pleasure.

I'd like to thank my friends also undertaking their PhDs at Cardiff University – the knowledge that I wasn't alone in experiencing stress, and their ability to provide advice and guidance was very much appreciated at all times. The same applies to my korfball friends; thanks for continually supporting and believing in me (and putting up with my rants over a couple of drinks). Also my thanks go to my long-suffering friends who have been there since forever; without you I'd have been lost.

My sincere thanks go to my family, to grandparents who have been wonderful throughout, to Mum for her endless love, support and tolerance, and efforts to help whenever she could. To Vicki, Adam, Nicola and Caryn for their support and confidence in my ability. Thanks to Dominic and Kieran, without whom I would not have undertaken this (yeah, thanks!). Lastly and importantly I'd like to thank Smeeth, for his unquestioning support, faith and ability to provide fun as a distraction from the massive work load that loomed; for this I am grateful.

CHAPTER 1

INTRODUCTION

1.1. Rheumatoid Arthritis

RA is a multifactorial systemic disease characterised by chronic inflammation, primarily of the small synovial joints in the hands and feet. It is an autoimmune disease in which cells of the normally protective immune system propagate an aggressive attack on host antigens resulting in pain and disability for the sufferer. The exact trigger for this change in immunity is unknown (Goronzy and Weyand 2005).

Processes underlying the disease include hyperplasia of the synovial membrane and infiltration of inflammatory cells resulting in structural damage to bone, cartilage and ligaments within the joint (Cho, Cho et al. 2007). Patients experience tenderness, stiffness, joint swelling and fatigue (Makelainen, Vehvilainen-Julkunen et al. 2008) and a subsequent poorer quality of life. Progression of the disease from a self-limiting phase to a chronic progressive stage can result in extra-articular manifestations with which comes an increased mortality rate and lower life expectancy (Myllykangas-Luosujarvi, Aho et al. 1995; Kaplan 2006; Cho, Cho et al. 2007; Turesson, Jacobsson et al. 2008). It is now widely acknowledged throughout the literature that patients with RA are at risk of developing cardiovascular complications. Indeed approximately half the deaths observed in RA patients can be attributed to cardiovascular disease (Goodson 2002).

1.1.1. Epidemiology and Aetiology of Rheumatoid Arthritis

The disease affects approximately 0.5 - 1% of the population (Gabriel 2001); women account for two thirds of this number with typical age of onset between forty and sixty. While the aetiology of RA is unknown, a combination of environmental and genetic factors including smoking, viral infections, mechanical stress and specific human

leukocyte antigen (HLA) alleles have been associated with its development (Silman and Pearson 2002). However, no strong evidence exists for any hypothesis.

1.2. Pathogenesis of Rheumatoid Arthritis

Numerous cellular mechanisms and signalling pathways drive the inflammatory processes leading to joint destruction in RA. Cells from both the innate and adaptive immune system are involved, the innate system being the primary producer of cytokines, chemokines and matrix metalloproteinases (MMPs), all of which propagate the destructive process. To understand the pathogenesis of RA it is important to first understand the normal environment of a joint, and how this subsequently changes with disease.

1.2.1. The Normal Joint

The synovial joints are composed of two opposing bone surfaces covered in cartilage providing a smooth low friction exterior, responsible for weight-bearing and shock absorption. The articular faces of the bone are surrounded by a capsule filled with synovial fluid, giving joint lubrication and a medium for the passage of nutrients and other molecules between this fluid and the surrounding tissue (Knedla, Neumann et al. 2007; Otero and Goldring 2007). The synovial membrane lines this fluid filled capsule covering the joint cavity from bone to bone. This membrane is composed of synovial fibroblasts (SFs) and macrophages which secrete a rich combination of products essential for maintenance of the joint including cytokines and proteases such as MMPs (Knedla, Neumann et al. 2007) (see figure 1.1a). The latter are secreted in balance with endogenous inhibitors, a factor that is of crucial importance in preserving homeostasis of the joint. For an overview of the cells and their function in a normal joint see table 1.1.

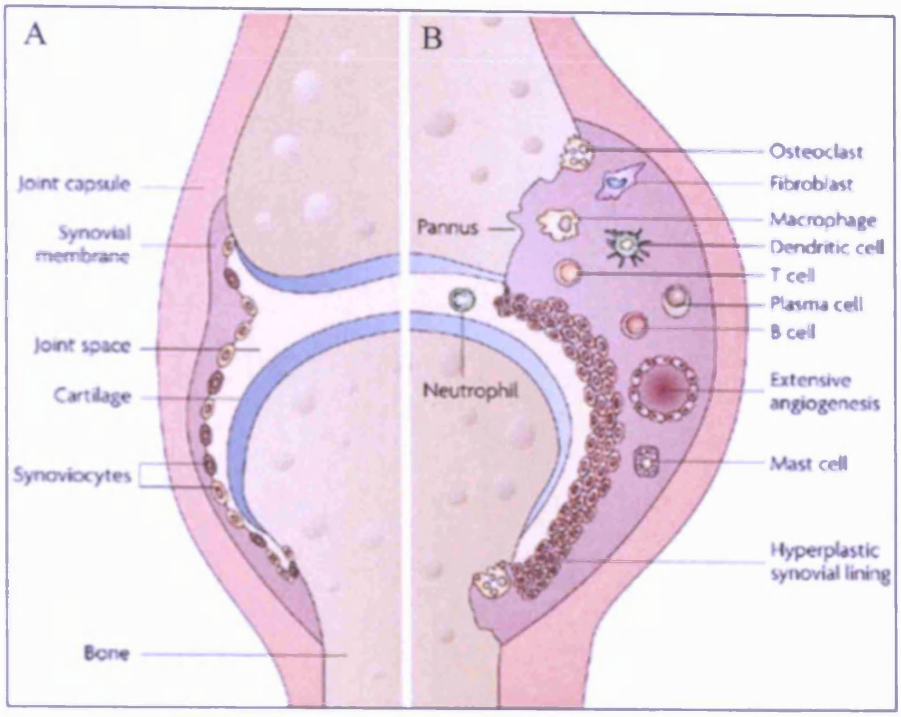

Figure 1.1. Overview of a Normal and a Rheumatoid Joint. A) The healthy joint. The thin synovial membrane consisting of synovial fibroblasts lines the joint capsule and contains the synovial fluid encapsulated between the articular ends of the two bones. The fluid is acellular and there are no infiltrating cells in the joint. B) In the rheumatoid joint, the synovial membrane becomes hyperplastic, and inflammatory cells invade the membrane and surrounding area. Inflammatory cells such as neutrophils migrate into the joint space. Taken from Strand (2007)

Cell Type	Function in the Normal Joint
Synovial Fibroblasts	Maintain membrane
Osteoclasts/Osteoblasts	Maintain bone synthesis/degradation
Chondrocytes	Maintain cartilage
Innate Immune Cells	Protect joint from infection
	Maintain membrane

Table 1.1. Cell Function in a Normal Joint. The predominant cell types and their roles within the healthy synovial joint.

SFs have general "house keeping" roles in ensuring the synovial fluid is kept at a constant volume and clear of debris, and as such maintain capsule integrity. The

secretion of hyaluronic acid, lubricin and other glycoproteins also ensures that fluid viscosity and function are sustained, protecting the joint from excessive pressure and general wear and tear (Mor, Abramson et al. 2005).

In the cartilage, chondrocytes sustain the balance of collagen and proteoglycan, the chief protein components of cartilage. They obtain their nutrients by diffusion from the articular cartilage surface or the subchondral bone allowing continued synthesis and degradation of the glycosaminoglycan components of aggrecan and other cartilage matrix constituents. Under normal conditions the chondrocytes have low cell turn over and proliferation is limited. No other cell types from bone or joint space enter the cartilage in the healthy joint (Otero and Goldring 2007).

In the bone, osteoclasts and osteoblasts are responsible for bone resorption and bone synthesis respectively. In a highly regulated fashion, they control the volume of bone tissue and ensure it is being constantly renewed (Fujisaki, Tanabe et al. 2007). Osteoblasts secrete bone extracellular matrix (ECM) proteins which become mineralized to form functional bone. In contrast, osteoclasts remove bone by attaching themselves to the periosteum, the bone membrane, and sealing it off from the extracellular environment. Proteolytic enzymes are pumped into the sealed-off area degrading the membrane of the bone, following which acid is secreted by the osteoclast into the bone causing degradation. This process leaves pits and leads to an overall weakening of the bone surface (Horowitz, Xi et al. 2001). Importantly in a normal joint these two processes are carefully balanced.

Cells of the innate immune system are also resident within the normal synovial joint. Macrophages cover the synovial lining and mast cells are found near the capsule, their primary role being to protect the acellular synovial fluid from invading cells and pathogens (Eklund 2007). In health, these cells play a small role in preventing infection. However in RA they become destructive, with significant detrimental consequences for the joint.

1.2.2. The Arthritic Joint

In the arthritic joint an orchestrated catalogue of events occur, with each subset of chain reactions playing a role in the process as a whole. The multifactorial nature of the disease implicates many cells and effector molecules in the progressive damage to the joints. The specific trigger for RA is as yet unknown and investigations to elucidate this are ongoing.

Initially dendritic cells (DCs) play an important role in both the innate and adaptive immune responses in RA as well as providing an ongoing immune stimulus throughout the duration of disease. In the presence of inflammatory stimuli they mature and adapt their gene expression to favour an antigen-presenting function. As such they are able to present arthritogenic molecules to the invading T-cells via the major histocompatibility complex (MHC) II (Gorman and Cope 2008; Lebre and Tak 2009). This stimulates invading T-cells resulting in adaptive immunity (Lebre and Tak 2008), and attraction of both helper and cytotoxic T-cells to the site of inflammation (Miossec 2008). Additionally DCs are also capable of secreting mediators which attract mononuclear cells, leading to broad expression of chemokines and upregulation of adhesion molecules further exacerbating the inflammatory response.

The T-cells stimulated by the antigen-presenting cell (APC) nature of the DCs can elicit subsequent activation of B-cells resulting in antibody producing plasma cells (Lebre and Tak 2009). Furthermore, T-cells can also differentiate into Th17 cells producing large volumes of the deleterious interleukin (IL) – 17 (IL-17) inducing inflammation in the cells of the synovium (Miossec 2008). Other cytokines such as IL-1 and tumour necrosis factor-α (TNF-α) cause damage to the joint and also result in further attraction of T- and B-cells (Miossec 2008) to the inflammatory site. In summary initiation of the adaptive immune response as a result of DC and T-cell interactions and influences result in a chronic inflammatory environment.

In conjunction with this immune reaction, changes within the cells of the joint begin to occur. The rather quiescent normal phenotype is pushed via the actions of other cells and cytokines towards a highly inflammatory destructive state. SFs become highly proliferative, stimulated by growth factors which further propagate cell multiplication by the production of mitosis factors, behaving in a "positive feedback" fashion. These cells also experience a decreased apoptosis and senescence rate. As a result the thickness of the synovial membrane can increase from a single cell layer of SFs, to a depth of more than 15 cells (see figure 1.1b). The thickening of the membrane so close to the articular surface of the bone forms the pannus, a sheet of granulated inflammatory tissue which drives into the extra-cellular matrix of the cartilage and subchondral bone, resulting in destruction of both (Abeles and Pillinger 2006; Otero and Goldring 2007). Macrophages are also present here, helping to form the destructive face of the pannus.

Throughout the onset and progression of disease there is a large influx of macrophages into the joint. Indeed the number of macrophages in the tissue correlates directly with disease severity (Kim, Kim et al. 2005) implying that they play an important role in inflammatory damage. Macrophages migrate into the joint as a result of inflammatory cytokines, for example Il-1 and TNFα, and chemokines stimulate their movement (Drexler, Kong et al. 2008). Additionally, these inflammatory mediators initiate neovascularisation within the joint, resulting in an increased blood flow to the site of inflammation. This allows continued infiltration of blood-borne cells (Knedla, Neumann et al. 2007), and helps to sustain the prolonged initiation of inflammation and subsequent damage to the joint (Tak and Bresnihan 2000; Mor, Abramson et al. 2005). The effect of inflammation on macrophages and SFs causes additional production of inflammatory factors such as Il-1β, TNF-α, transforming growth factor-β (TGFβ), inducible nitric oxide synthase (iNOS), prostaglandin E2 (PGE2) and a range of chemoattractants (Mor, Abramson et al. 2005) (see table 1.2).

Cell Type	Inflammatory Mediators Produced
Chondrocytes	MMPs, cathepsin, RANKL
Synovial Fibroblasts	Interleukins: IL-1β, -4, -6, -8, -10, -12, -13, -17, -18, -21, TNF-α, TGFβ, iNOS, PGE2 and a range of chemoattractants
Macrophages	Inflammatory cytokines, chemokines and MMPs after activation, induced by IL-1 and TNFα/RANKL
Neutrophils	RANKL, inflammatory cytokines, C-reactive protein, NO and MMPs.
Mast Cells	Eicosanoids, cytokines, histamine and the proteolytic enzymes chymase and tryptase

Table 1.2. Cells and their Contribution to Inflammation in RA.

On the articular end of the bone there is a loss of proteoglycan from the cartilage attributed to this infiltrating inflammatory milieu and a subsequent change in expression/activation of matrix degrading enzymes like the MMPs in the synovial fluid. The function of chondrocytes in the cartilage is also altered after activation by inflammatory cytokines such as TNFα, IL-1β and IL-17 and leads to the further production of MMPs, cathepsin, and aggrecan-degrading enzymes, all of which contribute to collagen degradation (Otero and Goldring 2007; van den Berg, van Lent et al. 2007). At this stage the joint is a site of increased tissue catabolism and suppressed repair.

Also during this inflammation, neutrophils infiltrate into the joint and contribute to inflammation by producing receptor activator for nuclear factor κ B Ligand (RANKL), a member of the TNF superfamily. This ligand is also produced by SFs, macrophages and chondrocytes (Haynes 2007) and is a key molecule involved in influencing osteoclast differentiation; expression of the ligand stimulates further production of RANKL, and pushes the function of osteoclasts towards degradation (Drexler, Kong et al. 2008).

The mast cells that reside in the synovium of a normal joint are also activated during arthritis leading to degranulation and release of eicosanoids, cytokines, histamine and the proteolytic enzymes chymase and tryptase. The latter two can directly degrade the matrix resulting in cartilage and bone destruction (Kobayashi and Okunishi 2002; Eklund 2007). Mast cells are activated by interaction with key components of the complement system. They initiate and perpetuate the inflammatory reaction promoting tissue destruction and can recruit and stimulate other cell types. Moreover, these cells also stimulate angiogenesis (Eklund 2007) resulting in increased blood flow and further infiltration of plasma cells exacerbating the prolonged inflammatory attack in the joint.

The combination of all the above factors contributes to the aggressive and destructive nature of the disease. In addition to the physical disability and pain experienced, RA patients also face a poorer quality of life, and decreased life expectancy due to the systemic effects of RA. The severe inflammation characteristic of RA can exert damaging effects elsewhere in the body.

1.3. Rheumatoid Arthritis; a Systemic Disease

RA is a systemic disease and consequently, in addition to polyarthritis, other organs and tissues can be affected by the inflammatory overload in the circulation resulting in the development of extra-articular diseases (Kaplan 2006). These are described in detail throughout the literature although some difficulty lies in distinguishing between side-effects that are a complication of RA and those that manifest as a direct result of the

disease process (Young and Koduri 2007). For example, skin thinning is a direct result of the inflammatory burden, while an observed general malaise could be a result of the inactivity imposed on the patients due to pain upon movement. As such the latter is a consequence of being afflicted with RA, but not a direct disease response. Therefore, for the purpose of this thesis all complications and manifestations have been grouped together. Importantly, these extra-articular manifestations are associated with a shortening in the life expectancy of the RA sufferer. It has now been established that co-morbid diseases play a large role in determining the health of RA patients with respect to both disability, disease severity and mortality (Mikuls 2003).

Complications of Rheumatoid Arthritis
Skin Thinning
Infection
Systemic Vasculitis
Rheumatoid Nodules
Lung Disease/Infection
Renal Amyloidosis
Anaemia
Cataract
Osteoporosis
Psoriasis
Myocardial Infarction
Congestive Heart Failure
Stroke
Perhipheral Vascular Diseases
Leukaemia
Skin Cancer

Table 1.3. Extra-Articular Features of RA.

Many RA-associated co-morbidities have been identified, of which, a significant proportion are related to CVD. Such diseases are now recognised as being major contributors to the increased mortality rate among this patient cohort (Voskuyl 2006; Turesson, Jacobsson et al. 2008) and are responsible for one-third to one-half of all RA-related deaths (Reilly, Cosh et al. 1990). Cardiovascular events on average occur a decade earlier in RA patients than in the general population in the absence of traditional cardiovascular risk factors (Goodson 2002; Mikuls 2003; Kaplan 2006; Turesson and Matteson 2007). Indeed it is now commonly perceived that RA alone is an independent

risk factor for the development of CVD events (Montecucco and Mach 2009). Such manifestations include pericarditis, myocarditis, cardiac amyloidosis, coronary vasculitis, arrhythmia, valve diseases, congestive heart failure (Voskuyl 2006) and coronary calcification (Chung, Oeser et al. 2005). Suggested explanations for the CVD-related morbidity and mortality include:

- Secondary effects of physical inactivity due to the sedentary lifestyle led by RA patients,
- Drugs used in the management of disease (Turesson and Matteson 2007),
- The direct impact of the systemic inflammatory load (Sattar and McInnes 2005).

These are discussed below, however it is the general consensus amongst the literature that (1) and (2), cannot explain the stark increase in risk without the presence of (3).

1.3.1. Physical Inactivity

In the general population, lack of exercise has a major impact on the likely development of CVD, and an increase in physical activity has been shown to improve the mortality rate for patients with CVD in the Western World (Gielen, Sandri et al. 2009). Moreover there is significant evidence that in "at risk" populations, exercise benefits the patient by reducing cholesterol, dyslipidaemia, hypertension (Metsios, Stavropoulos-Kalinoglou et al. 2008), and possibly reducing inflammation (Kasapis and Thompson 2005). It is logical therefore that the immobility that RA can impose on the affected individuals leads to a greater risk of developing CVD. However, given the multifactorial nature of both RA and CVD it would be far too simplistic to suggest that lack of exercise/mobility alone could account for the reduced life expectancy.

1.3.2. Drugs Used in Management of RA

1.3.2.1. Current Therapies for RA

The current therapies used to treat RA can be divided into three broad spectrum groups; non-steroidal anti-inflammatory drugs (NSAIDS), disease modifying anti-rheumatic drugs (DMARDS) and biological therapies. While these drugs variously manage pain and/or inflammation, some have unwanted side-effects that are detrimental to organs and tissues, including the vasculature (see table 1.4).

DRUG	MECHANISM OF ACTION	EXAMPLE	SIDE EFFECTS
NSAIDS	Broad inhibition of COX isoforms preventing synthesis of eicosanoids. Results in pain relief and is anti-inflammatory	Paracetamol, ibuprofen, diclofenac	Gastric bleeding and ulceration.
COXIBS	Specific inhibition of COX-2 preventing synthesis of COX-2 product. Analgesic and anti-inflammatory.	Celecoxib, rofecoxib	Can have cardiovascular side-effects due to increased amounts of thromboxane, and decreased amounts of prostacyclin leads to a prothrombotic environment
DMARDS	Modify disease progression by suppressing disease activity and reducing joint damage. Is anti-proliferative and an immunosuppressant	Methotrexate	Can increase homocysteine levels in the serum and cause subsequent vessel damage.
BIOLOGICAL THERAPIES	Work by inhibiting various cytokine pathways.	Infliximab, etanercept, adalimumab (anti-TNF), anakinra (anti-IL-1), rituximab (anti-B-cell)	Infection, irritation at injection site, cancer, immune diseases. May promote atherogenesisand has been shown to exacerbate existing CVD-related problems.

Table 1.4. Therapies Used for Treatment of RA. Summary of the Drugs used in the treatment of RA, their mechanism of action and possible side-effects.

1.3.2.2. NSAIDS

NSAIDS act by inhibiting cyclooxygenase (COX) enzymes, the key enzymes responsible for the formation of eicosanoids from arachidonic acid. The eicosanoids produced encompass a sub-class called prostanoids, several of which play important roles in the vasculature (see table 1.5).

Prostanoid	Function
Prostaglandin E2	Vasodilator
Prostacyclin	Vasodilator
Thromboxane A2	Prothrombotic, Vasoconstrictor

Table 1.5. Important Prostanoids in the Vasculature.

The eicosanoids produced by COX are potent mediators of inflammation and produce oedema, pain and vasodilation. Blocking production of these PGs is associated with analgesia and a reduction in inflammation (Green 2001), hence their widespread use in RA treatment. There are two isoforms of COX; the constitutively expressed COX-1 found in most tissues including vascular endothelium, stomach mucosa and kidneys (Mitchell and Warner 1999), and the inducible COX-2 induced in inflammatory cells after stimulation by inflammatory cytokines (Grosser, Fries et al. 2006; Gluszko and Bielinska 2009) and is largely responsible for inflammation and hyperalgesia (Marnett and Kalgutkar 1999).

The prostanoids produced by COX-1 play a role in gastric protection [50] and therefore broad spectrum inhibition has detrimental effects on gastric function. Due to this, COX-2 specific inhibitors (COXIBs) were produced which had a positive effect, halving the incidence of gastric side effects (Capone, Tacconelli et al. 2003). However these drugs are not without problems and have now been linked to an increased risk of cardiovascular events (Moodley 2008), probably due to the development of an imbalance between thromboxane and prostacyclin production. Given that these prostanoids have pharmacologically opposing actions, thromboxane being a potent platelet aggregator and vasoconstrictor, and prostacyclin being an inhibitor of platelet aggregation and a potent vasodilator, COXIBS decrease the release of prostacyclin and can therefore result in a disruption between pro- and anti-thrombotic prostanoids favouring a pro-thrombotic environment. This promotes thrombosis and subsequent

CVD events (Mikuls 2003). In addition any underlying vascular problems could be exacerbated by the use of these drugs.

1.3.2.3. DMARDS

DMARDs act to modify the progression of RA by suppressing disease activity and reducing joint damage. Of this group the most popular and commonly used agent is methotrexate (MTX). This drug acts in an anti-proliferative and immunosuppressive manner, decreasing cell proliferation and increasing cell apoptosis, cytokine production, bone formation and adhesion molecule expression (Wessels, Huizinga et al. 2008; Braun and Rau 2009).

With respect to cardiovascular-related problems, DMARDs can have protective effects. It has been observed that use of these drugs has a positive effect on the lipid profile of RA patients. Normally in early RA disease a higher low density lipoprotein (LDL) to high density lipoprotein (HDL) ratio manifests, predisposing patients to a risk for atherosclerosis. In a study where general DMARDs were used, often in combination therapy (with other drugs such as corticosteroids), this ratio can be lowered, reducing the CVD risk (Park, Choi et al. 2002). Epidemiological studies have also indicated that MTX can provide a substantial survival benefit for the patients, largely by lowering cardiovascular mortality (Choi, Hernan et al. 2002). A review of the literature reaffirms this (Salliot and van der Heijde 2009).

Contrastingly however, MTX has been associated with an increase in cardiovascular risk due to its use being associated with an increase in serum levels of homocysteine. Elevated plasma homocysteine is related to CVD and is a recognised risk factor for thrombosis (Desouza, Keebler et al. 2002; Lonn, Yusuf et al. 2006), and so could possibly exacerbate existing problems or cause further damage in the vasculature. The deleterious mechanism of action of homocysteine is still a controversial topic of research. However a significant role in endothelial damage via oxidative stress and the

subsequent promotion of atherosclerosis is the most widely accepted (Welch and Loscalzo 1998).

1.3.2.4. Biological Therapies

Biological therapies have been developed and are a direct result of the clearer understanding behind disease mechanism. They encompass a wide range of drugs which act by inhibiting specific cytokines/inflammatory cells within the inflammatory pathways (see table 1.6).

Drug	Action
Leflunomide	Inhibits Pyrimidine Synthesis
Etanercept	Binds TNF-α and TNF-β
Adalimumab	Human anti-TNF-α antibody
Infliximab	Chimeric anti-TNF-α antibody
Anakinra	Interleukin-1 receptor antagonist.

Table 1.6. Biological Therapies in RA.

A popular drug used within this cohort is the anti TNF-α therapy; examples of this are etanercept, infliximab and adalimumab which all interact with TNFα signalling.

With respect to anti-TNFα therapy safety, initial reports were positive and encouraging. The post-marketing data on the drug reassured its safety, reporting that after five years of clinical use there was generally excellent tolerance (Day 2002). However wider use of these various biological therapies has lead to the discovery of a broad spectrum of side effects including infections, cancer, immune diseases, malignant disease, injection site irritation and heart failure (Olsen and Stein 2004). Additionally there has since been negative data reporting that TNF-α antagonists could exacerbate existing cardiovascular

problems (Kwon, Cote et al. 2003). With regard to RA, recent evidence supports that such anti-TNFα therapy does not completely suppress inflammation and can indeed promote atherogenesis (Cuchacovich and Espinoza 2009).

Use of these therapies can increase the risk for developing or exacerbating existing cardiovascular problems. However the inflammatory burden on these patients is huge and is the main cause for the development of dysfunction/CVD-related problems. The interactions between the traditional and disease-related risk factors with respect to CVD development are complex and therefore any therapy administered should take into consideration the risks and benefits to the patient (Hall and Dalbeth 2005).

1.3.3. Inflammatory Load

Much attention has been paid to the chronic inflammation experienced in RA and the subsequent systemic damage this wages on the rest of the body. Importantly, considerable evidence also exists to support the role of inflammation in the pathogenesis of atherosclerosis and CVD in general.

It is widely suggested within the literature that atherosclerosis and CVD are both true inflammatory disorders with the latter sharing a common pathology with synovitis and pannus formation (Mikuls 2003). This has progressed into the hypothesis that inflammatory mediators characteristic of RA become systemic and in doing so exert their effects at extra-articular regions within the rheumatoid patient (Kaplan 2006). This is shown not only in cardiovascular-related problems but also through a higher incidence of lung problems, the development of Reynauds phenomenon and pleuritis, all prime examples of systemic extra-articular problems (Young and Koduri 2007).

Although several factors contribute to the high risk of CVD, systemic inflammation is the most influential. The sequence of events that lead to inflammation in RA is mimicked by events that occur in the vasculature. However to appreciate the damage

this could exert on the vessel it is first important to understand the structure and function of the healthy vasculature.

1.4. Vascular Function

1.4.1. Normal Structure and Function of the Arteries

Blood is ejected from the left ventricle of the heart into the aorta thus supplying organs and tissues of the body with oxygen and essential nutrients. Due to the regular pumping of the heart the arteries must be able to withstand high pressures, and as such have thick muscular walls rich in elastin and collagen, important for maintaining both vascular compliance and the elasticity of the vessel (Rang H.P 2003) (see figure 1.2).

1.4.1.1. The Tunica Intima

The tunica intima, the innermost layer of the artery, is comprised of a single layer of endothelial cells supported by an underlying internal elastic lamina. The endothelial cells form an interface between the circulating blood and the cells of the vasculature through which nutrients can pass. Changes in local stimuli (eg an increase in pressure resulting in shear stress, or a change in humoral substances) affect endothelial cells, and in response these cells are able to alter their structure by secreting potent vasodilators or constrictors in order to maintain vascular tone (Bell, Johns et al. 1998). The endothelium is also important in vessel relaxation and protection as these cells are the primary producers of the potent vaso-dilator and -protector, nitric oxide (NO) (Forstermann and Munzel 2006). The endothelium is attached to a connective tissue bed containing basement membrane and ECM molecules. The supporting internal elastic lamina consists of a band of elastic tissue separating the intima from the tunica media (Ratcliffe 2000).

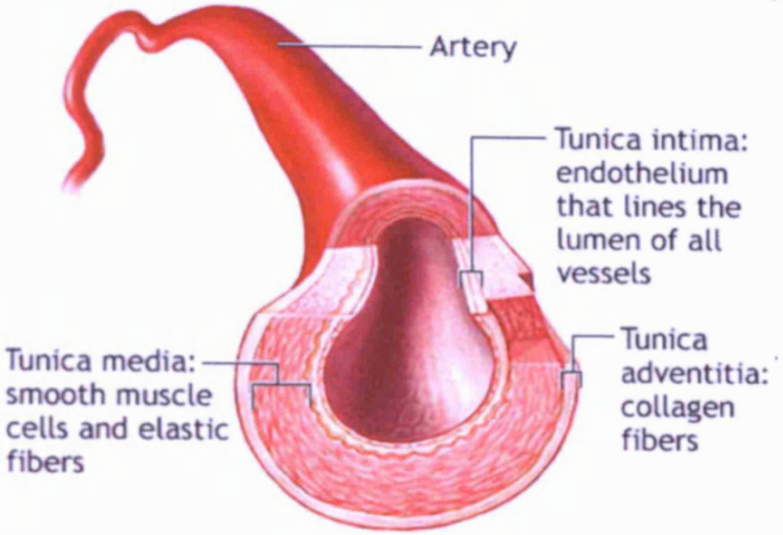

Figure 1.2. Simplified Structure of an Artery.

1.4.1.2. The Tunica Media

The tunica media consists of a dense population of vascular smooth muscle cells (VSMCs) arranged concentrically with additional bands of elastin fibers between the layers. These cells contain the contractile filaments myosin and actin which allow the cells to constrict providing vessel resistance. Constriction occurs following a change in intracellular calcium (Ca^{2+}) levels and subsequent downstream phosphorylation cascades (see below) (Hirano 2007).

1.4.1.3. The Adventitia

The external elastic lamina separates the media from the adventitia; an area rich in collagenous ECM molecules which also contains fibroblasts, blood vessels and nerves. The combination of the layers add rigidity to the vessel and provides elasticity, tensile stiffness and the ability to withstand compression (Ratcliffe 2000).

1.4.2. Vascular Smooth Muscle Constriction

VSMC constriction is mediated via an initial increase in intracellular Ca^{2+} levels (see figure 1.3). The initial stimulus for this rise is the binding of a specific agonist (such as

noradrenaline, adrenaline, endothelin-1, serotonin, angiotensin II, phenylephrine etc.) to its G-protein coupled receptor (GPCR). Subsequently, phospholipase C (PLC), an enzyme specific for the membrane lipid phosphatidylinositol 4,5-bisphosphate (PIP2), is activated resulting in cleavage of PIP2 and the production of the secondary messengers inositol phosphate (IP3) and diacylglycerol (DAG). IP3 migrates to the sarcoplasmic reticulum (SR) and binds to specific IP3 receptors thus releasing intracellular Ca^{2+} from the SR into the cytoplasm (Somlyo and Somlyo 1994; Webb 2003; Dale M. M 2004).

The increase in cytoplasmic Ca^{2+} triggers the formation of the Ca^{2+}-calmodulin (Ca^{2+} /CaM) complex, capable of activating myosin light chain (MLC) kinase (MLCK) which subsequently phosphorylates MLC. This activates myosin ATPase and results in cross-bridge cycling and contraction. The termination of the signal reduces the intracellular Ca^{2+} and thus decreases the activity of MLCK. Subsequently MLC is dephosphorylated by MLC phosphatase (MLCP) and relaxation ensues (Hirano 2007).

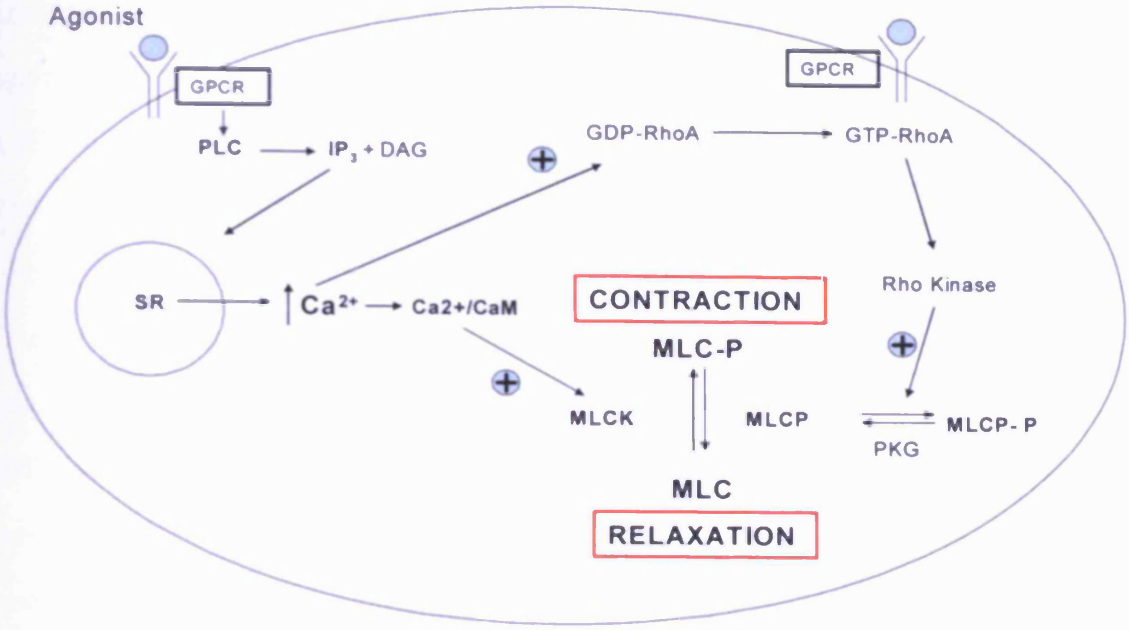

Figure 1.3. Regulation of SMC Constriction. Agonists interact with their specific GPCR to promote contraction. Subsequent to this binding, intracellular levels of PLC are increased promoting formation of IP3 and DAG. IP3 then binds to surface receptors on the SR and triggers the release of Ca^{2+} from intracellular stores. This promotes formation of the Ca^{2+}/CaM complex which activates MLC kinase causing phosphorylation of MLC. Additionally the rise in intracellular calcium and the binding of agonists to their specific receptor can result in the conversion of GDP bound RhoA to GTP bound RhoA. This activates Rho kinase which phosphorylates MLCP rendering it inactive and unable to dephosphorylate MLC, maintaining contraction. Protein kinase G (PKG) antagonises the effect of Rho kinase resulting in active MLCP, which subsequently dephosphorylates MLC and the cell relaxes.

Once phosphorylated MLC has an increased sensitivity to intracellular Ca^{2+}. This is due to a change in the Ca^{2+}/tension relationship and allows for a high level of constriction to be maintained with less Ca^{+2} present (high levels of Ca^{+2} are toxic to the cell). The exact mechanism behind this is not fully elucidated but is thought to be regulated by the level of MLC phosphorylation (Hirano 2007). MLCP can only dephosphorylate MLC when accompanied by correct sub-units, one of which is the regulatory sub-unit, MYPT1. MYPT1 allows the correct configuration of the enzyme, increasing its specificity for MLC and can inhibit these interactions by becoming phosphorylated which prevents the necessary contact between MLCP and MLC (Hirano 2007). This is another way in which contraction is regulated within the VSMC.

The RhoA/Rho kinase pathway is the most extensively studied with regard to MLCP inhibition. GPCR stimulation leads to activation of Rho guanine exchange factors (GEFs) which result in the change of the inactive GDP (guanosine diphosphate) bound Rho A to the active RhoA-GTP (guanosine triphosphate). This is able to then bind and activate Rho kinase, which phosphorylates MYPT1 inhibiting MLCP activity (Sakurada, Takuwa et al. 2003; Hirano 2007; Wang, Zheng et al. 2009) (see figures 1.3, 1.4) and causing increased calcium sensitivity of the contractile filaments (Gao, Portugal et al. 2007). This pathway has been shown to be sensitive to intracellular Ca^{+2} levels with removal of Ca^{+2} decreasing the amount of GTP bound RhoA, although the exact mechanism behind this is not known (Sakurada, Takuwa et al. 2003). This means that under slightly increased levels of intracellular Ca^{+2} (which occur after VSMC stimulation) contraction can be sustained.

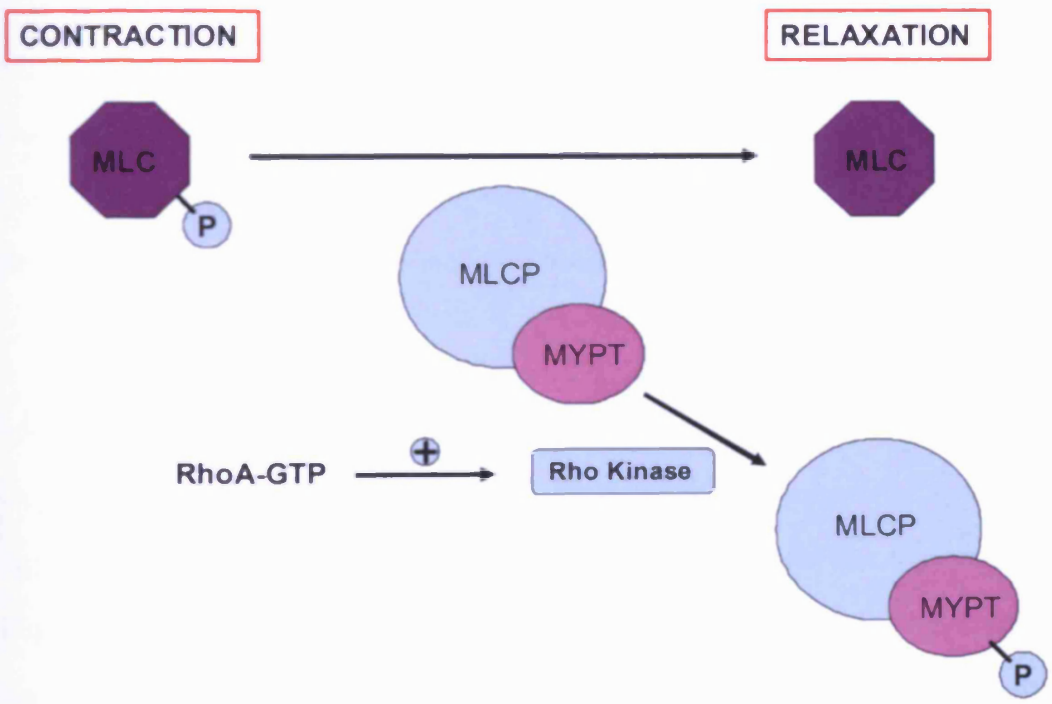

Figure 1.4. Regulation of MLC Phosphorylation. Rho kinase phosphorylates the regulatory MYPT sub-unit of MLCP rendering it unable to dephosphorylate MLC. This sustains contraction.

1.4.2.1. VSMC depolarisation

Additionally there are two different membrane channels which can affect intracellular Ca^{+2} concentrations; the voltage-gated calcium channels or receptor-operated calcium channels. The former are opened when the cell membrane becomes depolarised, for instance following exposure to a high potassium concentration, allowing the influx of extracellular Ca^{+2} into the cell resulting in constriction (Rang H.P 2003; Catterall, Perez-Reyes et al. 2005). Similarly receptor-activated Ca^{+2} channels are opened following agonist stimulation with the same end result.

1.4.2.2. Endothelin

Constriction can also occur via the action of endothelin (ET), of which there are three isoforms, ET-1, ET-2 and ET-3. ET-1 is expressed constitutively in endothelial cells and plays a role in vascular homeostasis (Pollock, Keith et al. 1995). ET1 binds to ETA and ETB receptors on VSMCs to exert vasoconstriction and ETB receptors on endothelial cells to produce NO and subsequent vasodilation. (Dashwood and Tsui 2002). In the vascular system ET-1 behaves as a potent vasoconstrictor and can also produce other vasoactive molecules such as prostcyclin (PGI_2) and NO which may regulate its actions via their opposing vasodilatory function (Dashwood and Tsui 2002).

1.4.2.3. Angiotensin II

Angiotensin II (Ang II), produced as part of the angiotensin-renin system, plays a significant role in vascular homeostasis and is a major target for blood pressure lowering drugs. It is formed following a series of proteolytic cleavages of angiotensinogen to angiotensin I (Ang I) by renin, and subsequent cleavage of Ang I to Ang II by angiotensin converting enzyme (ACE), the latter being found on endothelial cells. Ang II exerts its effects when it binds to its specific GPCR (de Gasparo, Catt et al. 2000) and stimulates activation of the PLC and IP3 pathway raising intracellular Ca+2 levels and eventually resulting in activation of MLCK and subsequent contraction. Its

physiological role is to maintain vascular homeostasis via vasoconstriction-induced blood pressure control, and control of intracellular Ca^{+2} levels (de Gasparo, Catt et al. 2000; Do, Kim et al. 2009).

1.4.3. Endothelium-Dependent Relaxation

In normal conditions the endothelium behaves in a protective manner and exerts anti-thrombotic, anti-inflammatory and anti-atherosclerotic effects (Ignarro and Napoli 2004) through fibrinolytic and anti-platelet mechanisms. This is achieved via release of the vasoprotective molecules PGI_2 and NO, the latter being able to regulate leukocyte adhesion, cytokine expression, VSMC proliferation/migration and platelet aggregation (Hetzel, Balletshofer et al. 2005). Healthy endothelial cells undergo continual repair in response to mechanical and chemical injuries, crucial for homeostasis (Lerman and Zeiher 2005) and help in preventing the development of thrombosis (Kirkpatrick, Wagner et al. 1997)

1.4.3.1. Nitric Oxide

In 1980 Furchgott and Zawadzki made the observation that vessel relaxation via acetylcholine (ACh) was dependent on the presence of intact functional endothelial cells. This was discovered by assessing vascular responses to ACh in isolated rabbit thoracic aorta. This work indicated that the action of ACh on muscarinic receptors stimulated the release of a vasodilator substance, then named endothelial-derived relaxing factor (EDRF) (Furchgott and Zawadzki 1980). Following many observations that EDRF shared several similarities to NO in terms of its mechanism of action, in 1987 the identity of EDRF as NO was confirmed (for a more detailed review of the decade of discoveries surrounding NO see (Stuart-Smith 2002).

1.4.3.2. Nitric Oxide Production

NO is produced via the action of nitric oxide synthase (NOS). There are three isoforms of NOS; the two constitutively expressed isoforms, neuronal NOS (nNOS) and endothelial NOS (eNOS) and the endotoxin- and cytokine-inducible NOS (iNOS) (O'Shaughnessy, Vetsika et al. 2006).

1.4.3.3. Structure of NOS

NOS is a homodimer and utilises both reductase and oxidase properties within different structural domains. The C-terminus is the reductase domain and contains the binding sites for the co-factors flavin mononucleotide (FMN) flavin adenine dinucleotide (FAD) and nicotinamide adenine dinucleotide phosphate (NADPH). This is linked to the N-terminal oxygenase of the other monomer, which carries a prosthetic heme group and binds 5,6,7,8-tetrahydrobiopterin (BH_4) and L-arginine (Forstermann and Munzel 2006; Xia, Misra et al. 2009). There is also a Ca^{2+}/CaM binding site in NOS; binding of Ca^{2+}/CaM to this site initiates electron transfer which ultimately produces NO (Welland, Garnaud et al. 2008; Xia, Misra et al. 2009).

1.4.3.4. Electron Transfer and Production of NO

Electrons are transferred from the reductase domain bound NADPH via a mobile FMN group, which serves as a one electron donor, to the oxygenase haem group (Welland, Garnaud et al. 2008). When the electrons reach the haem group they activate and reduce oxygen (O_2). This process must occur twice to produce NO. Dimerisation of the enzyme is essential for the flavin to haem transport as electron transfer occurs from the reductase domain of one monomer to the oxygenase domain of the other (Siddhanta, Presta et al. 1998) (see figure 1.5)

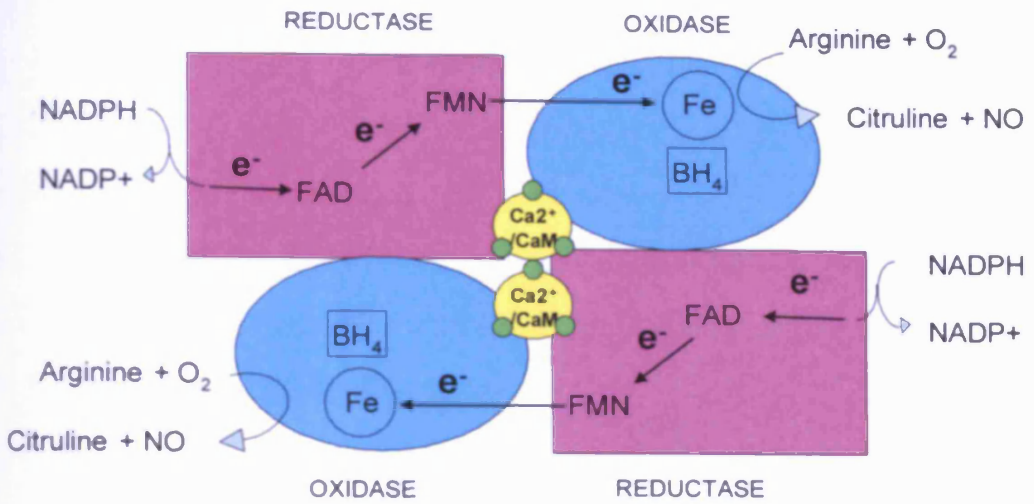

Figure 1.5. Structure of NOS. Electrons are shuttled from the reductase terminus of one NOS monomer, to the oxidase component of the adjoining monomer via FMN. The electron, upon reaching the haem group (Fe) reduces and activates the O_2 molecule producing NO.

1.4.3.5. NO-Mediated Vasorelaxation

An essential initiating step in the production of NO is Ca^{2+}/CaM complex formation in the endothelial cells. This can be induced in response to an agonist binding to a GPCR on the cell membrane (for example ACh to muscarinic receptors), or more likely in the intact blood vessel in-situ in response to increased shear stress. Binding of this complex to eNOS activates the enzyme thus catalysing the formation of NO from L-arginine and molecular oxygen (Sullivan and Pollock 2006). This highly lipophilic and reactive molecule rapidly diffuses across the plasma membrane and extracellular space from the endothelial cells to the VSMCs. Once in the VSMC, NO activates the heme-containing target enzyme soluble guanylate cyclase (sGC) resulting in the conversion of guanosine triphosphate (GTP) to cyclic guanosine monophosphate (cGMP) (Bohme, Graf et al. 1978) and a subsequent increase in the cellular levels of this secondary messenger. cGMP then activates cGMP-dependent PKG which phosphorylates downstream targets (see below) that regulate intracellular levels of Ca^{2+} (Birschmann and Walter 2004). The overall result is a reduction in the Ca^{2+} concentration resulting in smooth muscle relaxation (see figure 1.6).

PKG can phosphoryate MYPT1 at sites adjacent to the phosphoylation site of Rho kinase, exerting opposing actions to Rho kinase and activating the catalytic action of MLCP (Lincoln, Dey et al. 2001; Gao, Portugal et al. 2007). This activates MLCP resulting in depohsphorylation of MLC and subsequent relaxation. Additionally PKG has also been implicated in RhoA-dependent Ca^{2+} sensitisation, phosphorylating RhoA via cGMP, inhibiting it's contact with Rho kinase and thus contributing to NO-mediated vasodilation (Sauzeau, Le Jeune et al. 2000).

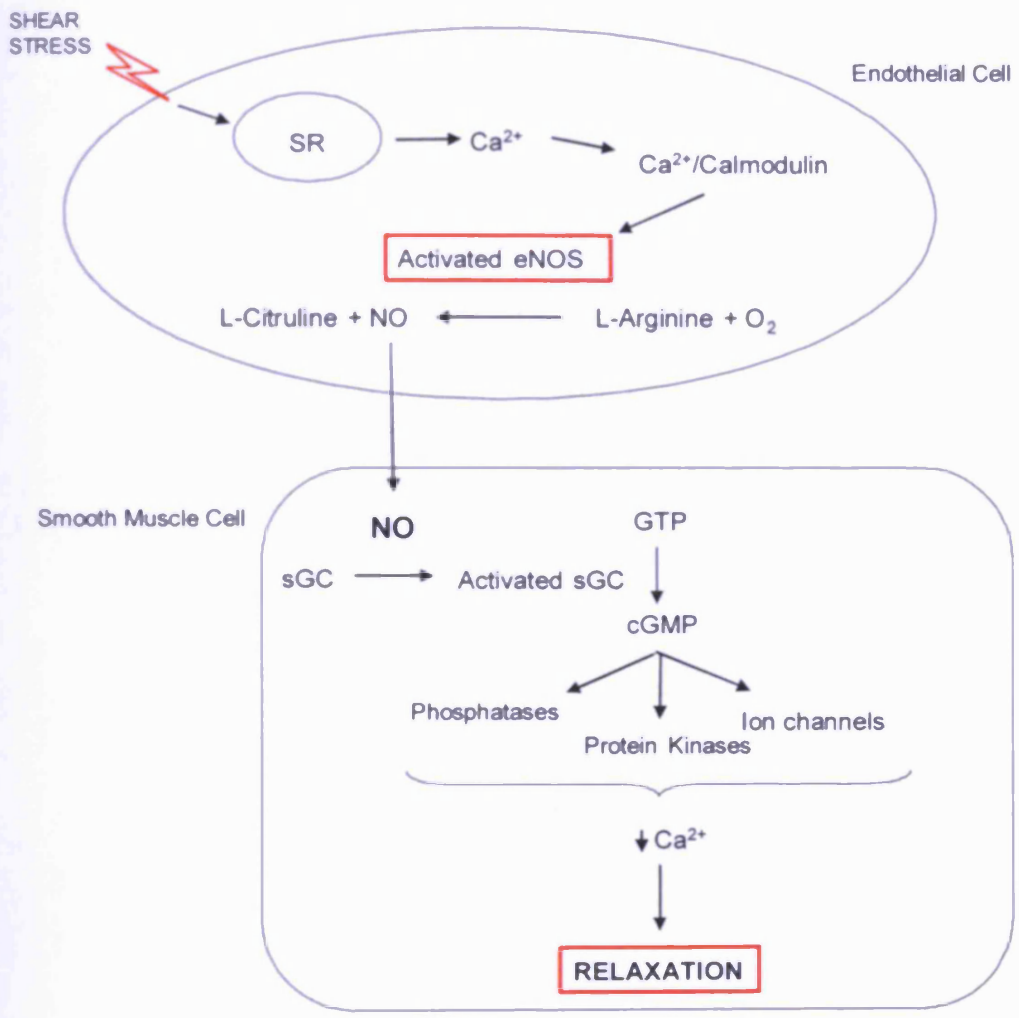

Figure 1.6. Mechanism of SMC Relaxation. Shear stress stimulates a release in calcium from the SR promoting formation of the Ca^{2+}/CaM complex. This activates eNOS resulting in production of NO. NO diffuses to the VSMC and activates sGC resulting in production of cGMP and initiating a downstream cascade of events, culminating in a decrease in Ca^{2+} availability and subsequent vessel relaxation.

1.4.3.6. Prostacyclin (PGI_2)

PGI_2 is from the family of eicoasnoids, and is itself a prostaglandin. It is synthesised alongside other prostanoids by the conversion of arachidonic acid by cyclooxygenase (COX) in both the endothelium and VSMCs but largely by the former. It is a potent vasodilator and an inhibitor of platelet aggregation (Vane and Botting 1995). It induces vasodilation via activation of adenylate cyclase-coupled GPCR on VSMC and elevation of cAMP levels (Vanhoutte 1998). Subsequent activation of cAMP-dependent protein kinase (protein kinase A, PKA), leads to removal of calcium from the cytoplasm and thus promotes relaxation.

Both the endothelium and VSMC work in conjunction to ensure vascular integrity and importantly to protect the blood vessels from everyday insults. However in a highly inflammatory environment, as observed systemically in RA, this protective function can become compromised and lead to vascular damage. It is such alterations in normal vascular function that are thought to be involved in the genesis and progression of CVD in RA patients.

1.5. From Rheumatoid Arthritis to Cardiovascular Disease

1.5.1. Similarities between RA and CVD

As mentioned previously cardiovascular-related problems are a huge burden for patients suffering from RA (Turesson, Jacobsson et al. 2008), to the extent that RA is now recognised as an independent risk factor for CVD (DeMaria 2002).

There is a large body of evidence in the literature supporting a role for inflammation in the development of CVD in RA. That striking similarities exist between both diseases reinforce this hypothesis. For instance the mechanism of damage in the synovium is paralleled by that which occurs in vascular disease (Pasceri and Yeh 1999; Flammer,

Sudano et al. 2008). Moreover, the cascade of events that lead to atherosclerosis resembles stages that also occur in the rheumatoid joint; T-cell and mast cell activation, an increased production of inflammatory cytokines, and increased expression of leukocyte adhesion molecules are observed in both cases (Libby 2008) (see table 1.7).

	Atherosclerosis	Rheumatoid Arthritis
Macrophage Activation	↑	↑
TNF-α	↑	↑
MMP Expression	↑	↑
IL-6	↑	↑
Mast Cell Activation	↑	↑
T-Cell Activation	↑	↑
B-Cell Activation	↑	↑
Adhesion Molecule Expression	↑	↑
Neoangiogenesis	↑	↑

Table 1.7. Upregulated Processes Shared by RA and CVD.

In both RA and CVD, the secretion of proinflammatory cytokines is increased and the subsequent effect of this is of utmost importance in disease progression. Elevated levels are deleterious in the joint, and similar damaging metabolic effects are exerted in the vasculature and can promote atherogenesis (Sattar, McCarey et al. 2003). Atherosclerosis develops into a chronic, systemic and diffuse disease which focuses at distant and multiple sites in various vascular beds. The mechanism behind the varying distribution of disease is unknown, but the seemingly sporadically affected regions have led to the hypothesis that the interactions between the vascular wall and circulation are the primary cause of the damage (Lerman and Zeiher 2005). IL-1, IL-6 and TNF-α are notably high in plasma during RA disease and are therefore in prime position to alter the

function of distant tissues, the vascular wall being an example of this (Sattar, McCarey et al. 2003).

Figure 1.7 summarises the role of inflammation in the development of early vascular disease in RA. Elevated levels of inflammatory cytokines characteristic of RA could elicit vascular changes (Libby 2008), resulting in endothelial dysfunction, now proposed to be an early event in the atherogenic process and a novel predictor of CVD (Sattar and McInnes 2005).

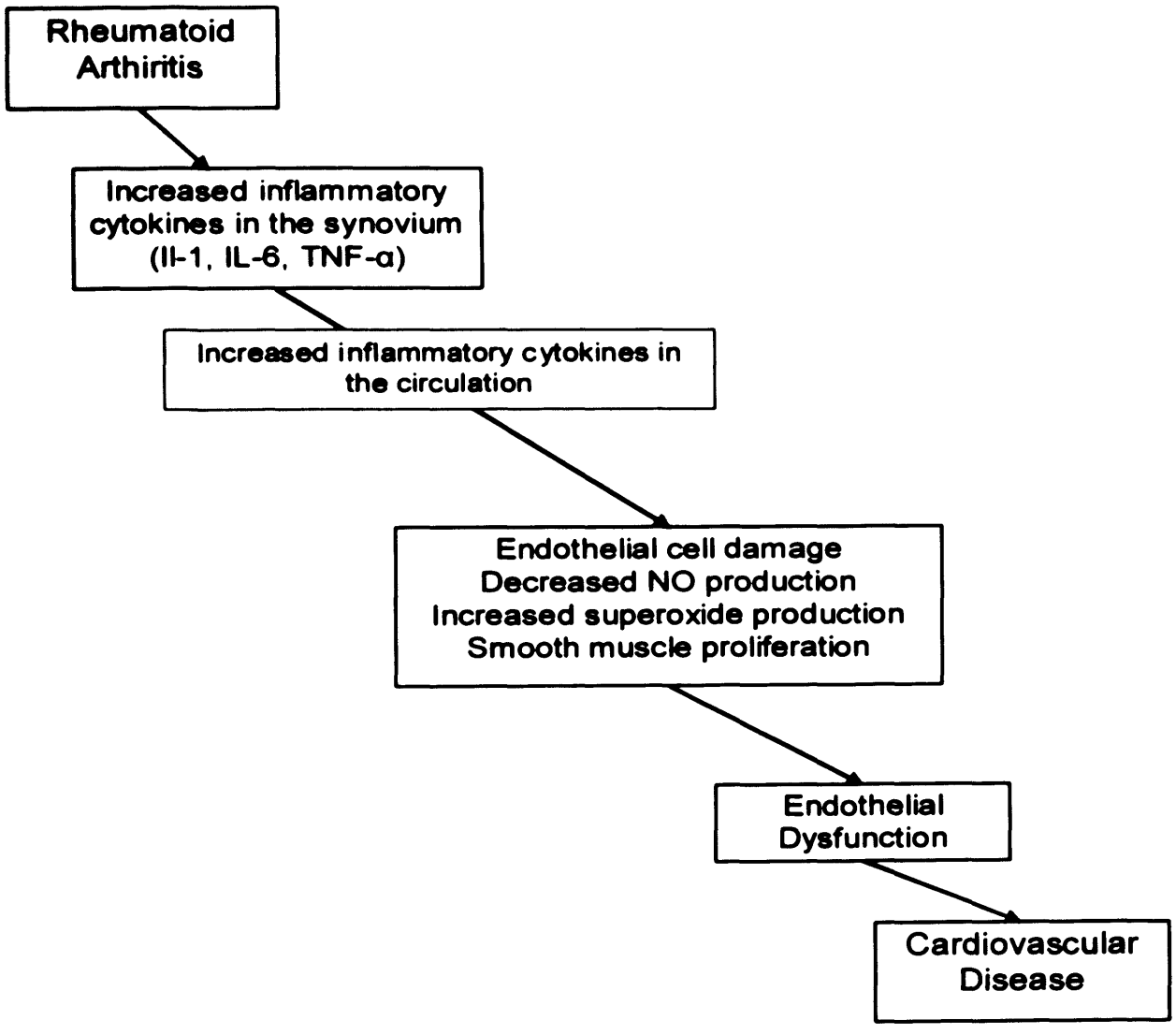

Figure 1.7. Hypothesised Progression from RA to CVD.

1.5.2. Endothelial Dysfunction

Following inappropriate endothelial cell activation (in response to various pathological insults) endothelial cell dysfunction ensues. Increased exposure to inflammatory cytokines is a prime example of such an insult that induces characteristic changes in endothelial function including loss of vascular integrity, increased expression of leukocyte adhesion molecules such as VCAM and ICAM, phenotypic switch from protective to prothrombotic, increased production of cytokines and subsequent upregulation of HLA genes and MHC molecules (Bijl 2003)

Normally endothelial cells do not bind leukocytes, a process inhibited by NO (Hetzel, Balletshofer et al. 2005). However in inflammatory situations such as in RA, the presence of IL-1 and TNFα can induce production of MHC molecules which are able to activate neutrophils and subsequently induce endothelial cell injury (Bratt and Palmblad 1997). These early changes to the environment surrounding the endothelium cause phenotypic changes, including the production of leukocyte adhesion molecules and chemokines which attract mononuclear cells to the vessel wall. The adhesion molecules facilitate the binding of monocytes to the endothelium which results in the widening of intracellular spaces between the endothelial cells. This induces increased endothelial permeability allowing the movement of leukocytes from the lumen into the sub-endothelial space and arterial intima. Such cell migration provides the stimulus for the initiation and progression of inflammation within the arterial wall itself (Libby 2008). The now injured endothelium also has increased susceptibility to other insults resulting in an exaggerated response to the classical risk factors (Bacon, Stevens et al. 2002) such as smoking. Once monocytes have migrated into the intima, they differentiate into macrophages where they encounter modified lipids. These modified lipids are a result of oxidation of HDL and LDL by ROS in the blood and can be engulfed by macrophages forming "foam cells". This represents the initial stage in the production of a fatty streak (Carter 2005), a significant precursor to chronic disease. With respect to RA the key step

in this sequence of events is the initial insult followed by endothelial activation and dysfunction.

A significant consequence of endothelial cell activation and dysfunction is impaired endothelium-dependent relaxation. This is a key issue in the advancement of disease, and while largely due to a decrease in the bioavailability of endothelium-derived NO (Kawashima and Yokoyama 2004; Hetzel, Balletshofer et al. 2005), decreased synthesis of prostacyclin (Simionescu 2007) has also been reported. Given that a large body of literature suggests that CVD in RA patients may be associated with endothelial dysfunction, the mechanism(s) underlying that underlie this process warrant further investigation.

1.5.3. Endothelial Nitric Oxide Synthase Dysfunction

While the development of endothelial dysfunction is normally associated with a reduction in bioavailable NO (Kawashima and Yokoyama 2004; Hetzel, Balletshofer et al. 2005), the latter may have various origins, for instance a decrease in expression/activation of eNOS. Indeed this has been demonstrated in a pig model of physical endothelial injury by denudation (Lee, Tse et al. 2007) where significantly lower concentrations of eNOS were evident in subsequently isolated and cultured regenerated endothelial cells compared to native cells, and therefore less bioavailable NO.

Studies have also demonstrated that a decrease in functional eNOS is associated with the production of superoxide ($\bullet O_2$-) (Rabelink and Luscher 2006), a significant contributor to the pathogenesis of endothelial dysfunction. Under normal conditions eNOS catalyses the formation of NO and L-arginine (see section 1.4.3), however due to the high redox potential of the enzyme it has the ability to produce $\bullet O_2$- and due to the electron transfer across the eNOS dimer is normally tightly controlled (Forstermann 2006). If the movement of electrons to L-arginine and molecular O_2 becomes

dysregulated, for instance in the absence of BH_4 or other co-factors (see figure 1.8) (Gross and Levi 1992; Forstermann and Munzel 2006; Rabelink and Luscher 2006) electrical "uncoupling" of eNOS can lead to the production of damaging $\bullet O_2$- anions instead of NO, thus promoting oxidative stress. Importantly, uncoupled eNOS has been identified as a risk factor for athrerosclerosis (Rabelink and Luscher 2006) as it is observed as a result of smoking, high blood pressure and other traditional risk factors (Forstermann and Munzel 2006).

The result of this uncoupling is an overall decreased production/bioavailibility of NO and subsequent removal of vascular protection. Moreover, $\bullet O_2$- reacts very rapidly with any residual (or perhaps iNOS-derived) NO producing peroxynitrite (ONOO). This molecule is extremely harmful to the cells of the vasculature (Forstermann and Munzel 2006; Sullivan and Pollock 2006) causing oxidative damage to proteins, lipids and DNA (Beckman 1996) and exacerbating endothelial dysfunction. Interestingly, recent studies indicate that peroxynitrite may also have a deleterious effect on prostacyclin synthase (Zou and Ullrich 1996) thus also removing the protective benefits of this molecule.

Other reactive oxygen species which are not so rapidly broken down are products of $\bullet O_2$- metabolism such as hydrogen peroxide and hypochlorous acid, both possessing oxidizing capabilties and therefore contributing further to oxidative stress in the vascular tissue (Munzel, Daiber et al. 2005). Moreover it has been suggested that once vessels are subjected to oxidative stress, the dysfunctional eNOS becomes further upregulated (Hink, Li et al. 2001). This therefore contributes to added damage and dysregulation, exacerbating the proinflammatory environment of the tissue, removing the protective molecules and increasing endothelial/vascular dysfunction.

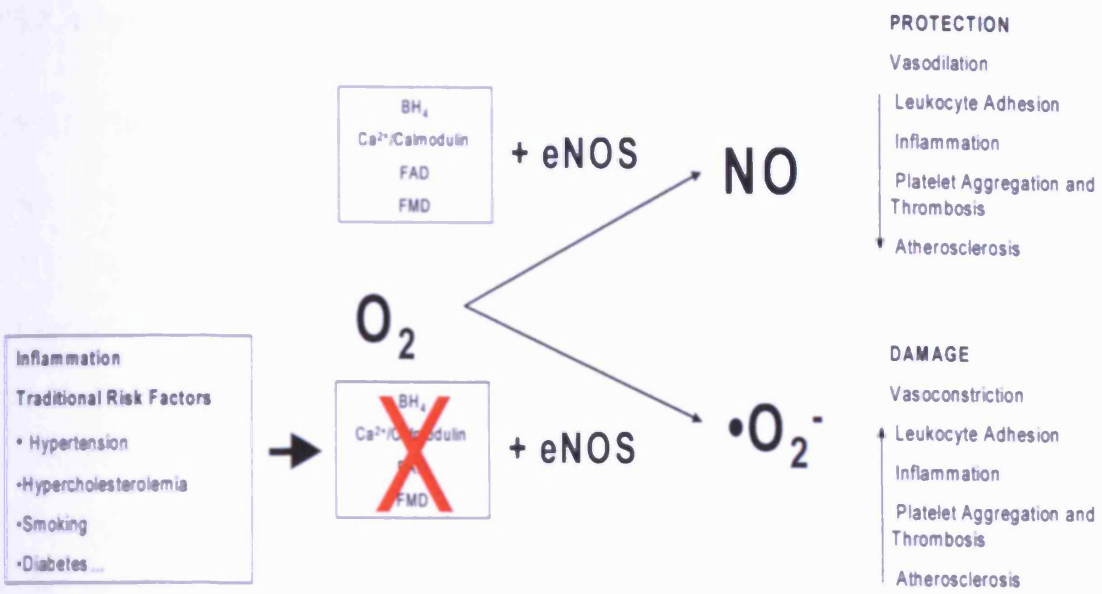

Figure 1.8. eNOS Uncoupling. eNOS uncoupling due to unavailability of the essential cofactors results in production of superoxide and a decrease in the natural protective mechanisms of the endothelial cells.

Hypotheses surrounding the development of CVD in RA centre largely on endothelial dysfunction, and in particular the uncoupling of eNOS and as such, experimental evidence exists in support of this (Haruna, Morita et al. 2006). This is thought to arise following insult to the endothelium by inflammatory cytokines characteristic of RA. However problems that arise within the vasculature are normally multifactorial and other underlying changes to the structure and function of cells within the vessel wall can occur after an initial damaging insult. This could result in other changes that are deleterious to function.

1.5.4. Changes to Smooth Muscle Cell Function

1.5.4.1. Phenotypic Switching

Many vascular diseases are characterised by intimal hyperplasia; the proliferation of SMCs within the intimal layer of the arteries and an additional increase in the volume of extracellular matrix proteins within the vessel wall (Newby and Zaltsman 2000). Under normal conditions the VSMCs exhibit a quiescent contractile phenotype with a low level of proliferation, serving to maintain vascular tone by playing a role in contraction and expressing contractile proteins (Owens 1995) (see figure 1.9). It is thought that inhibitory actions derived from cell-matrix interactions between basement membrane components, cell surface integrins and soluble mediators maintain the quiescent state (Thyberg, Blomgren et al. 1997).

In response to injury VSMCs rapidly increase their rate of proliferation and migration (from the media to the intima) and additionally start to play a critical role in vessel repair. This is similar to the phenotype expressed during development and is regarded as a "synthetic phenotype" (Owens, Kumar et al. 2004). The result of this phenotypic switching is to produce a thickening of the arterial wall, thus eventually narrowing the vessel lumen (see figure 1.9). It is important to note that there are many varying phenotypes, other than those mentioned above, which can be seen throughout cell maturation as well as disease progression. For example during development there will be differential expression of various proteins over time to achieve the fully functioning adult cell. However the two definitions described help to establish the alteration of VSMC from the normal function with respect to vascular changes without confusing other intermediate phenotypes the cells may exhibit at various times. The change in this vascular phenotype is important in the development and progression of many diseases including hypertension and atherosclerosis. Additionally it has been observed that in patients with RA intimal-media thickening is commonplace and correlates directly with

disease severity and moreover often is a predictor for the development of atherosclerotic plaques (for a recent review see (Tanasescu, Jurcut et al. 2009)).

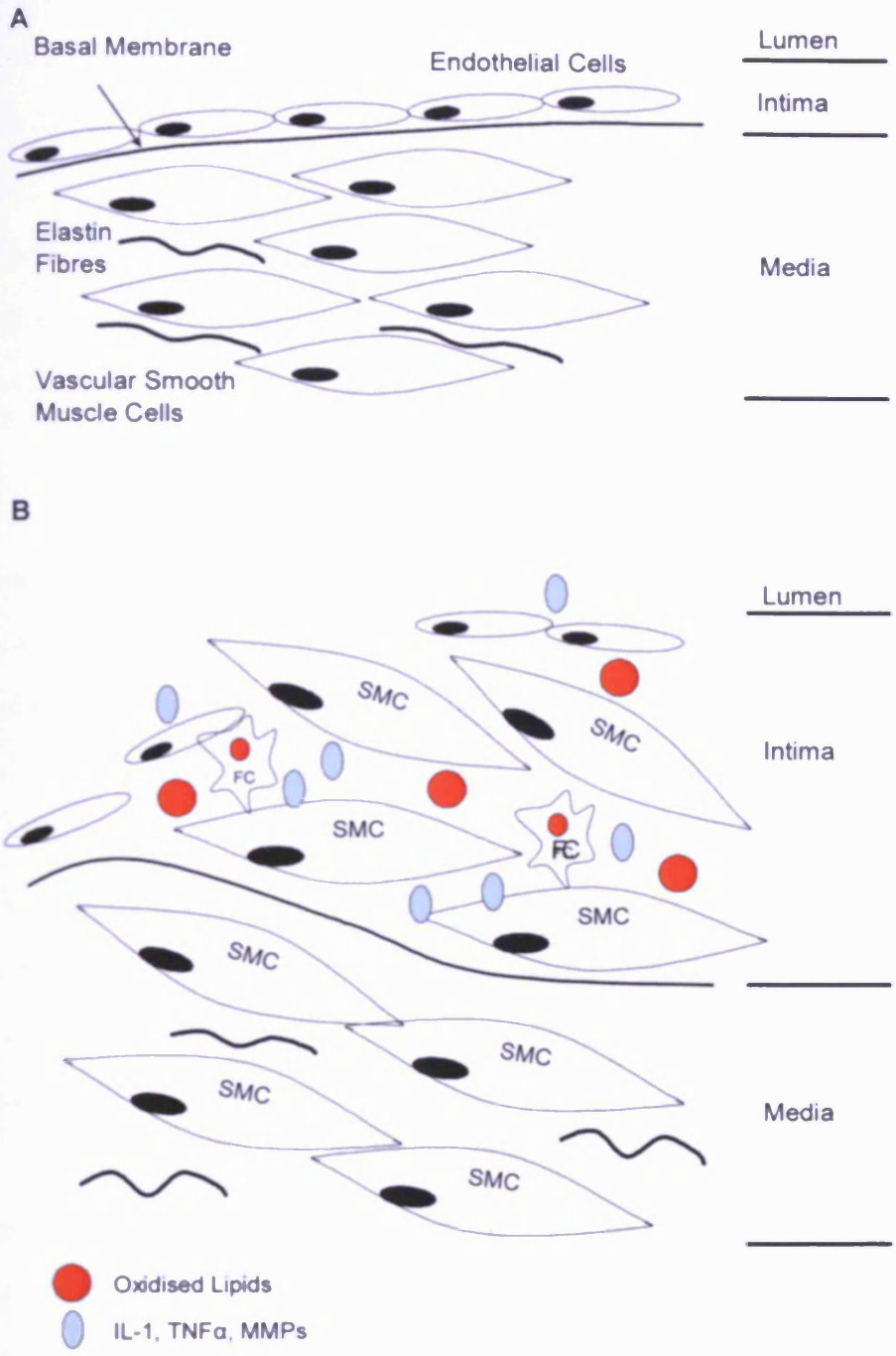

Figure 1.9. Changes to the Vasculature and Intimal Thickening. A. Normal structure of the vessel showing the intima and media. B. Inflammation in the vessel. Inflammatory mediators such as IL-1, TNFα and MMPs are present in the layers of the vessel. VSMCs, endothelial cells, and foam cells (FCs) are activated promoting proliferation and migration of VSMCs. These move from the media into the intima.

Phenotypic switching is a complex process, and is regulated by a variety of factors present in the circulation such as cytokines, chemokines, inflammatory mediators, lipids and reactive oxygen species (ROS) (Owens, Kumar et al. 2004). Physical factors such as mechanical stretch, a result of the high pulsatile force of the blood that the vessel is exposed to (Shyu 2009), can also induce changes within the VSMC that affect cell alignment, cell differentiation, migration and vascular remodelling. VSMC phenotype is also regulated by cell-cell and cell-matrix contacts. It must be noted that intimal thickening is a multifactorial process with migration of other cell types to the vessel wall (Bayes-Genis, Campbell et al. 2002).

Chronic inflammation can play a role in this process by disrupting normal vessel function. Leukocytes secrete inflammatory mediators causing damage and influencing cells elsewhere to further produce cytokines and chemokines. These can assist in cell activation and proliferation and as such, the actions of leukocytes are widespread (Singer, Salinthone et al. 2004).

The cytokines produced by inflammatory cells can have additional detrimental effects on vessel function; TNFα and IL-1 can both promote smooth muscle proliferation and ECM remodelling (Wills, Thompson et al. 1996), confirmed through extensive experimental investigations. Moreover with regard to the progression of vessel damage, these cytokines can stimulate adherence of LDL to the endothelium and VSMCs (Ross 1999) propagating further harm. With respect to VSMC proliferation, Rectenwald et al (2000) conducted a series of experiments investigating neo-intimal hyperplasia following vessel injury. Here it was observed that mice lacking functional TNFα, and in a separate experiment, mice lacking the IL-1 receptor, both failed to produce intimal thickening as observed in their control counterparts (Rectenwald, Moldawer et al. 2000), indicating a key role for these cytokines in the progression of this anomalie. Furthermore, other animal studies have confirmed the positive role cytokines can play in the development of vessel disease, observing that in an IL-1 knockout mouse model, atherosclerosis progression is notably reduced (Hoge and Amar 2006). Moreover, the

inflammatory effects of these cytokines are not limited to inducing changes to VSMCs only. For example IL-1 also acts as a growth factor for fibroblasts and lymphocytes, and can activate T- and B- cells (Libby, Warner et al. 1988) which can all exert a damaging effect in the vessel wall.

Another contributor to damage is the production of $\bullet O_2^-$ by inflammation-activated monocytes (Peri, Chiaffarino et al. 1990). This not only causes endothelial dysfunction (see 1.5.3) but can also contribute to damage to the VSMCs alongside that caused by inflammatory cytokines and growth and chemotactic factors also produced by these cells under inflammation (Assoian, Fleurdelys et al. 1987).

In addition to inflammation there are also extracellular structural changes in the vessel wall which can affect VSMC function and proliferation. These are novel pathways and are not entirely characterised, but have the potential to lead to exciting new developments in this field.

An example of this is the cadherin family of proteins which form extracellular cell-cell contacts. This is discussed in more detail in subsequent chapters. Briefly, when these contacts become compromised it is thought to have an effect on downstream signalling cascades which can result in changed protein expression. Experimental work has shown that a change in the structure, or cleavage of the extracellular component of these molecules can result in VSMC proliferation. In one case a reduction in the amount of N-cadherin on the VSMC membrane was observed following stimulation of cultured VSMCs with platelet derived growth factor (PDGF), a change which was attributed to the proteolytic activity of MMP and resulted in disruption of cell-cell contacts. These observations occurred during VSMC proliferation highlighting a role for MMPs in this change (Uglow, Slater et al. 2003).

The MMP family of proteins is a group of enzymes involved in extracellular matrix remodelling and is thought to be heavily involved in structural damage to the vessel wall

(Raffetto and Khalil 2008). Specific MMPs have been shown to play an important role in cadherin signalling as well as partaking in extracellular remodelling (Uglow, Slater et al. 2003). It is known that throughout the inflammation in RA there is an increase in the expression of MMPs both locally in the synovial fluid, and also in the serum of these patients (Tchetverikov, Ronday et al. 2004). Hypothetically this increase could have a detrimental effect on the vasculature causing cadherin shedding or other damaging changes, and could possibly stimulate the proliferation of VSMCs and promote subsequent intimal hyperplasia.

1.6. Matrix Metalloproteinases

An important group of enzymes that would seem to be common denominators in the pathogenesis of RA and cardiovascular-related diseases are the MMPs. These are a family of proteolytic enzymes capable of degrading and remodelling the ECM and connective tissue proteins (Raffetto and Khalil 2008). They are essential in biological processes such as embryonic development, morphogenesis, reproduction, tissue resorption and remodelling, but also play an important role in pathologies such as inflammation, CVD, arthritis and cancer (Ram, Sherer et al. 2006). While MMPs are mainly found in the extracellular milieu, it has been reported that some are found intracellularly (Ganea, Trifan et al. 2007).

While the many MMPs have a variety of expression patterns and functions, they are classified into subgroups according to their substrates, for example gelatinases, stromelysins, and collagenases (Chow, Cena et al. 2007) (see table 1.8.). MMPs are zinc-dependent endopeptidases and are all synthesised in the latent form of the molecule, as a pro-MMP or zymogen. They require activation by proteolytic removal of a pro-peptide domain before becoming fully functional (Tallant, Marrero et al. 2009). This is achieved by removal of the pro-domain which inteferes with the catalytic zinc to maintain dormancy (Chow, Cena et al. 2007) – removal of this domain exposes the

catalytic site. This "Cysteine Switch" is a common feature of all the MMPs (Van Wart and Birkedal-Hansen 1990) and is crucial for MMP regulation.

	MMP	Expression or Function	Substrates
Collagenases	Colagenase-1/MMP-1	Development, tissue repair, malignant tumours.	Col I, II, III, VII, VIII, X aggrecan
	Colagenase-2/MMP-8	Leukocytes, cartilage	Col I, II, III, aggrecan
	Colagenase-3/MMP-13	Bone development, invasive tumours	Col I, II, III, IV, IX, X, XIV, gelatin, fibronectin, laminin, aggrecan
Gelatinases	Gelatinase A/MMP-2	Degradation of basement menbrane and of fibrillar collagens after intial cleavage by collagenases. Invasion of malignant tumours.	Col I, IV, V, VII, X gelatin, fibronectin,
	Gelatinase B/MMP-9		Col IV, V, VII, XI, XIV, XVII, gelatin, elastin, fibrillin
Matrilysins	Matrilysin-1/MMP-7	Constitutively expressed in ductal epithelial cells of exocrine glands	Col IV, elastin, fibronectin, laminin, nidogen, tenascin, osteonectin
	Matrilysin-2/MMP-26	Uterus, placenta, reproductive processes	Col IV, gelatin, fibronectin, fibrin, fibrinogen, type I gelatin
Stromelysins	Stromelysin-1/MMP-3	Keratinocytes and fibroblasts	Col IV, V, VII, IX, X, XIV, fibronectin, elastin, gelatin, laminin, aggrecan
	Stromelysin-2/MMP-10		Col IV, V, IX, X, XIV, fibronectin, elastin, gelatin, laminin, aggrecan

Table 1.8. Examples of MMP Sub-groups. Table showing examples of some of the MMP sub-groups, their substrates and functions.

1.6.1. Gelatinases

Of the many MMPs described above, the gelatinases MMP-2 and MMP-9, (gelatinase-A and gelatinase-B respectively) are of particular importance in disease pathology. These enzymes differ in their expression; MMP-2 is expressed constitutively in many cells (Salo, Lyons et al. 1991) whereas MMP-9 is induced in inflammatory conditions in certain cells (Chakraborti, Mandal et al. 2003), and as such this molecule plays important roles in the pathology of inflammatory disease. As the name would suggest, their main substrate is gelatin (a denatured collagen) though a wide range of substrates has now been reported (see table.1.9).

Substrates for MMP-9
Gelatin
Elastin
Fibronectin
Proteoglycan core protein
Myelin
Collagen Type 17
Collagen Type 11
Collagen Type 10
Collagen Type 7
Collagen Type 5
Collagen Type 4

Table 1.9. Substrates for MMP-9.

MMP-9 has several regions within it which allow for correct enzymatic function. The N-terminal signal peptide domain directs the pro-MMP to the endoplasmic reticulum (Ram, Sherer et al. 2006) in order for it to follow the normal secretory pathway (Moscana A 2003) before removal of the pro-peptide domain and emzyme activation. Other sub-units within the molecule confer specificity for the substrate(s), allow cleavage by inhibitors of the molecule, and provide structural support for the enzyme (see figure 1.10) (Ram, Sherer et al. 2006).

It is crucial that MMP function is tightly controlled to avoid excess catabolism of the ECM and as such, there are several ways in this is achieved; the enzymes can be degraded and cleared to remove enzymatic function, or it can be compartmentalised for later secretion when appropriate. The cysteine switch, common to all MMPs is an important mechanism for regulation and enzymes which can are able to activate MMPs wil be under further regulation. Moreover transcription of these proteins can altered to increase and decrease gene expression (Chakraborti, Mandal et al. 2003). With respect to MMP-9, the enzyme is under strict control at gene transcription, synthesis, secretion, activation inhibition and glycosylation (Ram, Sherer et al. 2006).

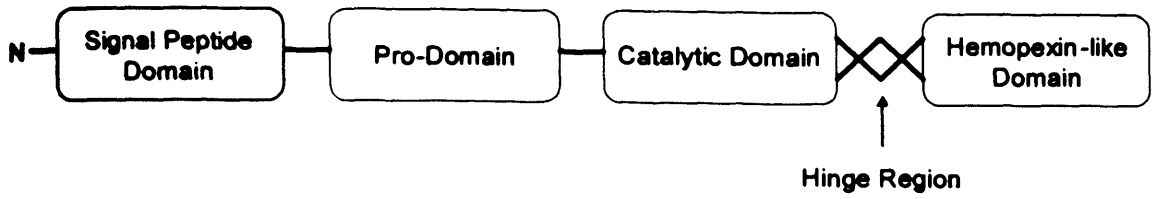

DOMAIN	FUNCTION
Signal Peptide Domain	N-Terminal domain which directs MMP-9 to the endoplasmic reticulum.
Pro-Domain	Maintains MMP-9 in inactive form. Within this is the cysteine residue which, when cleaved is essential for activity. This is the Cysteine Switch.
Catalytic Domain	Contains the catalytic machinery - the zinc binding site, a calcium ion and a methionine group. These help to conserve the three dimensional structure, the stability and activity of the enzyme.
Hemopexin-like Domain	The C-terminal domain. Plays a large role in substrate binding and interactions with TIMPS.
Hinge Region	Proline rich region connecting the catalytic domain to the hemopexin domain.

Figure 1.10. Structure of MMP-9. Schematic of the structure of MMP-9 and the function of the individual sub-units.

The gelatinases are under varying levels of transcriptional control due to the contrasting constitutive and inducible nature of the enzymes. MMP-2 is expressed widely in almost all cells and is affected minimally by growth factors and cytokines (Salo, Lyons et al. 1991), whereas conversely MMP-9 is induced in certain cells under the influence of IL-1β, TNF-α, PDGF, endothelial growth factor (EGF) (Chakraborti, Mandal et al. 2003), and TGF-β (Salo, Lyons et al. 1991). Interestingly growth factors and cytokine have been reported to have a synergistic effect on MMP expression emphasising the varying control this enzyme is under (Fabunmi, Baker et al. 1996; Bond, Fabunmi et al. 1998). Contrastingly neutrophils, which produce MMP-9 during their development, store the protein and thus when activated release it via de-granulation (Ram, Sherer et al. 2006). These mechanisms allow for varying control and secretion throughout inflammation.

Gelatinase activity can also be regulated via secretion and activation; MMP-9 like other MMPs is secreted as an inactive zymogen, and must be activated by removal of a pro-peptide domain. This enables conformational changes resulting in the zinc ion being accessed by a hydrolytic water molecule and thus activation of the enzyme can occur. Several different proteases are able to activate MMP-9, for example stromelysin and MMP-2. Additionally chemical mediators and extreme environments can also activate MMP-9, such as ROS, low pH and changes in temperature (Visse and Nagase 2003). Interestingly leukocytes are able to activate MMP-9 via chemical mediators; neutrophils produce hypochloric acid which can activate pro-MMP-9 (Ram, Sherer et al. 2006).

In addition to activation, MMP activity can be hindered by the presence of tissue inhibitors of MMPs (TIMPS) (Ganea, Trifan et al. 2007) of which there are four (TIMP-1, -2, -3 and -4) (Brew, Dinakarpandian et al. 2000). These are secreted alongside variable amounts of MMPs (Van den Steen, Dubois et al. 2002; Ram, Sherer et al. 2006) and can inhibit at a 1:1 ratio. The overall structure of the TIMP molecule behaves like a wedge and is able to fit into the active site of the MMP just as the substrate would. Most TIMPs can inhibit the majority of MMPs with a few exceptions (Visse and Nagase 2003). Active MMP-9 is inhibited by both TIMP-1 and TIMP-2 (Gruber, Sorbi et al. 1996). Naturally occurring antagonists of MMPs also exist, such as α2 macroglobulin and plasminogen activator inhibitor (PAI), but the MMP-inactivating ability of these is limited (Rannou, Francois et al. 2006).

Following translation MMP-9 is regulated in three ways via glycosylation, dimerisation and degranulation (see section 1.7.1.2). Primarily MMP-9 is heavily glycosylated with three possible sites for N-linked glycans assisting with maintaining the stability of the protease. Secondly, due to free cysteine residues the enzyme is able to form covalently bonded dimers and complexes, used to control activation of the enzyme (Van den Steen, Dubois et al. 2002; Ram, Sherer et al. 2006). The method of granulation prevents release of MMP-9 until the cell that stores the MMP-9 itself is activated.

In normal tissues, MMP-9 and the TIMPs are in a balance vital for maintaining homeostasis. When this balance tips the effect can become deleterious and damaging to cells and tissues. It is important to note that not all MMPs are deleterious in disease, in fact in certain circumstances they can be beneficial.

1.6.2. MMP-9 in RA

There are many studies relating MMP-9 and RA in both humans and animal models of disease. It is widely accepted that this enzyme is upregulated in the joints and is a primary cause of destruction to cartilage (Yoshihara, Nakamura et al. 2000). Moreover, an imbalance between MMP-9 and TIMP has been observed with a decrease in the amount of TIMP being secreted by the synovial cells of RA patients (Jackson, Arkell et al. 1998) exacerbating the effect of MMP-9. This, accompanied with the excess activation of other degrading enzymes, swiftly contributes to the chain of events associated with cartilage destruction (Ram, Sherer et al. 2006). Indeed a study performed by Itoh et al using a mouse model of arthritis emphasises the impact MMP-9 has on the joints and demonstrates that elevated MMP-9 plays a pivotal role in damage showing that while arthritis still develops in the absence of this enzyme, it takes on a significantly milder form (Itoh, Matsuda et al. 2002).

In RA MMP-9 is produced by inflammatory cells and inflammatory mediators. Primary cellular sources of the enzyme are macrophages, osteoclasts, synovial fibroblasts and neutrophils, while cytokines such as IL1-β, TNF-α and interferon-γ (IFNγ) can promote MMP-9 activation and secretion (Van den Steen, Dubois et al. 2002; Tchetverikov, Ronday et al. 2004; Chia, Chen et al. 2008; Garvin, Nilsson et al. 2008). A role for MMP-9 in RA is supported by the observation of a ten fold increase in circulatory MMP-9 in patients with RA compared to healthy control patients (Chang, Lin et al. 2008).

1.6.3. MMP-9 and Vascular Disease

MMPs have also been implicated in vascular disease as defects in the synthesis and breakdown of the ECM are seen as key processes in the development and stability of atherosclerotic plaques (Rodriguez, Orbe et al. 2007). ECM remodelling is maintained via a careful balance of proteases and their inhibitors and disruption can result in damage and atherothrombosis as shown in figure 1.11 (Rodriguez, Orbe et al. 2007). As in RA they are secreted as propeptides and need activation before they are enzymatically functional.

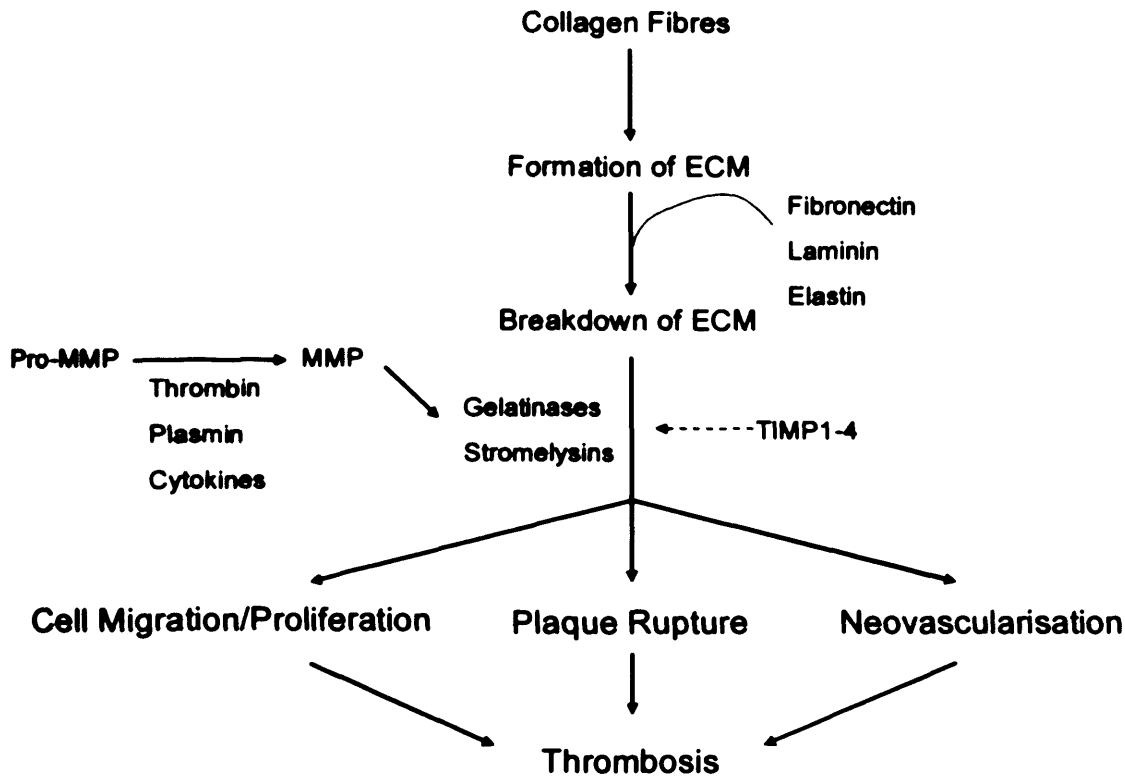

Figure 1.11. Maintenance and Breakdown of the ECM.

MMPs and in particular the gelatinases have been associated with destructive roles within the vasculature. Primarily, with regard to plaque formation, they have been seen to be essential for the formation of new blood vessels, contributing to neovascularisation of the plaque (Moreno, Purushothaman et al. 2004). As such there is substantial evidence in the literature supporting the role that MMPs play in the formation, progression and subsequent de-stabilising of the atherosclerotic plaque. In addition to

MMPs there are a plethora of other proteases which may play a detrimental role at the vessel wall however MMPs will form the main focus of this thesis.

MMP-9 has also been associated with other destructive roles resulting in compromised vessel function. In an animal model of Kawasaki disease, a disease characterised by vasculitis or inflammation of middle sized arteries, it was observed that such arterial inflammation was associated with MMP-9 upregulation, resulting in breakdown of elastin and subsequent aortic aneurysm (AA) formation (Lau, Duong et al. 2008). Although AA is associated with autoimmune diseases, there is no evidence in the literature that it is a co-morbidity of RA. Despite this, the active role that MMPs play in vessel diseases such as AA and atherosclerosis makes investigating the behaviour of this enzyme of high importance. Further supporting this is the observation that MMP-9 has been implicated in the progression of AA in other diseases. For instance in a mouse model of Marfan syndrome, a connective tissue disorder within which thoracic AA is a life threatening complication, weakening of the aortic wall is associated with a loss of vascular compliance. The degeneration of elastic fiber integrity observed in this model has been associated with an increased presence of gelatinases (Chung, Au Yeung et al. 2007) implying they could be responsible for this degeneration. Since elastic fibers within the vessel wall are responsible for elasticity, fragmentation of this structure by both MMP-9 and -2 is associated with a deterioration in compliancy and this has been proven by appropriate experimental work (Chung, Au Yeung et al. 2007). Importantly it has also been observed that MMP-9 and -2 inhibition by doxycyclin (a MMP inhibitor) prevents AA in the mouse model of this syndrome (Chung, Yang et al. 2008) supplying further support for the role of MMPs in this process. Additionally, in a knock-out mouse model, MMP-9 gene deletion reduces the formation of AA also highlighting the role the enzyme plays in this mechanism (Ikonomidis, Barbour et al. 2005). All of these results provide evidence for the deleterious nature of MMP-9 in the vessel wall.

Furthermore there have been suggestions that MMP-9 could play a role in the modulation of aortic contraction. Chew et al 2004 hypothesised as a result of their work

in AA, that MMP-9 is upregulated and results in subsequent aortic dilation by inhibiting Ca^{2+} mobilisation and influx (Chew, Conte et al. 2004). The decrease in intracellular Ca^{2+} as a result of this would prevent formation of the Ca^{2+}/CaM complex and subsequent MLCK activation and SMC contraction. This was shown after incubating rat tissue in the presence of MMP-9 and MMP-2 which prevented vessels reaching and maintaining their maximal constriction. Additionally, alongside this, MMP-9 appeared to have an inhibitory effect on KCl induced constrictions. In this work, the elastin structure was maintained (Chew, Conte et al. 2004), indicating that MMP-9 did not damage the ECM in the manner seen in the AA models. An interesting study by Raffetto et al 2007 concluded that MMP-2 could potentiate vascular hyperpolarisation in veins resulting in vascular relaxation. This is achieved via the Bka Ca^{2+} channel and subsequent blocking of the channel halted the MMP-2 effect, suggesting that MMP-2 may activate the potassium (K^+) channels causing lack of Ca^{2+} influx and thus relaxation (Raffetto, Ross et al. 2007).

The evidence above supports various theories for the role that MMP-9 could play in vascular damage and the loss of function that ensues. Due to the highly inflammatory nature of RA it is possible that this could be happening as a direct result of an increase in circulating MMPs and subsequent damage to the vasculature, however more reaserch must be done in the RA context to elucidate mechanisms behind this.

In summary, RA is a multifactorial systemic disease, a result of which is a damaging inflammatory environment within the circulation with detrimental effects upon the rest of the body. This systemic inflammatory burden results in cardiovascular-related disease and a subsequent lower quality of life with shortened life expectancy. Little is known regarding the pathology behind this and in order to increase our knowledge, significant research is underway to determine the mechanisms and key factors involved. To facilitate such activity, animal models are widely utilised as valid tools in determining underlying mechanisms in such pathologies.

1.7. Models of Rheumatoid Arthritis

There are several models of inflammatory arthritis all designed to further the understanding of disease pathology, some of which are discussed in more detail later on in this thesis. Defining the molecular and pathological events that lead to the severe inflammatory arthritis seen in RA patients is essential and could lead to new approaches for controlling the disease.

Despite the fact that none of the models are a perfect replica of the human disease there are compelling reasons for the use of such representations in the laboratory. Conditions surrounding the disease can be tightly controlled allowing for direct comparison of results. Secondly it can be induced with ease, with a high rate of incidence permitting straightforward tissue sampling, and thus relatively simple characterisation of tissue, cellular and molecular mechanisms. Pharmacologically-speaking therapies can be administered in tightly regulated doses and blood/tissue responses can be easily quantified.

In human RA external factors and person to person variability play a huge role in the development and progression of the disease, and as such, the disease can manifests itself in patients in very different ways. This can prove difficult with respect to treating each individual, and cause variations in observations made between patients. Therefore with regard to disease discovery, the simplicity of these models is a great benefit for the researcher. Of particular interest to this thesis is the murine collagen-induced arthritis (mCIA) model, which involves development of an inflammatory arthritis in mice post-inoculation with type II collagen (CII) in complete Freunds adjuvant.

1.7.1. Murine Collagen-Induced Arthritis

In 1977 Trentham et al reported in the rat that following immunization with CII, an erosive polyarthritis, mediated by an autoimmune response to the rat joint CII, subsequently developed (Trentham, Townes et al. 1977). This procedure has since been

replicated in the mouse (Courtenay, Dallman et al. 1980; Bruhl, Cihak et al. 2009; Hartog, Hulsman et al. 2009; Lindblad, Mydel et al. 2009; Palframan, Airey et al. 2009; Svelander, Erlandsson-Harris et al. 2009). The significance of this model is the production of auto-antibodies to CII. The latter forms a major component of the joint cartilage and indeed is expressed exclusively in the joints (Cho, Cho et al. 2007). During disease CII becomes a significant focus for aggressive inflammation. Importantly antibodies to CII have been found in RA patients in the early stage of the disease indicating that CII could play an important role in initiating the human condition (Cho, Cho et al. 2007).

From a pathological point of view this mCIA model and human RA are very similar. Histologically, they both involve synovitis and pannus formation, the latter progressing to cartilage damage and bone erosion. Susceptibility of animals to induction of this disease is dictated by expression of specific MHC class II molecules (Wooley, Luthra et al. 1981). This has parallels with the human condition as it is well established that inherited susceptibility to RA is associated with the genes encoding the human MHC class II molecules (HLA-DR4 and HLA-DR1 alleles) (Todd, Acha-Orbea et al. 1988)

1.7.2. Animal susceptibility to CIA

As susceptibility is conferred by the expression of MHC genes, mCIA is a largely T-cell-dependent disease (Staines and Wooley 1994). The MHC molecules are highly polymorphic integral membrane proteins which serve the following functions. Firstly they act as 'self' structures so the antigen-specific T-cells can recognise them, and secondly can behave as receptors which bind antigens and present them to T-cells in order to provoke an immune response (Luross and Williams 2001).

Extensive variation exists within the MHC subgroups of molecules; the class II chromosomal region encompasses nearly 1,000,000 base pairs, and includes at least 14 different genes (in humans). During splicing these genes can be differently assorted to

produce a highly variable set of proteins which are expressed on the cell surface (Gregersen, Silver et al. 1987). It has been observed that animals possessing the MHC II I-A isotype and within this the allele I-A^q, are susceptible to mCIA (Myers, Rosloniec et al. 1997; Luross and Williams 2001). This is analogous to the situation in human RA, in which expression of particular subtypes of the DR4 and DR1 alleles are strongly associated with susceptibility to the disease (Williams, Inglis et al. 2005). Subsequently the DBA/1 strain of mice is commonly used for the induction of arthritis as they posses this allelic variation, and therefore have a heightened susceptibility for positive induction of the disease.

In mCIA it is proposed that APCs capable of presenting the CII antigen complexed with the I-A^q MHC variant on the T-cell surface can promote initiation of arthritis. This results in production of T-cells that are specific for CII (Luross and Williams 2001). In mice, if this allelic variation is present, a strong T- and B-cell response will occur due to this antigen presenting complex following immunisation with heterologous (chick) CII. Specificity of the allele was described by Wooley et al in 1980 who found that despite the ability of several murine strains to mount a large anti-CII immune response after inoculation, only the animals with the I-A^q allele present developed arthritis (Wooley, Luthra et al. 1981). Similarly another variant, the I-A^r allele confers susceptibility to porcine or bovine collagen-induced arthritis in mice. The severity of arthritis has been observed to be dependent on the collagen source. Immunisation with heterologous collagen seems to elicit a more aggressive arthritis compared to an autologous collagen injection (Holmdahl, Karlsson et al. 1989).

1.7.3. Pathogenesis of CIA

mCIA is induced after the administration of two identical inoculations, consisting of an emulsion of complete Freund's adjuvant and chick CII, administered three weeks apart. It has been noted that during the period between inoculations, an increase in levels of IL-6 and TNFα occur and after the second immunisation, concentrations of these and

additionally IL-1β are higher in the joint (Marinova-Mutafchieva, Williams et al. 1997). This again represents a similarity to the human condition where increased plasma levels of IL-1 (Shore, Jaglal et al. 1986), and TNF-α are observed and have been associated with joint damage (van den Berg 2001).

In the mCIA model, immediately after the second immunisation, DCs begin to present CII, increase MHC II expression and thus induce T-cells to activate B-cells in a highly specific immune attack against the CII component (Cho, Cho et al. 2007). At the same time, DCs also start to express higher levels of chemokines and cytokines. At this initial phase in the disease, and prior to clinical signs of arthritis, MHC II-expressing cells (DCs and T-helper cells) are found to accumulate in the synovial membrane. In parallel with, and as a direct result of this cell accumulation, neutrophils and macrophages also begin to invade the joint (Luross and Williams 2001) secreting proteolytic enzymes and cytokines as they do so.

The anti-CII antibodies produced in this environment by the DCs and T-helper cells, are of the IgG_2 subset, a family of IgG molecules involved in induction of the complement system (Cho, Cho et al. 2007). The activation of the complement system results in the production of chemokines and infiltration of inflammatory cells helping to supplement the initial stages of the inflammatory attack. This process has similarities to human disease as complement activation occurs as described in section 1.2.2. The autoantibodies produced in this response work in a similar way to natural antibodies normally produced against invading antigens. Antibodies specific for the self-CII initiate a specific attack against the CII residing in the cartilage (Fleming and Tsokos 2006).

The infiltrating macrophages and proliferating SFs that invade the joint, begin to attack the cartilage and bone, as in human disease, producing the eroding pannus. Other cells which reside here, for example the DCs and granulocytes also produce destructive factors (Luross and Williams 2001) contributing further to cartilage and bone destruction (see figure 1.12).

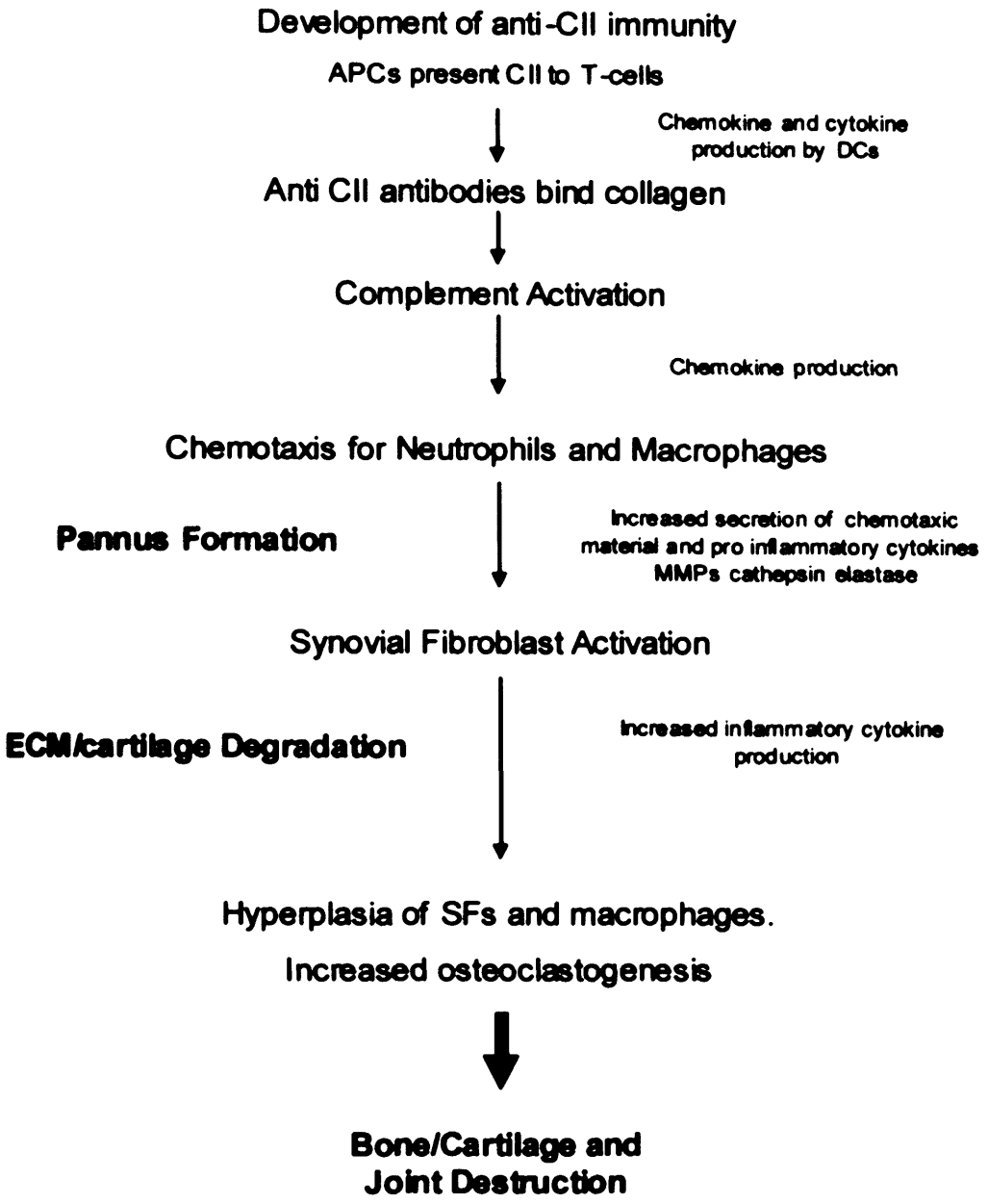

Figure 1.12. Pathogenesis of mCIA.

Once disease is initiated, each event in the inflammation pathway assists in maintaining and furthering the aggressive immune response. The downstream cascade of events is aggressive and fast acting with every step favouring tissue damage and destruction. In short, mCIA is a self-perpetuating disease driven by tissue damage and cellular changes.

1.7.4. Relevance of the mCIA Model

The mCIA model is a highly relevant model of RA due largely to the similarities in the histopathology of both diseases shown by pannus development, a large inflammatory cell infiltration, joint damage, synovitis, neovascularization and bone erosion (Holmdahl, Karlsson et al. 1989; Quinones, Estrada et al. 2005) and both have genetically restricted susceptibility as mentioned in section 1.7.2. They are both immune diseases with production of antibodies to CII, the importance of this in mCIA is shown by induction of inflammatory arthritis in naïve animals after transfer of CII autoantibodies from an arthritic animal (Staines and Wooley 1994). There are also similarities in factors that affect the disease, for example it has been noted that RA and mCIA are similarly influenced by female sex hormones and pregnancy (Waites and Whyte 1987; Holmdahl, Karlsson et al. 1989).

The mCIA model provides a valuable research tool due to its "controllability", and most important in validating its use as an experimental model is the emergence of therapeutic strategies for the management of RA patients as a direct result of the use of mCIA.

Although knowledge has been gained with regard to underlying pathologies of RA, more is still to be done in order to appreciate it as a systemic disease. It is increasingly recognised that RA patients have other underlying health problems, particularly those of a cardiovascular nature. Moreover it is becoming clear that this could be due to the burden of inflammation their body must withstand.

1.8. Hypothesis

In this thesis the following hypothesis will be investigated:

Due to the highly inflammatory nature of RA and similarities of this exhibited in the murine model of RA vascular dysfunction will ensue following the clinical onset of arthritis. This will be characterised by a decrease in bioavailable NO both in the vessel and circulation. Serum levels of inflammatory mediators will be increased and thus contribute to the detrimental effect on the vasculature. Endothelial dysfunction will be observed in isolated blood vessels.

1.9. Aims

Assess endothelial dependent relaxation in aortic tissue from experimentally arthritic and normal mice.

Measure vessel levels of eNOS and iNOS in vessels from experimentally arthritic animals.

Assess plasma levels of NO, TNFα, IL-6, and IL-1β levels in these vessels.

Compare $\bullet O_2^-$ and ONOO in normal and arthritic vessels as a marker of oxidative stress.

CHAPTER 2

EXPERIMENTAL MATERIALS AND GENERAL METHODS

2.1 Mice

All work with animals was performed in accordance with the United Kingdom Animals (Scientific Procedures) Act 1986 and under the authority of Home Office Personal (30/7627) and Project (30/2361) Licences. The technique used to create the animal model of arthritis is an adapted vesion of the method developed by Trentham et al (Trentham, Townes et al. 1977). Throughout the work pertaining to arthritis assessment, DBA/1 animals were used due to their heightened susceptibility for mCIA as a result of their genetic make-up (as discussed in section 1.7.2).

Male DBA/1 mice aged 6-8 weeks were purchased from Harlan Sprague Dawley Inc. and housed in conventional cages. All mice had ad libitum access to normal chow and water and were given a settling in period of one week before being used for experimentation. Mice were subjected to a continual light:dark cycle of 12:12 hours, between the hours of 8am to 8pm. The temperature range in the animal house was maintained between 19 - 23°C, and humidity at 55±10%. At appropriate time points (see below for more detail), mice were euthanised under Schedule 1 of the United Kingdom Animals (Scientific Procedures) Act 1986 by inhalation of carbon dioxide (CO_2). Each mouse was placed in a chamber and exposed to a rapidly rising concentration of CO_2 at a flow rate of 3 l/min until no vital signs of life were observed.

2.2 Induction of Murine Collagen Induced Arthritis

Following the settling in period (see section 2.1), mice were anaesthetised with isofluorane (5 l/min) and oxygen (4l/min) and immunised (see below) with type II chick

sternal collagen (C-9301, Sigma Aldrich) and complete Freunds adjuvant (CFA). This adjuvant was used to assist with initiating the immune reaction in the presence of chick CII. CFA was prepared by grinding 100mg Mycobacterium tuberculosis (dried weight) (H37 RA, DIFCO) into 20ml of incomplete Freunds adjuvant (F-5506, Sigma Aldrich) using a mortar and pestle. The chick CII (5mg) was dissolved overnight at 4°C in 2.5ml of 0.02% (v/v) acetic acid (A/0400/PB17, Fisher Chemicals) and then added to an equal amount of CFA. This mixture was emulsified by passing through a 19 gauge needle ~20 times before injection.

On day 0 mice received 100µl of the CII/CFA emulsion in two 50µl injections intradermally (ID) via a 27 gauge needle after anaesthesia. Each injection was given at a separate site on the right lateral side at the base of the tail. Mice were returned to their cages to recover, and were subsequently checked several times a week to ensure the injection site was not ulcerated and that their general health was satisfactory. Between days 0 and 21 the behaviour of the immunised mice was as observed prior to the first CII/CFA injection. On rare occasions animals did develop arthritis before day 21, this arthritis was very mild and animals were given the second CII/CFA injection (in line with our established protocol (Nowell, Williams et al. 2009) .On day 20 the chick CII was dissolved in 0.02% (v/v) acetic acid, and on day 21 was made into an emulsion with an equal volume of CFA as before. Animals were anaesthetised and ID injections administered to two separate sites at the right lateral side near the base of the tail. After day 21, arthritis progressively developed and to minimise suffering, all mice were given free access to the opiate-derived painkiller buprenorphine (temgesic) (Schering-Plough) via drinking water at a concentration of 0.4mg/l. This was the favoured pain killer as anti-inflammatory analgesics would hinder the progression of disease.

The onset of arthritis usually occurred from day 21 onwards. Throughout disease mice were regularly anaesthetised with isofluorane (as above, for restraint) and the severity of the arthritis measured by assigning a score to each of their paws and measuring paw

swelling. This was achieved by measuring the hind paw diameter using a micrometer (Kroeplin 0-100mm), and also by observing the physical appearance of the paws (see figure 2.1). The scoring criteria are outlined below. Animals were also weighed over the experimental timecourse. If the weight of any one animal dropped by >20% (compared with weight prior to arthritis development) on two consecutive days the animal was humanely removed from the experiment (less than 1% occurrence). To prevent malnutrition, food pellets were made more accessible for the animals by placement in the bottom of the cage.

Paw Score	Description
0	Normal
1	Mild/moderate erythema (redness) and swelling
2	Severe erythema and swelling affecting entire paw joint
3	Up to three joints affected by arthritis
4	Greater than three paws affected by arthritis
5	Deformed paw or joint with ankylosis (stiffness)

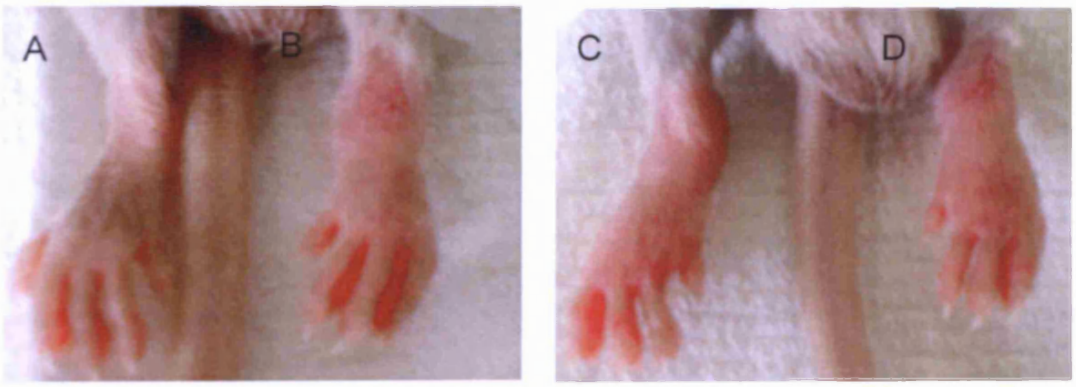

Figure 2.1. Hind Paws from mCIA Mice. Picture showing successful induction of arthritis in the hind paws. A. Paw scoring 0. This paw is normal with no signs of redness and the digits are thin. B Paw scoring 2. This paw is showing more inflammation with redness and swelling of the ankle joint and paw. C Paw scoring 2-3. The ankle joint is inflamed, as well as the two digits on the left (compared to the index digit). D. Paw scoring 4. The entire paw, ankle and all digits are inflamed and swollen.

The sum of the scores for the four paws in each mouse gave an indication of disease severity. Mice were euthanised at time points defined by mild, moderate and severe arthritis according to the criteria below:

Combined Paw Score	Severity
0 - 5	Mild
6-10	Moderate
11 – 14+	Severe

Any animal with a paw score of 5 in any one paw, or a combined clinical score of 14 or more, was humanely removed from the experiment.

2.3 Collection of Experimental Samples

2.3.1 Plasma

At appropriate time points mice were euthanised as described above (section 2.1). Blood (approximately 0.2 – 1ml) was then collected as soon as practical via cardiac puncture using a 19 gauge needle and transferred to EDTA-coated vacutainers (EDTA Coated Vacutainers, BD) on ice, or on occasion blood was collected using a heparin (10,000units/10ml, Leo Laboratories Ltd)-coated syringe and put on ice in an 1.5 ml Eppendorf tube. Subsequently all blood samples were transferred to 1.5ml Eppendorf tubes and centrifuged for 20 minutes at 14,000rpm (16464g) at 4°C. The resulting plasma supernatant samples were stored separately at -80°C until required for analysis.

2.3.2 Tissue

(i) Aortae

Following euthanasia and blood collection the chest cavity and abdomen were quickly opened using small scissors, and 200μl heparin injected into the left ventricle of the heart. The lungs, diaphragm, intestine, stomach and liver were removed for ease of

dissection. The exposed aorta was then vented just above the renal arteries and the left ventricle perfused slowly with ~1ml of gassed (95% oxygen/5% carbon dioxide) Krebs buffer (see appendix) to remove blood from the vessel. Subsequently the thoracic aorta was carefully excised from the chest cavity using curved scissors and placed in fresh Krebs buffer. Loose fat and connective tissue were then removed from the outside of the vessel which was then either;

a) cut into rings for myography (see 2.4)
b) embedded in OCT for histology (see 2.5.2i)
c) homogenised in RIPA buffer for protein analysis (see 2.5.1i)
d) snap frozen in liquid nitrogen (N_2) and stored at -80°C for further use.

(ii) **Paws**

Following euthanasia paws were collected from mice. Forepaws were removed just above the "wrist joint", quickly snap frozen in liquid N_2 and stored at -80°C for further use. Hind paws were removed near the base of the tibia and fibula, just before they meet the ankle. Hind paws were scored along the base of the paw with a scalpel blade, before being immersed completely in Neutral Buffered Solution Formalin (NBSF) (HT501128, Sigma Aldrich), to ensure the solution could penetrate the joint..

2.4 Studies of Aortic Function Using the Danish Multi-Myograph

This method represents a modification of the one used by Cai et al (Cai, Khoo et al. 2005) and based on a technique originally developed by Mulvaney and Halpern (Halpern, Mulvany et al. 1978).

At appropriate times points mice were euthanised as described in section 2.1, and blood and the aorta were removed as in sections 2.3.1 and 2.3.2i. After removal the vessel was cut in to rings of 2mm length (each individual aorta producing 4-5 rings) under a X20

microscope using a scalpel blade and a ruler for scale. These were mounted in separate baths of the Mulvany myograph (Multi-wire Myograph System 610M Danish Myo-Technology, with one or two four-bath myographs being used to study tissues from one or two animals respectively on any given day). Individual rings were bathed in 5ml Krebs buffer at all times and the temperature was maintained at 37°C, regulated by the steel block upon which the bath is placed. Baths were continually gassed with 95% oxygen/5% carbon dioxide. Once mounted, each ring was held between two prongs, one connected to a micrometer to allow manual increase of tension, the other connected to a force transducer to allow measurement of ring tension. The myograph output was connected to a PC and recorded and analysed using Myodaq and Myodata (Aarhaus, Denmark) software respectively. The data was also displayed on the myograph LED for each ring tension.

After mounting the rings were subjected to an equilibration period of 20 minutes following which any tension on the rings and gas were removed and the myograph was zeroed. A baseline tension of 5mN (or 15mN in preliminary experiments, see below) was then established manually via the micrometer over a gradual period of 30 or 10 minutes respectively, increasing the tension at a rate of 0.5mN/min. A rest period of 20 minutes then followed during which the tension was manually adjusted in order for it to maintain the desired baseline. The tissues were then exposed for five minutes to 6×10^{-2}M K^+ in Krebs to condition the vessels to contraction. Peak tension was noted at 5 minutes, following which vessels were washed 8 times with Krebs and left to rest for 20 minutes to re-equilibrate. If the baseline resting tension had decreased during this time (and at any other time in the experiment after washing) it was manually re-constricted to 5mN. After the equilibration period tissues were incubated for five minutes with the appropriate constricting agent (10^{-6}M) followed by 5 minutes with the appropriate relaxing agent (10^{-6}M). Following washing 8 times with Krebs solution a further resting period of 20 minutes was allowed. To ensure accuracy a stock solution of 10^{-2}M was

made up of the agonists was and then diluted accordingly to achieve the desired final concentration in the bath.

Unless stated otherwise constriction responses were measured using the agonist 5-hydroxytryptamine (5HT). To test tissue viability vessels were initially constricted to their maximum by adding increasing concentrations of 5HT (10^{-9}M to10^{-5}M) in half-log increments (see below). Following the plateau with the highest concentration of 5HT, a single bolus concentration of 10^{-6}M ACh was added to ensure normal endothelial function (by relaxation of the vessel via endothelium-derived NO generation). If any ring failed to relax they were subsequently excluded from further experimentation. Vessels were then washed 8 times in Krebs and left to re-equilibrate for 20 minutes.

Starting Agonist Concentration (M)	**Volume added to the Bath (µl)**	**Final Concentration in Bath (M)**
10^{-6}	5	10^{-9}
10^{-6}	10	$3e10^{-9}$
10^{-5}	3.5	10^{-8}
10^{-5}	10	$3e10^{-8}$
10^{-4}	3.5	10^{-7}
10^{-4}	10	$3e10^{-7}$
10^{-3}	3.5	10^{-6}
10^{-3}	10	$3e10^{-6}$
10^{-2}	3.5	10^{-5}

Subsequently vessels were reconstricted to 70-80% of the maximum established previously using increasing concentrations of 5HT as before. 70-80% was normally achieved at a concentration of either 10^{-7}M or $3e10^{-7}$M. After plateau at 70-80% vessels were subjected to a concentration response to ACh (10^{-9}M to10^{-5}M in half log

increments) (see below), each step following the previous only after the vessel was at a steady tension.

Starting Agonist Concentration (M)	Volume added to the Bath (µl)	Final Concentration in Bath (M)
10^{-6}	5	10^{-9}
10^{-6}	10	$3e10^{-9}$
10^{-5}	3.5	10^{-8}
10^{-5}	10	$3e10^{-8}$
10^{-4}	3.5	10^{-7}
10^{-4}	10	$3e10^{-7}$

ACh Concentration	Volume added to the Bath (µl)	Final Concentration in Bath (M)
10^{-6}	5	10^{-9}
10^{-6}	10	$3e10^{-9}$
10^{-5}	3.5	10^{-8}
10^{-5}	10	$3e10^{-8}$
10^{-4}	3.5	10^{-7}
10^{-4}	10	$3e10^{-7}$
10^{-3}	3.5	10^{-6}
10^{-3}	10	$3e10^{-6}$
10^{-2}	3.5	10^{-5}

Results were noted for each ring at the plateau of the response. Relaxation responses to Ach were then expressed as a percentage of the 5HT-induced tone. Where appropriate data was averaged for each animal/condition and counted as one n-value. Values for animal/condition were combined and expressed as mean ± SEM.

2.5 Sample Preparation

2.5.1 Homogenising

(i) Aortae

Aorta were homogenised in 100μl RIPA buffer (see appendix) using a 100μl close-fitting glass rod (attached to a drill (Black and Decker)) and homogenisation tube (Jencons). The frozen aorta was placed in ice cold RIPA buffer in the tube and homogenised for six 10 second bursts. The aorta was left on ice during the homogenising, essential for avoiding the build up of excess heat which could potentially damage the sample. The homogenate was removed from the tube using a glass pipette and transferred to a 1.5ml Eppendorf tube before spinning in a centrifuge for 30 minutes at 14000rpm (16464g) at 4°C. The supernatant was removed and frozen at -80°C for further use.

(ii) Paws

Paws were homogenised as the aortae but using 500μl RIPA buffer and a 1ml close-fitting glass rod and homogenisation tube (Jencons). The homogenate was centrifuged and the supernatant stored as described in 2.5.1(i).

2.5.2 Histology

(i) Aortae

Rings of 2mm were cut from the excised aorta (described previously 2.3.2i) and placed in OCT (LAMB/OCT Embedding Medium, Thermoshandon) on a metal chuck pre-cooled in liquid N_2. The aorta was held in the desired orientation using forceps while OCT was placed on and around the vessel segment and allowed to partially freeze in order to hold the aorta in place. Once the position of the aorta was secured it was immersed in OCT and the whole block was frozen in liquid N_2. Subsequently sections of 7μm were cut on a cryostat and mounted onto Colourfrost Plus glass slides (9991001,

Thermoshandon) to ensure maximum adherence to the glass slide. These were then stored at -80°C ready for staining.

(ii) Paws

Hind paw joints were removed from DBA/1 arthritic animals post euthanasia and immersed in NBSF for a week as previously described (2.3.2ii). It is necessary to decalcify the joints after fixing so that they can be cut, and this was achieved by soaking the paws in a decal solution consisting of 10% (v/v) formic acid (BDH), and 5% (v/v) formaldehyde (F1635 Sigma Aldrich) in distilled water. The solution was made up fresh and changed twice-weekly until paws were decalcified. The latter was confirmed using an ammonium oxalate assay adapted from (Gamble 2008) capable of detecting levels of calcium in the supernatant of the paw-bathing solution. Ammonium oxalate was prepared by dissolving ammonium oxalate in water over heat until it failed to dissolve and a precipitate formed. Following this an excess was added to ensure high saturation. Briefly to assess calcium in the joint, 2ml of supernatant was neutralised to pH7 using hydrochloric acid HCl, and mixed with concentrated ammonium oxalate in a universal container. The presence of calcium was indicated by the formation of a white precipitate (calcium hydroxide). When a precipitate no longer formed, the joints were deemed free of calcium and samples were ready for further processing. This normally occurred after approximately three weeks in the decal solution.

Subsequently joints were dehydrated using a Thermoshandon Tissue Processing Path Centre machine. The paws were immersed and agitated in increasing concentrations of ethanol; 70% (v/v) for 30 minutes, 90% (v/v) for 90 minutes, 100% ethanol for one hour (repeated three times) and then in xylene for three incubations each lasting an hour Finally joints were immersed in four changes of wax, following which they were removed an set in paraffin wax using the Thermoshandon Histocentre. Once set in wax joint sections of 7μm were cut on a microtome and mounted on Colourfrost Plus glass slides before storing at room temperature until ready for staining.

2.6 Histology

2.6.1 Haematoxylin and Eosin Staining

This method was used in order to assess the histological changes to the paws, and to confirm successful induction of mCIA. Haematoxylin and eosin (H & E) staining was used as the haematoxylin stains nuclei purple and eosin stains the cytoplasm and fibrous tissue pink. This provides the contrast necessary for evaluation of changes in cellular content of the joints.

Paws were removed and treated as mentioned in Section 2.5.2ii. After sectioning the slides were deparaffinised by immersing in three changes of xylene (3 x 5 mins) and then in descending concentrations of ethanol (100%, 100%, 90% and 70% all v/v) for three minutes each. Slides were then hydrated in running tap water for 5 minutes, rinsed in distilled water and stained in haematoxylin (351946T, Jencons) for 90 seconds. Slides were washed in tap water for a further 5 minutes and immersed in Scotts tap water (S-5134, Sigma Aldrich) for 30 seconds to enhance the blue stain of the haematoxylin. A 5 minute wash in tap water and rinse in distilled water followed this to remove any excess Scotts tap water. Slides were then stained with eosin (352065W, Jencons) for 90 seconds and washed in tap water for 5 minutes once more before dehydrating in 5 minute washes in ascending concentrations of ethanol (70%, 90%, 100%, 100% all v/v) and then in 3 changes of xylene for 5 minutes each. Slides were mounted with DePex and kept at 60° overnight in order for them to set.

Figure 2.2 shows an example section of a normal paw and an arthritic paw outlining the areas of inflammation. For more detail on the scoring are and criteria see section 4.4.2.

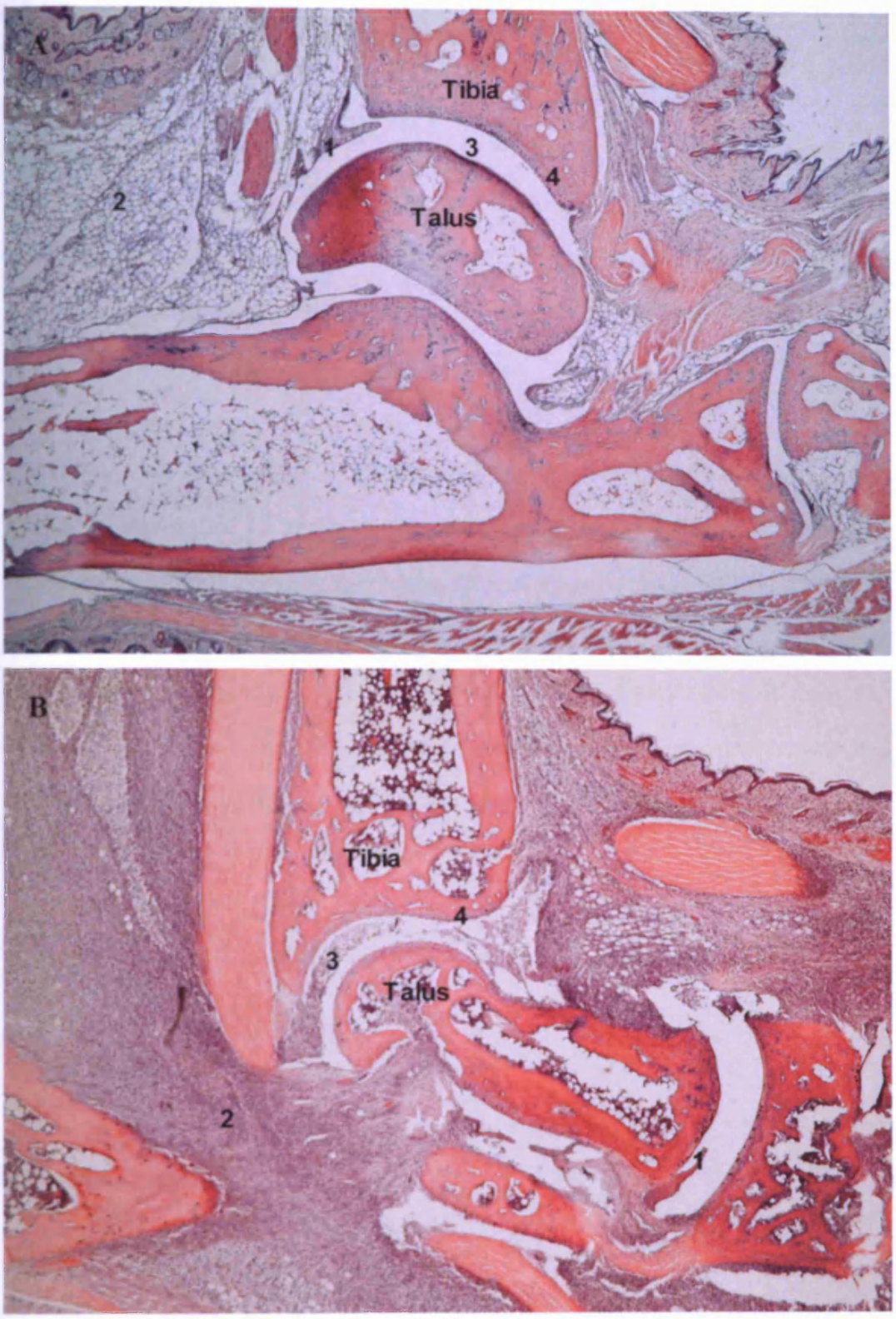

Figure 2.2. H and E Stained Joints. A. Normal Ankle Joint. 1. The synovial membrane, 2. The surrounding connective tissue, 3. The joint space, 4. The layer of cartilage covering the articular end of the bone. B. Severely arthritic ankle joint. 1. The inflamed synovial membrane, 2. Inflammatory cells in connective tissue 3. Exudate that has infiltrated the joint space. 4. Inflammatory cells invade the bone (at X4 magnification).

2.6.2 Safranin O and Fast Green Staining.

This method was used to highlight the areas of cartilage depletion within the joint. Safranin O binds to the cartilage (Rosenberg 1971) leaving a red band. As such when it is degraded there is a "bleaching" effect on the colour allowing the amount of depletion to be measured compared to the original depth of staining (see 4.4.2.2 for more detail). Fast green is the counter stain and stains the rest of the cells. Figure 2.3 shows a normal joint stained with Safranin O and Fast Green.

The slides were deparaffinised, hydrated and stained with haematoxylin as previously described (section 2.6.1). Sections were then washed and immersed in Scotts tap water before washing for 5 minutes in running tap water and staining in Fast Green (F-7252, Sigma Aldrich) for 5 minutes. After this, slides were immersed in 1% (v/v) acetic acid for 10 seconds and stained with Safranin O (S-2255, Sigma Aldrich) for a further 5 minutes. The Safranin O was washed off with two distilled water rinses and then immersed in 100% ethanol before dehydrating to xylene as described in 2.6.1. Slides were mounted using DePex and left over night at 60°C.

To measure cartilage depletion the overall depth of cartilage and the amount stained a "bleached" red was measured (see figure 2.4). These measurements were taken at five random points along the concave articular edge of the tibia using the inbuilt graticule in the microscope. The results were expressed as average original depth of cartilage along the bone edge ± SEM.

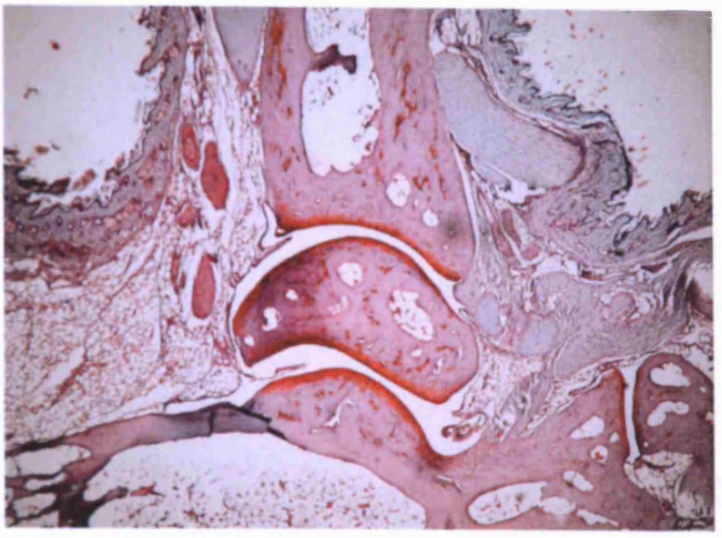

Figure 2.3. Normal Hind Paw Joint Stained with Safranin O and Fast Green. The Saf O shows the cartilage as a bright red band on the articular surfaces of the joint. (at X4 magnification).

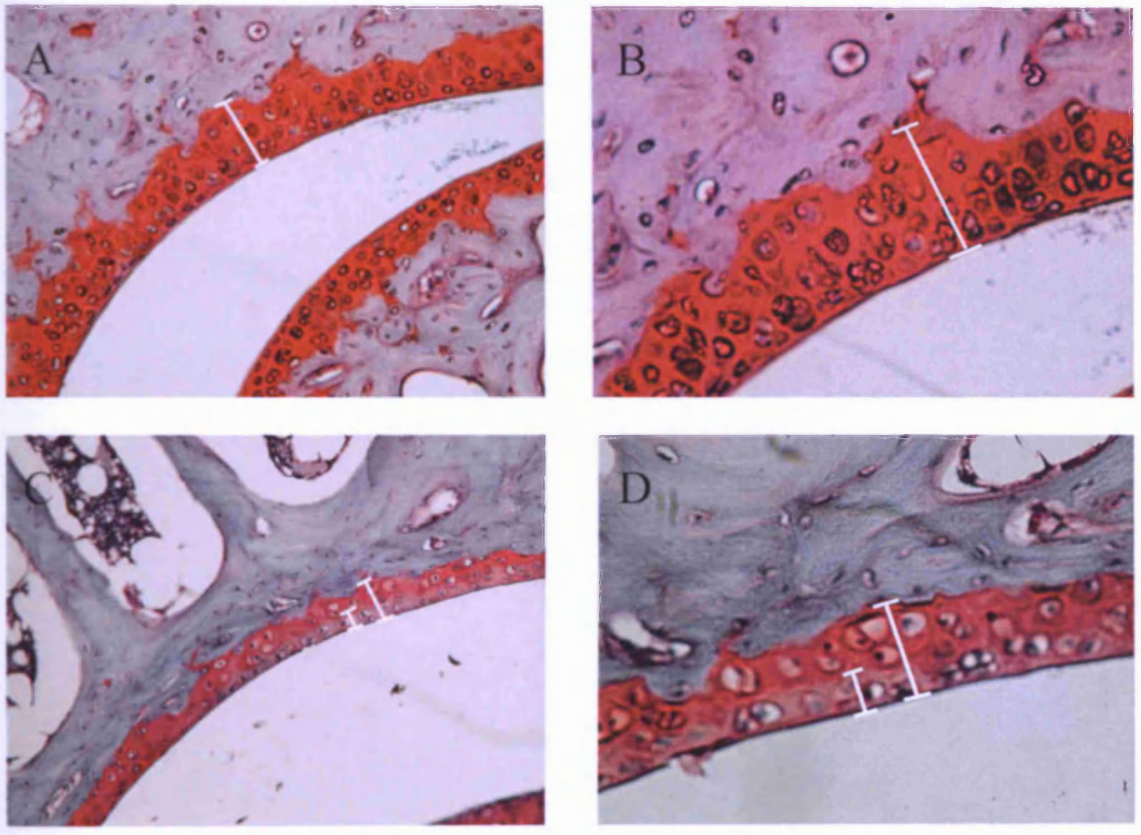

Figure 2.4. Safranin O and Fast Green Staining in Normal and mCIA Joints. A. Shows deep red staining of Safranin O in the cartilage of the tibia in a normal healthy joint. The white line indicates the depth of cartilage (x10 magnification). B. As A, at x20 magnification. C. Safranin O staining in a severely arthritic joint. The two lines indicate the original depth of cartilage, and the depth of depletion due to arthritis (at x10 magnification). D shows an example of this at a higher magnification (x20 magnification).

2.7 Protein Detection

2.7.1 Bradford Protein Assay

This method is a modified version of one developed by Bradford et al (Bradford 1976). This protein assay was performed using the Coomassie Plus (Bradford) protein assay kit (Thermoscientific). Two columns of Bovine Serum Albumin (BSA) (supplied) standards were set up with concentration limits of 10μg/ml to 0.3125μg/ml in a 96 well flat-bottomed plate. Standards and samples were diluted in 0.01M phosphate buffered saline (PBS) in a 1 in 100 dilution (total volume 200μl) in the top row of wells. All samples including the standard were run in duplicate. Standards and samples were diluted 1 in 2 by adding 100μl of protein dilution to the next well with 100μl PBS and mixing. This dilution was repeated 5 times down the plate with the last row of wells containing PBS only, thus behaving as a blank. 100μl of Coomassie Blue reagent was added to each well and allowed to react for 10 minutes before absorbance was measured using a spectrophotometer at a wave length of 595nm. A standard curve was plotted from the BSA results and the concentration of protein in the sample calculated from this.

2.7.2 ELISA

Paw specimens, serum and aortae were removed and treated as previously described in 2.3.

For all kits, experiments were carried out according to manufacturer's guidelines. Briefly all reagents were made as instructed and samples were thawed and diluted as appropriate. Plates came pre-coated with the primary antibody. 50μl of assay diluent and a further 50μl of standard, control or sample were added to each well. The plate was tapped to ensure thorough mixing before incubating for 2 hours at room temperature.

After this incubation period each well was aspirated and washed 3 times using the wash buffer provided. Excess liquid was removed from the wells by inverting and blotting against paper towels. 100μl of the mouse conjugate specific for the protein of interest was then added to the wells and left for 2 hours at room temperature before washing as before. The substrate solution was then added and the plate incubated in the dark at room temperature for 30 minutes. The stop solution was then added at a volume of 100μl and the plate was gently agitated to ensure full mixing. The optical density was measured at 450nm. A standard curve was plotted, and protein concentrations were calculated from this.

2.8 Statistical Analysis

The statistical analysis used to interpret data sets is discussed in more detail in each chapter. Briefly, in the case where two conditions are to be compared, the student's t-test was used to determine if the averages were significantly different. In the case of three or more data cohorts, a one-way ANOVA followed by Newman-Keuls was utilised.

It is important to note that in some experimental work, due to time constraints a small n-value was attained. Under these circumstances the experiments may not be sufficiently powered to adequately represent the sample mean, or to detect an actual difference between sample groups. In these cases more work is needed to determine this; the data was included in this thesis as a discussion point.

CHAPTER 3

OPTIMISING VASCULAR RESPONSES IN 8 – 10 WEEK OLD MALE DBA/1 MICE

3.1 Introduction

In order to measure functional changes to the vasculature in the mCIA model it was necessary to ensure that a reproducible "normal" model was established in DBA/1 mice for appropriate comparison. To do this, it was essential to perfect the technique of dissecting, cleaning and mounting the vessel on the myograph. Therefore in initial experiments vessels from C57BL/6 animals (surplus to requirement from other studies) were assessed. This was in-keeping with the principles of the "three R's" (reduction, re-use and refinement) as outlined in the Home Office Personal Licence guidelines, and had the additional benefit of being more financially viable. Once reproducible results had been attained with the C57BL/6 tissues, the technique would be repeated in the DBA/1 mice, and further optimised if necessary.

At the time of starting this work no measurements of isolated vascular function in the DBA/1 species, or in the mCIA model, were evident in the published scientific literature. While many such studies had been performed in other species and strains, varying responses were observed between them. Therefore it was deemed vital to optimise responses in DBA/1 animals in case they differed from the norm. At this point it was also decided that only male mice would be used for this study (for reasons outlined below).

3.1.1 Sex Differences

With respect to vessel function, differences have been observed between responses in tissue from male and female mice. In experiments conducted by Karanian et al (1996) male canine tissue appeared to be more reactive to constricting agents than that from female counterparts, resulting in a significantly larger constriction after exposure to the agonist (Karanian and Ramwell 1996). This was reiterated also in work done by Lamping et al (2001) who, whilst investigating serotonin-induced constrictions in male and female mice, saw a significantly larger response from the latter. Interestingly this was not echoed in the endothelium-dependent relaxations, with both sexes displaying similar responses (Lamping and Faraci 2001). This finding has been further supported in studies performed by Rubanyi et al (1997) who observed no difference in endothelial-mediated relaxation responses in aorta from both male and female mice (Rubanyi, Freay et al. 1997). Contrastingly however, studies by Huang et al (1998) and Kauser et al (1994) both showed a larger production of endothelium-derived NO in tissue from female compared to male mice. The resulting greater relaxation responses to ACh in the females was subsequently attributed to greater oestrogen production compared to males (Kauser and Rubanyi 1994; Huang, Sun et al. 1998). Interestingly oestrogen is now largely recognised as a protective molecule in the vasculature, exerting beneficial effects on endothelial cells by increasing their production of both NO and PGI_2 (Miller and Duckles 2008). For a review on the vascular actions of oestrogens see Miller and Duckles 2008. Furthermore, the finding that pre-menopausal women have a lower incidence of CVD compared with age-matched male counterparts and postmenopausal women also supports the role for oestrogen as a protective molecule, as the difference in incidence is attributed to the changes in the levels of this hormone between the three cohorts (Villar, Hobbs et al. 2008). See the introduction of Villar, Hobbs et al 2008 for further information regarding this.

Sex differences have also been observed in the successful induction of experimental arthritis. For instance male mice are more susceptible than female mice to mCIA, the increased oestrogens of the females seemingly preventing/suppressing the disease (Holmdahl, Jansson et al. 1986), why this is the reverse to the situation in human disease is unknown and thus open to speculation. In order to control for such variation it was decided that male mice would be used throughout this thesis.

In addition to differences observed between sexes, inter-species variation is also common and can affect expected outcomes with respect to experimental work. A relevant example of this is the elevated level of acetylcholinesterase observed in the DBA mouse strain versus C57BL/6 mice (discussed in section 3.1.2).

3.1.2 Acetylcholinesterase

Acetylcholinesterase (AChE) cleaves the neurotransmitter ACh, commonly found at synapse junctions, to produce choline and acetic acid (Rao, Swamy et al. 1991; Sussman, Harel et al. 1991). With regard to vascular biology ACh is commonly used to elicit endothelium-dependent relaxation in isolated blood vessels (see sections 1.4.3 and 2.4). It has been reported that levels of AChE can vary between species of mice, and in particular higher levels have been noted in DBA/1 animals compared to C57BL/6 mice (Schwab, Bruckner et al. 1990). Due to the lack of information in the literature regarding AChE levels in isolated tissues, it was unclear whether this enzyme could interfere with vessel relaxation during an ACh concentration response experiment. If the enzyme was upregulated in the vessels it could cleave ACh prior to it inducing vasorelaxation, and as such, falsely suggest endothelial dysfunction. In order to overcome this problem, whilst assessing the initial vessel function, carbachol (CC) was also used as a comparator. This is a drug that binds and activates muscarinic receptors in the same manner as ACh, but is resistant to degradation by AChE (Foster 1986; Streichert and Sargent 1992).

3.1.3 Common Vasoactive Agents

Vasoconstrictors commonly used in myography are the alpha adrenoceptor agonists phenylepherine (PE) and noradrenaline (NA), with ACh being a common vasodilator Along with serotonin (5-HT) these agents (see table 3.1.) were chosen to initially characterise responses in isolated vascular tissue from DBA/1 mice before deciding on appropriate agonists for subsequent studies. All vasoconstrictors in this table function by interacting with specific receptors on the VSMC triggering a downstream signalling cascade resulting in increased intercellular Ca^{2+} levels and subsequent vasoconstriction (see 1.4.2). The relaxing agents behave by increasing the formation of the Ca^{2+}/CaM levels resulting in stimulation of eNOS and thus production of the vasodilator NO (see 1.4.3).

AGONIST	RECEPTOR	MODE OF ACTION	EXPECTED RESULT
Phenylepherine	Alpha-adreno receptor α_1 on SMCs	PLC, IP3, DAG as secondary messengers	Constriction
Noradrenaline	Adrenoreceptors α_1 α_2 on SMCs	PLC – IP3, DAG as secondary messengers	Constriction
5-HT	$5HT_{1B}$ receptors on SMCs	Increases intracellular Ca^{2+}	Constriction
Acetylcholine	M_3 Receptors on endothelial cells	Activates eNOS	Relaxation
Carbachol	M_3 Receptors on endothelial cells	Activates eNOS	Relaxation

Table 3.1. Agonists and Expected Responses in the Vasculature. Vasoactive agents to be tested in the DBA/1 mice, their mode of action and the expected result. m3 is the muscarinic 3 receptor.

3.2 Aims

Optimise responses in C57BL/6 animals to ensure correct dissection/myography technique and obtain reproducible constriction and relaxation responses.

Establish a suitable method with appropriate vasoactive agents to obtain reproducible "normal" vascular responses in 8-10 week old male DBA/1 mice.

3.3 Experimental Materials and Methods

3.3.1 Mice

An in-house strain of C57BL/6 male mice aged 10-12 weeks were used for preliminary experimentation. DBA/1 male mice aged 8-10 weeks were used for subsequent determination of "normal" vascular function. For detail see section 2.1.

3.3.2 Collection of experimental Tissue

Aortic tissue was collected from both strains of animal as described in section 2.3.2i.

3.3.3 Studies of Aortic Function using the Multi Myograph.

Aortae from both C57BL/6 and DBA/1 mice were mounted on a myograph and responses to the vasoactive agents outlined in table 3.1 were measured as described in section 2.4. In order to assess duplicate responses with the same vessel, concentration responses were, on occasion, repeated. For duplicate responses, baths were washed out 8 times with fresh Krebs buffer following a constriction/relaxation response, and the tissues left to rest for 20 minutes before repeating the appropriate response.

3.3.2 Measurement of Constriction and Relaxation Function

3.3.2.1 Establishing Responses in C57BL/6 Mice

The vasoactive agents PE and ACh were used to measure preliminary constriction and relaxation responses respectively in tissues from male C57BL/6 mice. A baseline tension of 15mN as outlined in (Cohen, Weisbrod et al. 1999; Horvath, Orsy et al. 2005) was set manually, in order to mimic the mean arterial pressure that would be found *in vivo*, and the protocol outlined in section 2.4 then followed.

3.3.2.2 Establishing Responses in DBA/1 Mice.

The vasoconstrictors PE, NA and 5HT were used on separate occasions to assess constriction responses in DBA/1 male mice. To determine the most efficient relaxing agent, relaxation responses to increasing concentrations of either ACh or CC were assessed in tissues pre-constricted with the appropriate agent to 70-80% of the previous maximum. Initial experiments were carried out using PE following the establishment of a 15mN baseline tension set. However, it was immediately apparent that the vessel size in the DBA/1 strain was approximately 15% smaller (estimated) than the C57BL/6 animals. Following an abnormal first response to PE (see section 3.4.2.1) and due to the smaller size of the DBA/1 mice/vessels compared to C57BL/6 animals, it was deemed necessary to decrease the baseline tension. Following this, observational preliminary experiments were carried out in these vessels investigating a range of length-tension relationships. There was no available information in the literature regarding this technique in DBA/1 animals and subsequently the results of experiments involving varying baseline tensions deduced that 5mN was an appropriate level of tension for this work. Methods using a baseline tension of 5mN have been previously documented in experimental work performed in mouse aortae (Judkins, Sobey et al. 2006; Zemse, Hilgers et al. 2007).

3.4 Results

3.4.1 Responses in C57/BL6 Mice

Concentration responses to PE and ACh were utilised to measure constriction and relaxation responses respectively in the aortae of male C57BL/6 mice aged 10-12 weeks in order to obtain reproducible results. Vessels responded well, constricting to a maximum tension of ~20mN (~5mN developed tension) and relaxing to ~90% of the previously induced maximum (see figure 3.1). These results were reproducible and as such the method was repeated in the DBA/1 strain.

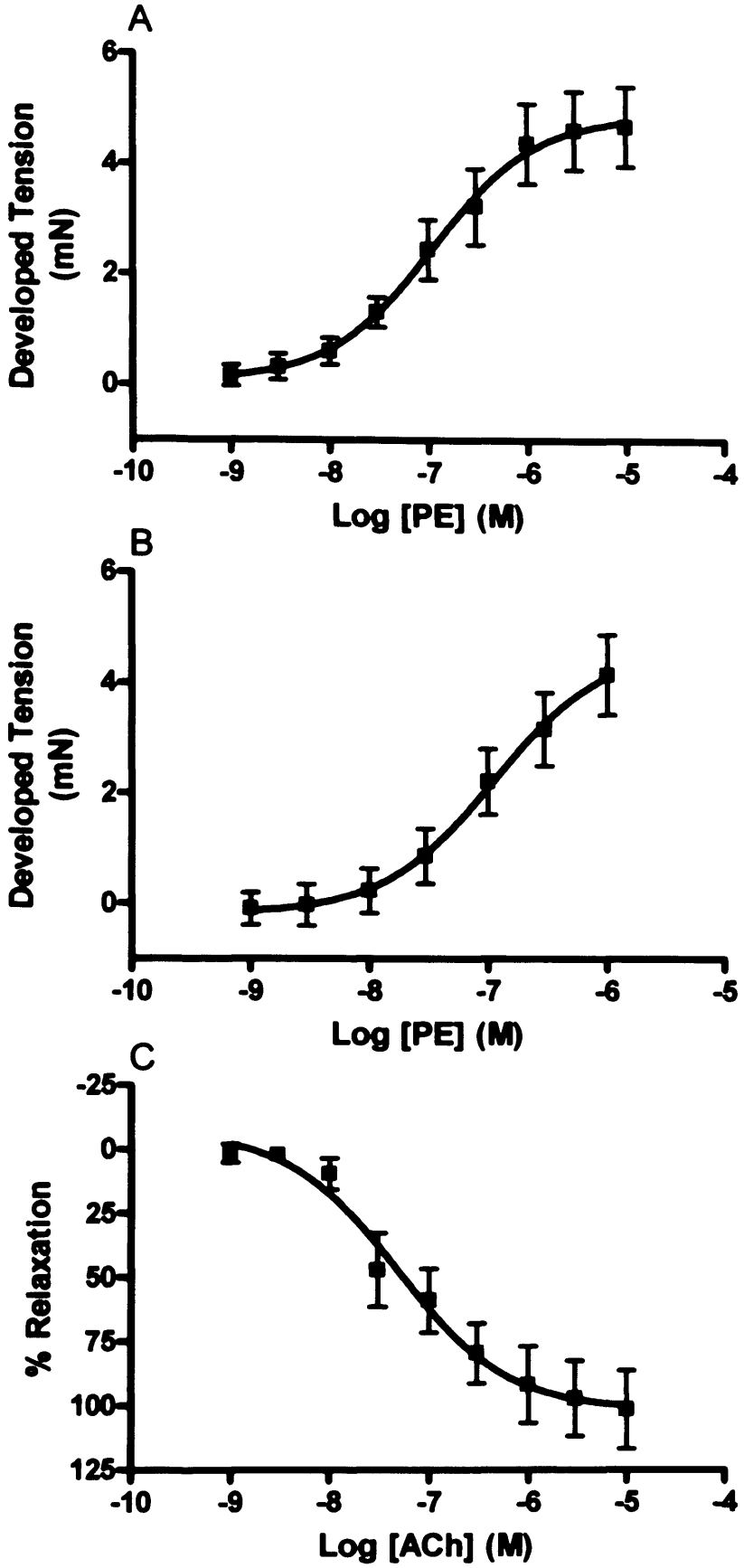

Figure 3.1. Vascular Responses in the Aorta of C57BL/6 Male Mice to PE and ACh. A. Maximum constriction response to the vasoconstrictor PE. B. Responses to the vasoconstrictor PE to 70-80% of maximum response. C. Response to vasodilator ACh following induced constriction of 70-80% of maximum (n=4).

3.4.2 Vascular Responses in DBA/1 Mice

3.4.2.1 Phenylepherine

Responses to PE were measured in the aortae of male DBA/1 mice aged 8-10 weeks. After the initial constriction tissues were washed x8 and left to rest. During this resting period vessels reconstricted to above the initial baseline tension. Vessels were washed again in an attempt to return the tension to baseline, however this could not be resumed (see figure 3.2).

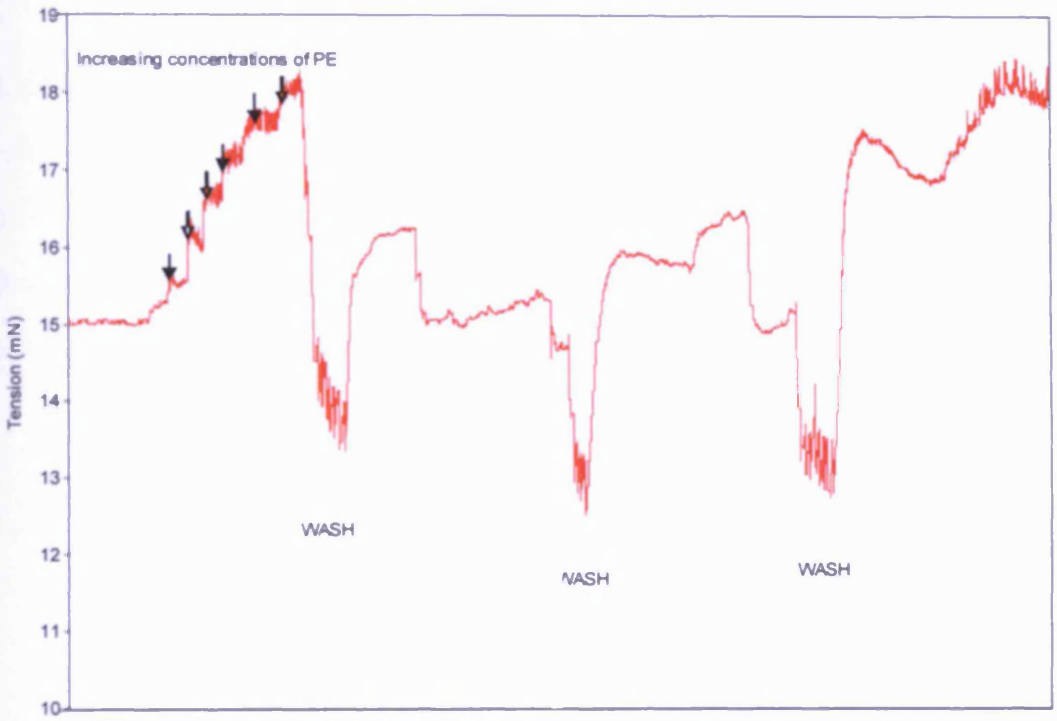

Figure 3.2. Vascular Responses in the Aorta of DBA/1 Male Mice to PE. PE was used to constrict the aorta at increasing half log increments using concentrations of 10-9M to 3e10-5M (arrow heads). After maximum constriction was reached, vessels were washed x8 to return to baseline (wash). Vessels did not return to baseline and re-constricted without presence of agonist after multiple washes.

3.4.2.2 Responses in DBA/1 mice to the Vasoconstrictor NA.

Due to the abnormal response of the DBA/1 vessels to PE, an alternative vasoconstrictor was assessed. In this instance responses were measured in the aortae of male DBA/1 mice aged 8-10 weeks to NA after a baseline tension of 5mN was manually set. The maximum constriction reached was not very large and to test the reproducibility of these responses the 70-80% responses were repeated several times. The vessels appeared to

become desensitized to the agonist, with each subsequent exposure resulting in a slightly smaller constriction (see figure 3.3).

3.4.2.3 Responses in DBA/1 mice to the Vasoconstrictor 5HT.

Responses were measured in the aortae of male DBA/1 mice aged 8-10 weeks to the vasoconstrictor 5HT. Prior to the constrictions the baseline was manually set to 5mN. This agonist elicited a large contraction that was found to be reproducible after numerous exposures (see figure 3.4).

3.4.2.4 Relaxation responses in DBA/1 Mice.

Responses were measured in the aortae of male DBA/1 mice aged 8-10 weeks to the relaxing agents CC and ACh after pre-constriction to 70-80% of the maximum by 5HT. Relaxation responses to CC were significantly smaller than those to ACh ($p<0.05$) and more variable (see figure 3.5).

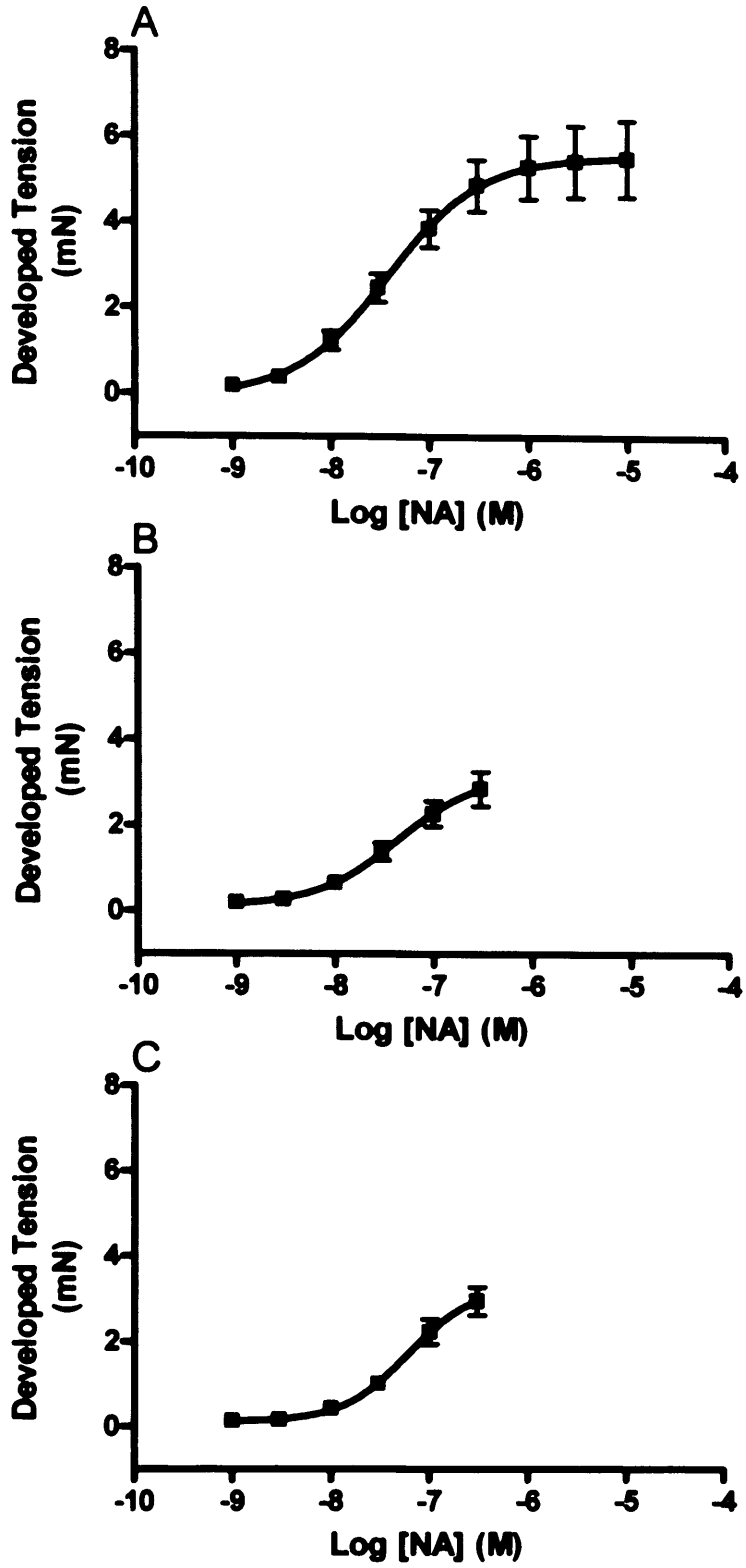

Figure 3.3. Vascular Responses in the Aorta of DBA/1 Male Mice to NA. A. The initial exposure to all concentrations of NA reaching their maximum constriction. B, C. Consecutive responses to NA to a concentration of 3e10-7M to reach ~70-80% of the previous maximum. (n=5).

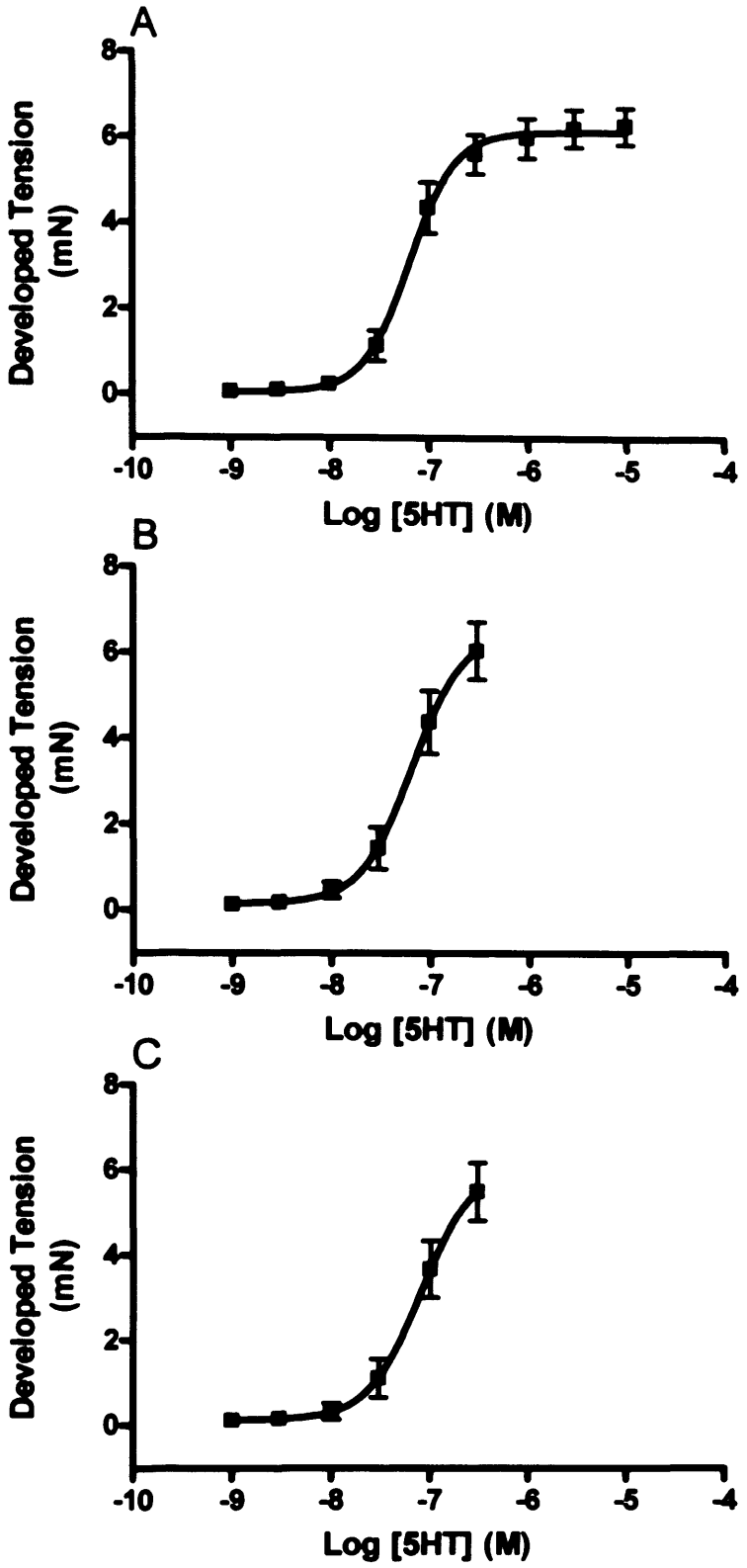

Figure 3.4. Vascular Responses in the Aorta of DBA/1 Male Mice to 5HT. A, Exposure to 5HT showing the maximum constriction reached. B and C show repeat responses to a stepwise concentration response of 5HT reaching 70-80% of the maximum (n=5).

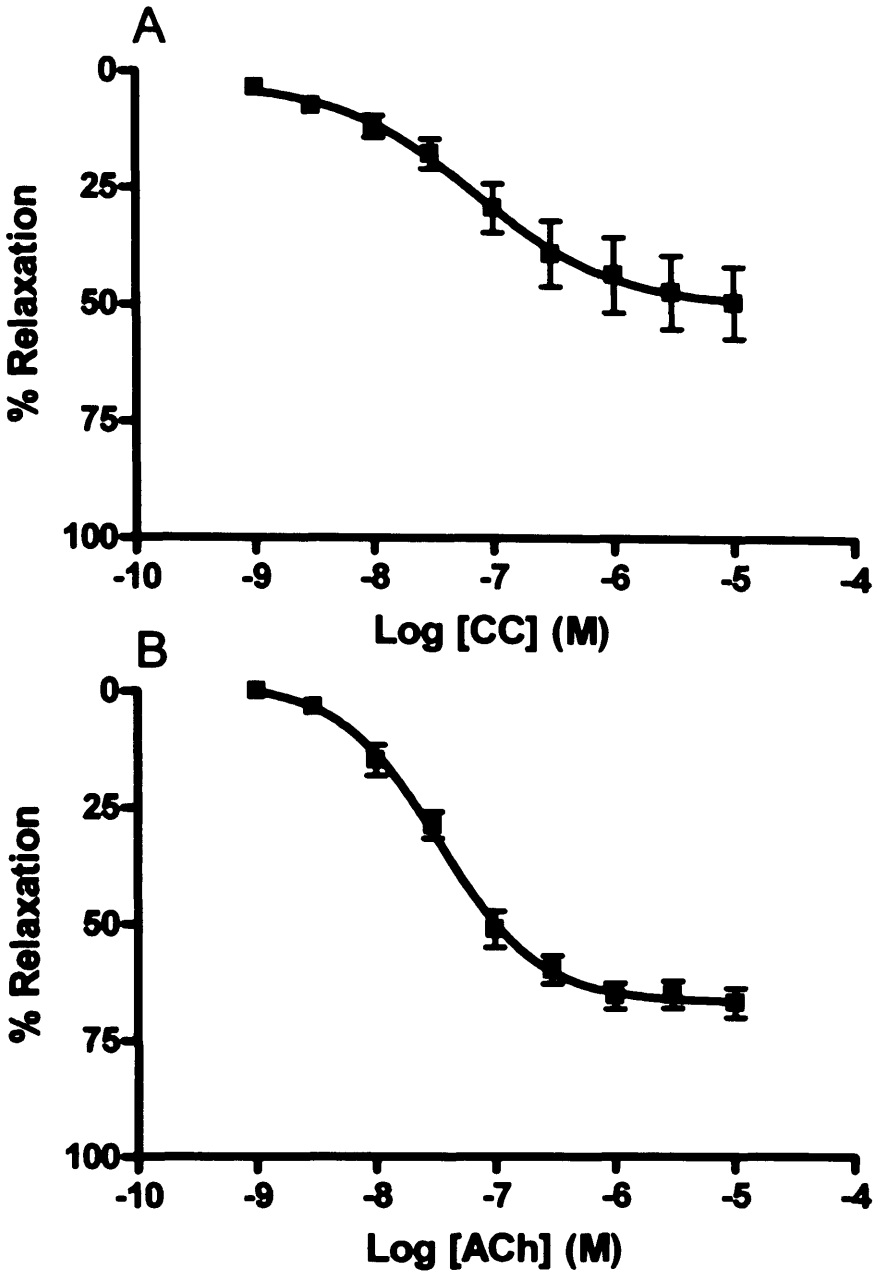

Figure 3.5. Vascular Responses in the Aorta of DBA/1 Male Mice to ACh. Responses to (A) CC and (B) ACh. Maximum relaxation values (Rmax) from each curve are significantly different as determined by students T-test ($p<0.05$, $n=5$).

3.4.3 Summary of Agonists.

Table 3.2 shows a summary of agonists tested and the responses achieved in the aorta from the DBA/1 animals.

AGONIST	RESULT IN DBA/1 TISSUE
Phenylepherine	Vessels contracted however the effect of the agonist could not be removed by washing and baseline tension could not be resumed.
Noradrenaline	Vessels contracted however repeat exposure caused desensitisation and contractions were quite small.
5-HT*	Vessels contracted and with reproducible results.
Acetylcholine*	Vessels relaxed
Carbachol	Vessels relaxed

Table 3.2. Table of Agonists Tested and Observed Results. * Denotes the agonists chosen for further work.

3.5 Discussion

3.5.1 Vessel Constriction

Responses to PE/ACh in C57BL/6 animals have been previously characterised and are well documented in the scientific literature. As such, results obtained from these experiments were to behave as a comparator for confirming correct technique. However when it came to reproducing the responses observed in the C57BL/6 mice in the DBA/1 strain the results differed.

PE appeared to have a high affinity for the receptors on the smooth muscle of the animals resisting removal by washing, for which there was no obvious explanation in the literature. A "one off" prasozin experiment was carried out, whereby the alpha adrenoreceptor blocker was added to the tissue (at 10^{-6}M) following PE-stimulated contraction. This effectively removed the effects of PE showing that binding was not entirely irreversible but as a result of this adverse response this agonist was deemed unsuitable for further work in the DBA/1 strain. Further investigations into the mechanisms behind this are outside the scope of this project.

Similarly, NA was considered unsuitable due to the decreased sensitivity exhibited by the vessels following repeat exposure. The initial constrictions were not very high and the gradual diminishment of them over time made the agonist an unfavourable one. The increased insensitivity could be to do with the receptor function, they could become dysfunctional after repeat exposure, or they could be internalised or degraded after stimulation. Interestingly with respect to this it has been observed that in the rat, following long term (6 days) *in vivo* infusion with NA, the receptor becomes desensitised exhibiting a decreased constriction (Seasholtz, Gurdal et al. 1997) however the instant effect of NA has not been investigated. Similarly after exposure there could be an upregulation in proteases capable of inhibiting NA function. Alternatively there could be fewer NA receptors found in the VSMCs than for example the 5HT receptors resulting in the smaller constriction exhibited here. However, as nothing is known about the distribution or expression of these receptors in the vessels from the DBA/1 strain, these are hypothetical suggestions, and investigating this further is again outside the scope of the project.

5HT produced non-variable large constrictions with each repeated concentration response and these were reproducible for at least four concurrent exposures. As a result of this, 5HT has been chosen as the appropriate agonist for measuring vascular function.

Three different responses were obtained with respect to each of the vasoconstrictors tested in these vessels, which could be in part due to the difference in their mode of action. The three agonists investigated here all elicit VSMC constriction, but do so via different receptors, and thus vary in their downstream signalling cascade (see figure 3.6). NA, a catecholamine, exerts effects via the α and β adrenoceptor subtypes, either activating PLC or inhibiting adenylate cyclase resulting in constriction (α_1 and α_2 subtypes respectively). PE is a selective α_1 antagonist and thus constricts smooth muscle by means of the PLC pathway via the increase of the intracellular secondary messengers IP_3 and DAG. 5HT contrastingly interacts with $5HT_{2A}$ receptors on the VSMCs, also

stimulating constriction in this manner. These receptors in the VSMCs of the DBA/1 strain have not been characterised and as such, differential expression/distributions of these may provide explanation for the difference in the observed responses. Alternatively the different downstream signalling initiated by NA could explain the difference in constriction observed between the small NA-induced constriction, and the significantly larger PE- and 5HT-induced constrictions.

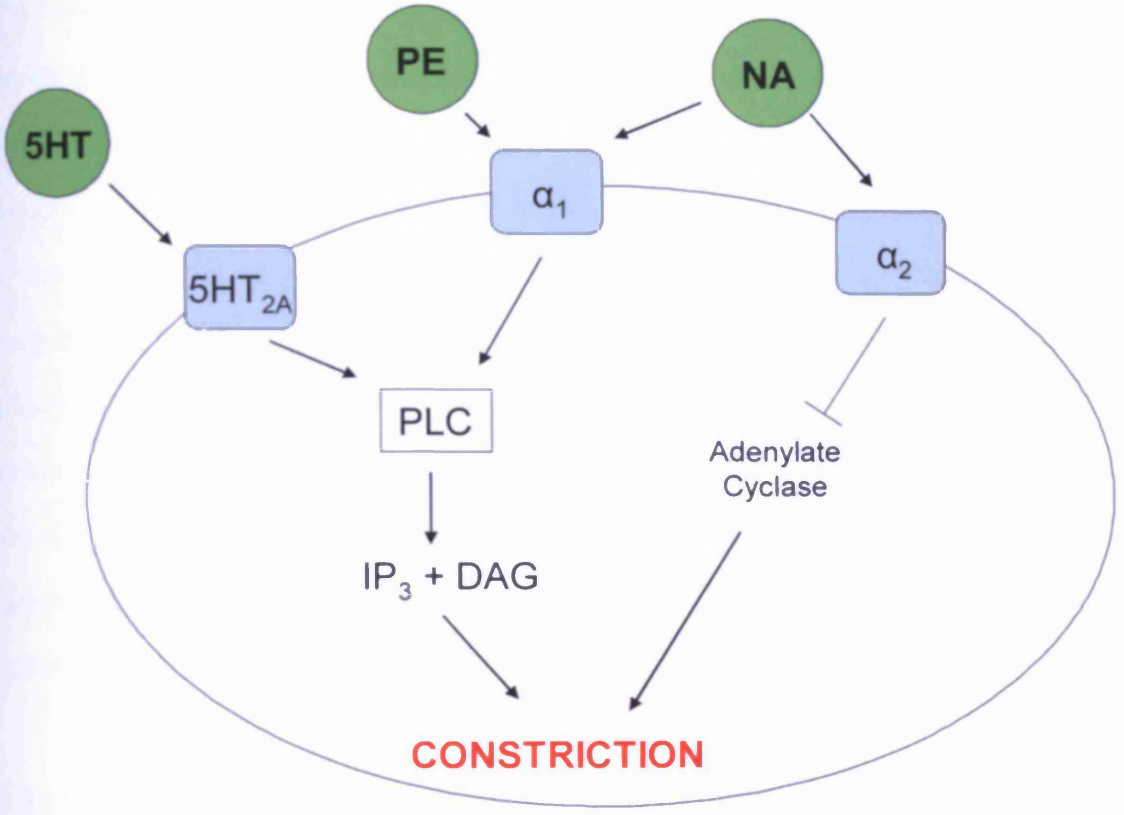

Figure 3.6. Pathways Involved in VSMC Constriction. Diagram showing the different receptors and pathways via which 5HT, NA and PE exert VSMC constriction

3.5.2 Vessel Relaxation

Relaxation responses to both ACh and CC in the DBA/1 animals were smaller than those observed in the C57BL/6 animals. This may suggest that the reported (Schwab, Bruckner et al. 1990) higher activity of AChE in the DBA/1 does have an effect on relaxation responses to these agents. However, the observation that ACh-induced

stimulating constriction in this manner. These receptors in the VSMCs of the DBA/1 strain have not been characterised and as such, differential expression/distributions of these may provide explanation for the difference in the observed responses. Alternatively the different downstream signalling initiated by NA could explain the difference in constriction observed between the small NA-induced constriction, and the significantly larger PE- and 5HT-induced constrictions.

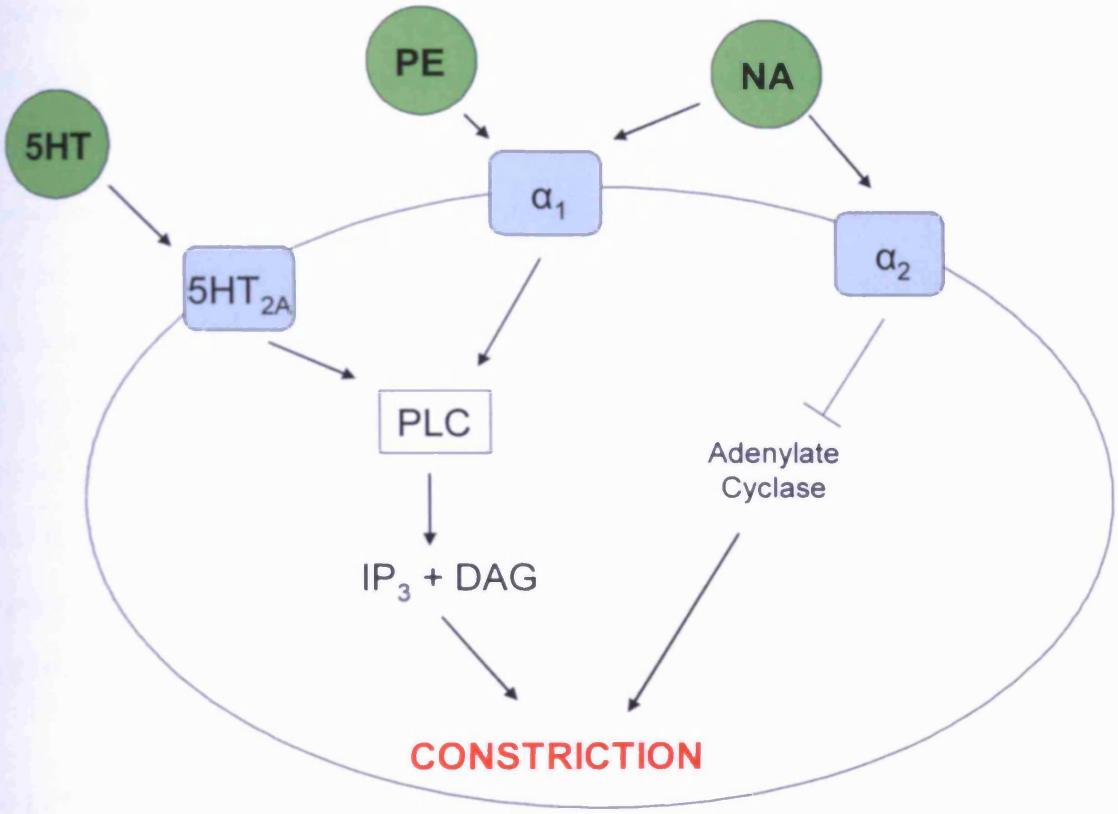

Figure 3.6. Pathways Involved in VSMC Constriction. Diagram showing the different receptors and pathways via which 5HT, NA and PE exert VSMC constriction

3.5.2 Vessel Relaxation

Relaxation responses to both ACh and CC in the DBA/1 animals were smaller than those observed in the C57BL/6 animals. This may suggest that the reported (Schwab, Bruckner et al. 1990) higher activity of AChE in the DBA/1 does have an effect on relaxation responses to these agents. However, the observation that ACh-induced

responses were greater than those achieved by CC (an agent that is resistant to AChE-induced hydrolysis) would argue against such an action. Moreover, this difference in responses to ACh and CC is not a novel finding, having been previously noted in studies by Walch et al. This group reported that in human pulmonary vessels, CC was a less potent agonist for binding and activating muscarinic receptors than ACh (Walch, Taisne et al. 1997).

Muscarinic receptors are G-protein coupled receptors and 5 subtypes (M_1- M_5) exist, of which three (M_1 – M_3) are well characterised. Stimulation of the receptors M_1, M_3 and M_5 activate the IP_3 pathway; M_2 and M_4 activate inhibition of AC and a subsequent reduction in intracellular Ca^{2+}. The role of the M_3 receptor, to which ACh and CC bind in the vasculature is excitatory however on the endothelial cells the end result is production of NO and subsequent vasodilation (Dale M. M 2004). That a limited selectivity of CC for certain muscarinic receptor subtypes has been reported (Walch, Taisne et al. 1997), may provide explanation for the varying responses elicited to ACh and CC in DBA/1 animals. However as the expression and distribution of the M_3 receptor has not been characterised in this strain there is no certainty for this explanation, and as such, is merely speculative.

It is possible therefore that the distribution of these receptors and their susceptibility to activation by these agents is different in DBA/1 mice compared to others. However, given the working hypothesis of this thesis and the fact that ACh elicited substantial and reproducible relaxation responses rendered further intricate pharmacological dissection of this issue a fool's errand. As such, ACh was used in all future experiments to assess endothelial function.

There are some very obvious differences observed in these animals compared to well documented results across the literature for the more commonly used C57BL/6 strain. Unfortunately the complete vascular phenotype of the DBA/1 animals is not defined, and to attempt to do so in order to validate and understand these results would be a

lengthy and time consuming process. For the purposes of this thesis and within this chapter the normal vessel function of male DBA/1 animals has been elucidated and optimal agonists and conditions to asses this confirmed. The next question to address is whether successful induction of mCIA in these animals leads to subsequent changes in vascular function. This will be assessed utilising the methodology determined in this chapter and using vessels taken from animals at various stages of the disease.

CHAPTER 4

VASCULAR AND HISTOLOGICAL CHARACTERISATION OF AN EXPERIMENTAL MODEL OF ARTHRITIS

4.1 Introduction

In Chapter One the large body of information regarding the role of endothelial dysfunction in the progression of human RA was summarised, and the main mechanisms discussed. It is widely suggested that the inflammation characteristic of RA, and once thought to simply affect the joints, becomes systemic and exerts damaging effects at the vessel wall. The consequence of the systemic inflammatory insult to the endothelium during RA is the development of endothelial dysfunction (see figure 1.7) (Sattar and McInnes 2005; Libby 2008). This evidence provides the reasoning behind the hypothesis that endothelial function will be compromised in the mCIA model.

4.1.1 Vascular Function in Experimental Arthritis

There is no documentation within the scientific literature outlining the effect of mCIA on vascular function. However in an alternative model, the adjuvant-induced arthritis (AdA) model (Henderson B 1995), endothelial dysfunction has been investigated in some depth (see below). Similar to mCIA, AdA is a T cell-dependent disease that shares some features of human RA; swelling of the paws, cartilage degradation (although to a lesser degree than mCIA and human disease), loss of joint function and inflammatory cell infiltration in the joints (Hegen, Keith et al. 2008).

Using the rat AdA model, Can et al (2002) investigated the presence of endothelial dysfunction by examining endothelium-dependent and -independent relaxations in the isolated thoracic aorta. This study demonstrated that endothelium-dependent relaxation was diminished in arthritic animals, and that this impairment was inhibited by the

antioxidant vitamin E, indicating a role for oxidative stress in the development of endothelial dysfunction in this model. Endothelium-independent relaxation remained unchanged (Can, Cinar et al. 2002) implying dysfunction at the endothelial but not vascular smooth muscle level. Further studies have observed endothelial dysfunction in this model to be associated with an increase in eNOS protein levels, ROS production and a decrease in levels of BH_4 (the essential eNOS co-factor), again suggesting a role for oxidative stress (Haruna, Morita et al. 2006). That treatment with BH_4 prevented the endothelial dysfunction, indicates that the latter could be the result of eNOS "uncoupling" in this model (Haruna, Morita et al. 2006) (see 1.5.3). Further support for a role for oxidative stress comes from observations of increased serum peroxynitrite, iNOS, eNOS and NO metabolites accompanying diminished relaxation responses in this pathology (Nozaki, Goto et al. 2007). Interestingly administration of fluvastatin (a cholesterol-lowering statin with pleiotropic anti-inflammatory effects (Ray and Cannon 2004)) in this model has positive effects on the vasculature, improving endothelium-dependent relaxation, increasing serum BH_4 levels and decreasing levels of oxidative stress markers (Haruna, Morita et al. 2007). That no such studies have been reported in the mCIA model suggests that further research in this more accurate model regarding the systemic effects of RA, is warranted.

In human RA it has been suggested that the development of an imbalance between ROS (normally produced as part of cell metabolism and protection) production and the antioxidant behaviour of the cells contributes to vascular pathology. Indeed, low circulating levels of antioxidants have been implicated in the development of RA in previously healthy patients (Filippin, Vercelino et al. 2008). Additionally there is evidence within the literature that oxidative stress plays a role in the development of CVD in RA. To this end inflammatory mediators produced at the synovial membrane are postulated to become systemic and produce a 'pro-atherogenic profile' in the patients. Consequently an increase in oxidative stress, as demonstrated by a higher level of ROS and impaired anti-oxidant activity (Ku, Imboden et al. 2009), leads to damage at the vessel wall. Importantly, whatever the mechanisms responsible for vascular

dysfunction in RA, it would seem that this process is multifactorial and complex. Indeed it is possible that the dysfunction may not only involve the endothelium given that changes in vascular smooth muscle structure/function are implicated in other vascular pathologies such as hypertension, arterial stiffness, atherosclerosis and aneurysm formation to name but a few.

With regard to AdA, while an increase in vascular smooth muscle contractility has recently been reported (Nozaki, Goto et al. 2007), rather contrastingly a previous study observed no change in contractility in this model compared to control animals (Fontaine, Herchuelz et al. 1984). That this information is conflicting and that no such studies in the mCIA model have been reported, again suggests that further research in this area is essential.

4.1.2 Histological Assessment of Arthritis.

As explained in Chapter One there are many changes occurring in the joint throughout the induction of experimental arthritis starting with a rapid infiltration of inflammatory cells in to the bone and culminating with cartilage and bone destruction. This also occurs in the human disease and can be seen through histological assessment.

To confirm successful induction of mCIA, clinical assessment of experimental arthritis is necessary. Paws should be scored routinely to determine the amount of swelling and redness (erythema) at any given time (see section 2.2 for examples of the clinical signs of experimental arthritis). Additionally histological assessment is necessary to assess the architectural changes to the joint; synovial inflammation, cartilage degeneration and erosion of bone are particularly useful measurements which are relevant to RA.

4.2 Aims

To induce mCIA in 8-10 week old male DBA/1 mice.

To determine the effect of mCIA on vascular function.

4.3 Method

4.3.1 Mice

Male DBA/1 mice aged 8-10 weeks were purchased (Harlan Laboratories) and housed according to section 2.1.

4.3.2 Induction of mCIA

Experimental arthritis was induced in DBA/1 mice and subsequently assessed according to the clinical scoring criteria described in section 2.2.

4.3.3 Collection of Experimental Samples

At appropriate time points (see section 2.2) animals were euthanised as described in section 2.1. Subsequently the thoracic aortae and paws were harvested as described in sections 2.3.2i and 2.3.2ii respectively.

4.3.4 H & E Staining.

7μm Sections from a representative sample of paw joints were stained with H & E for assessment of inflammation according to the method and criteria described in section 2.6.1. Scores for each paw from either the mild, moderate or severe cohort are expressed as the mean ± SEM. The criteria outlined in table 4.1 are based on previous studies in our laboratory (Bull, Williams et al. 2008). Synovial hyperplasia is assessed by the level of thickening at the synovial membrane. Normally one layer of cells thick, an increase in depth is observed as inflammation progresses. Infiltration is judged by the volume of infiltrating inflammatory cells into the joint itself, and is measured in the extracellular space by the talus and tibia joint. This is scored on a scale of 1-5 with increasing cell numbers/visible area of joint with inflammatory cells present. Bone and cartilage erosion can be observed by the attachment of inflammatory cells to the surface of the bone, slight pitting of the bone surface and subsequent apparent infiltration of

inflammatory cells into the bone. Finally cellular exudate is assessed by the presence of inflammatory cells infiltrating the normally acellular joint space between articular ends of the talus and tibia cells in the synovial space. For familiarisation purposes, initial scoring was carried out by two people. Subsequently this process was performed by the author of this thesis, though frequent checks were carried out by an experienced and independent observer to ensure consistent and impartial assessments were being made.

Scoring Criteria	Description	Score Scale
Synovial Hyperplasia	**Thickening of the synovial membrane surrounding the synovial capsule**	**0 - 3**
Infiltrate	**The volume of infiltrating cells in the surrounding tissue**	**0 - 5**
Cartilage Depletion and Bone Erosion	**The amount of cartilage and bone eroded by the infiltrating cells**	**0 – 3**
Exudate	**The amount of cells infiltrating into the joint space**	**0 - 3**

Table 4.1. Criteria for Scoring H & E Stained Paws.

4.3.5 Safranin O and Fast Green Staining

In order to assess pathological changes to the ankle joint, sections from the hind paws of normal animals and those with experimental mCIA were stained with safranin O and fast green. Cartilage depletion was then assessed histologically as described in 2.6.2. Results are expressed as the mean distance (μm) of cartilage depleted ± SEM.

4.3.6 Study of Isolated Vascular Function in the mCIA model

At appropriate time points aortae were removed from normal and arthritic mice and prepared for myography as described in section 2.3.2i. Responses were measured as described in section 2.4.

4.3.6.1 Vasoconstriction

Tissues were initially depolarised by exposure to $6x10^{-2}M$ K^+ for 5 minutes. Following washing and re-establishment of baseline tension the agonist 5HT was used for assessment of vasoconstriction as described in section 2.4.

4.3.6.2 Endothelium-Dependent Relaxation

Experiments to assess endothelium-dependent relaxation followed the protocol as described in section 2.4. Briefly, isolated vessels were first exposed to increasing concentrations of 5HT ($10^{-9}M$ to $10^{-5}M$) and a maximum constriction response obtained. Following washout they were re-constricted to 70-80% of their previous maximum before being exposed to increasing concentrations of ACh ($10^{-9}M$ to $10^{-5}M$) to assess endothelium-dependent relaxation. Following washing and appropriate reconstriction, endothelium-independent relaxation was assessed by exposing the tissues to increasing concentrations of the NO donor sodium nitroprusside (SNP, $10^{-9}M$ to $10^{-5}M$) (S0501, Sigma Aldrich).

4.3.7 Statistical Analysis

4.3.7.1 Histology

H & E stained sections of arthritic paws were scored and the results described as mean ± SEM for each criteria. To assess cartilage degradation the original depth and depth of depletion were measured at five points on the end of the bone and expressed as percentage depleted mean ± SEM, and compared using the one way analysis of variance (ANOVA) and subsequent Student Newman-Keuls multiple range test.

4.3.7.2 Isometric Tension Recording

All data are expressed as mean ± SEM. Constriction responses to K^+ and 5HT are expressed as developed tension in mN. Peak at 5 minute K^+-induced constrictions and Rmax (maximum response) and EC50 (concentration to produce 50% of maximum

response) values for responses to 5HT are compared by one way ANOVA followed by Student Newman-Keuls multiple range test. Relaxation responses to either ACh or SNP are expressed as a percentage of the appropriate 5HT-induced constriction. All concentration response data was first fitted to sigmoid curves using GraphPad Prism software and resulting EC50 and Rmax values then compared by ANOVA followed by Student Newman-Keuls multiple range test. Differences were considered significant where $p<0.05$.

4.4 Results

4.4.1 Arthritis Induction and Progression of the Disease

In all mice used in this thesis there was 100% incidence of mCIA. To assess disease progression of mCIA, paws were measured/clinically scored with regard to the criteria outlined in section 2.2. Figure 4.1 illustrates the timeline of arthritis development, the animals having been banded in three distinct groups of mild, moderate and severe according to their total paw score as appropriate (see section 2.2). For normal animals there were no physical changes to their paws (data not shown). Mild arthritis was evident around days 24 – 28, moderate arthritis was reached around days 28 – 32, and severe arthritis at around day 29/30 – 35.

It is important to note that arthritis progressed differently in each animal, and as such there are limitations of the scoring criteria. The existence of a "grey area" between the days of disease onset and a possible overlap between the severities is impossible to avoid. This can be seen in figure 4.1A; a minority of animals reached "moderate" on days 34 and 35. Despite this, the utmost care was taken to be consistent in the approach to scoring and in doing so minimise such issues.

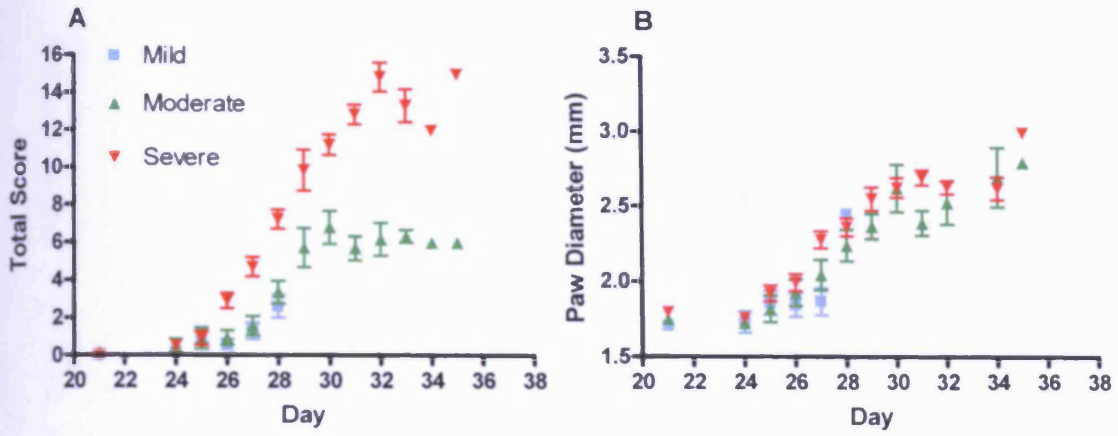

Figure 4.1. Arthritic Progression in mCIA. A. Progression of arthritis in animals scoring an overall severity of mild (blue) (n=17), moderate (green) (n=19) and severe (red) (n=19) arthritis. B. The increase in paw diameter thickness as disease progresses from mild (n=17), to moderate (n=19) and severe (n=24) arthritis. Mild n=, moderate n=, severe n= n ≥ 17

4.4.2. Histological analysis

4.4.2.1 H & E Staining

Sections taken from the appropriately diseased paws were stained with H & E. Histological assessment of each section was performed; four pathological features were scored namely: synovial hyperplasia, infiltration of inflammatory cells/fibroblasts into the joint, the level of exudate in the joint space and bone and cartilage degradation (see table 4.1).

Following H & E staining figure 4.2 outlines the areas of inflammatory arthritis within the paw that are scored as described in table 4.1. The clinical progression of arthritis from normal to mild, moderate and severe was reflected in the histological changes within the inflamed paw and the subsequent scores. A significant thickening of the synovial membrane in the joints of animals was observed with increasing disease severity (fig 4.2A). This progressive change was accompanied by a large influx of inflammatory cells (fig 4.2B), an increase in the level of exudate evident in the joint space (fig 4.2C), and extensive cartilage and bone damage (fig 4.2D). Unfortunately due to poor resolution the exact cell type can not be determined by the photos. It was presumed that these cells would be a mixture of macrophages, neutrophils, T-cells and fibroblasts. The scores and differences between severities are shown in figure 4.3.

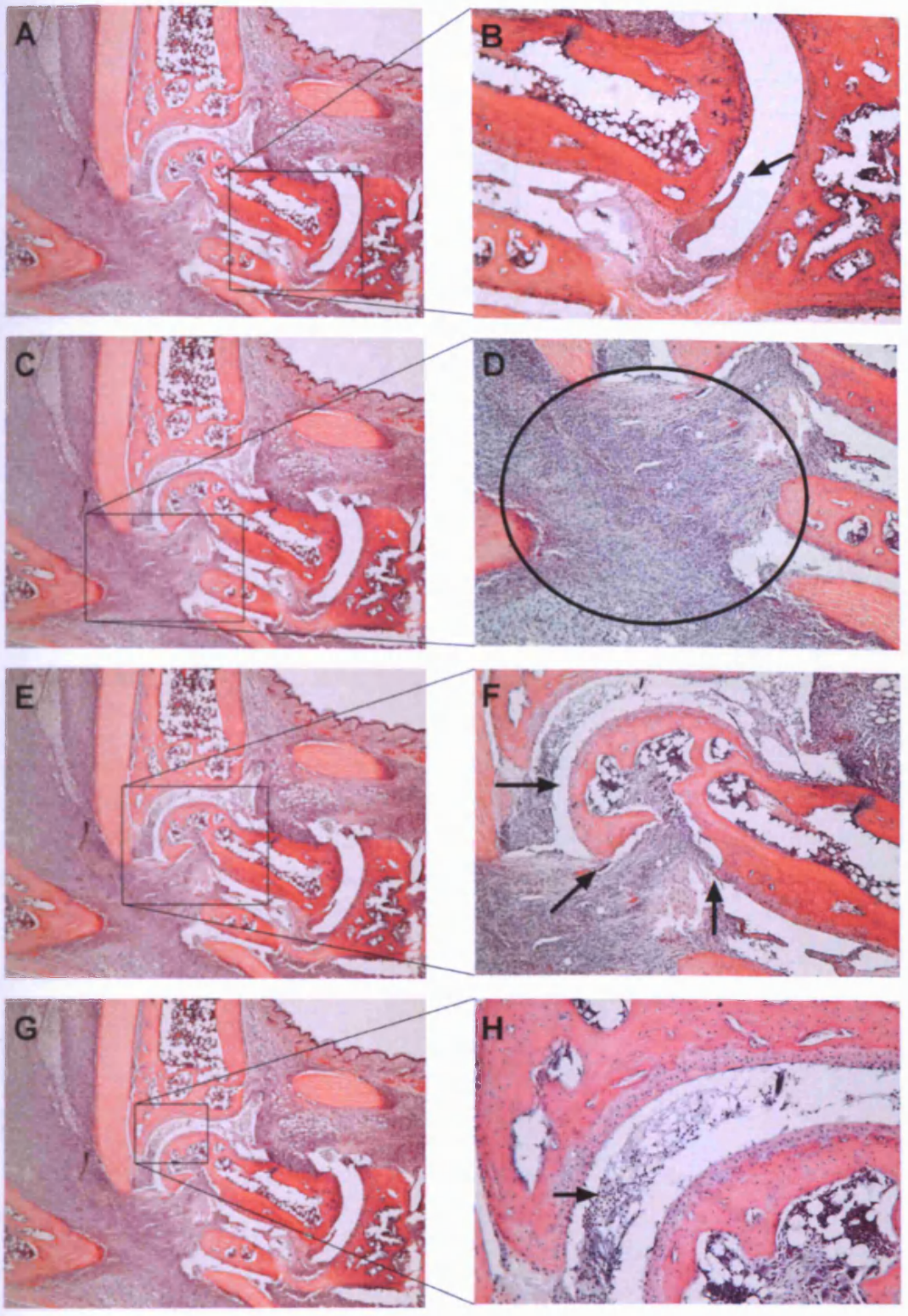

Figure 4.2. An Example of Severe Inflammation in the Joint. A, C, E and G. Ankle joint from an animal with severe inflammatory arthritis (Original magnification x4). B. Arrow indicates inflamed synovium (arrow) (at X10 magnification). D Circle defines an area within the joint affected by a large influx of inflammatory cells in to the synovium (magnification x10). F. Arrows show bone and cartilage damage inflammatory cells are visualised invading the bone (at X10 magnification). H. Black arrow signifies presence of joint exudate, nuclei of inflammatory cells stained purple (magnification x20).

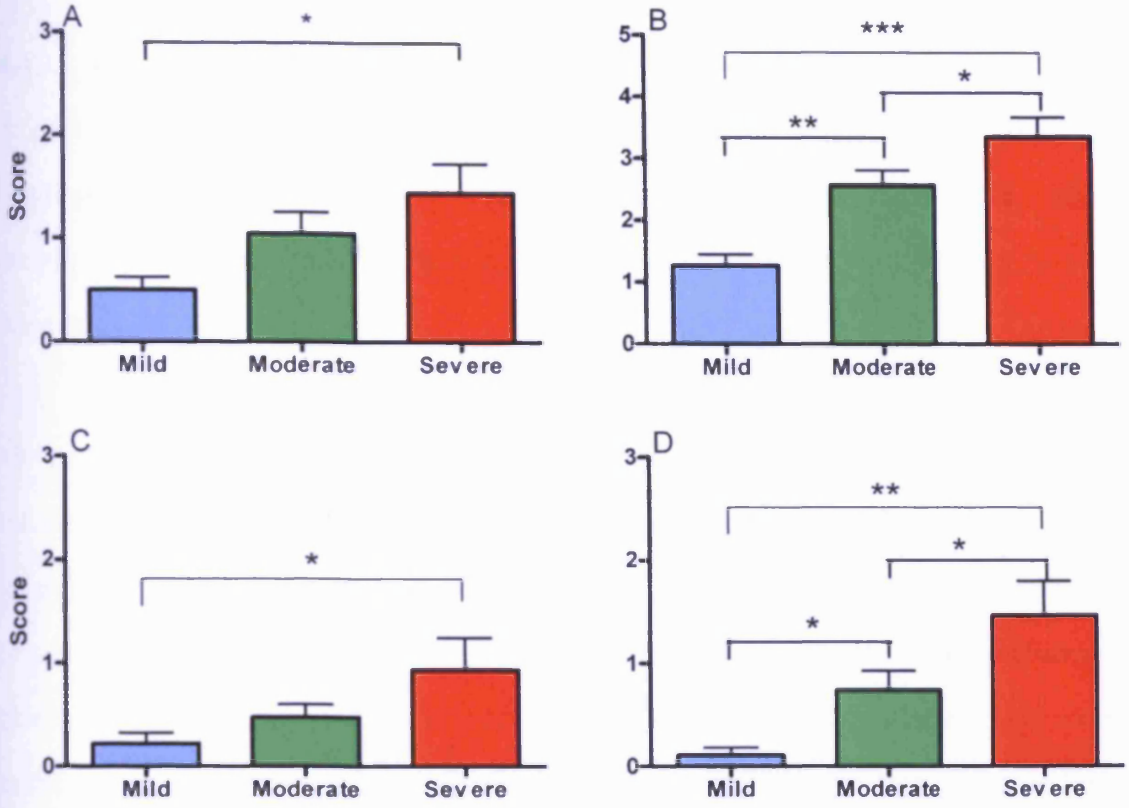

Figure 4.3. Analysis of H & E Staining in Paws from mCIA Animals. A. Graph showing the changes in synovial hyperplasia in differently affected paws, mild n=18, moderate n=23, severe n=16. B. Graph showing the changes in infiltrating cells in arthritic paws, mild n=15, moderate n=23, severe n=17. C. Results from paws scored for the level of exudate in the joint space, mild n=18, moderate n=23, severe n=15, and D. Results for paws scored for the degradation of cartilage and bone, mild n=18, moderate n=23, severe n=15. *$p<0.05$, **$p<0.01$, ***$p<0.001$ (according to one-way ANOVA followed by Newman-Keuls test for significance).

4.4.2.2 Safranin O and Fast Green Staining

Proteolytic degradation of articular cartilage and bone is a characteristic feature of RA. Cartilage destruction attributed mainly to serine proteinases and matrix metalloproteinases produced by SFs, macrophages and chondrocytes (Ronday, van der Laan et al. 2001).

Molecules of safranin O are small enough to penetrate the matrix of the cartilage following which they bind to the glycosaminoglycan side-chains of the cartilage in a 1:1 ratio (Kiviranta, Jurvelin et al. 1985) producing a deep red staining (see figure 4.4). Enzymatic digestion of the cartilage disrupts the binding of the dye producing a bleaching effect on the colour intensity. As the original band of cartilage is still visible in the section, the amount of cartilage that has been depleted can be measured (see figure 4.5)

Sections from paws with clinical signs of arthritis were stained with safranin O and fast green to assess the level of damage in the cartilage surrounding the bones. Measurements of the original depth of cartilage and the depth of the lighter staining areas were taken at 5 points along the band of cartilage on the end of the tibia (see figure 4.5). The depleted volume was expressed as a percentage of the original total. As the clinical score progressed, the percentage of cartilage depleted increased. Bones from normal paws showed no cartilage degradation (see figure 4.6)

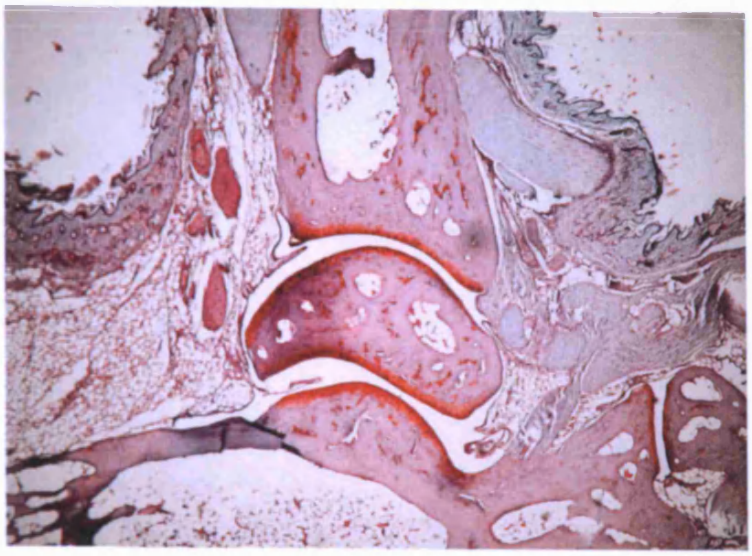

Figure 4.4. Normal Hind Paw Joint Stained with Safranin O and Fast Green. The Safranin O stains the cartilage and thereby a bright red band is visible on the articular surfaces of the bones (at X4 magnification).

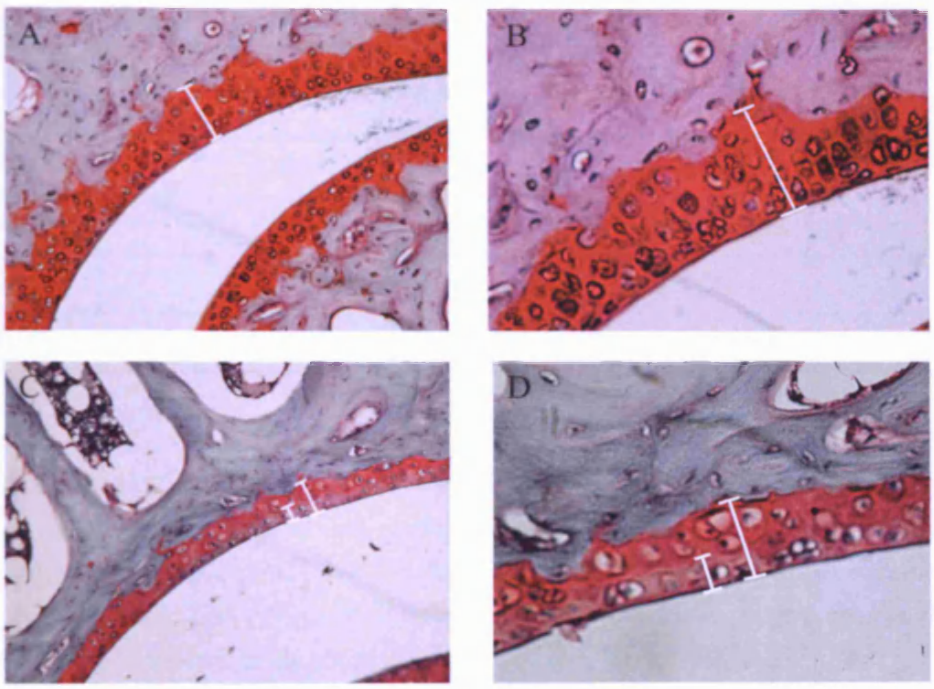

Figure 4.5. Safranin O and Fast Green Staining in Normal and mCIA Joints. A. Shows deep red staining of Safranin O in the cartilage of the tibia in a normal healthy joint. The white line indicates the depth of cartilage (x20 magnification). B. As A, at x40 magnification. C. Safranin O staining in a severely arthritic joint. The two lines indicate the original depth of cartilage, and the depth of depletion to arthritis (at x20 magnification). D. An example of the bleaching effect at a higher magnification (x40 magnification).

A

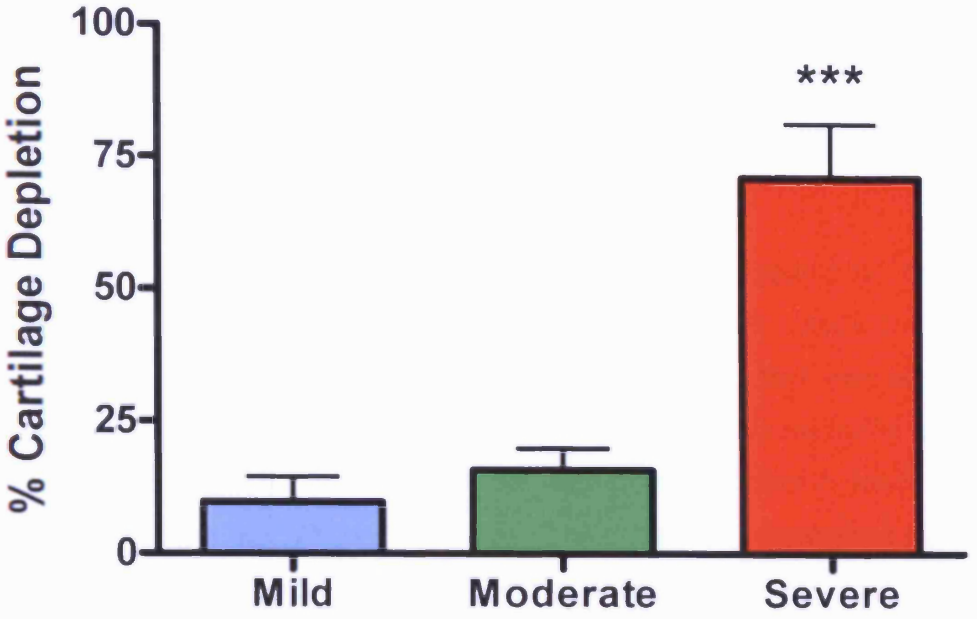

B

Severity	Cartilage Depth (µm ± s.e.m)	Cartilage Depletion (µm ± s.e.m)
Normal	3.80 ± 0.59	0
Mild	3.98 ± 0.23	0.45 ± 0.22
Moderate	3.78 ± 0.81	0.69 ± 0.21
Severe	3.30 ± 0.70	2.87 ± 0.41

Figure 4.6. Cartilage Depletion in mCIA. A. The increase in cartilage depletion (expressed as percentage depletion – calculated from data in table B) with the progression of arthritis. The paws from normal animals showed no degradation and thus there is no bar. *** indicates $p<0.001$ compared to mild and moderate according to one-way ANOVA analysis and Newman-Keuls post test for significance. B. Raw data for cartilage depletion in µm, mild n=8, moderate n=9, severe n=6.

4.4.3. Vascular Function in the mCIA model.

4.4.3.1 Constriction Responses

Vascular function was assessed in the aortae of mCIA animals at appropriate time points after disease induction. These were compared to responses of vessels from normal animals that were sacrificed as age matched controls. Firstly responses were measured by depolarisation of the VSMCs by the addition of $6x10^{-2}M$ K^+ in Krebs buffer in order to condition the tissue. Vessels were allowed to constrict for 5 minutes at which point the maximum constriction reached was recorded. These constrictions showed that tissues from animals with experimental mCIA failed to reach the same constriction as those from normal (see figure 4.7).

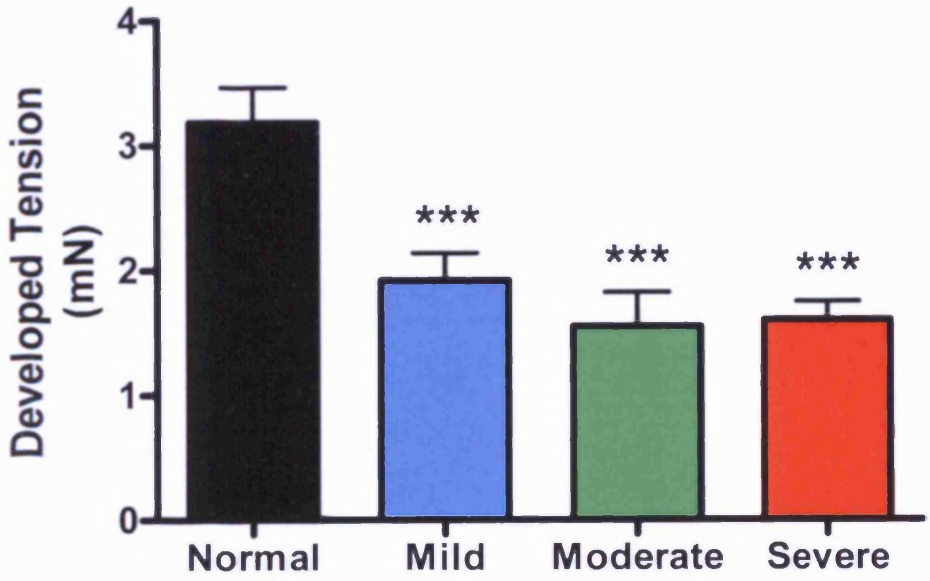

Figure 4.7. Developed Tension Following K+-induced Depolarisation in Normal and mCIA Animals. Vessels were depolarised using 6x10-2M K+ and the maximum constriction reached after 5 minutes was recorded, normal n=8, mild n=7, moderate n=6, severe n=7, ***$p<0.001$ compared to normal.

After depolarisation tissues were washed and allowed to equilibrate following which responses to 5HT were assessed. Similar responses to those observed for depolarisation with K^+ were observed; as arthritis progressed from mild to moderate and severe, the

ability of the vessels to constrict in response to 5HT was significantly reduced (see figure 4.8). All data sets for Rmax and EC50 values were compared to each other. Rmax values for responses from severe and moderate tissue were found to be significantly lower ($p<0.001$) than responses from both normal and mild tissue. Rmax values for mild tissue responses were also significantly higher ($p<0.05$) compared to those from normal tissue. EC50 values for diseased tissue were all significantly higher than EC50 values for normal tissue ($p<0.001$) however no statistical difference existed between disease cohorts.

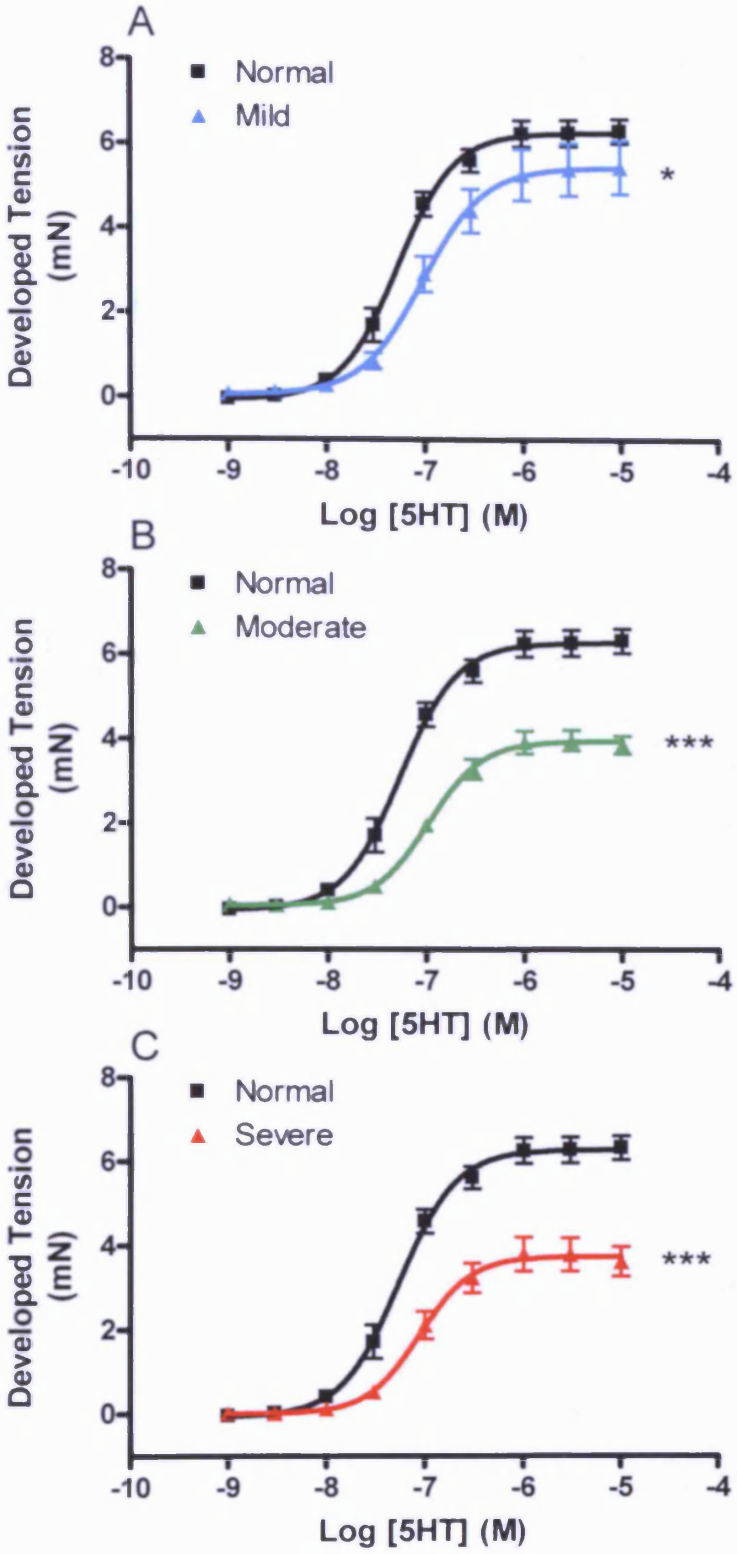

Figure 4.8. Vascular Responses in the mCIA Model. Graph showing concentration response curves to 5HT in vessels from normal (n=5) animals compared to vessels from A, mild (n=7), B, moderate (n=6) and C, severe (n=5) animals. *** $p<0.001$ compared to normal * $p<0.05$ compared to normal.

	Rmax Values (mN)	Level of Significance Compared to Normal
Normal	6.22 ± 0.14	
Mild	5.47 ± 0.28	*
Moderate	3.96 ± 0.11	***
Severe	3.75 ± 0.16	***

	EC50 Values (M)	Level of Significance Compared to Normal
Normal	5.46×10^{-8}	
Mild	9.69×10^{-8}	***
Moderate	1.05×10^{-7}	***
Severe	8.81×10^{-8}	***

Table 4.2. Rmax and EC50 values for Vascular Constriction in the mCIA Model. Rmax values shown as developed tension in mN, and EC50 in concentration (M). *$p<0.05$, ***$p<0.001$ (compared by one-way ANOVA followed by Newman-Keuls statistical analysis.

4.4.3.2 Relaxation Responses

Relaxation responses were originally measured using the method outlined in section 2.4 (all tissues were re-constricted to 70-80% of their maximum response to 5HT before exposure to ACh). Vessels from all animals relaxed fully, and no significant difference between groups were observed (see figure 4.9). Rmax and EC50 values are compared in table 4.3.

However, since the extent to which tissues are constricted can have a significant effect on their subsequent ability to relax (more constriction/less relaxation and *vice versa*), these experiments were repeated using a new protocol. To this end tissues from mild, moderate and severe animals were again constricted to 70-80% of their appropriate maximum response to 5HT. Importantly normal tissues were constricted to corresponding levels by altering the concentration of 5HT applied (for concentrations used see table 4.4). Concentration responses to ACh were then carried out as above. As shown in figure 4.10, this set of experiments confirmed that there was no apparent difference in relaxation responses between tissues from normal, mild, moderate and severe animals. For Rmax and EC50 values see table 4.5

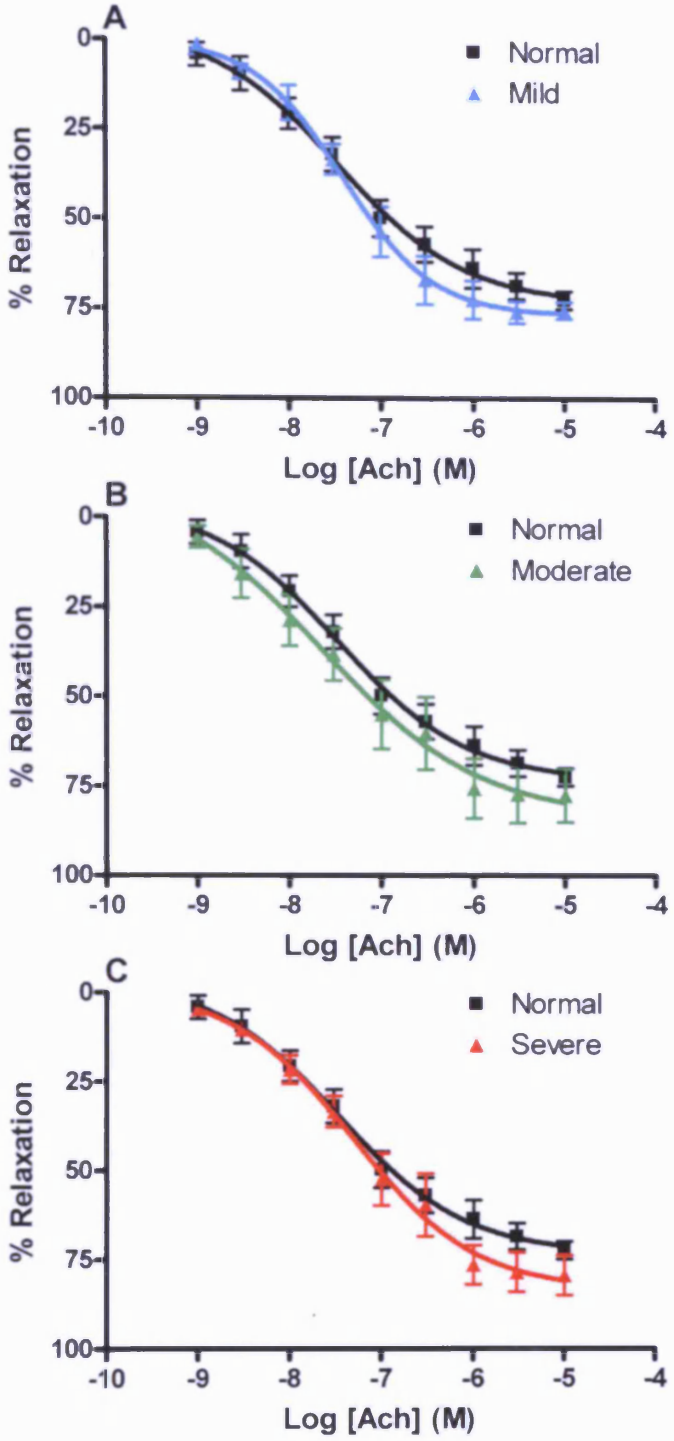

Figure 4.9. Initial Relaxation Responses to ACh in the mCIA Model. Vessels were constricted to 70-80% of their previously induced maximum before relaxing using the agent ACh. A. responses from normal (n=6) and mild (n=5) tissues, B. Responses from normal and moderate (n=5) tissues, C responses from normal and severe (n=5) tissues.

	Rmax Values (%)
Normal	73.37 ± 5.09
Mild	76.78 ± 3.37
Moderate	83.82 ± 12.52
Severe	83.42 ± 6.51

	EC50 Values (M)
Normal	3.44×10^{-8}
Mild	3.86×10^{-8}
Moderate	2.31×10^{-8}
Severe	4.94×10^{-8}

Table 4.3. Rmax and EC50 Values for the Initial Relaxation Responses. Values shown as developed tension for the Rmax values (%) and the EC50 values in concentration

	Developed constriction attained at 70-80% of maximum (approximate) (mN)	Concentration range needed to reach this (M)	Concentration range needed to reach this in normal tissue (M)
Mild	5.5	$3x10^{-7}$	10^{-7} - $3x10^{-7}$
Moderate	4	$3x10^{-7}$ - 10^{-6}	10^{-7} - $3x10^{-7}$
Severe	3.5	$3x10^{-7}$ - 10^{-6}	10^{-7}

Table 4.4. Concentrations of 5HT used to Obtain Similar Constrictions. The concentrations (approximate) listed were used to elicit the same level of constriction in vessels from normal animals as mCIA animals. Vessel relaxation responses were then measured from the same level of tension.

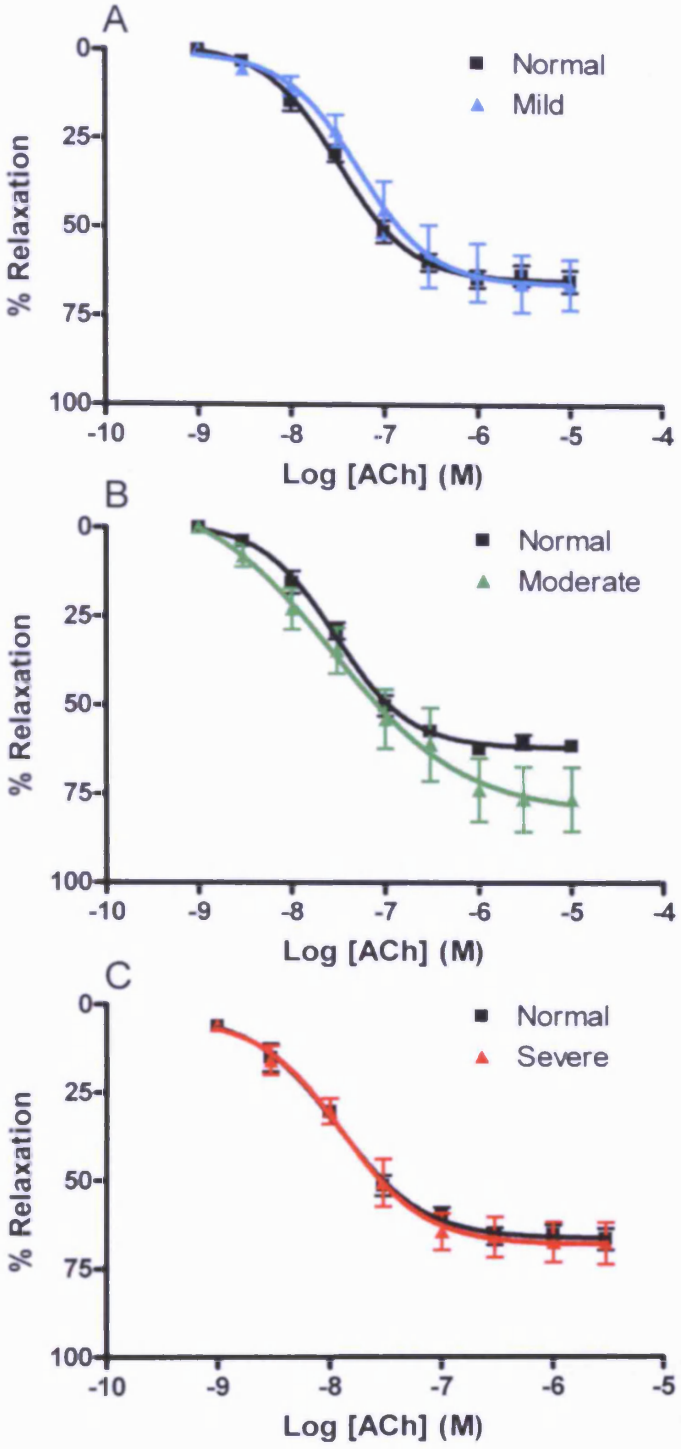

Figure 4.10. Relaxation Responses in the Aortae from the mCIA model. Vessels from normal animals were constricted to the same level of tension as vessels from mCIA animals in order to directly compare vessel relaxation. Responses from tissue taken from normal (n=6) animals compared to tissue taken from A mild (n=5), B moderate (n=5) and C severely (n=5) affected animals.

	Rmax Values (%)
Normal	65.00 ± 1.54
Mild	66.08 ± 4.14
Normal	61.65 ± 1.33
Moderate	80.26 ± 8.55
Normal	68.71 ± 2.14
Severe	68.16 ± 3.20

	EC50 Values (M)
Normal	3.24×10^{-8}
Mild	5.30×10^{-8}
Normal	2.54×10^{-8}
Moderate	2.72×10^{-8}
Normal	1.25×10^{-8}
Severe	1.29×10^{-8}

Table 4.5. Rmax and EC50 Values for Relaxation Data. Rmax values are expressed as maximum percentage relaxed (%), and EC50 values as the concentration (M) needed to obtain 50% of the relaxation observed.

To ensure that the relaxation capability of the VSMCs was not compromised in anyway responses to the NO-donor SNP were also measured. There were no apparent differences between these responses in any group of animal (see figure 4.11) with regard to EC50 values and Rmax values (see table 4.6).

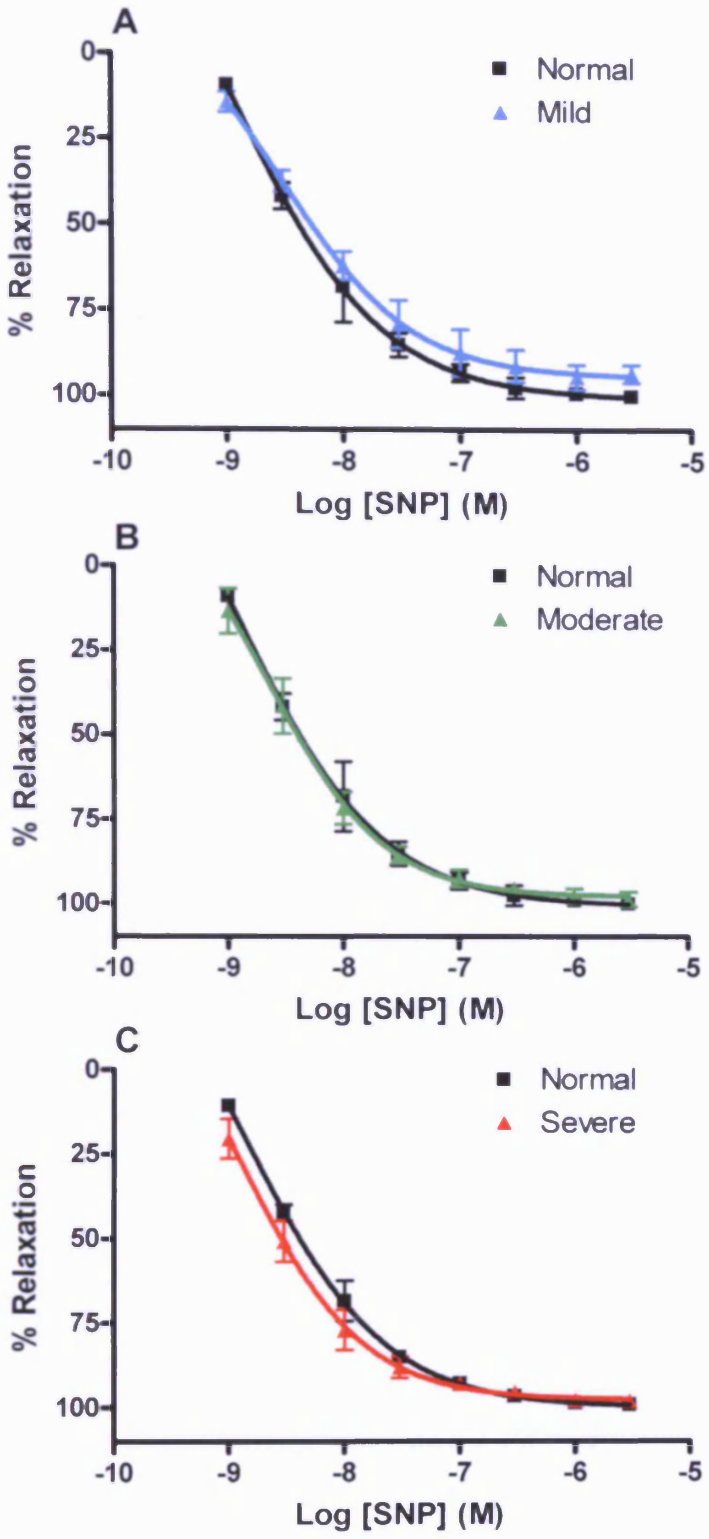

Figure 4.11. Relaxation Responses to SNP. A Relaxation responses to SNP from normal (n=3)and mild (n=5) vessels. B. Responses from normal and moderate (n=4) vessels, and C. From normal and severe (n=3) vessels.

	Rmax Values (%)
Normal	100.10 ± 2.01
Mild	94.67 ± 3.66
Moderate	98.10 ± 2.90
Severe	97.89 ± 2.48

	EC50 Values (M)
Normal	1.36×10^{-9}
Mild	3.08×10^{-9}
Moderate	2.29×10^{-9}
Severe	1.23×10^{-9}

Table 4.6. Rmax and EC50 values for Relaxation Responses to SNP. Rmax values are expressed as the maximum relaxation (%) and EC50 values as concentration (M).

4.5 Discussion

4.5.1. Successful Induction of mCIA

The successful induction of mCIA in DBA/1 mice was apparent by the level of paw swelling shown clinically and the extent of inflammatory cell influx and changes to cartilage and bone shown histologically. In all cases the progression in the clinical signs of arthritis were accompanied by sequential histological changes within the paw. These were shown by higher levels of inflammatory cells invading the joints and the joint space, synovial thickening within the joint and by the increased levels of cartilage and bone degradation. The latter was further confirmed using safranin O and fast green staining to assess in detail the progressive level of cartilage erosion.

The scoring criteria for this model attempts to distinguish between mild, moderate and severe arthritis and was established in order to effectively evaluate the relationship/timeline between the possible development of vascular dysfunction and the progression of experimental arthritis. While every effort was taken to adopt a consistent and unifying approach to the clinical assessment criteria, uncontrollable biological factors on occasion made this difficult. Since each mouse affected with mCIA has a unique timescale for the progression of disease, individual animals sometimes could reach mild, moderate or severe disease at different time points, post-second injection. The majority of animals reached the appropriate disease stage as outlined in section 4.4.1, however this was not always the case. For example arthritis in one animal may take 5 days to present itself, following which it progresses to severe in 3 days. Alternatively a mouse could show slight swelling on day 23 and from this point progress slowly to moderate arthritis at day 26, and reach severe at day 32. Every effort was therefore taken to group animals of similar disease aetiology when investigating the mild, moderate and severe categories. The "tight" nature of the data described above would suggest that any possible problems due to such idiosyncratic variations have been minimised.

4.5.2. Changes to the Vasculature as a Result of mCIA

From these experiments it was observed that as the number of joints affected increased and clinical symptoms of arthritis deteriorated, the ability of the isolated aortic rings to constrict to either K^+ or 5HT became significantly reduced. Interestingly, this was not accompanied by a reduction in the ability of the vessel to relax to ACh.

4.5.2.1 Vessel Constriction in the mCIA Model

The initial observation made with regard to vessel function in aortae from the mCIA animal was the change in the ability of the vessel to constrict following K^+-induced depolarisation, implying a change in the contractile ability of the VSMCs. This change was further confirmed by the responses to 5HT, with maximal constrictions in vessels from mCIA animals failing to reach those of their normal counterparts. Such responses for all diseased groups were significantly lower than the constrictions attained in normal tissues with regard to Rmax. The maximum contractile ability of the vessels from arthritic animals deteriorated with disease severity; aortae taken from mild animals had a

small decrease in the maximum constriction reached, moderate and severe vessels were further inhibited in this ability. In addition to the change in Rmax values, EC50 values were also significantly reduced in responses from diseased tissues compared to normal, implying that there may be a decrease in sensitivity to 5HT in these diseased vessels. This could be due to differential expression of receptors with progression of disease, or compromised interactions between agonist and receptor. Additional experiments could be performed to determine the levels of the receptor present (perhaps by western blot), or an attempt could be made to visualise the effect of binding on the cell (by calcium signalling) to determine the downstream effect of the agonist on the VSMCs. However, given that contractile responses to both K^+ and 5HT are impaired would argue against a defect in receptor-medicated responses. Moreover such experiments would prove time-consuming and somewhat outside the scope of this project. Instead focus will be placed on investigating the mechanistic changes that underlie the contractile dysfunction. While this will be addressed experimentally in later chapters of this thesis, as a prelude it is appropriate to speculate as to their nature here.

Within the inflammatory setting a large number of events are occurring resulting in upregulation of a wide range of cytokines, chemokines and inflammatory cells and mediators (Kaplan 2006) both in the joint and the vasculature. Once in the circulation, these individual factors may initiate a downstream cascade of events resulting in damage to the cells therein. In order to prevent this damage occurring, the cells of the vasculature may change their function in an attempt to self-protect, perhaps by increasing the production of protective molecules such as NO and PGI_2. These potent vasodilators are the products of NOS or COX activity respectively and possible "inflammation-induced" upregulation of these enzymes could lead to such an action. This in turn would serve to counteract the effects of K^+ and 5HT and dampen maximal constriction. The diminished constriction observed in the mCIA model could therefore be a result of an increase in the production of the vaso-protective and vasodilatory molecules. This may follow the pattern observed with constriction "dampening" increasing with arthritic severity and as such investigating production of these vasodilators is of utmost importance. This will be discussed below and investigated in the following chapters.

4.5.2.2 Changes in NO Levels

Upregulated levels of eNOS at both the mRNA and protein level have been shown to be associated with endothelial dysfunction in a model of diabetes mellitus (Hink, Li et al. 2001). In this model eNOS became dysfunctional, however the timeline for this change was not discussed, allowing for speculation that initially functional eNOS may be upregulated before endothelial dysfunction occurs. If this occurred in mCIA model, such upregulation could be the cause of an overproduction of NO.

A further possibility is the upregulation of iNOS and consequently uncontrolled overproduction of NO. Indeed, in RA it is well documented that iNOS is upregulated and is a producer of large amounts of NO (Cuzzocrea 2006). This is perhaps unsurprising as iNOS is speculated to be induced following a surge in inflammatory mediators such as IL-1β and TNFα (Gibson, Constantin et al. 2005), cytokines which are upregulated in both human disease (Shore, Jaglal et al. 1986; van den Berg 2001) and mCIA (Marinova-Mutafchieva, Williams et al. 1997). Moreover, in an alternative, bacterial cell wall-induced model of arthritis, increased production of inflammatory cytokines is associated with an upregulation of iNOS gene expression and increased circulating NO levels (Wahl, McCartney-Francis et al. 2003). Such an increase in the present model would certainly contribute to decreased responsiveness/sensitivity to 5HT in isolated tissues.

4.5.2.3 Changes in PGI_2 Levels

PGI_2 is a potent vasodilator and inhibitor of platelet aggregation and VSMC proliferation (Funk and FitzGerald 2007), and therefore plays an essential role in maintaining vessel tone. COX-2, a producer of PGI_2 is known to be upregulated under inflammatory conditions (Suleyman, Demircan et al. 2007) thus increasing circulating levels of this molecule in inflammatory systems. Additionally, an increase in the urinary metabolite of this molecule has been detected in human RA (Hishinuma, Nakamura et al. 2001). As such it is possible that in the mCIA model there will be higher levels of circulating PGI_2 indicating a role for this molecule in the development of decreased responsiveness to 5HT.

Currently there is limited evidence surrounding these hypotheses in the vasculature of the mCIA model and subsequent investigation will be provided in detail in the following chapter.

4.5.2.4 Vessel Relaxation in the mCIA Model

Despite many reports in the literature of endothelial dysfunction in RA-affected human (Sattar and McInnes 2005; Libby 2008) and animal models (Can, Cinar et al. 2002; Haruna, Morita et al. 2006; Haruna, Morita et al. 2007; Nozaki, Goto et al. 2007), it would appear that the model described in this thesis is not overtly characterised by this condition. Why this should be the case is open to speculation.

In line with current research publications, adult male DBA/1 mice were used for the studies (Inglis, Notley et al. 2007; Andreakos, Rauchhaus et al. 2009; Nowell, Williams et al. 2009) aged 8–10 weeks, an age at which they are considered adult. However, comparatively speaking, the age of arthritis onset in these animals is much younger than observed in human RA; DBA/1 mice are "skeletally" adult, (at 8-10 weeks their skeletal development is complete, personal communication Dr AS Williams) and so the age of onset would be proportional to a 16-18 year old human. Conversely the average age of disease onset in humans is 40-50 years. While the mice may be deemed adult, they may still be "vascularly" immature. This leads to speculation as to whether the "young" mouse vessels are prone to the development of endothelial dysfunction. It is well recognised that as vessels age they lose their natural resistance to ROS and other damaging agents (Csiszar, Labinskyy et al. 2007), and thus the relatively young age of these animals could mean compensatory mechanisms in response to mCIA prevent endothelial dysfunction. For example, the generation of anti-oxidant molecules such as superoxide dismutase, heme oxygenase, catalase, peroxidase/peroxiredoxin (Forstermann 2008) to name but a few are capable of protecting against ROS and superoxide damage.

Natural resistance of the vessel to these damaging species is diminished as the vessels age. Age-related vascular pathologies in humans have been attributed to an increase in ROS production, coupled with a decrease in natural resistance, an occurrence which becomes more frequent with age (Csiszar, Labinskyy et al. 2007). Indeed the longevity of a species is associated with the ability of the vessel to prevent damage by these reactive

species (Labinskyy, Mukhopadhyay et al. 2009). As such, due to the relatively short lifespan of the DBA/1 species (C57BL/6 in comparison live on average to 22 months (Storer 1966)) it may be speculated that the protective changes are perhaps unlikely to be occurring and in fact, these vessels may be more prone to oxidative damage. Nonetheless, endothelial dysfunction remains absent in this model.

An additional argument opposing this "age theory" is that endothelial dysfunction has been reported in children who present risk factors such as diabetes mellitus, or have high circulating levels of C-reactive protein (Urbina, Williams et al. 2009). Moreover, juvenile arthritis has been described to affect children under the age of 16 (Hayward and Wallace 2009), and be accompanied by vascular impairment; capillaries of the microcirculation become widened and exhibit other structural abnormalities speculated to herald the onset of endothelial dysfunction (Gorska, Kowal-Bielecka et al. 2008).

An alternative theory is that endothelial dysfunction might be present in the mCIA model, but the means by which it was assessed may not be appropriate/sensitive enough. For instance in rabbit aortic segments incubated with oxidised-low density lipoprotein (ox-LDL), varying relaxation responses were observed depending on the vasodilator used (Bocker, Miller et al. 2001). In this study relaxation responses to thrombin were impaired while those to ADP unaffected. In the present studies ACh was used and elicited responses comparable to those of "normal" animals, indicating no change in endothelial function. ACh is an M3 muscarinic receptor agonist and the "agent of choice" in *in vitro* experiments investigating endothelial function. While further studies with other endothelium-dependent vasodilators were a possibility, it was deemed of higher importance to assess the possible mechanical changes occurring to the VSMCs and to investigate changes in endogenous vasodilator production.

These results do not entirely discount the presence of endothelial dysfunction in the mCIA model. Since disease progression is only permitted over a short time course there may not be enough time for this condition to become overt. Indeed other changes that could be less noticeable in the patients with human disease may develop first in the animal model. However it does not appear that the changes relating to endothelial dysfunction outlined in the hypothesis are occurring in this model in our hands.

As a result of this experimental work it is obvious that the original proposed hypothesis for the endothelial dysfunction that would present in a model of mCIA can be discounted. However this work has deduced that there is a problem with the contractile function of the vessel and as such, the aim is to elucidate the mechanism(s) responsible for such changes. In order to do this, the theory that constriction is muted due to an over production of vasodilatory compounds will be investigated.

CHAPTER 5

VASCULAR DYSFUNCTION IN MCIA: A ROLE FOR NO AND COX?

5.1 Introduction

In Chapter Four no discernable endothelial dysfunction was observed in the mCIA model. Furthermore, the ability of the VSMC to relax to exogenous NO (in the form of SNP) was not compromised. It was observed that vessels from diseased animals constricted in response to agonist stimulation; this vascular response decreased with increasing arthritis severity. Although defects in the contractile apparatus may be present in the VSMCs, given the ability of NO and PGI_2 to dampen vessel contraction it is important to first assess any possible role these vasodilators may play in the development of this dysfunction.

5.1.1 Upregulation of NOS Isoforms

Information regarding the activity and expression of NOS isoforms in this model remains unclear. Although it has been suggested that upregulation may occur (see Chapter Four) this is merely speculation. Aberrant NOS isoform activity could potentially affect basal tone; excess production of NO may result in a continual partially dilated vessel and the possibility of low blood pressure. Alternatively, the change in vessel function observed could be due to the loss of compliance leading to vessels becoming stiffer and unable to constrict. In this scenario, hypertension could ensue (Zieman, Melenovsky et al. 2005; Tsioufis, Dimitriadis et al. 2007). Indeed the observation that vessel stiffening occurs in hypertensive patients, and that such hypertension is not an uncommon pathology observed in patients suffering from RA (for a recent review see (Panoulas, Metsios et al. 2008)) gives fuel to this theory. Interestingly, levels of both iNOS and eNOS are upregulated in spontaneously hypertensive rats (Vaziri, Ni et al. 1998) emphasising the need to investigate the roles of these enzymes in this model.

If eNOS levels/activity remain stable and functional, the proposed change in NO bioavailability may be due to altered iNOS activity, which perhaps would not be an

unexpected occurrence in this inflammatory disease. Indeed in human RA an increased level of endogenous NO due to upregulation of iNOS, reflected as an increase in serum NO metabolites, has been described (Yki-Jarvinen, Bergholm et al. 2003). Moreover, *in-vitro* observations show an increase in iNOS mRNA levels in cultured human VSMCs following stimulation with inflammatory cytokines IL-1 and TNF-α (MacNaul and Hutchinson 1993), both of which are characteristic of mCIA and human RA. Additional factors may also play a role in this "NO hypothesis". For instance, vascular endothelial growth factor (VEGF), a pro-angiogenic cytokine, is upregulated in the paws of mCIA animals (Choi, Kim et al. 2009) and plays an important role in the initial stages of arthritis (Lu, Kasama et al. 2000). It has been observed that during angiogenesis VEGF can induce expression of both eNOS and iNOS resulting in an increased production of NO (Kroll and Waltenberger 1998). Contrastingly a decrease in endothelial cell eNOS mRNA and protein levels following stimulation with TNFα has been observed (Jantzen, Konemann et al. 2007) perhaps questioning a role for eNOS in the vascular pathology observed in this thesis.

Due to the multifactorial nature of the disease model a myriad of events are occurring throughout disease progression. Taken together the above observations certainly suggest that a role for increased NO production in the mCIA model merits greater scrutiny.

5.1.2 Markers of NOS Activity

A common method of assessing *in-vivo* eNOS activity is by determining plasma concentrations of the more stable oxidative products of NO metabolism, namely nitrite (NO_2^-) and nitrate (NO_3^-), subsequently described widely as total NO (NO_x). This measurement is based on the fact that eNOS-derived NO rapidly reacts with both oxy- and deoxy-haemaglobin (deoxy-Hb) to produce NO_3^- and iron-nitrosylhaemoglobin respectively (Liu, Miller et al. 1998). Alternatively NO that fails to react with Hb is oxidized to NO_2^- in the plasma (Shiva, Wang et al. 2006) and can be further converted to NO_3^- (Kelm, Schafer et al. 1997). Moreover, NO when inhaled or added to the blood, is also rapidly converted to these NO-metabolites (Lauer, Preik et al. 2001). Importantly circulating NO_x levels in eNOS -/- animals are reduced by half compared to normal

counterparts (Godecke, Decking et al. 1998) confirming the usefulness of this parameter in assessing *in vivo* eNOS activity.

There are several things to consider when measuring NO_x since the rate of NO metabolism is highly dependent on its location, concentration and indeed the concentration of other bioreactors in the immediate environment. For example juxtaposition with cellular membranes, differences in pO_2, the presence of ROS, changes in pH and the concentration of transition metals all have various positive and negative influences on NO bioavailability (for review see (Kelm, Schafer et al. 1997). Moreover, additional quantification difficulties may arise due to the abundant nature of NO_2^- in the laboratory. Extra precautions are therefore required to limit contaminating NO_2^- in blood collection tubes and avoid overestimation of NO_x levels (Dejam, Hunter et al. 2005). Importantly, the above parameters should not overtly affect measurements taken in the present study since they should have equal influence on both control and diseased animals. Indeed changes in NO_x should appropriately reflect disease activity and the role of NO therein.

5.1.3 Upregulation of COX products

COX products such as prostanoids play important roles in vascular homeostasis and both COX-1 and -2 may potentially mediate changes to vessel function under the inflammatory conditions imposed by the mCIA model. For instance, COX-1 is upregulated in human umbilical vein endothelial cells (HUVECs) following exposure to VEGF (Bryant, Appleton et al. 1998). Interestingly concomitant NOS isoform upregulation was absent in this study, possibly reflecting differential regulation of vein and arterial enzymes. However, upregulation of COX-1 in endothelial or smooth muscle cells in the mCIA model could lead to a significant increase in the production of PGI_2, the vasodilatory properties of which could mediate the observed dampening of contraction.

The more likely mediator in the disruption of normal vessel function in RA is inducible COX-2, widely demonstrated to be upregulated in inflamed tissues (Suleyman, Demircan et al. 2007) and the primary producer of PGI_2 (for review see (Funk and FitzGerald 2007). That a four-fold increase in the urinary metabolite of PGI_2 has been described in

human RA (Hishinuma, Nakamura et al. 2001) indicates a possible role for PGI_2 regulation in this inflammatory disease. Further investigations in the present model are therefore warranted.

5.1.4 Inhibition of NOS and COX

5.1.4.1 N^G-Nitro-L-Arginine Methyl Ester (LNAME) and 1400W

Inhibition of NOS activity was assessed using the L-arginine analogue N^G-nitro-L-arginine methyl ester (L-NAME), and N-(3-(Aminomethyl)benzyl)acetamidine (1400W). L-NAME is a widely used non-specific competitive NOS inhibitor while 1400W is the most selective inhibitor of iNOS known to date (Garvey, Oplinger et al. 1997). Indeed 1400W is 5000- and 200-fold more potent against purified human iNOS than eNOS and nNOS respectively (Garvey, Oplinger et al. 1997). By conducting separate experiments with these agents the relative roles of eNOS and iNOS in the contractile dysfunction observed in the mCIA model was investigated.

5.1.4.2 Indomethacin

Indomethacin is a non-steroidal anti-inflammatory (NSAID) drug administered for pain relief in conditions such as RA (Hart and Boardman 1963), and widely used as a pharmacological tool in investigations of vascular-derived COX products. By insertion of a methyl group into the active site of COX (Prusakiewicz, Felts et al. 2004) indomethacin acts as an inhibitor (Ersoy, Orhan et al. 2008). Its use will initially provide general information with regard to the role of COX-derived products in the contractile dysfunction observed in the mCIA model. More specific experiments may follow as appropriate.

5.2 Aims

To assess the role of NOS in vessel dysfunction in the mCIA model utilising broad spectrum and specific NOS inhibitors.

Determine plasma levels of NO metabolites to assess NO bioavailability in the mCIA model

To assess the role of COX in vessel dysfunction in the mCIA model utilising a broad spectrum COX inhibitor.

5.3 Method

5.3.1 Induction of mCIA

mCIA was induced in male DBA/1 mice as described in section 2.2.

5.3.2 The role of NOS

5.3.2.1 Analysing the Effect of the non-specific NOS inhibitor L-NAME

At appropriate time points mCIA and control animals were euthanised and blood (see below) and aortae removed. The latter was then prepared for myography as detailed in section 2.3.1 and 2.3.2ii. To assess the general role of NOS isoforms in the aortic responses a non-specific inhibitor was used initially. To this end constriction responses were measured as outlined in section 2.4 but with the addition of an incubation period with L-NAME (N5751, Sigma Aldrich). Following the constriction response to K^+ vessels were incubated with L-NAME ($3x10^{-4}$M, a concentration widely used in the literature to completely inhibit NO production) for 30 minutes before responses to bolus additions of 5HT and ACh were assessed as before (section 2.4), though this time to ensure inhibition of endothelium-dependent relaxation. Following washing L-NAME was re-added to the bath and incubated for a further 30 minutes. Concentration responses to 5HT were then assessed as before (section 2.4).

5.3.2.2 Analysing the Effect of the iNOS Inhibitor 1400W

Experiments as 5.3.2.1 above were repeated with 1400W (10^{-5}M, W4262, Sigma Aldrich) (Alvarez, Briones et al. 2008) in place of L-NAME. Following incubation with 1400W for 30 minutes vessels were subjected to bolus responses to 5HT and ACh as described in section 2.4. Importantly, endothelium-dependent relaxation to this bolus addition of ACh (10^{-6}M) was not affected by this agent (see results section 5.4.2). Constriction responses to 5HT were then assessed as before (section 2.4).

Endothelium-dependent relaxation was also measured in these experiments as outlined in section 2.4 and 4.3.6.2. Briefly, following the maximum constriction response, vessels were washed, 1400W re-added and the tissues left to re-equilibrate before being re-constricted to 70-80% of their previous maximum and subsequently exposed to increasing concentrations of ACh (10^{-9}M to 10^{-5}M).

5.3.2.3 NO Metabolites in the Blood

The Sievers® 280i NO Analyzer (NOA, Analytix UK) is a highly sensitive system with detection limits of less than 1 picomole (MacArthur, Shiva et al. 2007). The principle of using chemiluminescence to detect NO_x is based on the reaction between NO and ozone (O_3), which produces NO_2 in an excited state (NO_2*, see equation below). When the excited electron returns to its ground state it emits a photon (*hv*) that is detectable and amplified by a photomultiplying tube in order to generate an electrical signal.

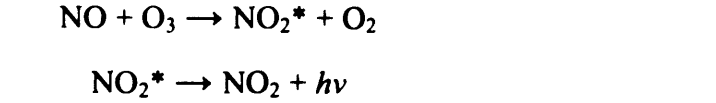

$$NO + O_3 \longrightarrow NO_2^* + O_2$$

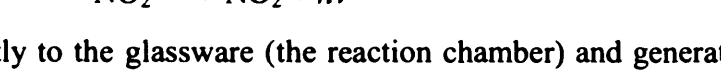

$$NO_2^* \longrightarrow NO_2 + hv$$

The NOA is attached directly to the glassware (the reaction chamber) and generates the O_3 for reacting with NO. The glassware contains a redox-active chemical solution which reduces the NO_x to NO (MacArthur, Shiva et al. 2007). Samples are injected into this chemical solution in the reaction chamber where NO metabolites are reduced to NO and subsequently forced by the flow of oxygen-free nitrogen into the NOA for detection.

At appropriate time points, serum was prepared from blood samples collected at the time of aortic tissue harvesting as described in section 2.3. Concentrations of NO metabolites were subsequently measured using ozone-based chemiluminescesce (Rogers, Khalatbari et al. 2005). Briefly, 5ml of tri-iodide reagent (70ml glacial acetic acid, 650mg iodine (I_2), 20ml HPLC grade water, 1g potassium iodide (KI)) was added to the reaction chamber with 20µl of anti-foam (A5633, Sigma Aldrich) (to prevent foaming of the serum), before heating to 50°C on a thermostatically-controlled hot plate (see figure 5.1). Oxygen-free nitrogen gas was bubbled through the reaction chamber to force the NO towards the NOA. On route the NO passes by a sodium hydroxide (NaOH) (1M) chemical trap necessary for removal of oxygen-nitrogen compounds (eg N_2O_3) as well as preventing damage to the NOA from acid vapour (due to the acidic nature of the tri-iodide). Sodium nitrite standards for the calibration curve were made up in increasing concentrations from 62.5nM to 1000nM and HPLC water was used as a control. 100µl

standards were injected into the reaction chamber and the peak electrical signal was recorded using the data collection package "Liquid" (part of the NOAnalysis software suite). Serum samples were thawed in a 37°C water bath for one minute before injection. All standards and samples were repeated three times and measurements then averaged.

For signal analysis purposes the signal to noise ratio (and accuracy of area under curve (AUC) analysis) was improved by exporting the Liquid file to the data analysis and graphing software Origin 8.1 (Originlab®) and the "peak analysis" feature was utilised. Adjacent signal averaging was used to smooth the peak and determine manually the start and end point of each peak. The AUC for each sample was measured and averaged and sample values for each group combined. This analysis results in improved repeatability of measurement.

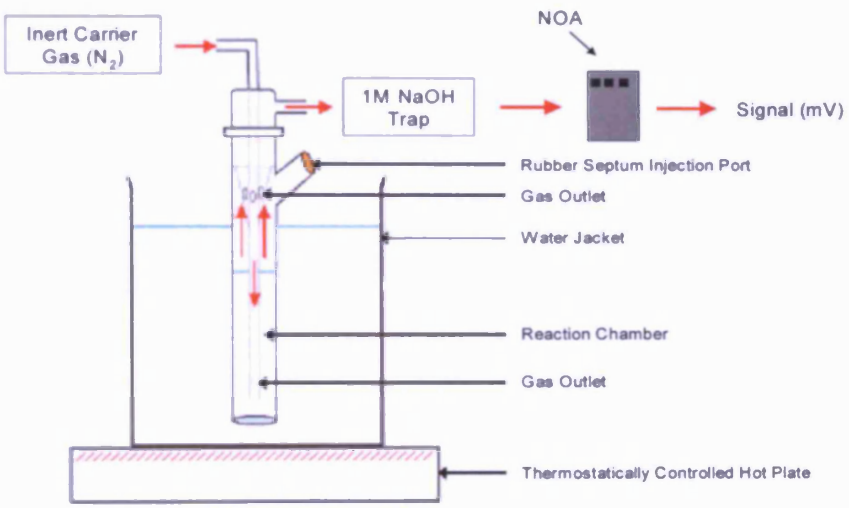

Figure 5.1. Apparatus for Nitric Oxide Analysis. The sample is injected into the injection port, NO-related species are reduced/converted to NO and carried with the oxygen-free nitrogen through the chemical trap to the NOA, where the electrical signal is created. Reproduced with kind permission from Dr Andrew Pinder (Pinder, Rogers et al. 2009).

5.3.3 The role of COX

5.3.3.1 Analysing the Effect of the non-specific COX Inhibitor Indomethacin

To assess the general role of COX isoforms in the aortic responses, a non-specific inhibitor was used. Experiments as 5.3.2.1 above were repeated with indomethacin (10^{-6}M, 57413 Sigma Aldrich,) (Quinn, O'Brien et al. 2003) in place of L-NAME.

Indomethacin was initially dissolved in ethanol and then diluted in Krebs buffer ensuring the final ethanol concentration at the tissue was no higher than 0.01% (v/v) (a concentration widely known to have no effect on vascular tone, personal communication Dr D Lang). Importantly, endothelium-dependent relaxation to a bolus addition of ACh (10^{-6}M) following constriction with 5HT (10^{-6}M) was not affected by this agent (see results section 5.4.5). Concentration responses to 5HT and ACh respectively were then performed as described above (see 5.3.2.2).

5.3.4 Statistical Analysis

All data are expressed as mean ± SEM. 5HT-induced increases in tension are expressed as developed tension in mN. Relaxation responses are expressed as a percentage of the immediately previous, agonist-induced maximum constriction. Isometric tension data were first fitted to sigmoid concentration curves using GraphPad Prism software and EC50 (concentration to produce 50% of maximum response) and maximum constriction/relaxation (Rmax) values analysed by one-way ANOVA followed by Student Newman-Keuls multiple range test. Rmax values were plotted on a bar graph to compare values. For direct comparison of EC50 values the negative log of the mean value and the standard error of this mean was taken and plotted in a bar graph.

Data from NO analysis were expressed as average levels of NO_x in the serum, mean ± SEM. Results were analysed by one-way ANOVA followed by Student Newman-Keuls multiple range test. For all data sets, differences were considered significant where $p<0.05$.

5.4 Results

5.4.1 Vessel Constriction in the Presence of L-NAME

Preliminary experiments showed that the presence of L-NAME had no significant effect on the constriction responses to 5HT in normal tissues (see figure 5.2). Importantly the tissues failed to relax in response to ACh confirming complete eNOS inhibition (an example of this is shown in the trace in figure 5.3). Vessels from experimentally arthritic animals exhibited the same impairment in 5HT-induced tension as observed in Chapter

Four. In the presence of L-NAME, while Rmax values for tissues from all three disease cohorts were marginally greater than those in the absence of the eNOS inhibitor, these responses were still significantly lower than those observed in normals (see figure 5.4). No differences in EC50 values between any groups were observed (see table 5.1 for graphs and values).

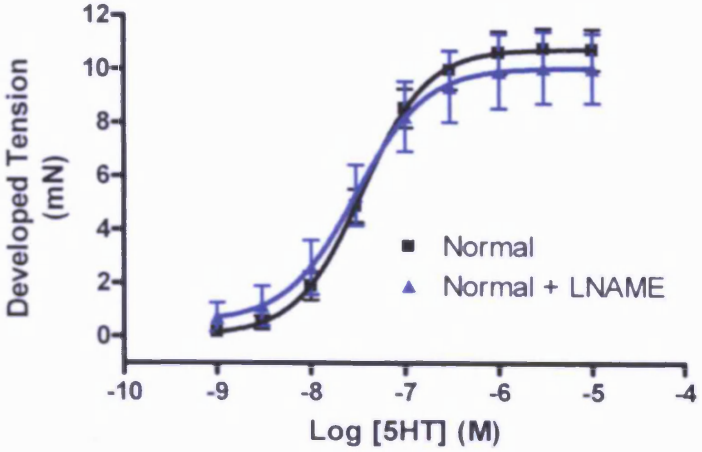

Figure 5.2. Responses from Normal Tissue in the Absence and Presence of L-NAME. No significant difference between responses (n=4).

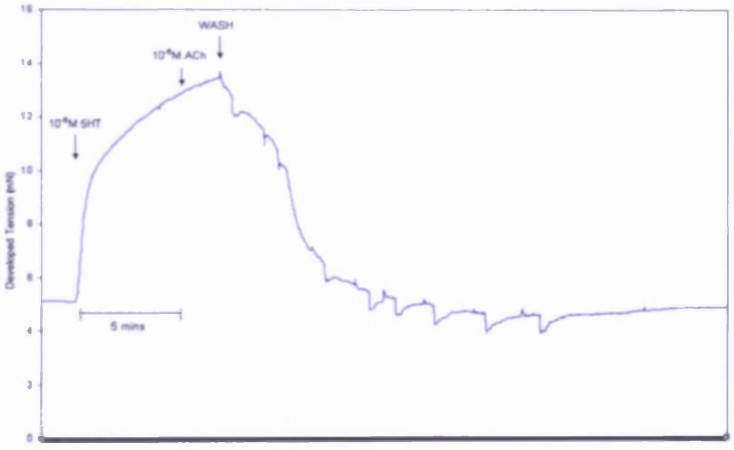

Figure 5.3. Representative Trace Showing Constriction and Relaxation Responses to Bolus Concentrations of 5HT and ACh (both 10^{-6}M) in Normal Tissues in the Presence of L-NAME. Arrows show the point at which agonists were added.

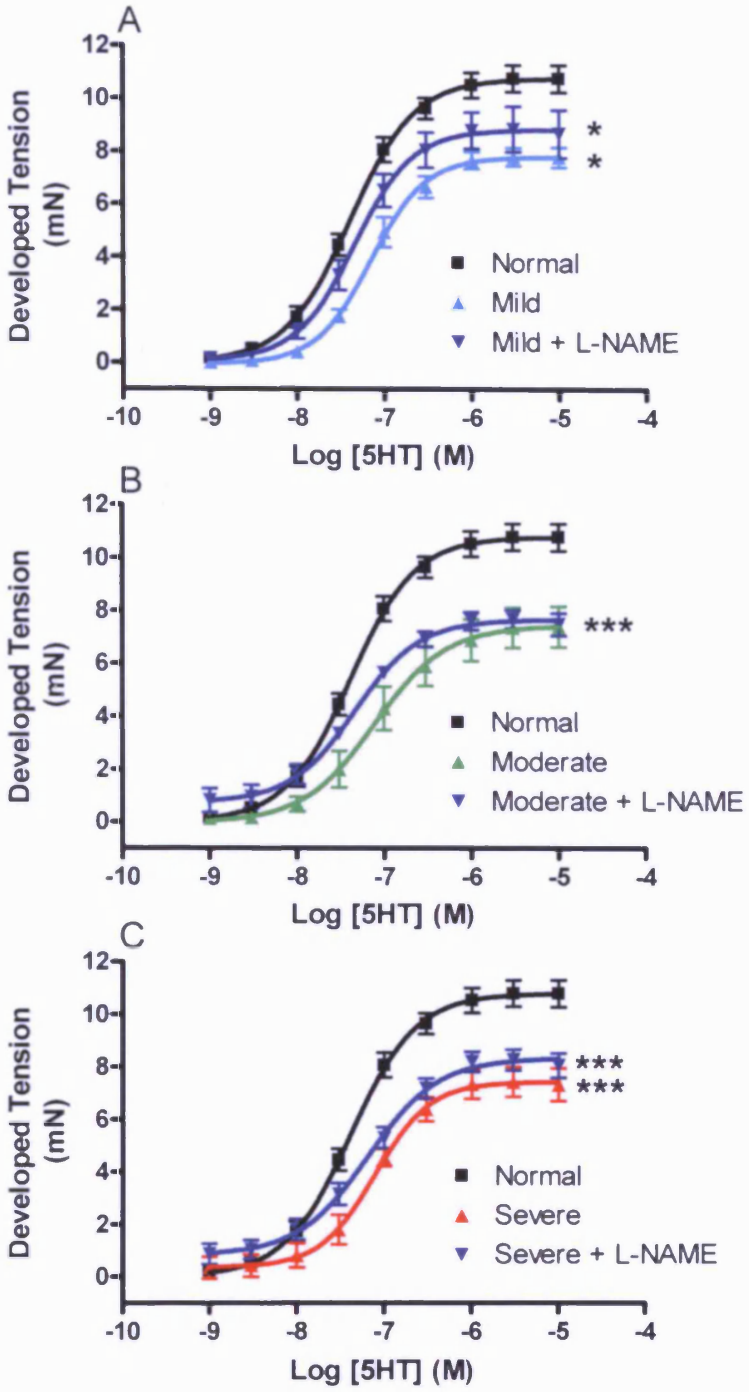

Figure 5.4. Graphs Showing Contractile Responses in Vessels from Normal and mCIA Animals in the Absence and Presence of L-NAME. A. Responses from normal (n=5) and mild (n=6) tissue, the latter in the absence and presence of L-NAME (n=6). B. The same responses in tissue from moderately (n=4) diseased animals with LNAME (n=4). C Responses in vessels from severe (n=5) animals and with LNAME (n=6). *$p<0.05$, **$p<0.01$ and ***$p<0.001$ for Rmax compared to normal analysed by one-way ANOVA followed by Newman-Keuls test.

	Rmax Values (mN)	Level of Significance Compared to Normal
Normal	10.80 ± 0.25	-
Mild	7.82 ± 0.92	*
Mild and LNAME	8.86 ± 0.36	*
Normal	10.80 ± 0.25	-
Moderate	7.44 ± 0.46	***
Moderate and LNAME	7.67 ± 0.22	***
Normal	10.80 ± 0.25	-
Severe	7.44 ± 0.30	***
Severe and LNAME	8.34 ± 0.28	***

	EC50 Values (M)	Level of Significance Compared to Normal
Normal	4.08×10^{-8}	-
Mild	7.04×10^{-8}	-
Mild and LNAME	4.55×10^{-8}	-
Normal	4.08×10^{-8}	-
Moderate	7.69×10^{-8}	-
Moderate and LNAME	4.56×10^{-8}	-
Normal	4.08×10^{-8}	-
Severe	7.79×10^{-8}	-
Severe and LNAME	6.45×10^{-8}	-

Table 5.1. Rmax and EC50 Values for Constrictions in the Absence and Presence of L-NAME. Raw data for responses shown in figure 5.5. *$p<0.05$, ***$p<0.001$ compared to normal.

5.4.2 Vessel Constriction in the Presence of 1400W

Preliminary experiments showed that 1400W had a minor, but not significant effect on 5HT-induced constriction responses in tissues from normal animals (see figure 5.5). Additionally the iNOS inhibitor had no effect on normal vessel relaxation indicating the preservation of fully functional eNOS (see figure 5.6). Vessels from experimentally arthritic animals exhibited the same impairment in 5HT-induced tension as observed in Chapter Four. Incubation of tissue from diseased animals with 1400W appeared to further dampen (significantly so in moderate ($p<0.01$) and severe ($p<0.05$) tissues) the maximum 5HT-induced tension (Rmax). Importantly all Rmax values for constriction responses in vessels from diseased animals (in the absence or presence of 1400W) were significantly ($p<0.05$) lower than those observed in normals (see figure 5.7). There was no significant statistical difference between the EC50 values for any groups (see table 5.2)

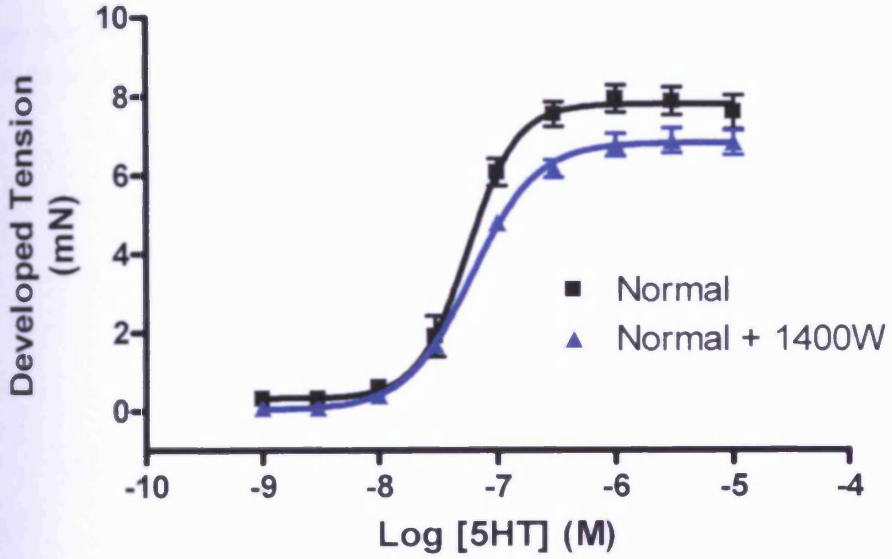

Figure 5.5. Constriction Responses in the Absence and Presence of 1400W in Normal Tissue. Constriction responses from normal tissue to 5HT in the presence and absence of 1400W (n=4).

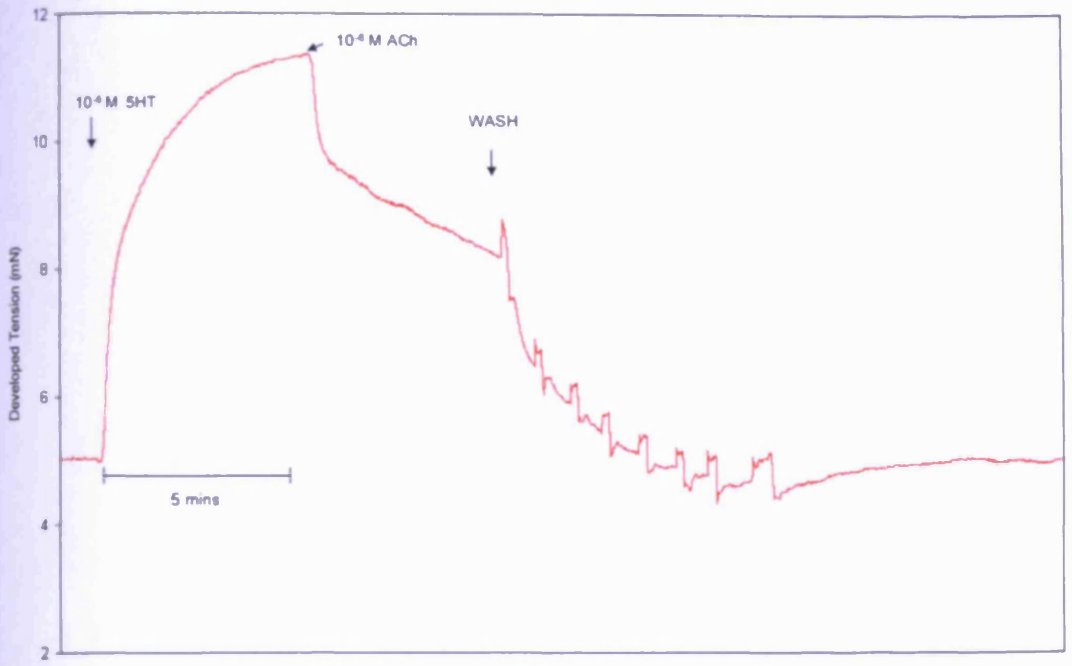

Figure 5.6. Representative Trace Showing Vessel Constriction and Relaxation in response to Bolus Concentrations of 5HT and ACh (both 10^{-6}M) in Normal Tissues in the Presence of 1400W. Arrows show the points at which the agonists were added.

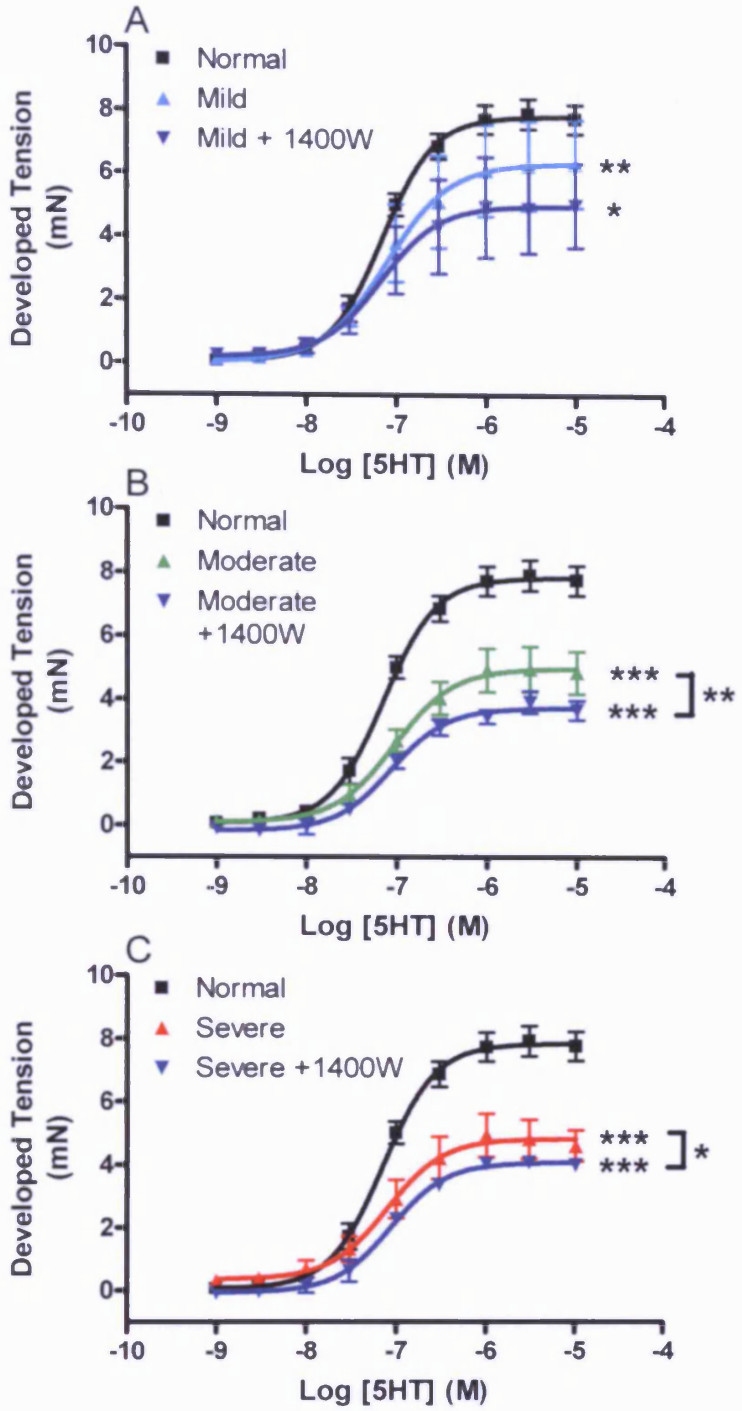

Figure 5.7. Graphs Showing Constriction Responses in Tissue from Normal and mCIA Animals in the Absence and Presence of 1400W. A. Constriction responses to 5HT from normal (n=5) and mild (n=4) tissue, the latter in the presence of 1400W. B. The same responses from moderate (n=3) tissue. C Responses from severe (n=3) tissues *p<0.05, **p<0.01 and ***p<0.001 for Rmax compared to normal analysed by one-way ANOVA followed by Newman-Keuls test. Bar indicates there is a significant difference between the two groups.

	Rmax Values (mN)	Level of Significance Compared to Normal
Normal	7.85 ± 0.21	-
Mild	6.34 ± 0.68	*
Mild and 1400W	5.00 ± 0.60	**
Normal	7.85 ± 0.21	-
Moderate	4.99 ± 0.29	***
Moderate and 1400W	3.74 ± 0.15	***/** compared to normal/moderate
Normal	7.85 ± 0.21	-
Severe	4.83 ± 0.30	***
Severe and 1400W	4.08 ± 0.11	***/** compared to normal/moderate

	EC50 Values (M)	Level of Significance Compared to Normal
Normal	7.10×10^{-8}	-
Mild	7.90×10^{-8}	-
Mild and 1400W	7.64×10^{-8}	-
Normal	7.10×10^{-8}	-
Moderate	9.32×10^{-8}	-
Moderate and 1400W	8.71×10^{-8}	-
Normal	7.10×10^{-8}	-
Severe	7.83×10^{-8}	-
Severe and 1400W	8.68×10^{-8}	-

Table 5.2. Rmax and EC50 Values for Constrictions in the Absence and Presence of 1400W. Raw data for responses shown in figure 5.9. *$p<0.05$, ***$p<0.001$ compared to normal unless indicated otherwise.

5.4.3 Vessel Relaxation in the Presence of 1400W

Relaxation responses were measured in vessels from normal and mCIA animals following 5HT-induced constriction to 70-80% of maximum in order to compare maximum relaxation responses in the presence of 1400W. The responses observed confirm that this agent had no effect on the eNOS-mediated relaxation responses to ACh. Incubation of tissue from mild and severely diseased animals with 1400W had no effect on relaxation responses. However in tissues from moderately affected animals, relaxation responses were significantly ($p<0.01$) greater in the presence of 1400W (see figure 5.8). EC50 values were not different between any groups (see table 5.3)

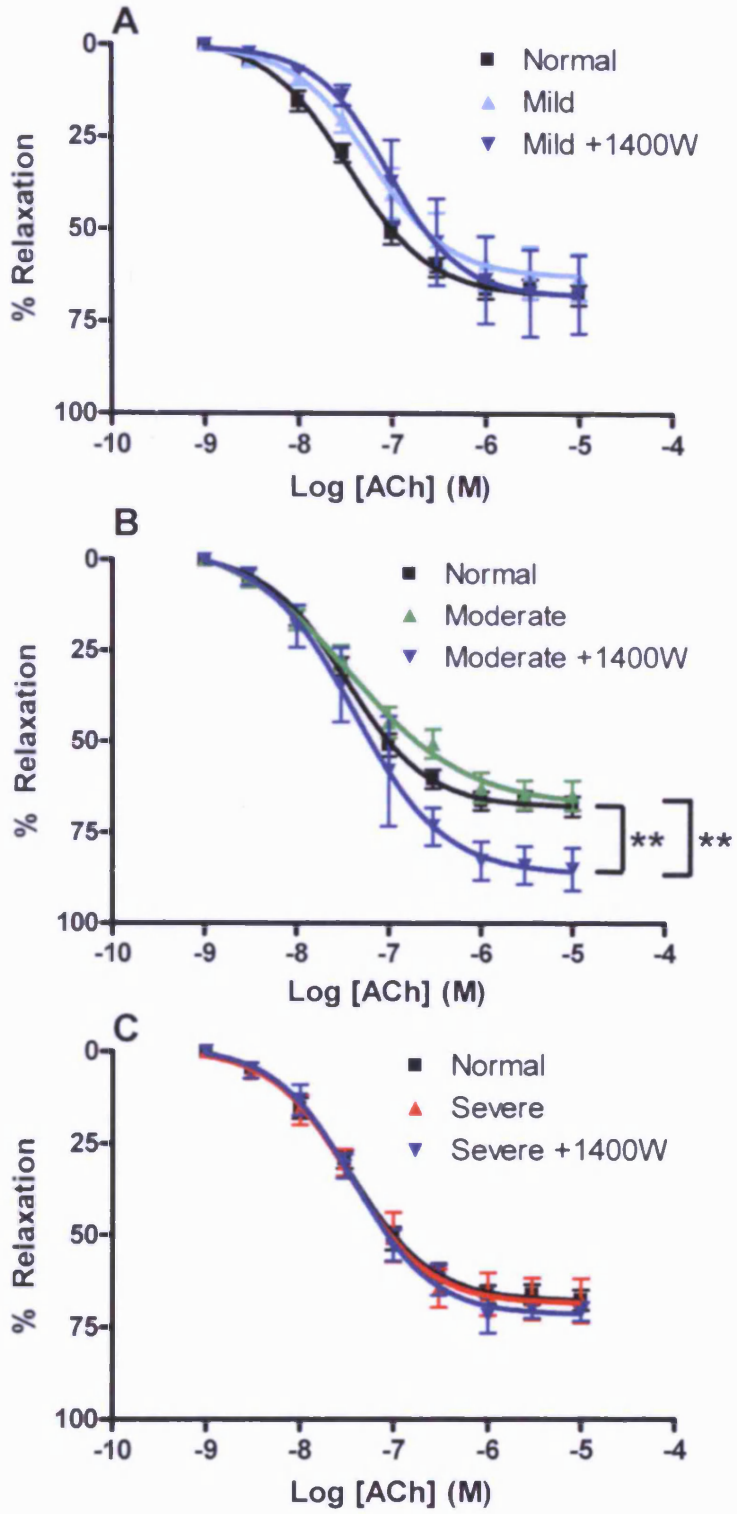

Figure 5.8. Graphs Showing Relaxation Responses in Tissue from Normal and mCIA Animals in the Absence and Presence of 1400W. A. Relaxation responses to ACh from normal (n=5) and mild (n=4) tissue, the latter in the presence of 1400W. B. The same responses from moderate (n=3) tissue. C Responses from severe (n=) tissues **$p<0.01$ for Rmax compared to normal, analysed by one-way ANOVA followed by Newman-Keuls test. .

	Rmax Values (%)	Level of Significance
Normal	67.93 ± 1.67	-
Mild	62.78 ± 3.92	-
Mild and 1400W	68.11 ± 5.86	-
Normal	67.93 ± 1.67	-
Moderate	67.52 ± 3.63	-
Moderate and 1400W	86.55 ± 5.29	** Compared to Normal/Moderate
Normal	67.93 ± 1.67	-
Severe	68.60 ± 3.10	-
Severe and 1400W	71.62 ± 2.23	-

	EC50 Values (M)	Level of Significance Compared to Normal
Normal	3.44×10^{-8}	-
Mild	5.97×10^{-8}	-
Mild and 1400W	9.15×10^{-8}	-
Normal	3.44×10^{-8}	-
Moderate	3.67×10^{-8}	-
Moderate and 1400W	4.13×10^{-8}	-
Normal	3.44×10^{-8}	-
Severe	3.46×10^{-8}	-
Severe and 1400W	3.76×10^{-8}	-

Table 5.3. Rmax and EC50 Values for Relaxations in the Absence and Presence of 1400W. Raw data for responses shown in figure 511. **$p<0.01$ compared to normal unless otherwise stated.

5.4.4 Analysis of Serum NO Metabolites Using Ozone-Based Chemiluminescence

Serum was prepared as appropriate from normal and mCIA animals. NO metabolites were analysed using ozone-based chemiluminescence. No differences between groups were observed (see figure 5.9).

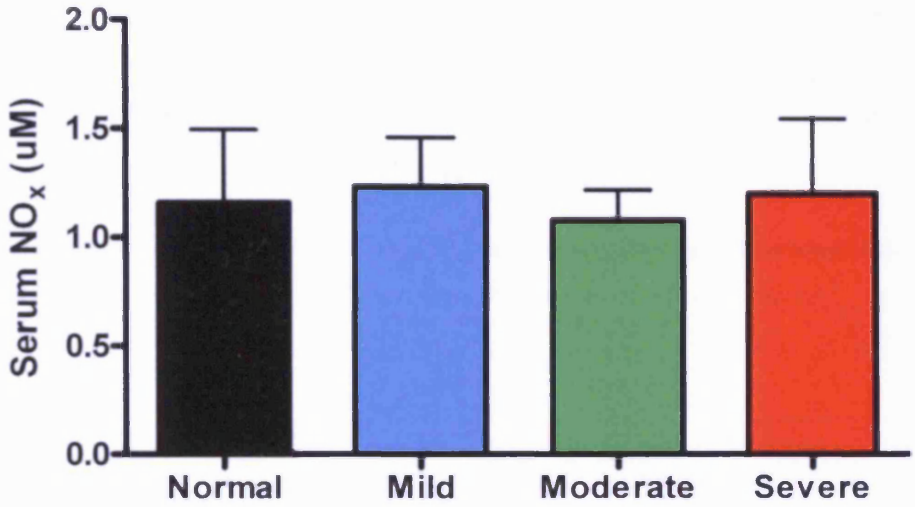

Figure 5.9. Serum NO Concentrations. NO metabolites were measured in the serum of normal (n=7) and mild (n=9), moderate (n=4) and severely (n=4) arthritic animals and expressed as serum NO_x (μM).

5.4.5 Vessel Constriction in the Presence of Indomethacin

Preliminary experiments showed that the presence of indomethacin had no significant effect on the constriction responses to 5HT in normal tissues (see figure 5.0), or the endothelium-dependent relaxation response to ACh (see figure 5.11). Incubation of tissue from diseased animals with indomethacin had no significant effects on their ability to constrict in response to 5HT (see figure 5.12). Rmax values were significantly ($p<0.01$) lower in vessels from mild, moderate and severely diseased animals compared to normal in both the absence and presence of indomethacin. There was no difference between EC50 values for these constrictions (see table 5.4).

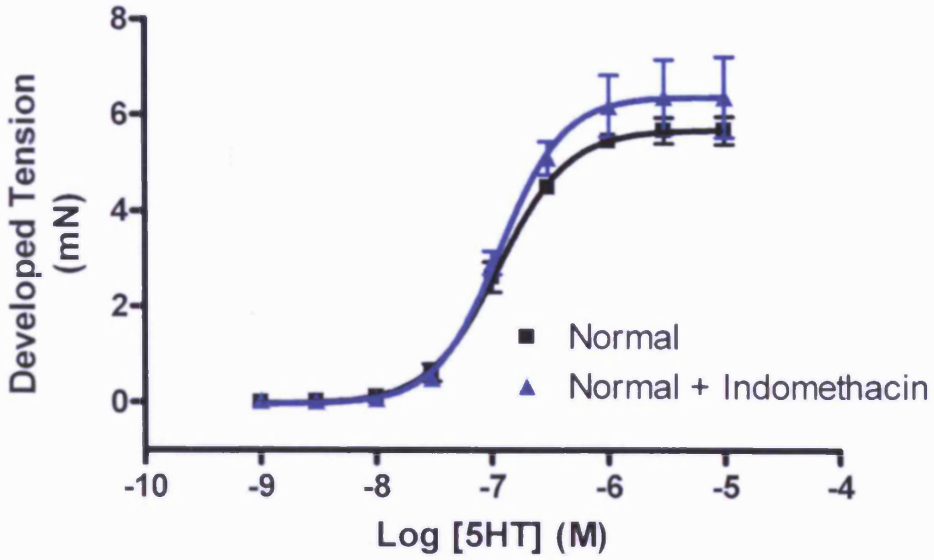

Figure 5.10. Constriction Responses in Normal Tissue in the Presence of Indomethacin. Constriction responses from normal tissue to 5HT in the presence and absence of indomethacin, n=3.

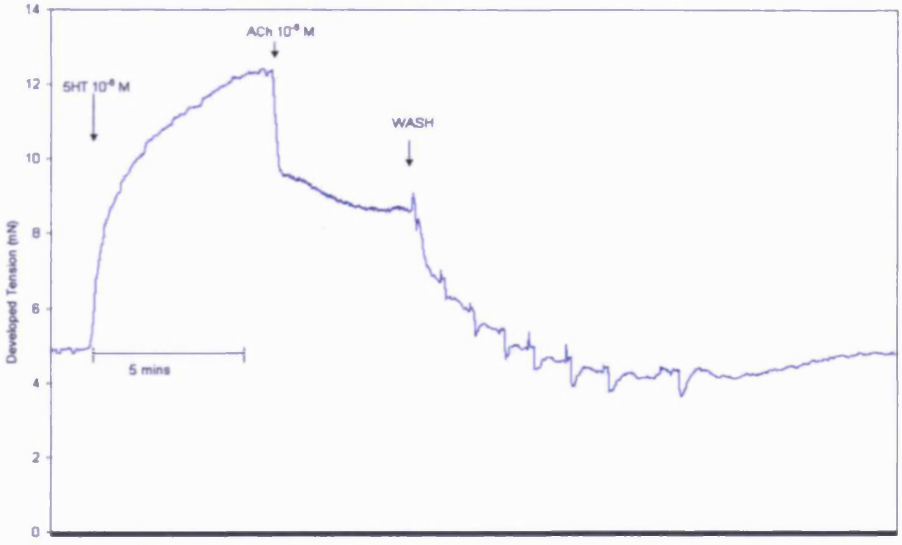

Figure 5.11. Representative Trace Showing Vessel Constriction and Relaxation in Normal Tissues in Response to Bolus Concentrations of 5HT and ACh (both 10^{-6}M) in the presence of Indomethacin. Arrows show the point at which agonists were added.

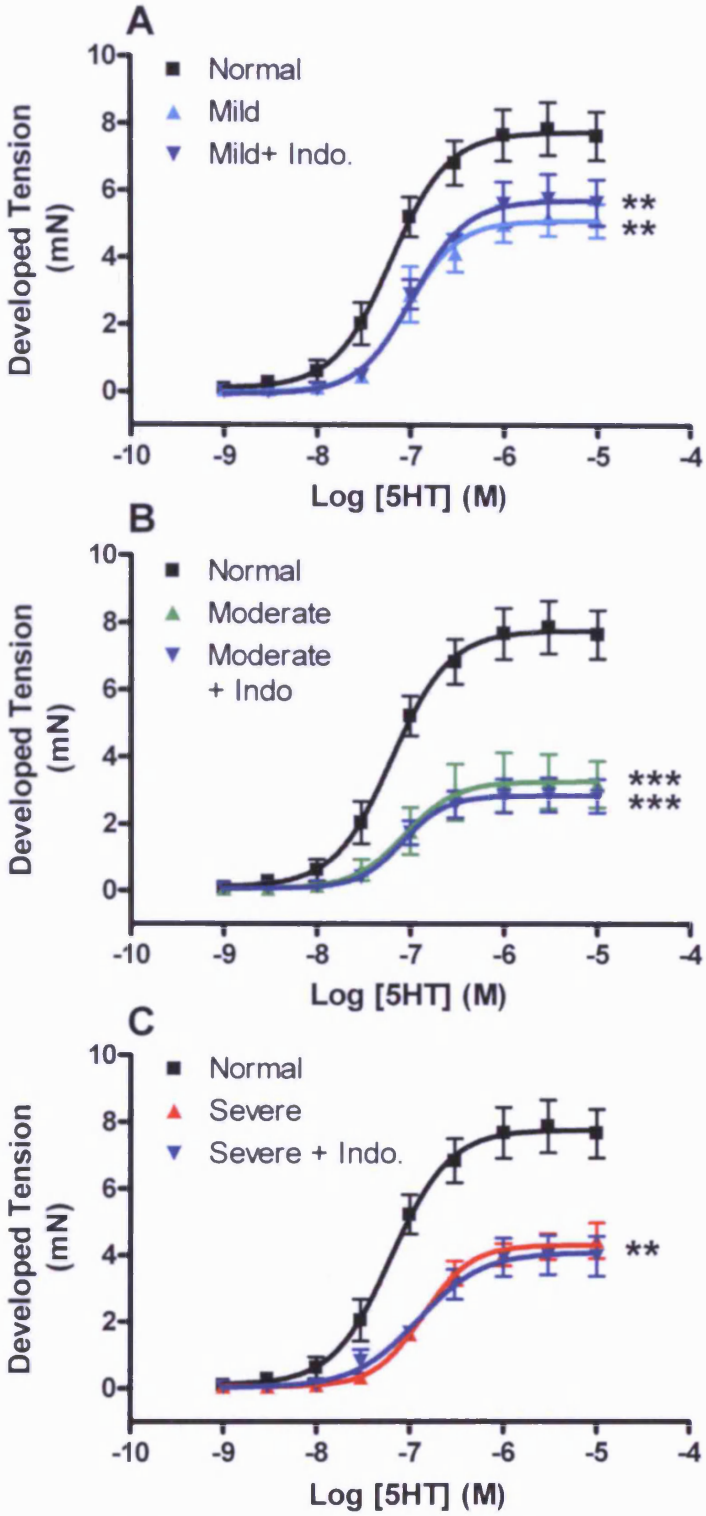

Figure 5.12. Graphs Showing Constriction Responses in Tissue from Normal and mCIA Animals in the Absence and Presence of Indomethacin. A. Constriction responses to 5HT from normal (n=3) and mild (n=3) tissue, the latter in the presence of indomethacin. B. The same responses from moderate (n=4) tissue. C Responses from severe (n=4) tissues **p<0.01, ***p<0.001 for Rmax compared to normal analysed by one-way ANOVA followed by Newman-Keuls test.

	Rmax Values (mN)	Level of Significance Compared to Normal
Normal	7.77 ± 0.32	-
Mild	5.11 ± 0.26	**
Mild and Indomethacin	5.72 ± 0.26	**
Normal	7.77 ± 0.32	-
Moderate	3.27 ± 0.34	***
Moderate and Indomethacin	2.85 ± 0.18	***
Normal	7.77 ± 0.32	-
Severe	4.28 ± 0.25	**
Severe and Indomethacin	4.17 ± 0.33	**

	EC50 Values (M)	Level of Significance Compared to Normal
Normal	6.34×10^{-8}	-
Mild	9.39×10^{-8}	-
Mild and Indomethacin	1.06×10^{-7}	-
Normal	6.34×10^{-8}	-
Moderate	8.64×10^{-8}	-
Moderate and Indomethacin	8.16×10^{-8}	-
Normal	6.34×10^{-8}	-
Severe	1.40×10^{-8}	-
Severe and Indomethacin	1.39×10^{-8}	-

Table 5.4. Rmax and EC50 Values for Constrictions in the Absence and Presence of Indomethacin. Raw data for responses shown in figure 5.16. **$p<0.01$ compared to normal. Bar indicates statistical difference between groups.

5.4.6 Vessel Relaxation in the Presence of Indomethacin

Relaxation responses were measured in vessels from normal and mCIA animals following 5HT-induced constriction to 70-80% of maximum in order to compare relaxation responses in the presence of indomethacin. The responses in the presence of indomethacin demonstrated this agent had the ability to increase the amount of relaxation the vessel could achieve (see figure 5.13). Rmax relaxation values in tissues from mild, moderate and severe animals were significantly ($p<0.05$) lower in the presence of indomethacin compared to normal and the disease counterparts (see table 5.5). EC50 values showed no difference for either moderate or severe cohorts, however, mild relaxation in the presence of indomethacin demonstrated a lower EC50 value compared to normal.

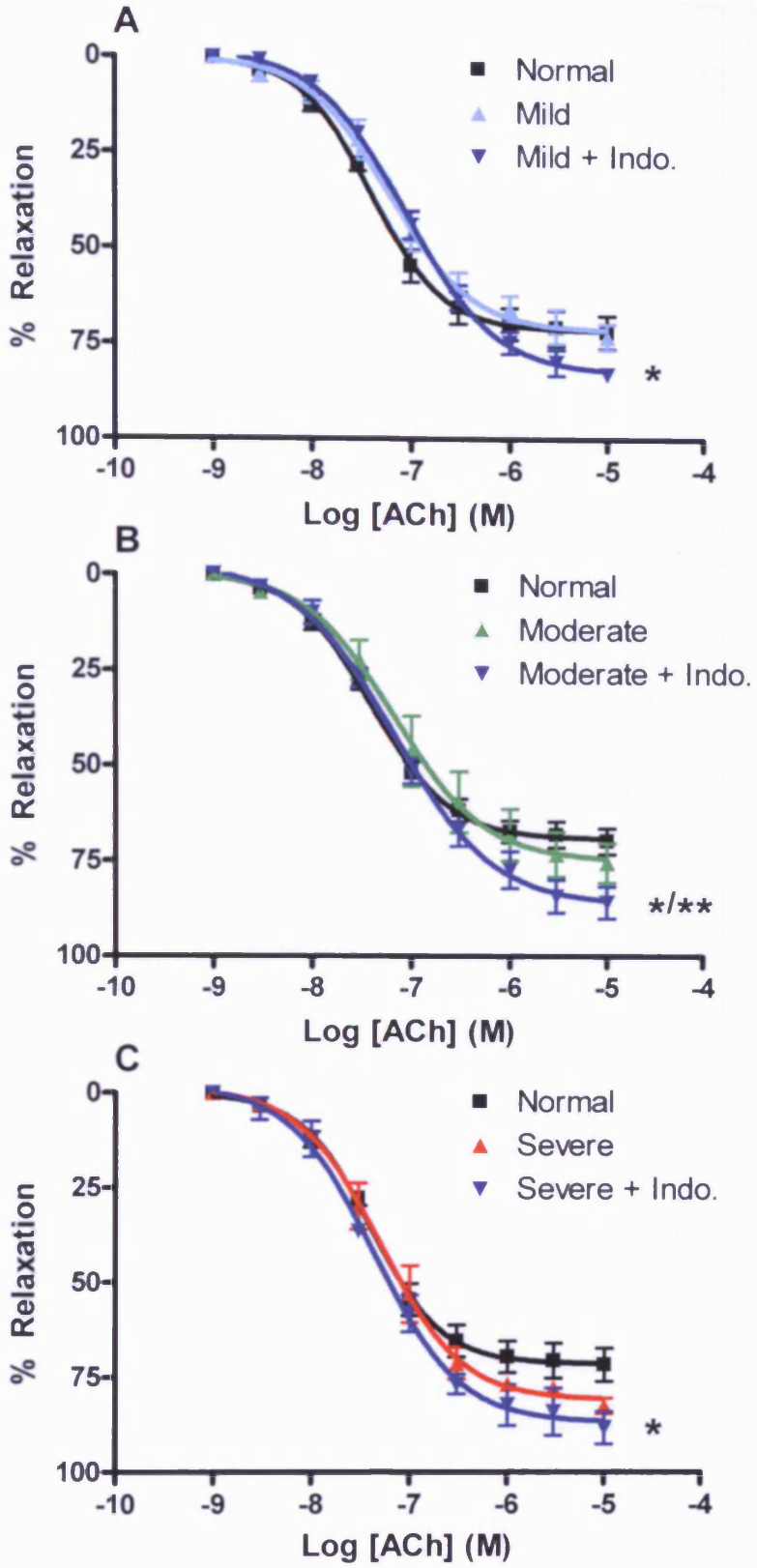

Figure 5.13. Graphs Showing Relaxation Responses in Tissue from Normal and mCIA Animals in the Absence and Presence of Indomethacin. A. Relaxation responses to ACh from normal (n=6) and mild (n=4) tissue, the latter in the presence of indomethacin *$p<0.05$ compared to normal and mild. B. The same responses from moderate (n=4) tissue *$p<0.05$ compared to moderate, **$p<0.01$ compared to normal. C Responses from severe (n=3) tissues *$p<0.05$ compared to normal determined by one-way ANOVA followed by Newman-Keuls test.

	Rmax Values (%)	Level of Significance
Normal	71.47 ± 2.07	-
Mild	71.62 ± 2.40	-
Mild and Indomethacin	82.82 ± 1.81	* Compared to Normal/Mild
Normal	71.47 ± 2.07	-
Moderate	75.02 ± 4.33	-
Moderate and Indomethacin	86.48 ± 2.92	*/** Compared to Moderate/Normal
Normal	71.47 ± 2.07	-
Severe	80.96 ± 2.18	-
Severe and Indomethacin	86.96 ± 2.56	* Compared to Normal

	EC50 Values (M)	Level of Significance Compared to Normal
Normal	4.08×10^{-8}	-
Mild	6.10×10^{-8}	-
Mild and Indomethacin	8.82×10^{-8}	*
Normal	4.08×10^{-8}	-
Moderate	6.70×10^{-8}	-
Moderate and Indomethacin	6.68×10^{-8}	-
Normal	4.08×10^{-8}	-
Severe	5.01×10^{-8}	-
Severe and Indomethacin	4.35×10^{-8}	-

Table 5.5. Rmax and EC50 Values for Relaxations in the Absence and Presence of Indomethacin. Raw data for responses shown in figure 5.18. *$p<0.05$, **$p<0.01$.

5.5 Discussion

5.5.1 The Role of NO in Impaired Constriction Responses in the mCIA Model

5.5.1.1 Inhibition of NOS Isoforms

Following the observation of impaired agonist-induced constriction responses in tissue from the mCIA model (Chapter Four), it was considered that excess production of NO may play a role in this dysfunction. To investigate this possibility 5HT-induced constriction was assessed in the presence of a broad spectrum NOS inhibitor, L-NAME. Preliminary experiments showed that L-NAME did not induce increased constriction responses in normal tissues but did completely inhibit the relaxation responses to ACh, the latter confirming total eNOS inhibition. Subsequent studies confirmed the observations of Chapter Four in that vessels taken from diseased animals exhibited blunted constriction responses. Interestingly, incubation with L-NAME produced only minor non-significant improvements in constriction responses in these tissues. While the latter may indicate that basal NOS activity is increased in the disease state, overall these data would suggest that increased production of NO is not involved in the impaired agonist-induced constriction responses in the mCIA model.

To eliminate a specific role for iNOS in the mCIA impaired constrictor responses, experiments in the presence of 1400W were also carried out. Importantly this agent had no effect on relaxation responses to ACh and therefore had no discernable action on eNOS. With regard to constriction responses to 5HT in tissues from diseased animals, in the presence 1400W further significant (at least for moderate and severe tissues) impairment was observed. While the reason for this action is unknown, there is a possibility that 1400W could interfere with the receptor function/reactivity to 5HT preventing the agonist from exerting its full effect. However these receptors are not characterised in this strain nor is any such phenomenon reported in the literature making this pure speculation. Regardless of the mechanism underlying this minor effect of 1400W in these experiments, these results imply that with respect to the mCIA model,

an increased production of NO via iNOS is not the cause of the decreased constriction observed in the diseased tissue.

In the presence of 1400W relaxation responses to ACh in normal, mild or severe tissues showed no change compared to their appropriate controls. However, in tissue from moderately arthritic animals the presence of 1400W caused a significantly larger relaxation compared to untreated moderate tissues. Again while there is no specific explanation for this action, the reduced constriction achieved may result in the vessel being more susceptible to a higher relative relaxation following stimulation with ACh; the less tension a vessel constricts to, the less relaxation is needed for its return to baseline. However, that this observation was not reproduced in severe tissue, which exhibited similar constriction responses, would argue against this. A further possibility is that 1400W may act as a substrate for eNOS rather than inhibitor for iNOS thus providing greater vasodilatory potential, although considering the vast difference in the affinity of iNOS over eNOS for 1400W (Garvey, Oplinger et al. 1997; Boer, Ulrich et al. 2000), makes this unlikely. Indeed pinpointing this mechanism is not the main thrust of this thesis. Importantly, these data do not seem to support a role for NO in the dampened constriction responses in tissues from mCIA animals.

A confounding factor in the measurement of NO_x described above is the presence of excess haemoglobin (Hb) in the serum due to red blood cell (RBC) lysis. Hb has a high affinity for NO and thus binds rapidly, an action that may hamper the required reduction in the reaction chamber (described above). NO metabolites, Hb-bound or otherwise, will eventually be reduced. The Hb contamination has the disadvantage of producing a broader peak for analysis thereby reducing the sensitivity of the assay giving a lower estimation of NO_x (Rogers, Khalatbari et al. 2005). Interestingly, patients with RA have been reported to present haemolysis as a result of the disease (Maharaj 1986). Whether this occurs in the mCIA model has not been described.

Following centrifugation of blood samples, taken from mCIA and control mice by cardiac puncture, the resulting serum invariably displayed a certain level of "pinkness" due to the presence of Hb. It is most likely that this is derived from RBC lysis during sample collection/preparation rather than pathological haemolysis. Even with the greatest of care, and the fact that the procedure was standardised and identical for each blood retrieval, this was virtually impossible to avoid in our hands. As such this could certainly contribute to subsequent complications upon NO analysis. However given that serum taken from normal animals was similarly contaminated with Hb does not explain why a difference was not observed between mCIA animals and controls in the present study. More likely it would seem to confirm the data presented here indicating that the reduction in contractile ability in the mCIA model is not attributable to increased NO levels.

5.5.2 The Role of PGI_2 in Impaired Constriction Responses in the mCIA Model

5.5.2.1 Inhibition of COX Isoforms during Vascular Assessment

To eliminate a specific role for COX in the mCIA impaired constrictor responses experiments were carried out in the presence of indomethacin. This agent did not affect constriction or relaxation responses to 5HT and ACh respectively, the latter indicating no obvious effect on eNOS function. In the presence of indomethacin constriction responses in the mCIA model showed no change compared to their normal counterparts, suggesting increased production of COX products, namely PGI_2, are not responsible for the decrease in vessel contractility observed in Chapter Four.

In the presence of indomethacin relaxation responses from mCIA tissue exhibited a significantly lower maximum relaxation capability compared to untreated disease controls and normals. The possibility that indomethacin acts as a substrate for COX would explain this change however there is no evidence in the literature to support this. Indeed given the widespread use of indomethacin, this seems an unlikely theory. More likely is that another COX product may be affecting vessel tone. Endothelial COX is

responsible for the production of arachidonic metabolites, one of which is the vasoconstrictor thromboxane A1 (TXA_1) (Vanhoutte 2009). Removal of basal levels of TXA_1 by indomethacin may therefore increase the relaxing potential of the tissues seen here. While this is an interesting theory, to further characterise these issues is outside the scope of this thesis.

COX activity in experimental arthritis has however been investigated in some depth by other groups. In the collagen antibody-induced arthritis (CAIA) model, the presence of a PGI_2 receptor (IP) antagonist resulted in a reduction in the severity of arthritis developed in experimental arthritis (Pulichino, Rowland et al. 2006). Furthermore emphasising the importance of PGI_2 signalling is the development of a milder form of experimental arthritis in an IP knockout model of experimental arthritis (Honda, Segi-Nishida et al. 2006; Pulichino, Rowland et al. 2006). In this CAIA model increased synovial levels of PGI_2 were also reported throughout the development of disease (Pulichino, Rowland et al. 2006) an observation that has also been reported systemically in RA patients (Hishinuma, Nakamura et al. 2001). Why elevations of PGI_2 have been reported by others yet COX inhibition does not reverse the vascular dysfunction demonstrated in the present model is intriguing and there are several reasons why this may be. For instance the concentration of indomethacin used may not be sufficient for total inhibition of COX-2. That indomethacin is a broad spectrum inhibitor, and moreover was used at a concentration reported to be efficient by many in the published literature, makes this seem unlikely. However, the possibility remains that COX activity may have been upregulated to such an extent that it could not be inhibited by the *ex vivo* exposure to indomethacin.

Given that PGI_2 signalling in VSMC is mediated via plasma membrane IP receptors, leading to activation of AC, the production of cAMP and vasorelaxation (Vanhoutte 1998), a further way to assess the role of PGI_2 in mCIA vessel dysfunction would have been to measure the cAMP levels in the isolated vessels. If COX was extensively upregulated as suggested above then tissues would be expected to contain high levels of

cAMP which could mediate the dampened contraction responses. Unfortunately time constraints and availability of tissue did not allow for such experiments to take place. Obviously such measurements would have been useful, but given the observations that follow in subsequent chapters, their absence does not detract from the impact of this thesis.

Another possibility is that any change in COX-1 and COX-2 activity (which may or may not have occurred in the present model) could impact on the sensitivity of the vessels to 5HT. This theory is based on the observation that induction of inflammation is capable of upregulating COX-2 and subsequently impairs vessel reactivity to NA in internal mammary arteries (Foudi, Louedec et al. 2009). If this were the case in mCIA vessels it may explain the change in reactivity throughout the progression in disease. Indeed it would imply that changes to the vessel wall were permanent since indomethacin failed to reverse the diminished constriction. Without direct measurements of COX activity, which are notoriously difficult to make, this cannot be proven one way or the other and again remains a topic of speculation.

Essentially, the *ex-vivo* experiments described above demonstrate that indomethacin has no significant effect on vessel function and suggests that PGI_2 does not contribute directly to the observed impaired contractile responses. Indeed a multitude of other factors may be responsible for these irreversible alterations to vessel function. Some of these will be investigated in subsequent chapters

5.5.3 Batch Variation

Experiments carried out in this chapter have unearthed discrepancies in vessel function between batches. Constriction in normal vessels in the presence and absence of L-NAME saw an average Rmax for developed tension of 10.8mN. This surpassed previous observations described in Chapter Four where average Rmax values were 6.22mN. This was echoed in the mCIA tissue in this batch; constrictions from all three cohorts were

notably higher in the latter experiments. In addition to this, the trend in vessel dysfunction throughout the progression of mCIA in this chapter was not as observed in Chapter Four. As all batches and animals therein were subjected to the same housing environment and conditions surrounding mCIA induction, differences may be attributed to batch-dependent biological variation. One cause of this could be the age at which the mice were used; animals were purchased at 6-8 weeks, those falling into the lower spectrum may have slightly different vessel function. However, as animals were not subjected to experimentation until they are deemed adult, at 8-10 weeks, this would be an unexpected occurrence. Alternatively these differences could be attributed to the "grey area" described between cohorts. Animals from one cohort may display less or more severe characteristics due to the individual progression of arthritis. This would also provide explanation for the observation in the indomethacin condition, where vessels from moderate animals failed to reach the Rmax attained by severe vessels.

In addition to contractile difference, slight variances in normal vessel relaxation are shown. With respect to their batch-mates and the progression of mCIA no significant difference was seen between relaxations and adequate endothelial function was presumed.

Despite the changes shown here, throughout the work in this thesis the overall pattern was similar within each batch of animals. To avoid any discrepancies every effort was made to ensure that animals were used from their respective batch for each experimental condition.

5.5.4 Further Work

Eliminating the role of NOS and COX activity in the pathology of decreased vasculature function has led to the conclusion that the contractile mechanism of the smooth muscle is compromised. As such, this investigation will now focus on changes in the inflammatory milieu which could present structural/mechanical changes in VSMCs in

this model. At present no findings similar to these have been described in this model. However, in a mouse model of Marfans' syndrome a decreased contractile ability has been observed. Subsequently this has been attributed to an increase in MMP-9, with elastin fragmentation and loss of compliance observed as a consequence (Chung, Au Yeung et al. 2007). Related to this is the widely documented occurrence of high blood pressure in human RA (Zieman, Melenovsky et al. 2005; Tsioufis, Dimitriadis et al. 2007; Panoulas, Metsios et al. 2008), and that arterial stiffening is also an acknowledged pathology in this disease(Bazzichi, Ghiadoni et al. 2009). That these parameters have not until now been investigated in this model warrants further study.

CHAPTER 6

VASCULAR DYSFUNCTION IN MCIA: A ROLE FOR MMP-9

6.1 Introduction

The data collected in Chapter Five indicates that the vascular dysfunction present in mCIA animals cannot be directly attributed to changes in NOS or COX activity. It is more likely that structural/mechanical changes to the vascular wall contribute to this dysfunction, though how this arises remains unclear.

An extensive literature search established that similar observations have been made in the vasculature of the mouse model of Marfan syndrome (Chung, Au Yeung et al. 2007). The latter is a connective tissue disease in which thoracic aortic aneurysm (AA) is a life-threatening complication leading to aortic rupture, dissection and sudden death (El-Hamamsy and Yacoub 2009). In this model, receptor-mediated VSMC contraction and K^+-induced depolarisation were markedly reduced compared to normal animals. Moreover, this dysfunction was associated with an increase in expression of the gelatinases MMP-2 and MMP-9 and elastin fragmentation (digestion of the elastic component of the vessel wall) (Chung, Au Yeung et al. 2007). Importantly these MMPs play a significant role in the degradation of elastin (Yasmin, McEniery et al. 2005), and in the Marfan model such an action appeared to contribute to the loss of compliance in the vessel wall. It is important to note here that MMP-9 is not the only MMP with elastolytic capabilities, for example MMP-12 is also called metalloelastase. However the focus of this thesis is to be largely on MMP-9 and as such this MMP is discussed in detail in this thesis.

Both the constitutive MMP-2, and the inducible MMP-9 have been associated with the development of arterial stiffness and systolic hypertension (Yasmin, McEniery et al. 2005; Flamant, Placier et al. 2007), pathologies which have been described extensively in human RA (Panoulas, Douglas et al. 2007; Bazzichi, Ghiadoni et al. 2009; Galarraga,

Khan et al. 2009). That increased levels of MMP-9 in particular have been observed in human RA, and moreover in experimental models of the disease (Chia, Chen et al. 2008), demonstrates the need for more detailed investigations with regard to the role of MMP-9 in vascular/blood pressure changes in the mCIA model.

6.1.1 MMP-9 in RA

MMP-9 is intrinsically involved in both disease progression and pathology in RA (described in more detail in section 1.6.2). Briefly, in human RA, an imbalance arises between the activity/levels of MMP-9 and its endogenous inhibitor TIMP (Jackson, Arkell et al. 1998), and as such MMP-9 is regarded as a prime contributor to joint damage (Yoshihara, Nakamura et al. 2000). The importance of this enzyme in RA is further highlighted by the observation that MMP-9 knock-out mice fail to develop antibody-induced experimental arthritis to the same degree as wild-types (Itoh, Matsuda et al. 2002).

Primary cellular sources of MMP-9 include macrophages, osteoclasts, SFs and neutrophils, with various cytokines such as IL1-β, TNF-α and IFNγ promoting MMP-9 activation and secretion (Van den Steen, Dubois et al. 2002; Tchetverikov, Ronday et al. 2004; Chia, Chen et al. 2008; Garvin, Nilsson et al. 2008). Moreover, in a collagen type II-specific monoclonal antibody-induced arthritis model, limb joint MMP-9 levels are also increased in SFs, chondrocytes and monocytes (Chia, Chen et al. 2008). With regard to the present thesis, the question is whether an increase in MMP-9 associated with increasing arthritic severity is reflected in the vasculature and as such contributes to the observed vascular dysfunction.

6.1.2 Possible mediators of MMP-9 Upregulation

The extensive inflammatory pathways in the mCIA model (Marinova-Mutafchieva, Williams et al. 1997) imply that increased MMP-9 levels may be upregulated by a multitude of mediators (Stolina, Bolon et al. 2008). Of these the cytokine IL-1β would seem to be of particular relevance given that various studies have characterised a link

between MMP-9 and the activity of this cytokine. For instance following stimulation of rat VSMCs with IL-1β, an increase in the level of MMP-9 mRNA was observed (Gurjar, DeLeon et al. 2001; Gurjar, Deleon et al. 2001). Additionally stimulation of cultured myometrial smooth muscle cells with IL-1β also produced a similar dose-dependent increase in MMP-9 levels (Roh, Oh et al. 2000). As such these studies emphasise the positive effect IL-1β has on MMP-9 production.

Importantly blood serum and joint tissue IL-1β levels have been measured in the mCIA model (MD) thesis, Cardiff University, "STAT-1 and STAT-3 signalling in Collagen Induced Arthritis: Towards New Therapeutic Targets for Rheumatoid Arthritis" Dr Shaun Smale 2010). In both cases, while little change is observed following the initial immunisation, the gradual and significant rise from day 22 (see figure 6.1 and 6.2 respectively) follows the increase in disease severity described in the present thesis (see Chapter 4). As such the increase in IL-1β shown here is associated with tissue damage, and given the studies described above, could well be involved in upregulating MMP-9 production/activity. Whether changes in MMP-9 follow those of IL-1β is unknown. Further investigations are therefore essential.

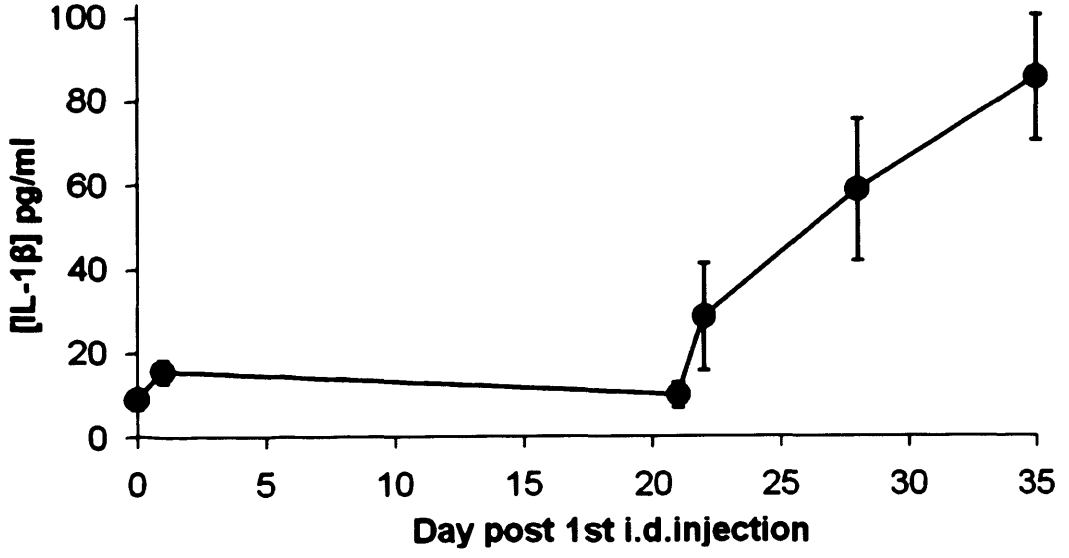

Figure 6.1. Serum IL-1β Levels in the mCIA model. Reproduced from MD, Cardiff University, "STAT-1 and STAT-3 signalling in Collagen Induced Arthritis: Towards New Therapeutic Targets for Rheumatoid Arthritis" (2010) Dr Shaun Smale with kind permission.

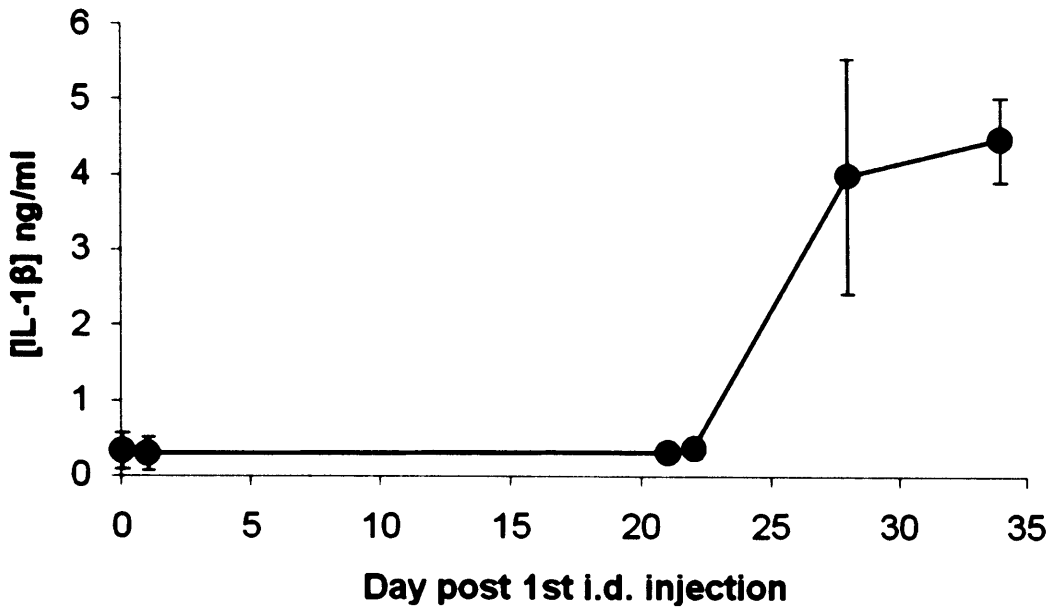

Figure 6.2. Paw Homogenate IL-1β Levels in the mCIA model. Reproduced from MD thesis, Cardiff University, "STAT-1 and STAT-3 signalling in Collagen Induced Arthritis: Towards New Therapeutic Targets for Rheumatoid Arthritis" (2010) Dr Shaun Smale with kind permission.

The working hypothesis of this chapter is that MMP-9 will be upregulated in the aorta in conjunction with increasing arthritic score and therefore contribute to increasing vascular dysfunction.

6.2 Aims

To investigate any changes to blood pressure following mCIA induction (measurement of this parameter in this model has not been reported previously).

To measure the levels of MMP-9 in the paw, serum and aorta from naïve animals and arthritic mice at varying stages of disease severity

To examine the effect of IL-1β on the contractility of aortic samples taken from naïve animals and whether this may also induce MMP-9 production.

To investigate the effect of exogenous MMP-9 on the contractility of naïve vessels.

To assess *ex-vivo* whether an MMP-9 inhibitor can reverse the vascular dysfunction observed in aortic tissues isolated from animals with mCIA.

To determine the site/where MMP-9 is localised within arthritic paws during mCIA.

6.3 Methods

6.3.1 Induction of mCIA

Animals were housed as described in section 2.1. Following a settling in period mCIA was induced in 6-8 week DBA/1 animals as described in section 2.2.

6.3.2 Blood Pressure Analysis by Photoplethysmography

Blood pressure analysis was carried out in a room preheated and maintained at 26-30°C and all readings were undertaken on a heated mat at 30°C to limit extraneous effects of temperature. Importantly at temperatures higher than 23°C blood flow to the caudal artery of the tail is enhanced as part of the mouse thermoregulation system, a process necessary for accurate blood pressure measurement (Krege, Hodgin et al. 1995). To achieve such measurements animals were restrained (for up to ten minutes) in a small mouse holder (Kent Scientific) enclosed in a dark tube to avoid over-saturation of the light signal (see below) and to minimise stress for the animal. To further minimise stress effects animals were trained prior to the commencement of this experimental procedure by subjecting them to daily ten minute periods in the restrainer whilst wearing the blood pressure measuring apparatus (see below) as previously suggested (Krege, Hodgin et al. 1995). Importantly it was also essential that the animals remained very still to avoid movement interference.

Systolic blood pressure was measured in the animals using a non-invasive Harvard Mouse Tail Photoplethysmography Pressure Monitor (Harvard apparatus USA). This apparatus utilises a tail cuff consisting of a plastic tube lined with a rubber bladder, placed at the base of the tail to occlude blood flow (the O-cuff), and a non-invasive infra-red light diode blood flow sensor placed distal to the occlusive cuff to monitor the pulse signal wave. The light source illuminates a small area of the tail, and attempts to measure the pulse, recording it as the pulse signal wave. Initially both cuffs were slipped on to the tail ensuring that the infra-red light was positioned to cross the tail in the same orientation every time. The balloon within the O-cuff was then inflated to a given pressure (around 200mm Hg) in order to halt blood flow. Following careful and slow cuff release the infra-red sensor detected the first appearance of blood flow on its return to the tail vessel. At the point where the increase in pulse signal wave becomes linear (see figure 6.5) the pressure value of the cuff is noted to represent the animal's systolic blood pressure. Maximum cuff pressure (mm/Hg), cycling interval (min), and inflation-deflation rates (mmHg/sec) were kept constant by the Harvard Mouse Tail Photoplethysmography Pressure Monitor to which the cuffs were attached. The BP monitor was connected to a PC via a PowerLab bridge amplifier and the data visualised using Chart for Windows (AD Instruments, UK).

Repeat measurements (a minimum of 8 for each animal) were taken over a period of ten minutes once the animal had settled calmly in the restraining cage. An average of these measurements was then calculated for each animal.

As can be seen from the trace in figure 6.3, there are several points at which the pulse could be taken. To avoid introducing bias into these measurements, the criteria for the point at which the measurement would be taken was pre-agreed; previously published mouse blood pressure has been seen to be around 120mm/Hg (Krege, Hodgin et al. 1995; Tilley, Audoly et al. 1999). In preliminary measurements, the point at which the pulse signal wave became linear that was closest to these values was taken as the reading point and subsequently used for all future measurement. Following which all measurements were taken blindly and by two different assessors to minimise variability.

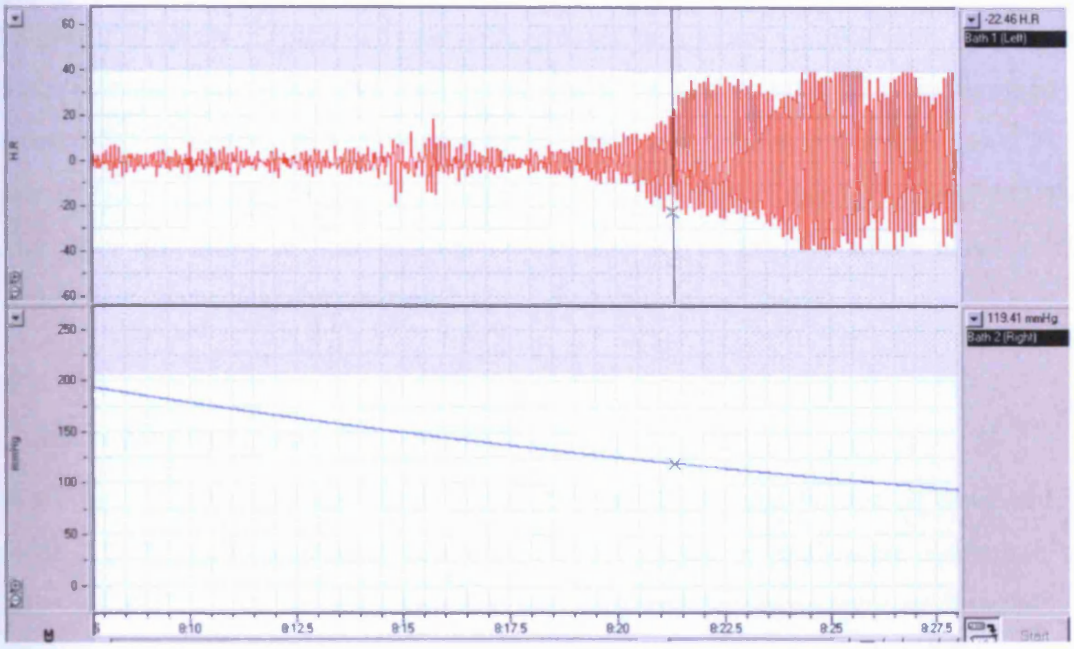

Figure 6.3. Diagram Depicting the Trace from the Blood Pressure Sensor. The top graph represents the pulse signal wave, the bottom the change in pressure. As the air is released from the balloon the pressure on the vessel decreases and blood flow resumes in the vessel. The pressure is taken when the increase in the pulse signal wave becomes linear – depicted here with the black line. From the graph below this the blood pressure can then be read. This trace shows the blood pressure as 119.41mm/Hg.

Blood pressure readings were taken in naive animals before the induction of arthritis, following which measurements were taken from each of the arthritic severity groups at appropriate time points.

6.3.3 Tissue and Serum Collection

Serum was collected from animals post-euthanasia at appropriate time points as described in section 2.3.1. Tissue and paws were removed and treated as described in section 2.3.2i, and 2.3.2ii respectively.

6.3.4 Analysing Levels of MMP-9 in the mCIA Model by ELISA

Total MMP-9 levels in aortic and paw homogenates, and serum samples were detected by ELISA (Mouse Total MMP-9 Quantikine ELISA Kit R and D, MMPT90) as described in section 2.7.2. Following this the total protein levels were elucidated (see section 2.7) in order to normalise the data. It is important to note here that measuring total MMP-9 levels does not allow a determination of the role active MMP-9 solely plays in the development of vascular dysfunction.

6.3.5 Myography: Incubations with IL-1β

DBA/1 mice aged 6-8 weeks were obtained from Harlan and housed as described in section 2.1. At appropriate time points mCIA and control animals were euthanised by inhalation of CO_2 and the aorta removed and prepared for myography as described in section 2.3.2i. Following excision and cleaning, aortic rings were incubated following a previously described protocol (Zemse, Hilgers et al. 2007). Briefly rings were placed in 2ml of Dulbecco's Modified Eagle Medium (DMEM) (1X), liquid (low glucose) (22320-022, GIBCO), supplemented with foetal calf serum (FCS) (10% v/v), penicillin/streptomycin (100μg/ml) and 200 mM glutamine. To this IL-1β (401-ML/CF, R&D Systems) was added to a final concentration of 70pg/ml (as observed previously in mCIA plasma, (University of Wales School of Medicine, Cardiff University) "STAT-1 and STAT-3 signalling in Collagen Induced Arthritis: Towards New Therapeutic Targets for Rheumatoid Arthritis" Dr Shaun Smale) or 700pg/ml (see figure 6.3). Tissues were then incubated for twenty four hours (see Results) in a 37°C humidified CO_2 buffered 5% incubator (Hera cell 150, Heraeus).

After twenty four hours aortic rings were removed and placed in the myograph bath with warmed (37°C) oxygenated Krebs solution before being mounted on wire prongs. Contractile function was measured by means of responses to high K^+ (60mM), increasing concentrations of 5HT and relaxation responses were measured to increasing concentrations of ACh following pre-constriction to 70-80% of the previously attained maximum (see section 2.4).

In subsequent experiments 24 hour incubations with 700pg/ml IL-1β were repeated in the presence of either L-NAME ($3x10^{-5}$M), 1400W (10^{-5}M), or indomethacin (10^{-6}M) (all as used in Chapter 5). Contraction and relaxation responses were then measured as described above and in section 2.4.

6.3.6 Investigating the Effect of IL-1β on MMP-9 Expression in the Aorta

Whole vessels were removed from naïve animals (section 2.3.2i) and incubated for 24 hours with 700pg/ml of IL-1β in supplemented DMEM as described in section 6.3.5. Following this vessels were removed and homogenised in 100μl RIPA buffer as described in section 2.3.2i. Subsequently the protein concentration was established as described in section 2.7.1., and MMP-9 levels were detected in this sample by ELISA (see 2.7.2.).

6.3.7 Myography: Incubations with MMP-9.

6.3.7.1 Preliminary Experiments: Vessel Exposure to MMP-9

6.3.7.1.1 The Effect of Active Human Recombinant MMP-9 on Pre-constricted Vessels.

In order to assess acute effects of MMP-9 on normal vessels, tissues were removed from naïve animals as described in 2.3.2i, before being mounted on a myograph and vessel function measured as described in section 2.4. Following this a bolus concentration of 5HT was added to the vessels and rings were allowed to constrict to ~70-80% of the observed previous maximum. At this point active human recombinant MMP-9 (75ng/ml) (PF024 Calbiochem) was added to two of the four rings to investigate a direct effect on vessel function. Responses were observed for approximately twenty minutes to investigate potential differences from the controls.

6.3.7.1.2 Acute Incubation with MMP-9.

In similar experiments tissues from naïve animals were incubated for one or three hours in the absence of presence of MMP-9 (75ng/ml added directly to the Krebs in the organ

baths) before contraction and relaxation responses were performed as described in section 2.4.

6.3.7.2 Acute and Chronic Exposure of Naïve Tissues To Normal and Pathological Levels of MMP-9 In Vitro.

Following measurement of MMP-9 levels in plasma from both normal (control) and mCIA animals (as described above), "normal" and "severe" values were established (15ng/ml and 75ng/ml respectively, see results section 6.4.2. Subsequently vessels from naïve animals were incubated *in vitro* with "normal" and "severe" concentrations of MMP-9 to mimic the *in vivo* RA conditions. Specifically aortic segments were placed into the well of a tissue culture plate containing 2ml of culture media (see section 6.3.5 for media constituents), in the absence or presence of MMP-9 (15ng/ml or 75ng/ml). These were then incubated for either three (acute) or twenty four (chronic) hours in an incubator at 37 °C gassed with 5% CO_2 in air before being mounted on the myograph and vascular function assessed using the previously described standard procedure (section 2.4).

6.3.7.3 Incubation with "Severe" Levels of MMP-9 in the presence of a MMP-9 Inhibitor.

In further experiments twenty four hour incubations with MMP-9 (75ng/ml) (as in 6.3.7.4) were repeated in the absence or presence of a MMP-9 inhibitor (10^{-7}M) (444252, Calbiochem) a concentration able to inhibit . Subsequently tissues were mounted on the myograph and vascular function assessed using the previously described standard procedure (section 2.4). It is important to note that at this concentration this inhibitor may also inhibit MMP-1 and MMP-13.

6.3.8 Ex vivo Effect of MMP-9 Inhibition on Vascular Function in Tissues from Moderately Diseased Arthritic Animal.

Aortic tissues from moderately diseased mCIA animals were harvested as described above (section 6.3.3) and then incubated in media (described in 6.3.5.) in the absence and

presence of a MMP-9 inhibitor (10^{-7}M) for twenty four hours. Subsequently tissues were mounted on the myograph and vascular function assessed using the previously described standard procedure (section 2.4).

6.3.9 Localisation and Cellular Sources of MMP-9 in mCIA joints by Immunohistochemistry

6.3.9.1 Localisation

Immunohistochemistry (IHC) was utilised to detect total MMP-9 and macrophages and neutrophils in the arthritic joint. Paws were removed from appropriate mCIA animals (see section 2.3.2ii) and fixed, sectioned, de-paraffinised and hydrated as previously described (section 2.5.2ii and 2.6.1 respectively). Detection of MMP-9 in the sections was achieved using the Vectastain ABC (goat) kit (PK-4005, Vector Laboratories). All incubations were carried out at room temperature. Following hydration, slides were immersed in tris-buffered saline (TBS) (0.02M Tris, 0.15M NaCl) for five minutes. Subsequently excess liquid was carefully removed while avoiding disturbance or drying and the sample then enclosed by a hydrophobic barrier drawn on the glass using a pap pen (22309, Ted Pella. Inc). The latter helped to minimise the volume of antibody used, and also to standardise the volume of each incubation. Using a plastic Pasteur pipette sections were then covered with two drops of hydrogen peroxide (0.03% v/v) (216763, Sigma Aldrich) and incubated at room temperature for thirty minutes in order to quench any hydrogen peroxidase activity. Next sections were immersed for five minutes in TBS before incubating with diluted normal serum (supplied in kit) for twenty minutes. Excess liquid was then blotted from the sample before incubation with the primary antibody; anti-MMP-9 (1/200) (sc-6841, Santa Cruz). This was left for thirty minutes before washing for five minutes in TBS and then applying the biotinylated secondary antibody (supplied in kit) for a further thirty minutes. Following this samples were incubated for five minutes with Vectastain ABC reagent (supplied in kit), washed in TBS and then incubated with two drops of the DAB substrate solution (SK-4100, Vector Laboratories) for five minutes. Slides were then immersed in tap water and counterstained with haematoxylin for ninety seconds, followed by a wash in tap water for five minutes, and a

rinse in Scotts tap water (to enhance the blue of the haematoxylin) for thirty seconds. After this slides were dehydrated by washing in ascending concentrations of alcohol (70%, 90%, 100% v/v x 3) for three minutes each and then immersing in three changes of xylene for five minutes. Lastly slides were mounted with DePex/DPX and set by heating at 60°C overnight.

6.3.9.2 Macrophages

Paws were removed from appropriate mCIA animals (see section 2.3.2ii) and fixed, sectioned, de-paraffinised and hydrated as previously described (section 2.5.2ii and 2.6.1 respectively). Detection of macrophages in the sections was achieved using the Vectastain ABC (rat) kit (PK-4004, Vector Laboratories). Subsequently slides were washed in TBS, sections circled with a pap pen and exposed to hydrogen peroxide and further TBS washing as above. They were then incubated with 2x (the block was increased by this value to prevent background staining) diluted normal (supplied in kit) serum for 20 minutes. Next excess liquid was blotted from the sample before being incubated with the primary antibody; rat anti-F4/80 (1/100) (a monoclonal antibody used widely as a marker for mouse macrophages) (GTX26640, AutogenBioclear). This was left on the sample for thirty minutes before washing for five minutes in TBS and then applying the biotinylated secondary antibody (supplied in kit) for a further thirty minutes. Samples were then incubated for five minutes with two drops of the Vectastain ABC reagent (supplied), washed in TBS and then exposed to two drops of the DAB substrate solution (SK-4100, Vector Laboratories) for five minutes. Slides were immersed in tap water and counterstained with haematoxylin before dehydration and mounting as mentioned in section 6.3.9.1.

6.3.9.3 Neutrophils

Paws were removed from appropriate mCIA animals (see section 2.3.23ii) and fixed, sectioned, de-paraffinised and hydrated as previously described (section 2.5.2ii and 2.6.1 respectively). Neutrophils were detected using the Vectastain ABC (rat) kit (PK-4004, Vector Laboratories). Subsequently slides were washed in TBS, sections circled with a pap pen and exposed to hydrogen peroxide and further TBS washing as above. Following incubation with diluted normal serum (supplied in kit) for 20 minutes, excess liquid was blotted from the sample before exposure to the primary antibody; anti-Ly-6G (1/100) (a

mouse neutrophil marker) (551459, BD Pharmingen). This was left for thirty minutes before washing for five minutes in TBS and applying the biotinylated secondary antibody (supplied in kit) for a further thirty minutes. Samples were then incubated for five minutes with two drops of the Vectastain ABC reagent (supplied in kit), washed in TBS and then exposed to two drops of the DAB substrate solution (SK-4100, Vector Laboratories) for five minutes. Slides were immersed in tap water and counterstained with haematoxylin before dehydration and mounting as mentioned in section 6.3.9.1.

For all IHC positively stained cells were identifiable by their brown colour in contrast to the blue/purple of the haematoxylin stained nuclei of the negative cells. Sections were visualised using a microscope; staining was apparent from X4 magnification upwards.

6.3.9.4 Quantification of Immunohistological Staining of Joint Sections.

To quantify the percentage of infiltrating cells sections were initially visually analysed to ascertain areas high in staining. Subsequently the stained area of interest was photographed at X20 or X40 magnification and five areas of 250μm^2 identified within this field were quantified and averaged. Quantification involved calculating the area of staining (object) according to the colour intensity of the stain compared to the contrasting remainder of the slide (area) and was expressed as % object/area. This criteria was manually set using Image-Pro Analyzer software and applied to all pictures taken from that batch to control for any inter-batch variation in staining intensity that might occur.

With all staining a negative control; rat or goat IgG (2026, 2028 respectively Santa Cruz) was run on a serial section of the sample of interest. Staining was deemed satisfactory if the cells of interest were clearly shown by brown staining on the positive section and there was no false positive staining on the negative control.

6.3.10 Statistical Analysis

Blood pressure data, expressed as mean ± SEM, was analysed by one-way ANOVA followed by Student Newman-Keuls multiple range test. Data from MMP-9 ELISAs were expressed as average levels of total MMP-9 in either group for the paw homogenates,

serum ± SEM and analysed by one-way ANOVA followed by Student Newman-Keuls multiple range test if three or more groups required comparison. If only two groups were present for comparison the Student's t-test was utilised.

5HT-induced increases in tension are expressed as developed tension in mN. Relaxation responses are expressed as percentage relaxation of the previously induced maximum, following constriction to 70-80% of the maximum. Isometric tension data were first fitted to sigmoid concentration curves using GraphPad Prism software and EC50 (concentration to produce 50% of maximum response) and maximum constriction/relaxation (Rmax) values obtained. If three groups were present for analyses a one-way ANOVA followed by Student Newman-Keuls multiple range test was utilised. If only two groups were presented then data was analysed by the Students t-test.

For IHC results are expressed as mean ± SEM % object/area and analysed by one-way ANOVA followed by Student Newman-Keuls multiple range test. For all data sets, differences were considered significant where $p<0.05$.

6.4 Results

6.4.1 Blood Pressure

The tail-cuff systolic blood pressure measurements showed no apparent difference between any of the groups (see figure 6.4). Average results ± SEM were as follows; normal 112.5 ± 4.38 mm/Hg, mild 115.8 ± 4.25 mm/Hg, moderate 105.9 ± 3.35 mm/Hg and severe 119.5 ± 3.79 mm/Hg.

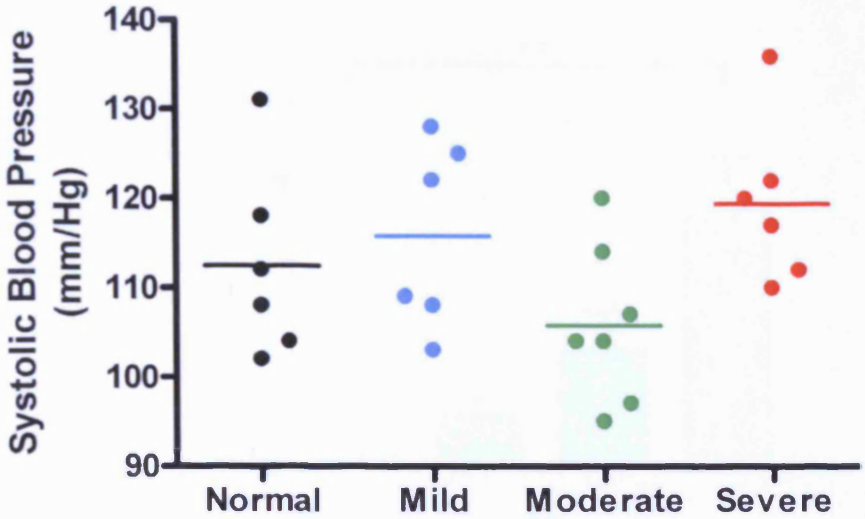

Figure 6.4. Blood Pressure Measurements. Systolic blood pressure readings from normal (n=7) (naïve) animals and animals with mild (n=6), moderate (n=7) and severe (n=6) experimental arthritis.

6.4.2 MMP-9 Levels in Normal and mCIA Animals

Tissue samples of aorta and paw, and blood serum was taken from DBA/1 normal animals, and those with mCIA at appropriate time points. Aorta and paw samples were homogenised and levels of total MMP-9 were detected by ELISA. In paw and aortic homogenates, levels of total MMP-9 were seen to increase following the onset of arthritis (see figure 6.5). In serum, levels of MMP-9 in severe disease surpassed those seen in mild and moderate disease (see figure 6.5C). In the aortic samples absolute levels of total MMP-9 were a lot lower than in the paws, however the pattern of change was similar with elevated levels associated with increasing arthritis severity.

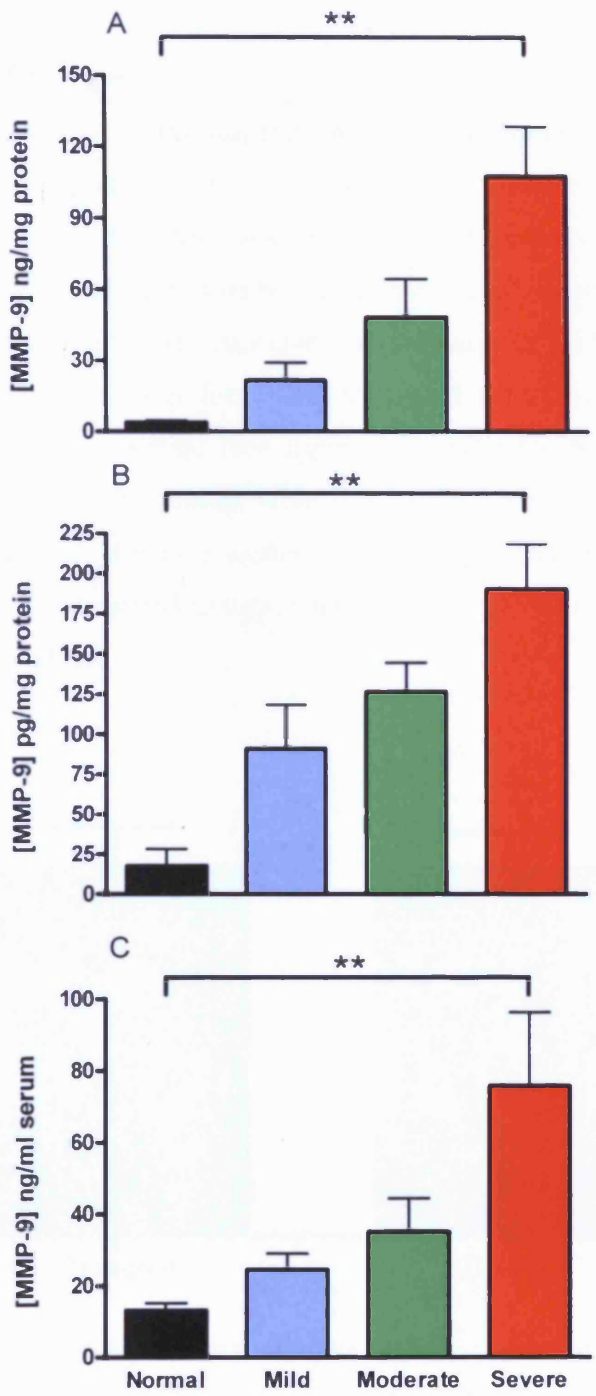

Figure 6.5. MMP-9 Levels the mCIA Model. MMP-9 levels in A. Paw, B. Aorta and C. Serum samples. Paw Samples; normal (n=5), mild (n=6), moderate (n=12) and severe (n=6). Aortic Samples; normal (n=3), mild (n=6), moderate (n=3) and severe (n=5). Serum Samples normal (n=10), mild (n=5), moderate (n=6) and severe (n=7). In all cases *$p<0.05$, **$p<0.01$ compared to Normal determined by one-way ANOVA followed by Newman-Keuls test.

6.4.3 Incubations with IL-1β.

6.4.3.1 Incubations with IL-1β (70pg/ml) for Twenty Four Hours.

Aortae from naïve normal animals were incubated in the absence or presence of IL-1β (70pg/ml) for twenty four hours as described above. Initial responses to high K^+ showed no difference in the maximum constriction between control and treated tissues (see figure 6.6). However, following a step-wise concentration response to 5HT the Rmax values were slightly yet significantly lower for tissues incubated with IL-1β. No differences between EC50 values were observed (see figure 6.7, and table 6.1). Following re-constriction to 70-80% of this maximum with 5HT (10^{-6}M), vessels were subjected to increasing concentrations of ACh (see section 2.4). A significantly impaired Rmax to this agent was seen in IL-1β-treated tissues, whereas EC50 values remained unchanged (see figure 6.7, and table 6.1).

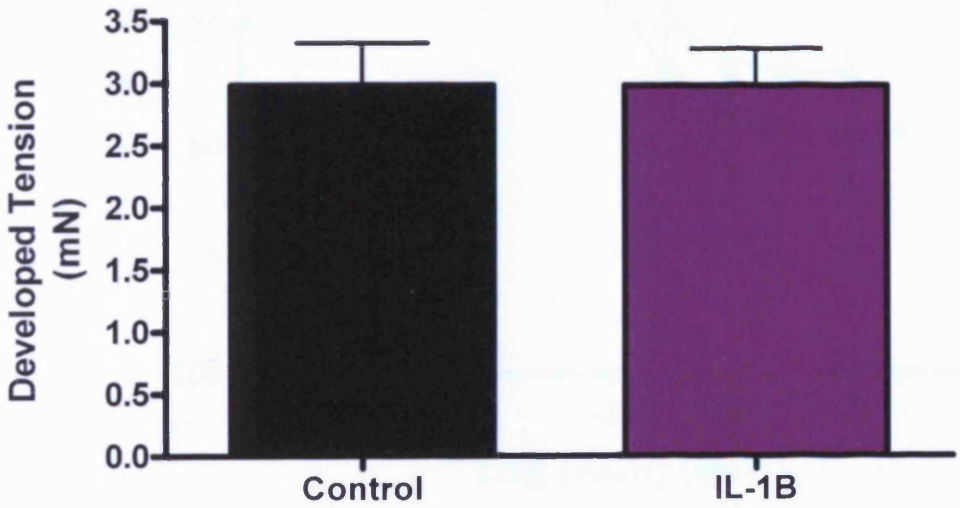

Figure 6.6. High K^+. Graphs showing constriction responses following exposure to K^+ ($6x10^{-2}$M) in the absence (Control) and presence of IL-1β (70pg/ml) for twenty four hours, n=6.

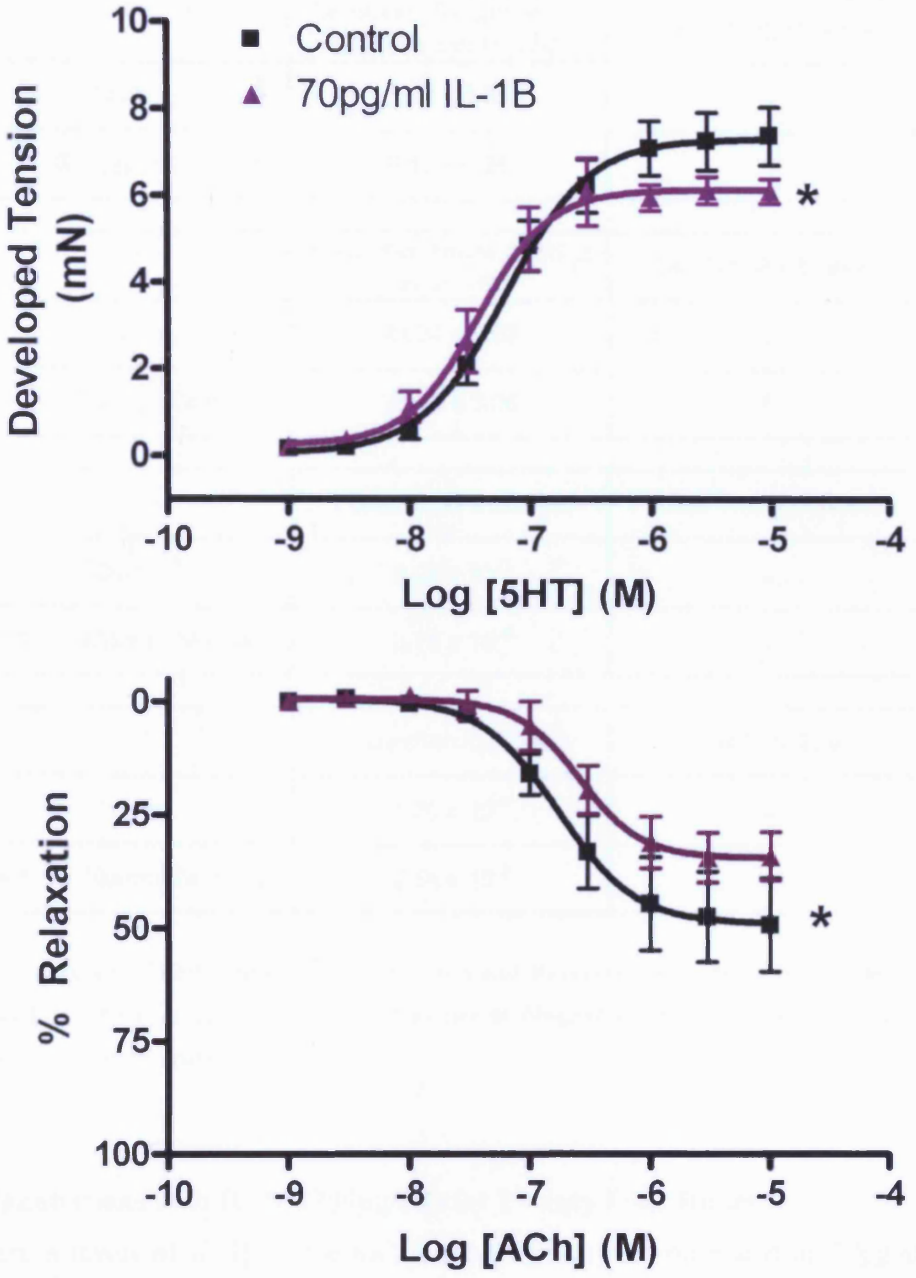

Figure 6.7. Graphs showing Constriction and Relaxation Responses to 5HT and ACh Respectively in Control Tissue in the Absence and Presence of 70pg/ml IL-1β for Twenty Four Hours. A. Constriction responses to 5HT in tissues from normal control animals treated in the absence and presence of IL-1β for twenty-four hours. B. Relaxation responses to ACh for the same tissue. Rmax *$p<0.05$ compared to normal, n=6.

	Developed Tension Rmax (Mean ± SEM) (mN)	Level of Significance
Control	7.32 ± 0.32	-
+ IL-1β 70pg/ml 24 hours	6.15 ± 0.26	*

	Relaxation Rmax (Mean ± SEM) (%)	Level of Significance
Control	48.94 ± 4.92	-
+ IL-1β 70pg/ml 24 hours	34.48 ± 3.06	*

	Constriction EC50 (M)	Level of Significance
Control	6.28×10^{-8}	-
+ IL-1β 70pg/ml 24 hours	3.75×10^{-8}	-

	Relaxation EC50 (M)	Level of Significance
Control	1.70×10^{-7}	-
+ IL-1β 70pg/ml 24 hours	2.54×10^{-7}	-

Table 6.1. Rmax and EC50 Values for Constriction and Relaxation Responses in Vessels Incubated for Twenty Four Hours in the Absence and Presence of 70pg/ml IL-1β. Raw data for responses shown in figure 6.8. *$p<0.05$ compared to normal.

6.4.3.2 Incubations with IL-1β (700pg/ml) for Twenty Four Hours

While serum levels of IL-1β in the mCIA model have been measured as 70pg/ml (MD Thesis, Cardiff University, "STAT-1 and STAT-3 signalling in Collagen Induced Arthritis: Towards New Therapeutic Targets for Rheumatoid Arthritis" Dr Shaun Smale 2010) the extent of IL-1β production at a cellular in the vessel wall is unknown. Given that such "local concentrations" could well be significantly higher than that seen in the serum, in these experiments a higher (10 fold excess) concentration of IL-1β (700pg/ml) was used to assess the potential effect on vessel function.

K^+ responses were again largely unaffected by incubation with IL-1β (see figure 6.8), however marked differences were observed in the Rmax values for constriction responses to 5HT. Indeed vessels incubated with IL-1β contracted to a significantly ($p<0.001$) lower level than control tissues (see figure 6.9). This was not echoed in the EC50 values for 5HT or the relaxation responses to ACh (see table 6.2).

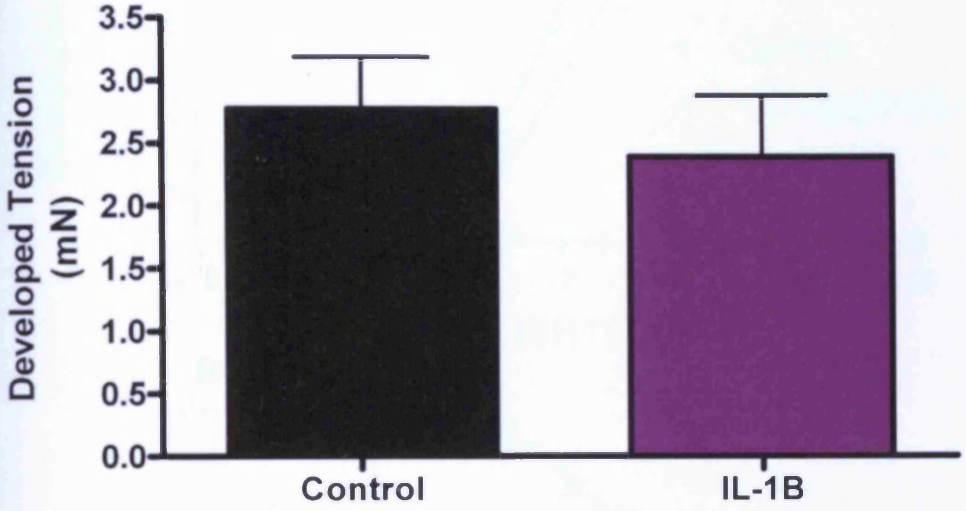

Figure 6.8. High K+. Graphs showing constriction responses following exposure to K^+ ($6x10^{-2}M$) in the absence and presence of IL-1β (700pg/ml) for twenty four hours. n=6.

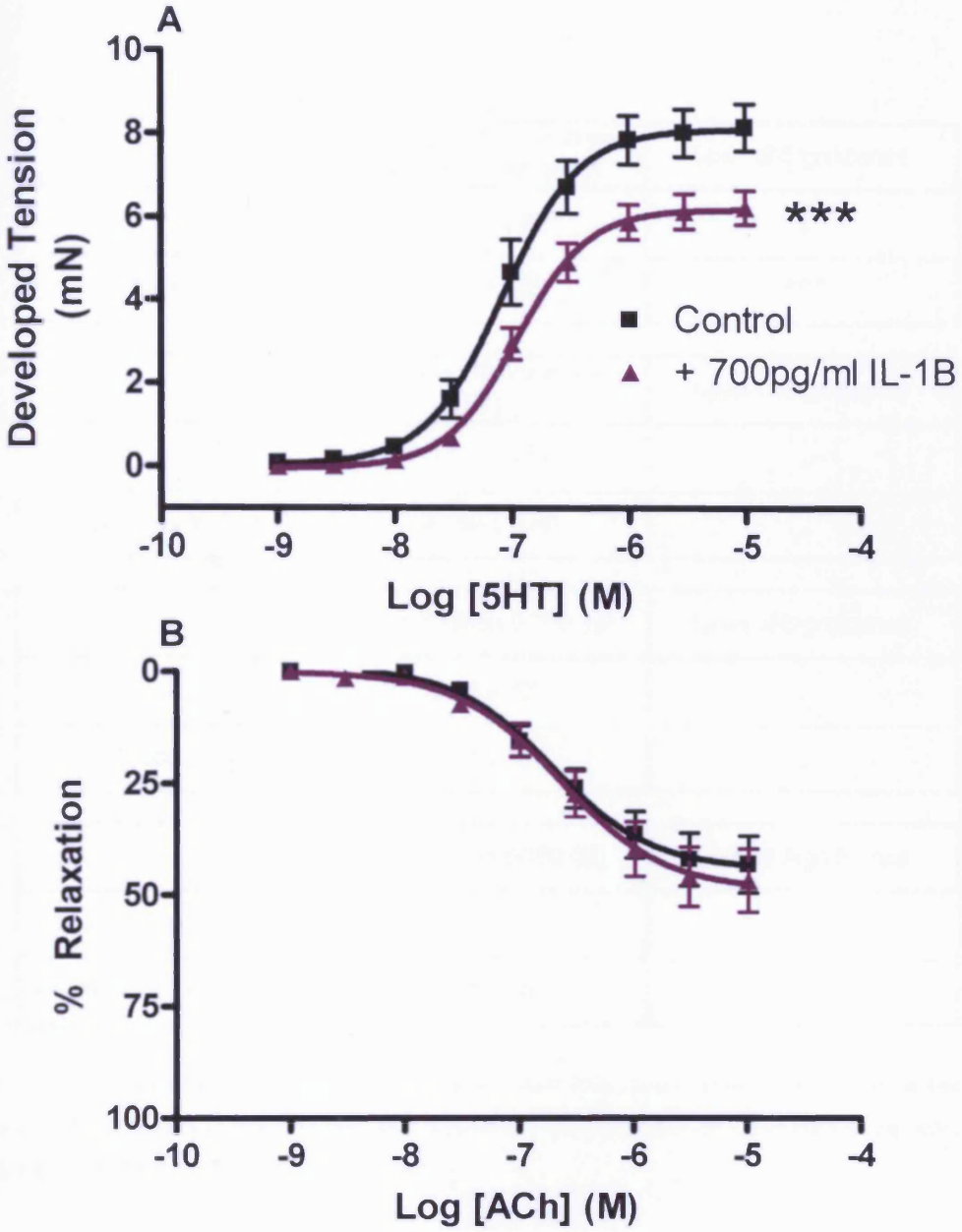

Figure 6.9. Graphs showing Constriction and Relaxation Responses to 5HT and ACh Respectively Following an Incubation period of Twenty Four Hours in Control Tissue in the Absence and Presence of 700pg/ml IL-1β. A. Constriction responses to 5HT B. Relaxation responses to ACh in the same tissue. Rmax ***$p<0.001$ compared to control determined by one-way ANOVA followed by Newman-Keuls test, n=6.

	Developed Tension Rmax (Mean ± SEM) (mN)	Level of Significance
Control	8.14 ± 0.32	-
+ IL-1β 700pg/ml 24 hours	6.21 ± 0.21	***

	Relaxation Rmax (Mean ± SEM) (%)	Level of Significance
Control	44.1 ± 3.87	-
+ IL-1β 700pg/ml 24 hours	48.69 ± 4.86	-

	Constriction EC50 (M)	Level of Significance
Control	8.39×10^{-6}	-
+ IL-1β 700pg/ml 24 hours	1.11×10^{-6}	-

	Relaxation EC50 (M)	Level of Significance
Control	1.94×10^{-7}	-
+ IL-1β 700pg/ml 24 hours	2.24×10^{-7}	-

Table 6.2. Rmax and EC50 Values for Constriction and Relaxation Responses in Vessels Incubated for Twenty Four Hours in the Presence and Absence of 700pg/ml IL-1β. Raw data for responses shown in figure 6.11. ***$p<0.001$ compared to control.

6.4.3.3 Incubations with IL-1β (700pg/ml) and L-NAME

It has been reported that IL-1β can upregulate iNOS activity and therefore increase NO production (Dinarello 2002). To investigate whether such an effect is responsible for the dampened response to 5HT described above, the experiments in section 6.4.3.3 were repeated in the presence of L-NAME (3×10^{-5}M). Subsequent constrictions to K^+ ($6 \times 10^{-}$

^{2}M were similar in control and treated tissues (see figure 6.10). In response to increasing concentrations of 5HT again no significant difference in either the Rmax or EC50 values were observed (see figure 6.11 and table 6.3). Therefore it would seem that NOS inhibition restored contractile function in IL-1β-treated tissues.

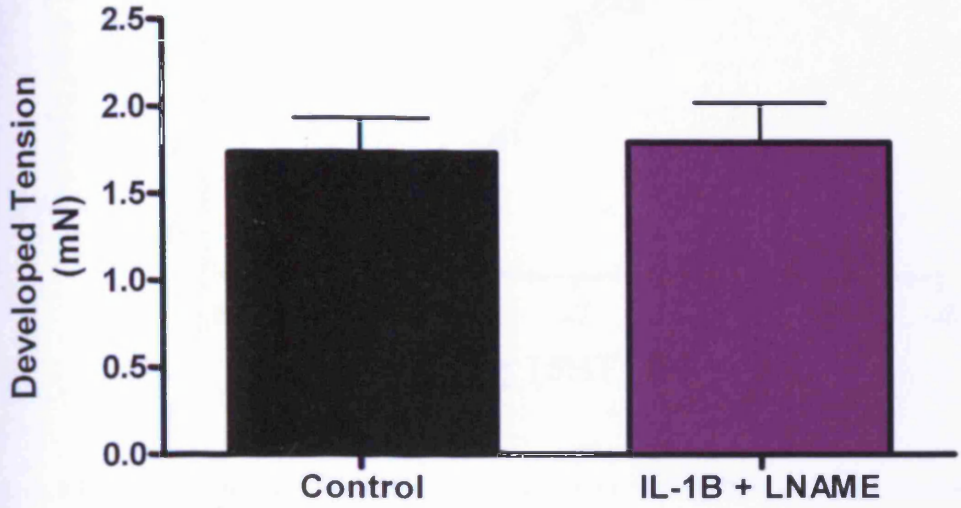

Figure 6.10. High K+. Graphs showing constriction responses following exposure to K^+ ($6x10^{-2}$M) in the absence and presence of IL-1β (700pg/ml) and LNAME ($3x10^{-5}$M) for twenty four hours. n=3

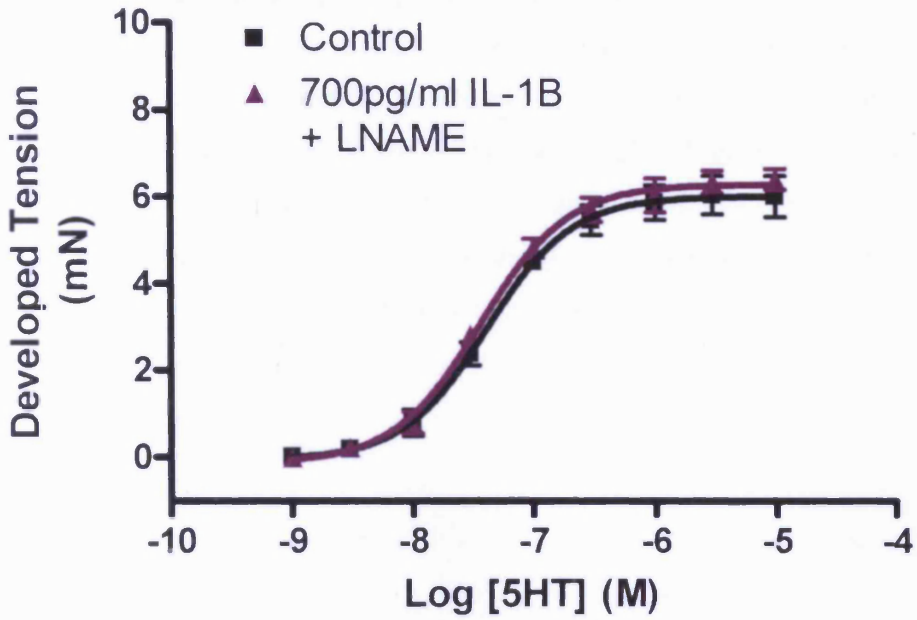

Figure 6.11. Graph Showing Constriction Responses to 5HT Following an Incubation period of Twenty Four hours in Control Tissue in the Absence and Presence of 700pg/ml IL-1β and LNAME ($3x10^{-5}$M). n=3.

	Developed Tension Rmax (Mean ± SEM) (mN)
Control	6.01 ± 0.18
+ IL-1β 700pg/ml 24 hours	6.30 ± 0.14
	Constriction EC50 (M)
Control	4.18×10^{-8}
+ IL-1β 700pg/ml 24 hours	3.67×10^{-8}

Table 6.3. Rmax and EC50 Values for Constriction Responses in Vessels Incubated for Twenty Four Hours in the Presence and Absence of 700pg/ml IL-1β and LNAME (3x10-5M). Raw data for responses shown in figure 6.11.

6.4.3.4 Incubations with IL-1β (700pg/ml) and 1400W

1400W was used to investigate the specific actions of iNOS. Vessels were incubated as previously for twenty four hours in the absence or presence of IL-1β (700pg/ml)/1400W (10^{-5}M). Although responses to K^+ ($6x10^{-2}$M) were slightly higher in the presence of IL-1β/1400W, this difference failed to reach significance (see figure 6.12). Constriction and relaxation responses to 5HT and ACh respectively, measured as in section 6.4.3.4, shown no significant differences between treatment groups for either Rmax or EC50 values (see figure 6.13 and table 6.4).

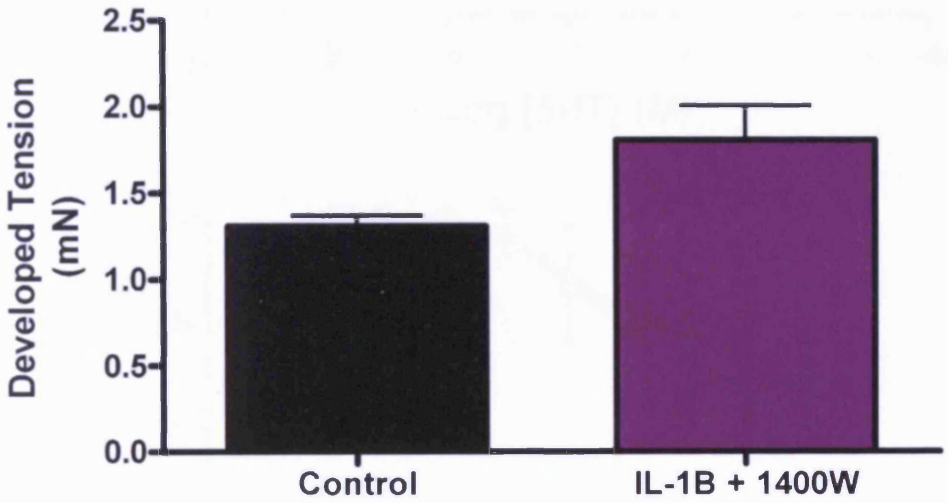

Figure 6.12. High K^+. Graphs showing constriction responses following exposure to K^+ ($6x10^{-2}$M) in the absence and presence of IL-1β (700pg/ml) and 1400W (10^{-5}M) for twenty four hours. n=3 check control responses.

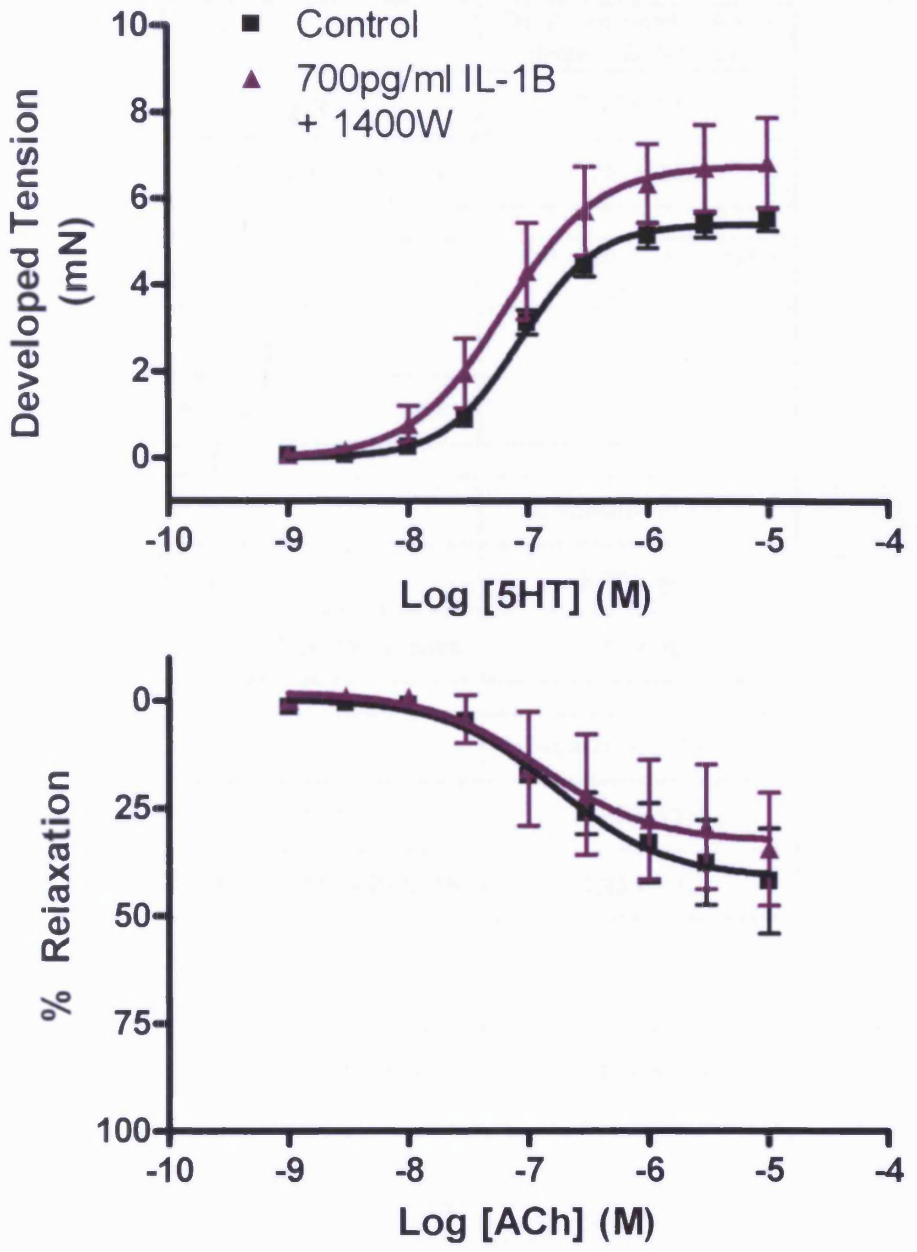

Figure 6.13. Graphs showing Constriction and Relaxation Responses to 5HT and ACh Respectively Following an Incubation period of Twenty Four Hours in Control Tissue in the Absence and Presence of 700pg/ml IL-1β and 1400W (10-5M). A. Constriction responses to 5HT. B. Relaxation responses to ACh in the same tissue. n=3.

	Developed Tension Rmax (Mean ± SEM) (mN)
Control	5.42 ± 0.13
+ IL-1β 700pg/ml 24 hours	6.79 ± 0.53

	Relaxation Rmax (Mean ± SEM) (%)
Control	41.09 ± 6.12
+ IL-1β 700pg/ml 24 hours	32.68 ± 9.06

	Constriction EC50 (M)
Control	8.72×10^{-8}
+ IL-1β 700pg/ml 24 hours	6.38×10^{-8}

	Relaxation EC50 (M)
Control	1.67×10^{-7}
+ IL-1β 700pg/ml 24 hours	1.23×10^{-7}

Table 6.4. Rmax and EC50 Values for Constriction Responses in Vessels Incubated for Twenty Four Hours in the Presence and Absence of 700pg/ml IL-1β and 1400W (10-6M). Raw data for responses shown in figure 6.13.

6.4.3.5 Incubations with IL-1β (700pg/ml) and Indomethacin

To investigate whether the IL-1β-mediated decrease in constriction demonstrated above was attributable to COX upregulation, responses were assessed following incubation with indomethacin. Tissues were incubated as before for twenty four hours in the absence or presence of IL-1β (700pg/ml)/indomethacin (10^{-6}M). Constriction responses to K^+ showed no difference between control and treated tissues (see figure 6.14). However, maximum constriction responses to 5HT were significantly ($p<0.05$) lower in IL-1β/indomethacin-treated tissues compared to controls (see figure 6.15), though no change

in EC50 values was observed (see table 6.5). No differences were observed for relaxations to ACh (see figures 6.15 and table 6.5).

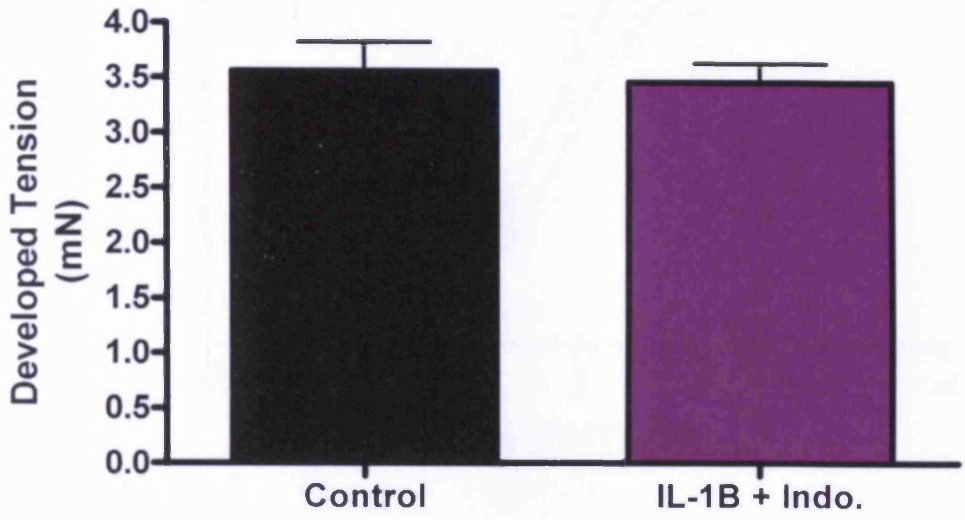

Figure 6.14. High K^+. Graphs showing constriction responses following exposure to K^+ ($6x10^{-2}M$) in the absence and presence of IL-1β (700pg/ml) and Indomethacin ($10^{-6}M$) for twenty four hours. n=3

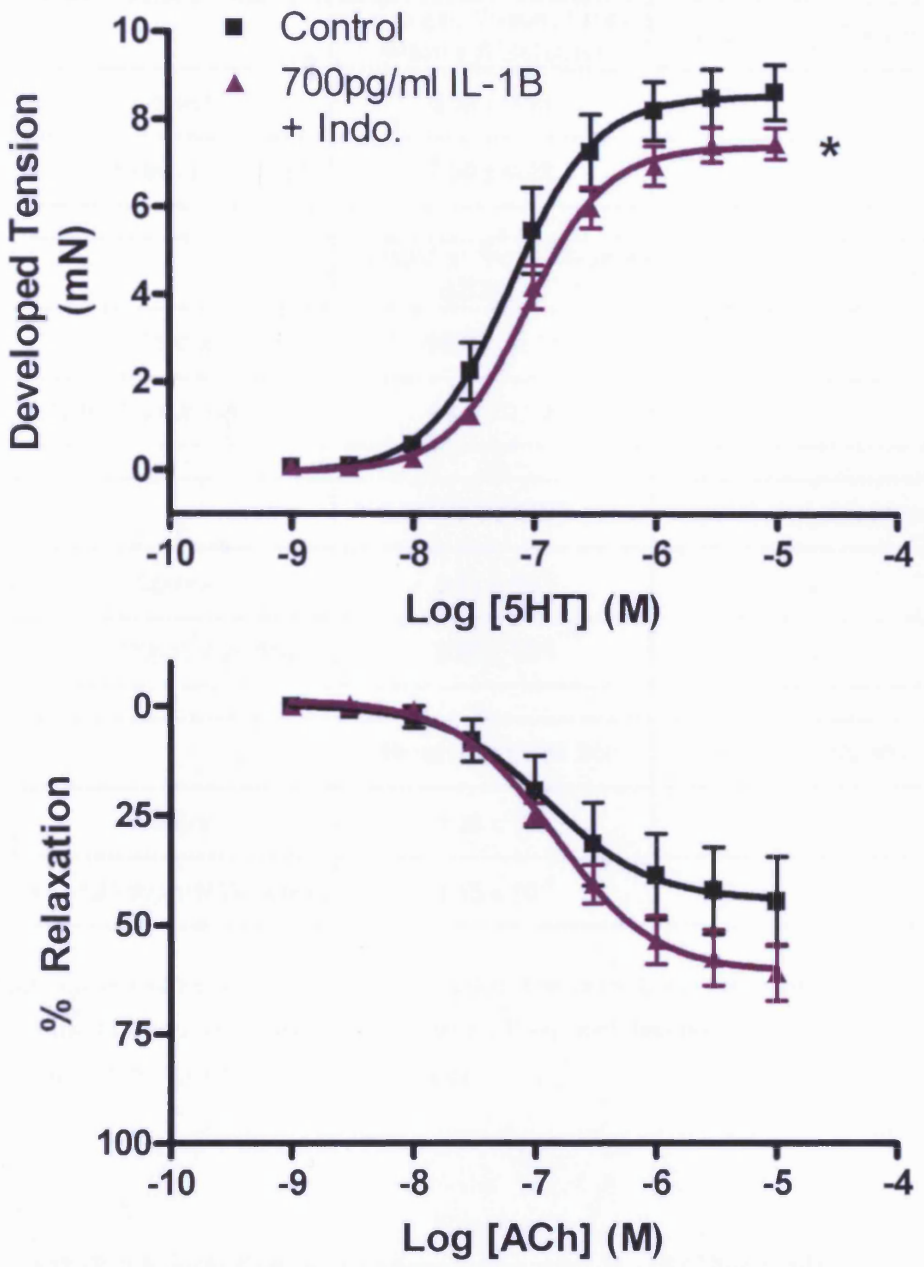

Figure 6.15. Graphs showing Constriction and Relaxation Responses to 5HT and ACh Respectively Following an Incubation period of Twenty Four Hours in Control Tissue in the Absence and Presence of 700pg/ml IL-1β and Indomethacin (10-6M). A. Constriction responses to 5HT B. Relaxation responses to ACh in the same tissue. *$p<0.05$ compared to normal determined by students t-test, n=4.

	Developed Tension Rmax (Mean ± SEM) (mN)	Level of Significance
Control	8.55 ± 0.38	-
+ IL-1β 700pg/ml 24 hours	7.39 ± 0.22	*

	Relaxation Rmax (Mean ± SEM) (%)	Level of Significance
Control	44.36 ± 6.17	-
+ IL-1β 700pg/ml 24 hours	60.7 ± 3.32	-

	Constriction EC50 (M)	Level of Significance
Control	6.61×10^{-8}	-
+ IL-1β 700pg/ml 24 hours	8.90×10^{-8}	-

	Relaxation EC50 (M)	Level of Significance
Control	1.28×10^{-7}	-
+ IL-1β 700pg/ml 24 hours	1.45×10^{-7}	-

Table 6.5. Rmax and EC50 Values for Constriction Responses in Vessels Incubated for Twenty Four Hours in the Presence and Absence of 700pg/ml IL-1β and Indomethacin. Raw data for responses shown in figure 6.20. *$p<0.05$ compared to control.

6.4.3.6 MMP-9 Levels Following Stimulation with IL-1β (700pg/ml).

Aortae isolated from naive animals were incubated as above in the absence and presence of IL-1β (700pg/ml) for twenty four hours before being homogenised and levels of MMP-9 therein assessed by ELISA (see figure 6.16.). No difference between control and treated tissues was observed; Control 27.92 ± 7.91 pg/mg protein, IL-1β incubation, 33.57 ± 12.02 pg/mg protein.

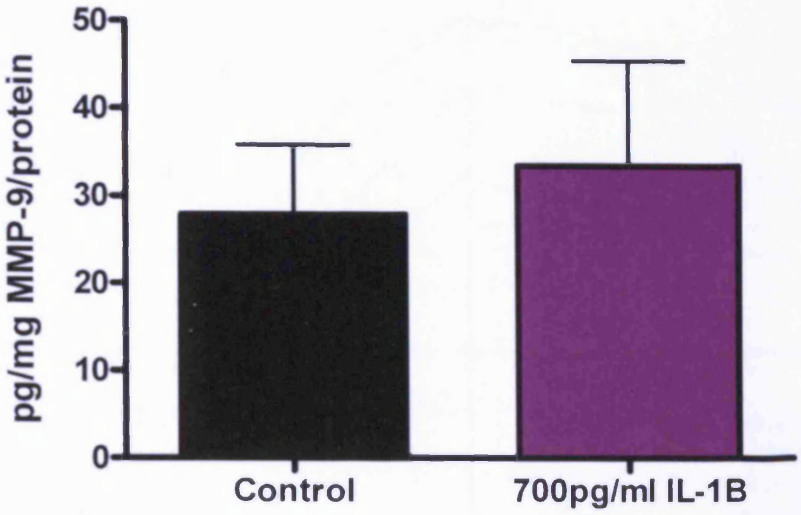

Figure 6.16. Levels of MMP-9 in Isolated Aortae from Control Animals Following Incubation with and without IL-1β (700pg/ml, twenty four hours). n=5 for both.

6.4.4 Incubations with MMP-9

6.4.4.1 The Acute Effect of MMP-9 on 5HT Pre-Constricted Tissues

Following constriction of aortic rings from naïve animals to 5HT (10^{-6}M) a bolus concentration of MMP-9 (75ng/ml, a concentration observed in the circulation of severely arthritic mCIA animals, see section 6.4.2) was added and left to incubate for 20 minutes. Subsequently no difference was observed between control and MMP-9-treated tissues, (see figure 6.17) both demonstrating the "drift" in tension towards baseline over time that is characteristic of this tissue (unpublished observations). Importantly this demonstrates that MMP-9 (at least at 75ng/ml) does not induce an acute endothelium-dependent (or indeed otherwise) relaxation response.

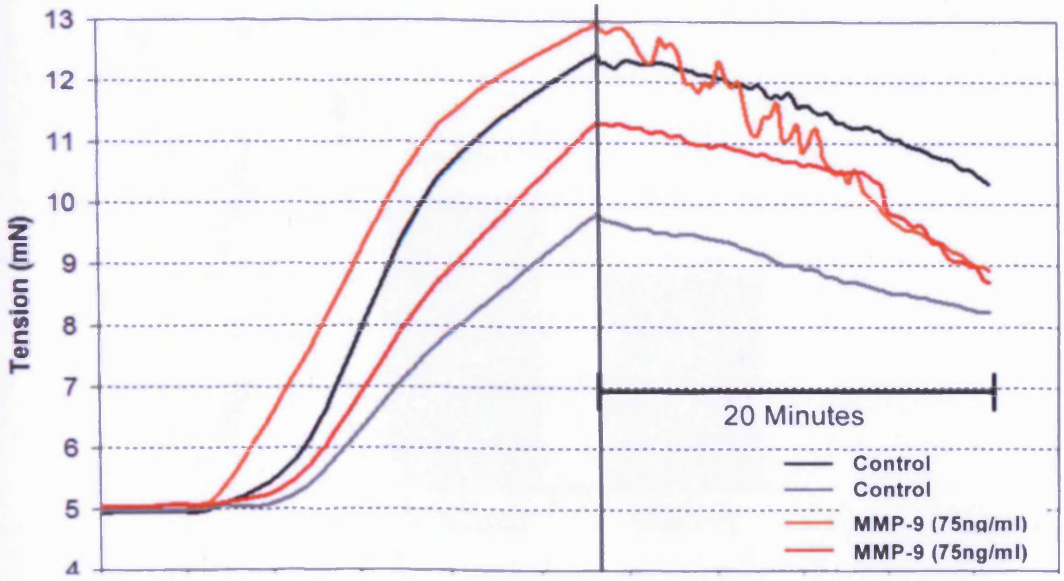

Figure 6.17. Vessel Responses to a Bolus Addition of MMP-9. Following constriction to 5HT a bolus concentration of MMP-9 was added to the vessels (depicted by the line) and left for 20 minutes.

6.4.4.2 One Hour Incubation with MMP-9 in the Myograph

Aortic rings from naive animals were incubated in the absence (control) or presence of MMP-9 75ng/ml for one hour as described above (see section 6.3.7.2). Subsequently constriction responses to K^+ ($6x10^{-2}M$) were measured and although MMP-9-treated vessels constricted slightly less, the difference to control was not significant (see figure 6.18). Furthermore constriction responses to 5HT were again no different (for either Rmax or EC50 values) (see figures 6.19 and table 6.7). Relaxation responses to ACh following re-constriction with 5HT to 70-80% of the maximum were again unaffected by this acute exposure to MMP-9. Rmax and EC50 values are shown in table 6.6.

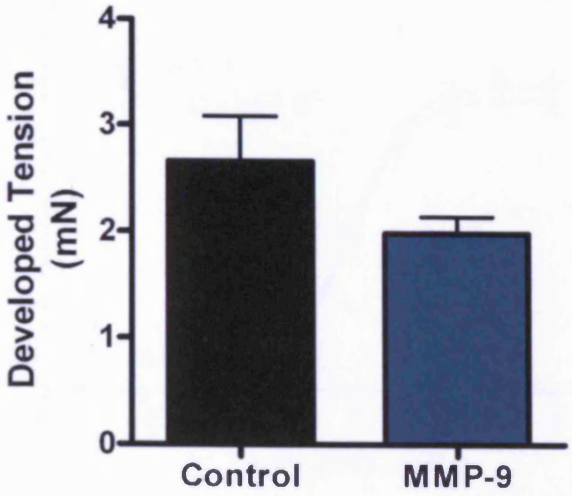

Figure 6.18 Graphs Showing Constriction to K^+ ($6x10^{-2}$M) Following One Hour Incubation in the Absence (Control) and Presence of MMP-9 (75ng/ml). n=3

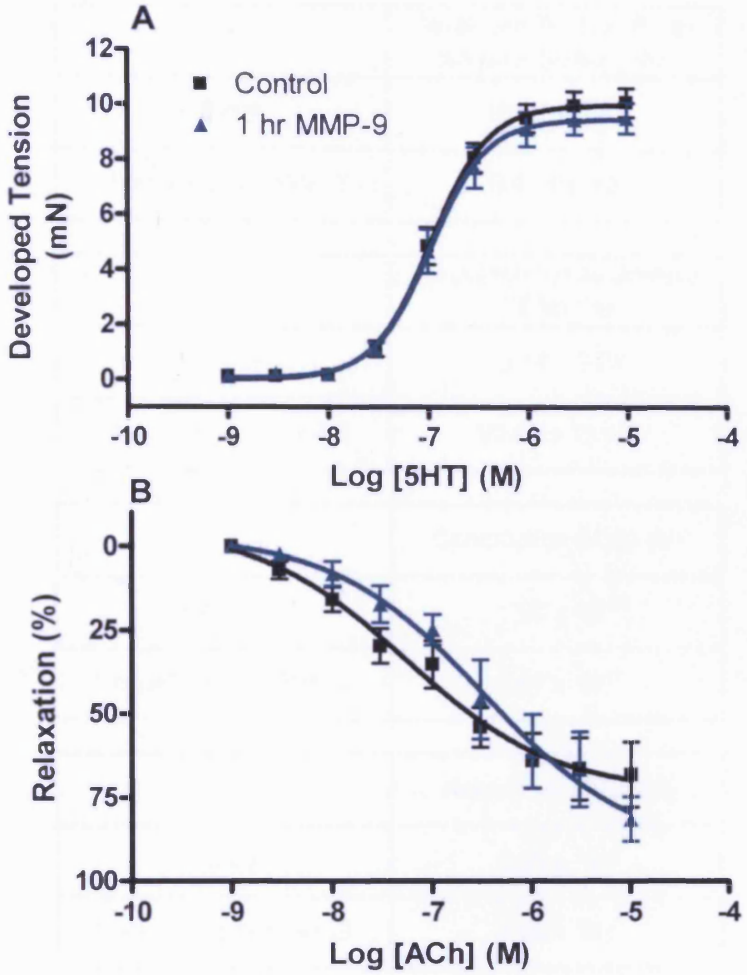

Figure 6.19. Graphs showing Constriction and Relaxation Responses to 5HT and ACh Respectively Following One Hour Incubation of Naïve Tissue in the Absence (Control) and Presence of MMP-9 (75ng/ml). A. Constriction responses to 5HT B. Relaxation responses to ACh in the same tissue. n=4.

	Developed Tension Rmax (Mean ± SEM) (mN)
Control	10.00 ± 0.26
1 hour 75ng/ml MMP-9	9.47 ± 0.30

	Relaxation Rmax (Mean ± SEM) (%)
Control	73.14 ± 9.24
1 hour 75ng/ml MMP-9	90.50 ± 19.43

	Constriction EC50 (M)
Control	1.09×10^{-7}
1 hour 75ng/ml MMP-9	1.07×10^{-7}

	Relaxation EC50 (M)
Control	5.38×10^{-8}
1 hour 75ng/ml MMP-9	3.15×10^{-7}

Table 6.6. Rmax and EC50 Values for Constriction Responses in Vessels Incubated for One Hour in the Absence and Presence of MMP-9 (75ng/ml). Raw data for responses shown in figure 6.25.

6.4.4.3 Three Hour Incubation with MMP-9 in the Myograph

Experiments were repeated as 6.4.4.3 above but incubations were for three hours. Subsequent contraction responses to K^+ were not different between control and MMP-9-incubated vessels (see figure 6.20). Maximum constriction responses to 5HT indicated that vessels incubated with MMP-9 failed to constrict to the level attained by control tissues (see figure 6.21), with a significantly ($p<0.05$) lower Rmax achieved. No difference was observed for EC50 values (see table 6.7). Relaxation responses to ACh showed no difference between treatment groups (see figure 6.21 and table 6.7).

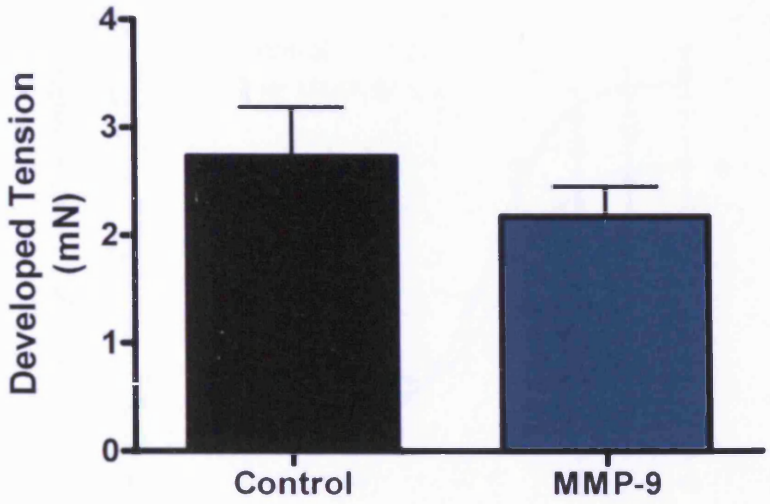

Figure 6.20. Graphs Showing Constriction to K^+ ($6x10^{-2}$M) Following Three hour Incubation in the Absence (Control) and Presence of MMP-9 (75ng/ml). n=4.

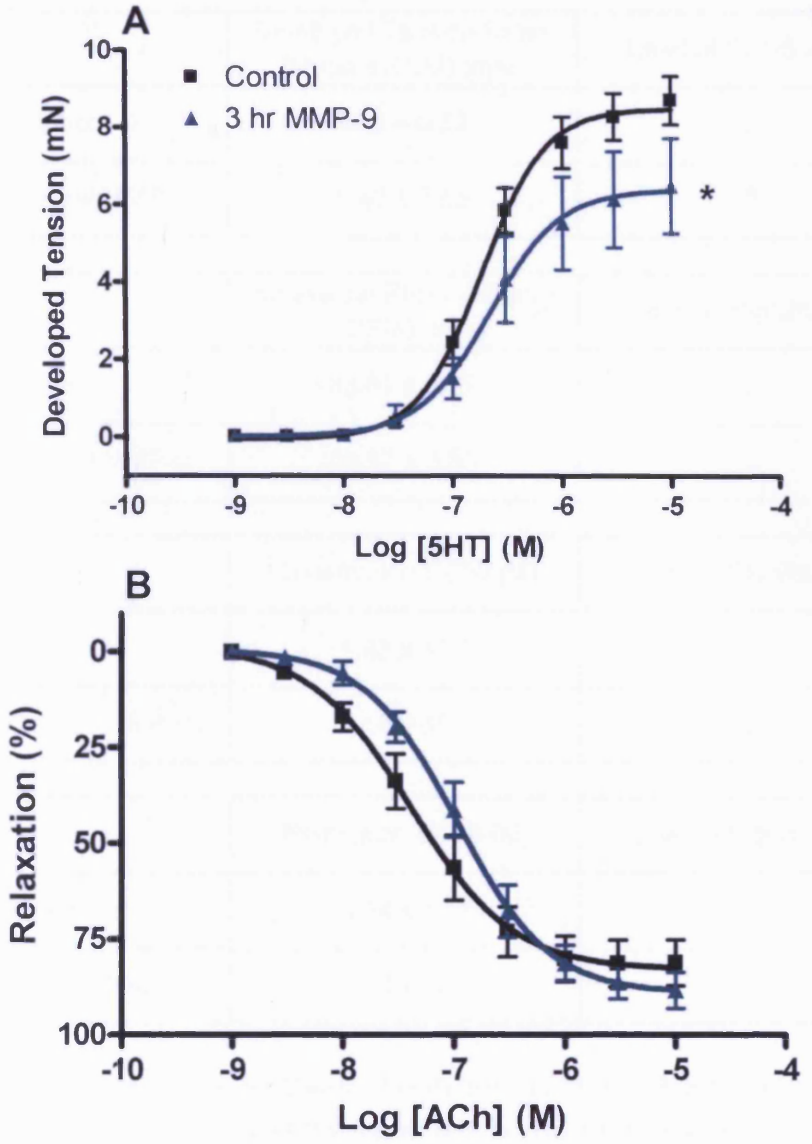

Figure 6.21. Graphs showing Constriction and Relaxation Responses to 5HT and ACh Respectively, Following Incubation of Naïve Tissue for Three hours in in the Absence (Control) and Presence of MMP-9 (75ng/ml). A. Constriction responses to 5HT B. Relaxation responses to ACh in the same tissue. *$p<0.05$ compared to control determined by students t-test, n=4.

	Developed Tension Rmax (Mean ± SEM) (mN)	Level of Significance
Control	8.52 ± 0.32	-
3 hour 75ng/ml MMP-9	6.40 ± 0.63	*

	Relaxation Rmax (Mean ± SEM) (%)	Level of Significance
Control	83.01 ± 3.97	-
3 hour 75ng/ml MMP-9	89.17 ± 3.53	-

	Constriction EC50 (M)	Level of Significance
Control	1.93×10^{-7}	-
3 hour 75ng/ml MMP-9	2.16×10^{-7}	-

	Relaxation EC50 (M)	Level of Significance
Control	4.14×10^{-8}	-
3 hour 75ng/ml MMP-9	1.06×10^{-7}	-

Table 6.7. Rmax and EC50 Values for Constriction Responses in Vessels Incubated for Three Hours in the Presence and Absence (control) of 75ng/ml MMP-9 *$p<0.05$ compared to control..

6.4.4.4 Three Hour Incubation with MMP-9 in Tissue Culture Medium.

Three hour incubations were repeated in the tissue culture media as a precursor to investigating long-term incubations, thus ensuring the media *per se* had no adverse effect on vessel function. Additional experiments were added to utilise the concentration of MMP-9 observed in naïve animals (15ng/ml, see 6.4.2). Following this incubation rings were suspended in the myograph (as described 2.4) before responses to K^+, 5HT and ACh were measured as before (see section 2.4). For experiments with MMP at 15ng/ml

subsequent responses to K^+ were not different between tissues (see figure 6.22). For maximum 5HT-induced constrictions Rmax values were significantly ($p<0.05$) lower for vessels incubated with MMP-9 (see figure 6.23). EC50 values for 5HT remain unchanged. Relaxations responses to ACh showed no difference following this incubation (see figures 6.23 and table 6.8).

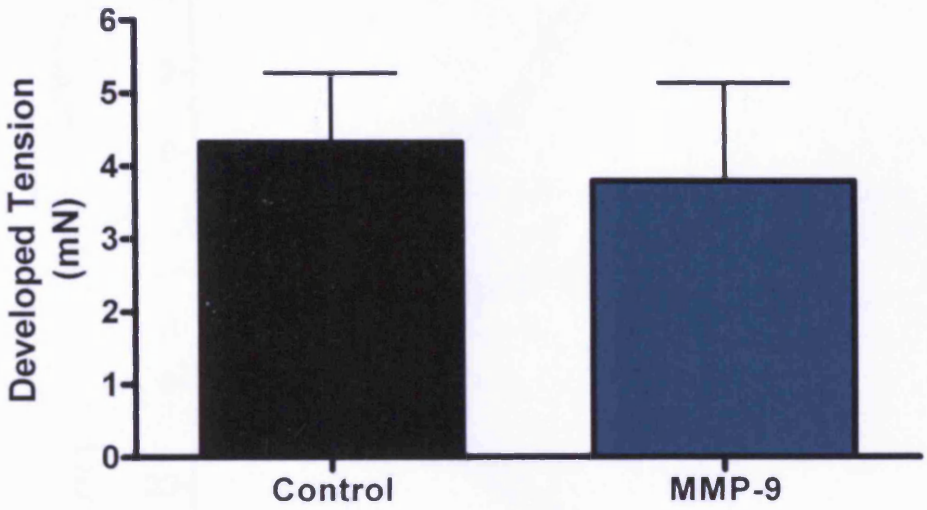

Figure 6.22. Graphs Showing Constriction to K+ (6x10-2M) Following Three Hour (TC) Incubation in the Absence (Control) and Presence of MMP-9 (15ng/ml). n=3

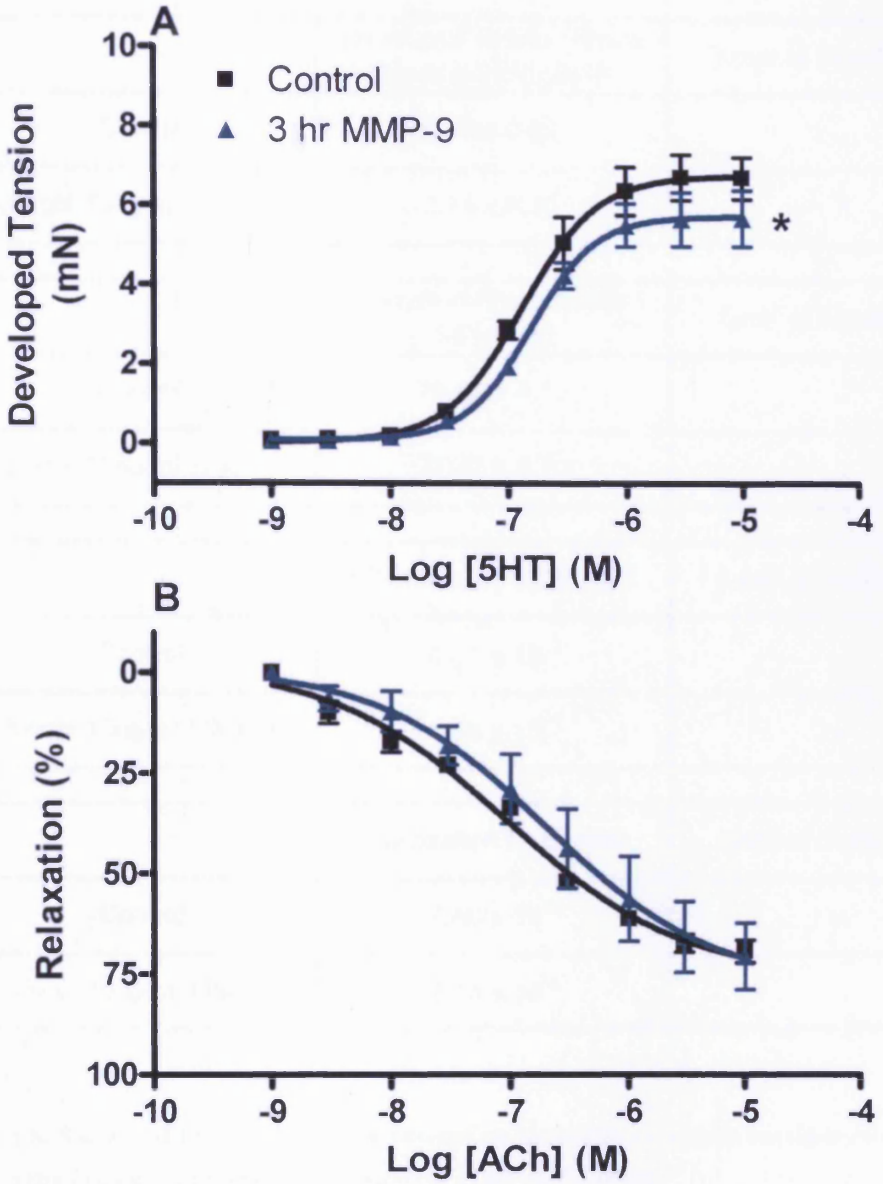

Figure 6.23. Graphs showing Constriction and Relaxation Responses to 5HT and ACh Respectively Following an Incubation period of Three Hours (TC) in Control Tissue in the Absence and Presence of MMP-9 (15ng/ml). A. Constriction responses to 5HT B. Relaxation responses to ACh in the same tissue. *$p<0.05$ compared to control determined by students t-test, n=3.

	Developed Tension Rmax (Mean ± SEM) (mN)	Level of Significance
Control	6.78 ± 0.26	-
3 hour 15ng/ml MMP-9	5.74 ± 0.25	*

	Relaxation Rmax (Mean ± SEM) (%)	Level of Significance
Control	75.44 ± 4.16	-
3 hour 15ng/ml MMP-9	77.47 ± 5.70	-

	Constriction EC50 (M)	Level of Significance
Control	1.31×10^{-7}	-
3 hour 15ng/ml MMP-9	1.56×10^{-7}	-

	Relaxation EC50 (M)	Level of Significance
Control	8.68×10^{-8}	-
3 hour 15ng/ml MMP-9	9.38×10^{-8}	-

Table 6.8. Rmax and EC50 Values for Constriction Responses in Vessels Incubated for Three Hours (TC) in the Presence and Absence (Control) of MMP-9 (15ng/ml).

For three hour incubations with MMP-9 at 75ng/ml, subsequent constrictions to K^+ showed no difference between control and treated tissues (see figure 6.24). Maximum constrictions to 5HT following exposure to MMP-9 were significantly ($p<0.05$) lower compared to control tissues (see figure 6.25), while EC50 values showed no change. There was no difference in relaxation responses to ACh (see figure 6.25 and table 6.9).

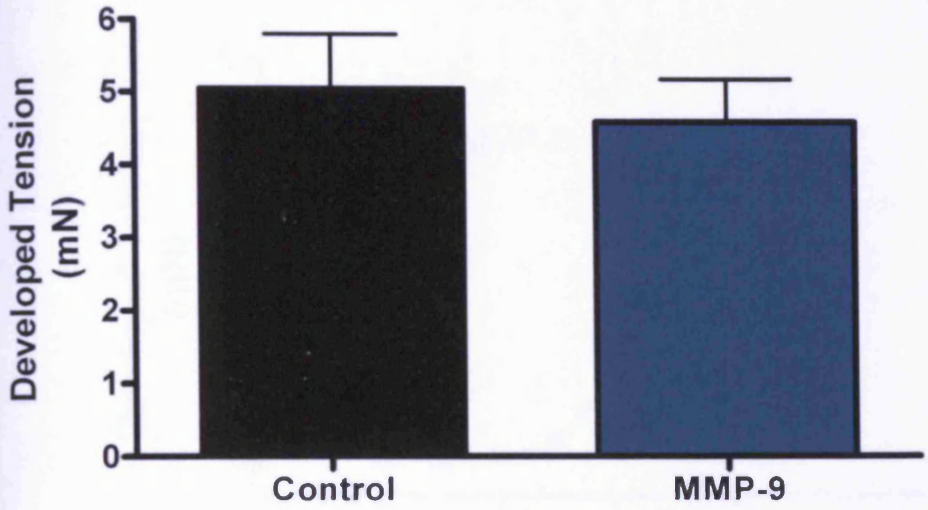

Figure 6.24. Graphs Showing Constriction to K^+ ($6x10^{-2}M$) Following Three Hour (TC) Incubation in the Absence (Control) and Presence of MMP-9 (75ng/ml). n=4.

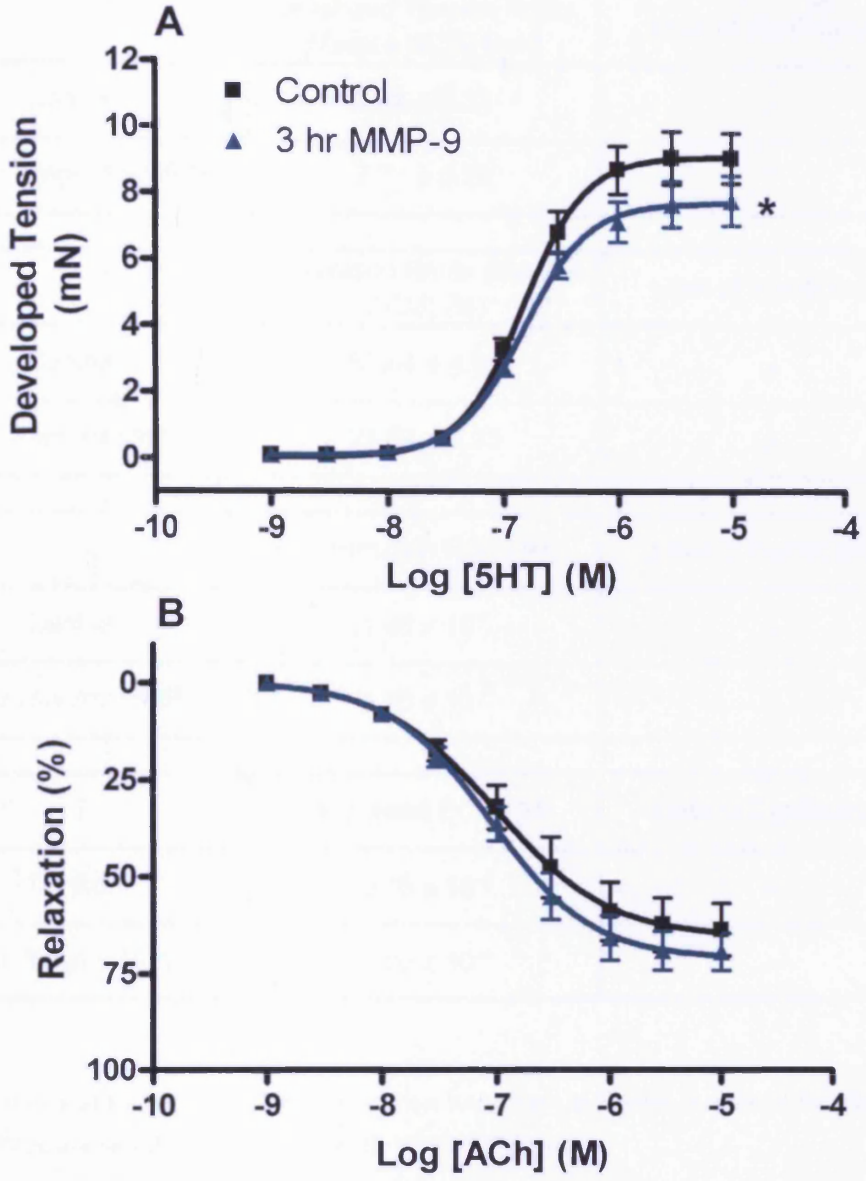

Figure 6.25. Graphs showing Constriction and Relaxation Responses to 5HT and ACh Respectively Following an Incubation period of Three hours (TC) in the Absence (Control) and Presence of MMP-9 (75ng/ml). A. Constriction responses to 5HT B. Relaxation responses to ACh in the same tissue. *$p<0.05$ compared to control determined by students t-test, n=4.

	Developed Tension Rmax (Mean ± SEM) (mN)	Level of Significance
Control	9.12 ± 0.32	-
3 hour 75ng/ml MMP-9	7.71 ± 0.28	*
	Relaxation Rmax (Mean ± SEM) (%)	Level of Significance
Control	65.44 ± 4.89	-
3 hour 75ng/ml MMP-9	71.02 ± 3.23	-
	Constriction EC50 (M)	Level of Significance
Control	1.48×10^{-7}	-
3 hour 75ng/ml MMP-9	1.50×10^{-7}	-
	Relaxation EC50 (M)	Level of Significance
Control	9.70×10^{-8}	-
3 hour 75ng/ml MMP-9	8.80×10^{-8}	-

Table 6.9. Rmax and EC50 Values for Constriction Responses in Vessels Incubated for Three Hours (TC) in the Presence and Absence (Control) of MMP-9 (75ng/ml).

6.4.4.5 Incubation with Normal and "Severe" Levels of MMP-9 in Tissue Culture Medium for Twenty Four Hours.

Aortae were removed from naive animals and incubated in tissue culture media for twenty four hours in the absence or presence of MMP-9 (15 or 75ng/ml). Vessel responses to K^+, 5HT and ACh were then measured as described in section 2.4. Constrictions to K^+ showed no difference in vessels incubated with MMP-9 (15ng/ml) compared to controls (see figure 6.26). Maximum responses to 5HT again showed no

statistical difference, however relaxation responses following exposure to MMP-9 failed to reach the same level as controls (see figure 6.27). For Rmax and EC50 values see table 6.10.

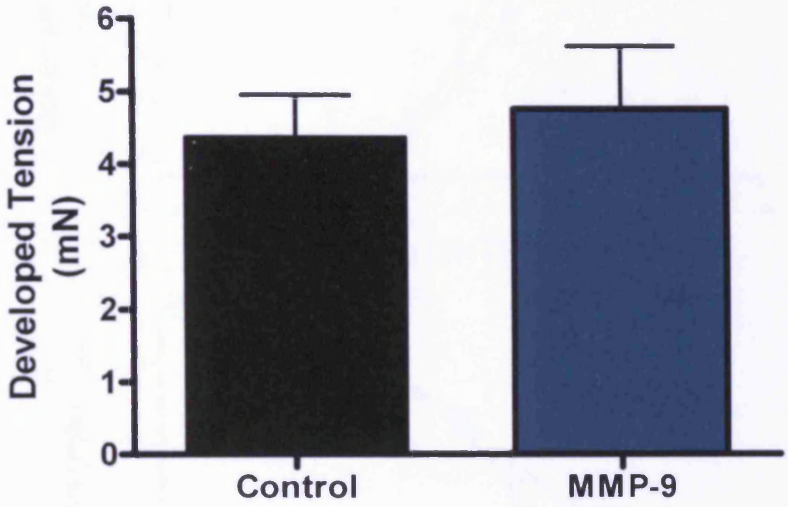

Figure 6.26. Graphs Showing Constriction to K+ (6x10-2M) Following Twenty Four Hour (TC) Incubation in the Absence (Control) and Presence MMP-9 (15ng/ml). n=3

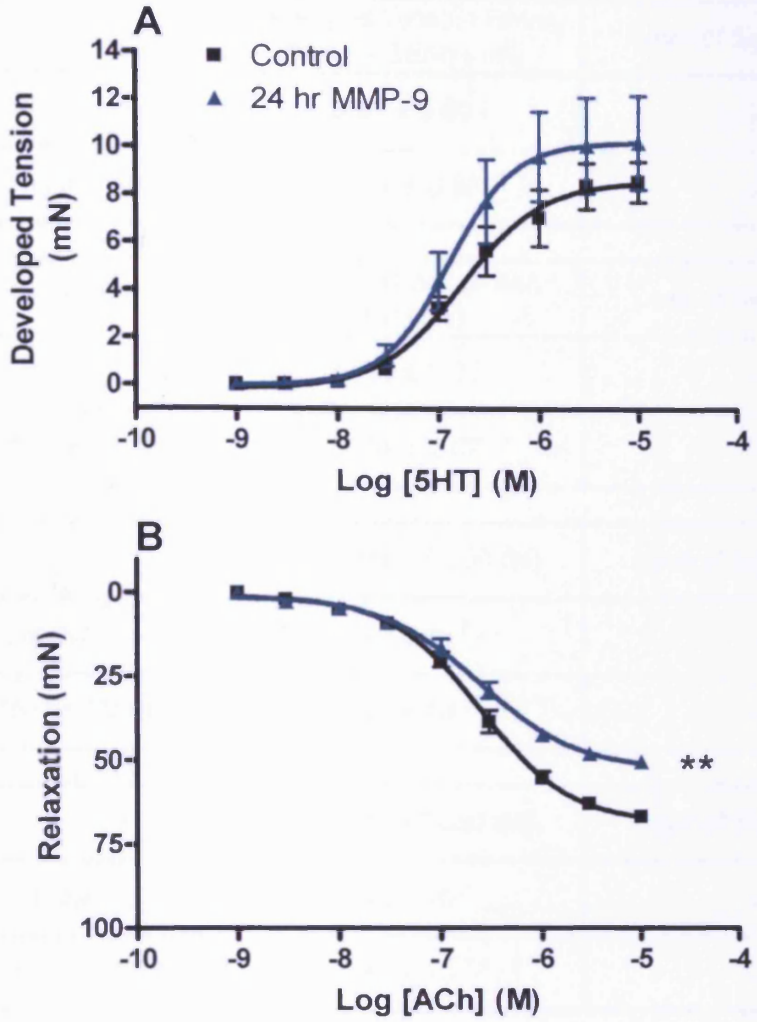

Figure 6.27. Graphs showing Constriction and Relaxation Responses to 5HT and ACh Respectively Following an Incubation period of Twenty Four hours (TC) in Control Tissue in the Absence and Presence of MMP-9 (15ng/ml). A. Constriction responses to 5HT B. Relaxation responses to ACh in the same tissue. **$p<0.01$ compared to control determined by students t-test, n=3.

	Developed Tension Rmax (Mean ± SEM) (mN)	Level of Significance
Control	8.61 ± 0.60	-
24 hour 15ng/ml MMP-9	10.27 ± 0.88	-

	Relaxation Rmax (Mean ± SEM) (%)	Level of Significance
Control	68.45 ± 2.05	-
24 hour 15ng/ml MMP-9	52.54 ± 2.07	**

	Constriction EC50 (M)	Level of Significance
Control	1.70×10^{-7}	-
24 hour 15ng/ml MMP-9	1.27×10^{-7}	-

	Relaxation EC50 (M)	Level of Significance
Control	2.45×10^{-7}	-
24 hour 15ng/ml MMP-9	2.42×10^{-7}	-

Table 6.10. Rmax and EC50 Values for Constriction Responses in Vessels Incubated for Twenty Four Hours (TC) in the Presence and Absence (Control) of MMP-9 (15ng/ml).

Constriction responses to K^+ showed no significant difference in tissues exposed to the higher concentration of MMP-9 (75ng/ml, see figure 6.28). However, responses (Rmax) to 5HT in the same tissues were significantly ($p<0.05$) lower than controls (see figure 6.29), with EC50 values presenting no change. Maximum relaxation responses to ACh were also significantly ($p<0.05$) different with those in MMP-9-treated tissues greater than controls. EC50 values again showed no difference (see table 6.11)

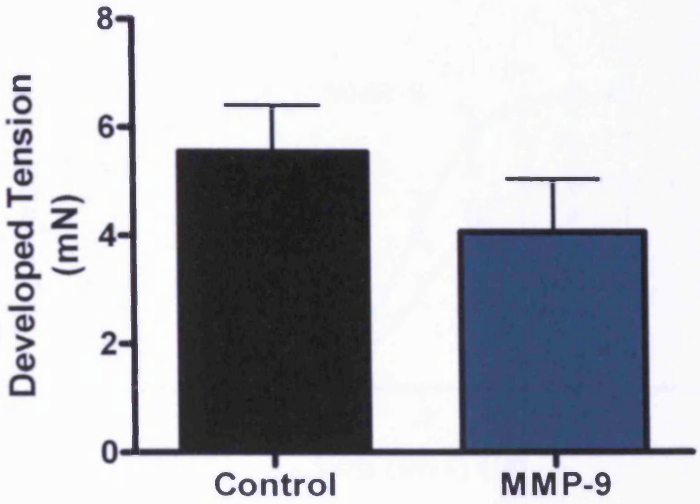

Figure 6.28. Graphs Showing Constriction K+ (6x10-2M) Following Twenty Four Hour Incubation in the Absence (Control) and Presence MMP-9 (75ng/ml). n=4.

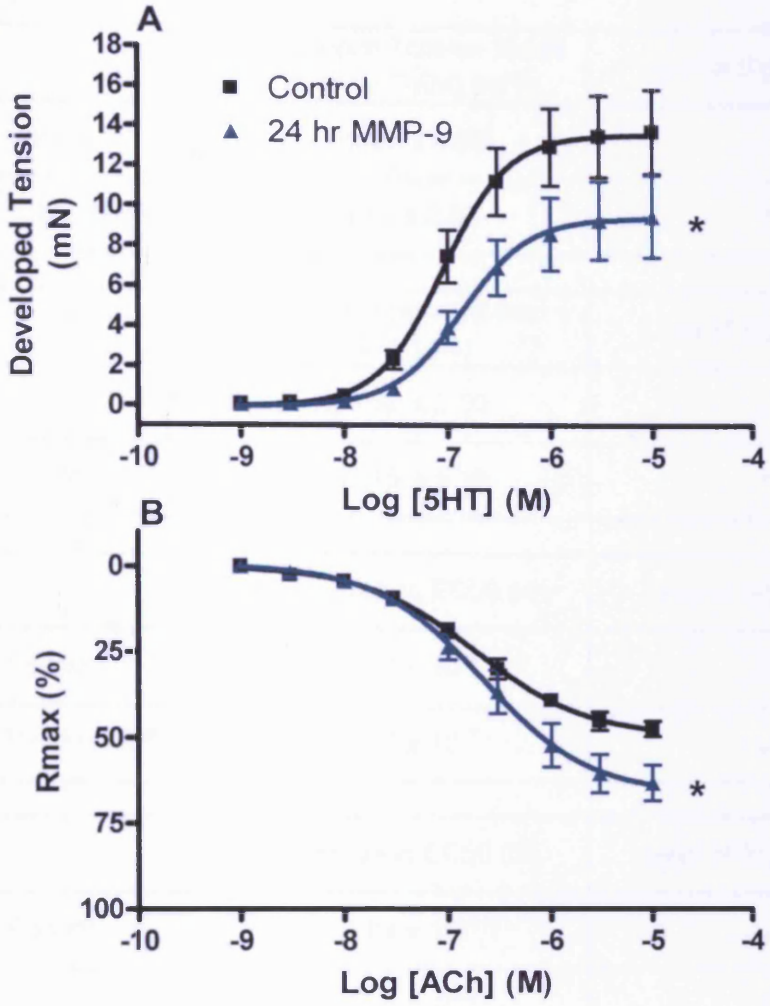

Figure 6.29. Graphs showing Constriction and Relaxation Responses to 5HT and ACh Respectively Following an Incubation period of Twenty Four hours (TC) in the Absence (Control) and Presence of MMP-9 (75ng/ml). A. Constriction responses to 5HT B. Relaxation responses to ACh in the same tissue. *$p<0.05$ compared to control determined by students t-test, n=4.

	Developed Tension Rmax (Mean ± SEM) (mN)	Level of Significance
Control	13.63 ± 0.86	-
24 hour 75ng/ml MMP-9	9.45 ± 0.86	*

	Relaxation Rmax (Mean ± SEM) (%)	Level of Significance
Control	44.92 ± 2.60	-
24 hour 75ng/ml MMP-9	66.15 ± 5.18	*

	Constriction EC50 (M)	Level of Significance
Control	8.99×10^{-8}	-
24 hour 75ng/ml MMP-9	1.35×10^{-7}	-

	Relaxation EC50 (M)	Level of Significance
Control	1.84×10^{-7}	-
24 hour 75ng/ml MMP-9	2.16×10^{-7}	-

6.11. Rmax and EC50 Values for Constriction Responses in Vessels Incubated for Twenty Hours (TC) in the Presence and Absence (Control) of MMP-9 (75ng/ml).

6.6 Incubation with "Severe" Levels of MMP-9 in the presence of an MMP-9 Inhibitor

Preliminary experiments were carried out to determine the effect of an MMP-9 inhibitor on naive vessels. As such, tissues were incubated in the absence or presence of the MMP-9 inhibitor for twenty four hours in tissue culture media as before. This exposure had no significant effect on subsequent constriction responses to K^+ (see figure 6.30) or 5HT or

relaxation responses to ACh (figure 6.31). Rmax and EC50 values for this data are shown in table 6.12.

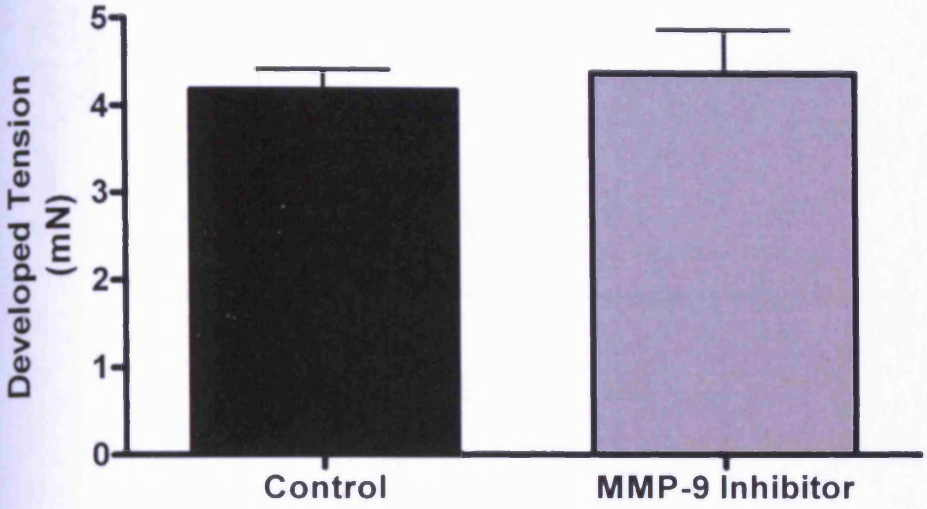

Figure 6.30. Graphs Showing Constriction Responses to K+ (6 x 10-2M) Following an Incubation period of Twenty Four hours (TC) in the Absence (Control) and Presence of an MMP-9 Inhibitor. n=4.

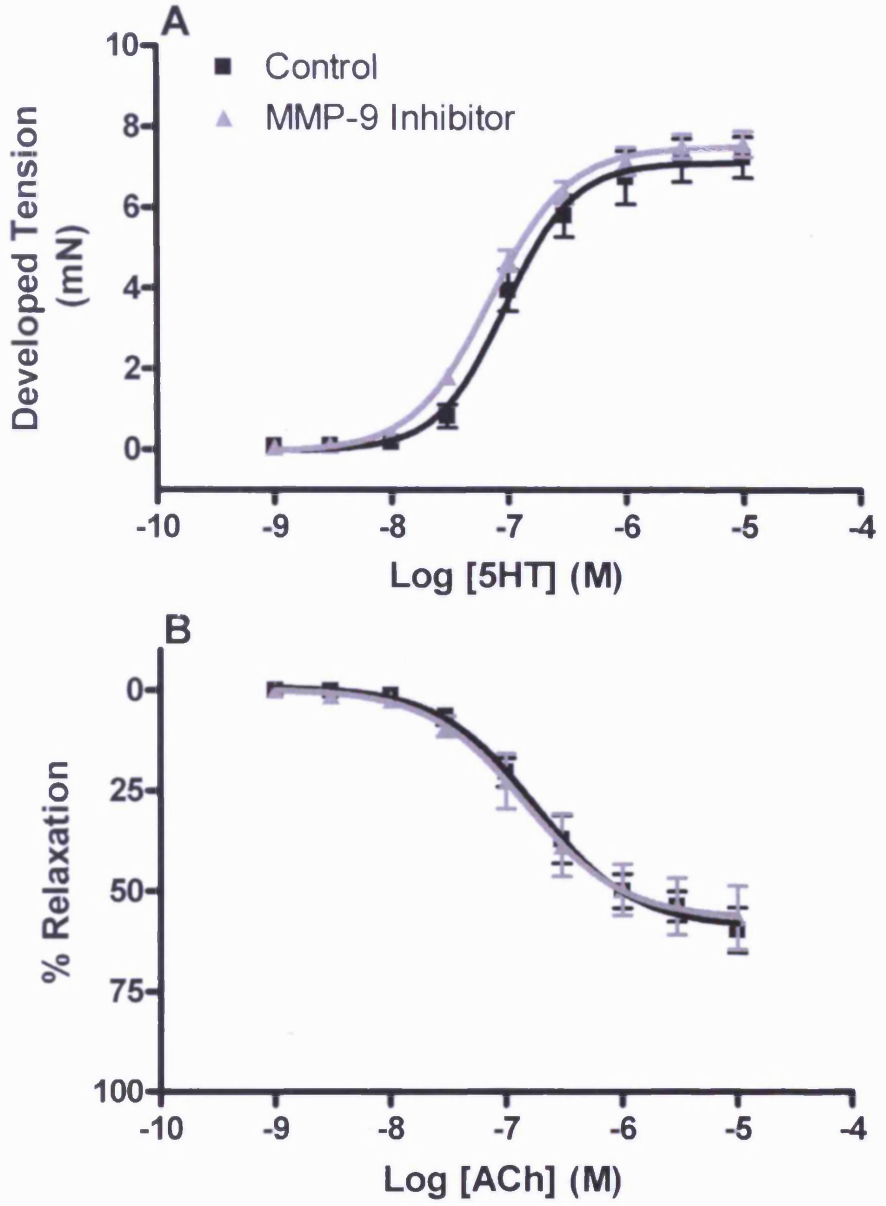

Figure 6.31. Graphs showing Constriction Responses to 5HT Following an Incubation period of Twenty Four hours (TC) in Control Tissue in the Absence and Presence of an MMP-9 Inhibitor. A. Constriction responses to 5HT B. Relaxation responses to ACh in the same tissue, n=4.

	Developed Tension Rmax (Mean ± SEM) (mN)
Control	7.12 ± 0.26
MMP-9 Inhibitor	7.51 ± 0.15

	Relaxation Rmax (Mean ± SEM) (%)
Control	58.89 ± 3.36
MMP-9 Inhibitor	56.74 ± 4.70

	Constriction EC50 (M)
Control	9.52×10^{-8}
MMP-9 Inhibitor	7.09×10^{-8}

	Relaxation EC50 (M)
Control	1.82×10^{-7}
MMP-9 Inhibitor	1.47×10^{-7}

Table 6.12. Rmax and EC50 Values for Constriction Responses in Vessels Incubated for Twenty Four Hours (TC) in the Presence and Absence (Control) of an MMP-9 Inhibitor.

Subsequently vessels from naïve animals were incubated in the absence or presence of MMP-9 (75ng/ml) for twenty four hours, with the MMP-9 inhibitor being added to some tissues as appropriate. Constriction responses to K^+ (6×10^{-2}M) were again largely unaffected by any of the incubation conditions (see figure 6.32). Incubation with the MMP-9 inhibitor reversed the dampening effect of MMP-9 on maximum constriction responses to 5HT (figure 6.33). EC50 values and relaxation responses to ACh showed no change (see figure 6.33 and table 6.13)

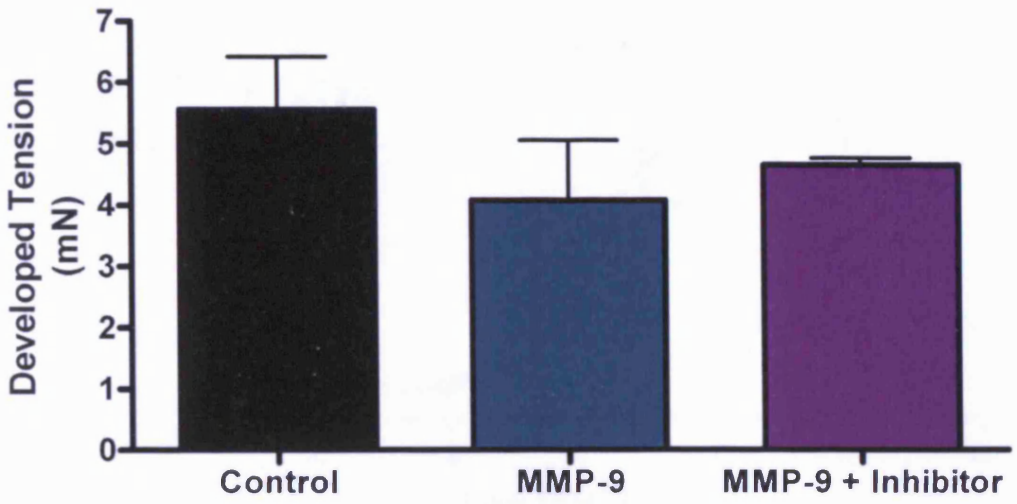

Figure 6.32. Graphs Showing Constriction Following Twenty Four Hour (TC) Exposure to K^+ ($6x10^{-2}$M) in the Absence (Control) and Presence of MMP-9 (75ng/ml), and MMP-9 and a MMP-9 Inhibitor. n=4 for all.

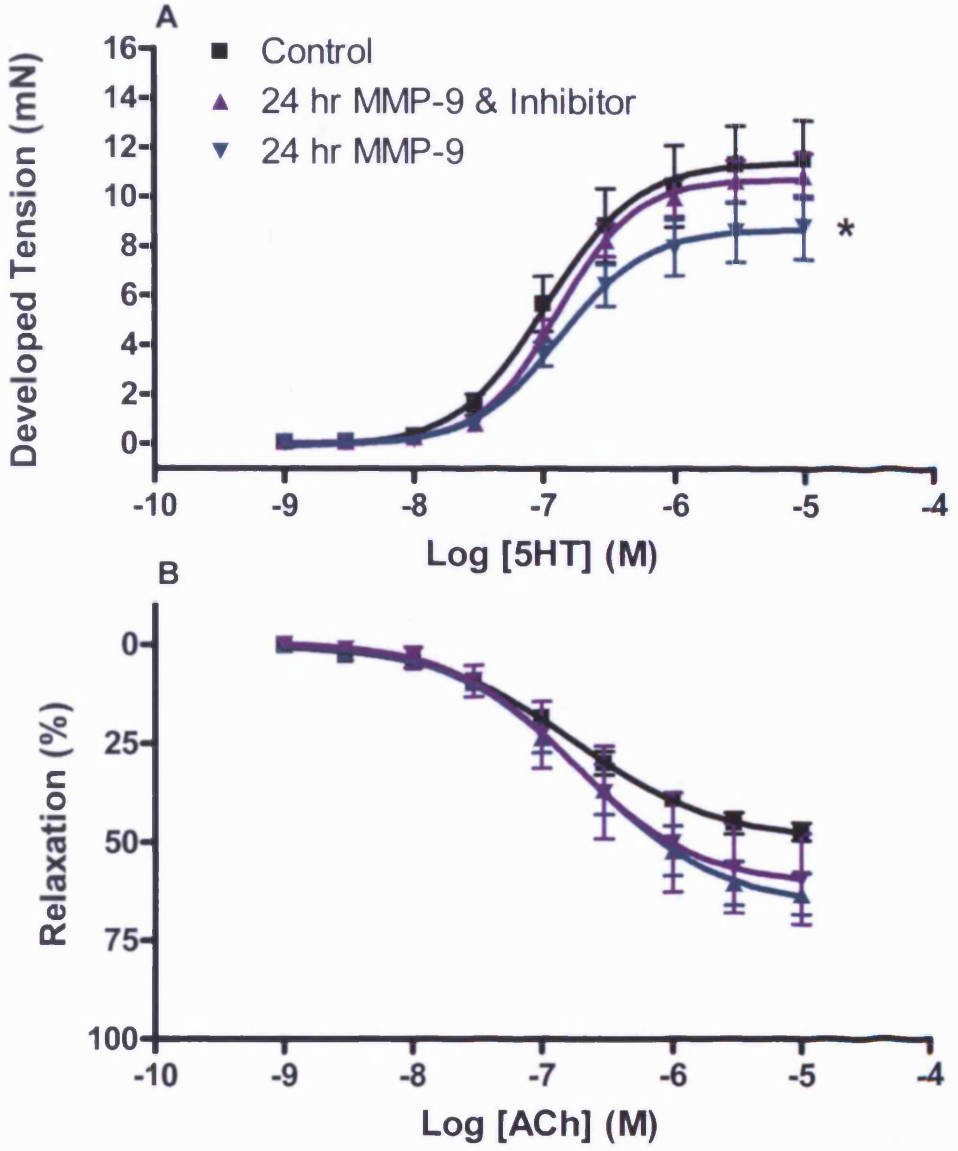

Figure 6.33. Graphs showing Vessel Responses with MMP-9 (75ng/nl) in the Presence and Absence (Control) of an MMP-9 Inhibitor. A. Constrictions responses. B. Relaxation responses. *$p<0.05$ compared to normal determined by one-way ANOVA followed by Newman-Keuls test n=4.

	Developed Tension Rmax (Mean ± SEM) (mN)	Level of Significance
Control	11.42 ± 0.79	-
24 hour 75ng/ml MMP-9	8.71 ± 0.56	*
24 hour 75ng/ml MMP-9 AND MMP-9 Inhibitor	11.20 ± 0.07	-

	Relaxation Rmax (Mean ± SEM) (%)	Level of Significance
Control	49.42 ± 2.60	-
24 hour 75ng/ml MMP-9	66.15 ± 5.18	-
24 hour 75ng/ml MMP-9 AND MMP-9 Inhibitor	60.69 ± 8.52	-

	Constriction EC50 (M)	Level of Significance
Control	1.07×10^{-7}	-
24 hour 75ng/ml MMP-9	1.35×10^{-7}	-
24 hour 75ng/ml MMP-9 AND MMP-9 Inhibitor	1.35×10^{-7}	-

	Relaxation EC50 (M)	Level of Significance
Control	1.84×10^{-7}	-
24 hour 75ng/ml MMP-9	2.16×10^{-7}	-
24 hour 75ng/ml MMP-9 AND MMP-9 Inhibitor	1.76×10^{-7}	-

Table 6.13. Rmax and EC50 Values for Constriction Responses in Vessels Incubated for Twenty Four Hours (TC) in the Presence and Absence (Control) of MMP-9 (75ng/ml) and MMP-9 with MMP-9 Inhibitor.

6.4.5 *Ex-vivo* Incubation of Aortae from Moderate-scored mCIA with MMP-9 Inhibitor

In these experiments tissue was removed from naïve and moderate-scored mCIA animals as appropriate and incubated in TC media in the absence and presence of the MMP-9 inhibitor for twenty four hours. Following this vessel responses to K^+, 5HT and ACh were assessed as previously described above. The presence of the MMP-9 inhibitor had no effect on K^+-induced contractions, "moderate" vessels still failing to reach the tension achieved by control tissue (see figure 6.34). Incubation with the inhibitor had a minor but not significant effect on the responses to 5HT in moderate tissue (see figure 6.35). EC50 values were not different. Relaxation responses to ACh were similar in all tissues. This was shown statistically with no difference between Rmax and EC50 values (see table 6.14).

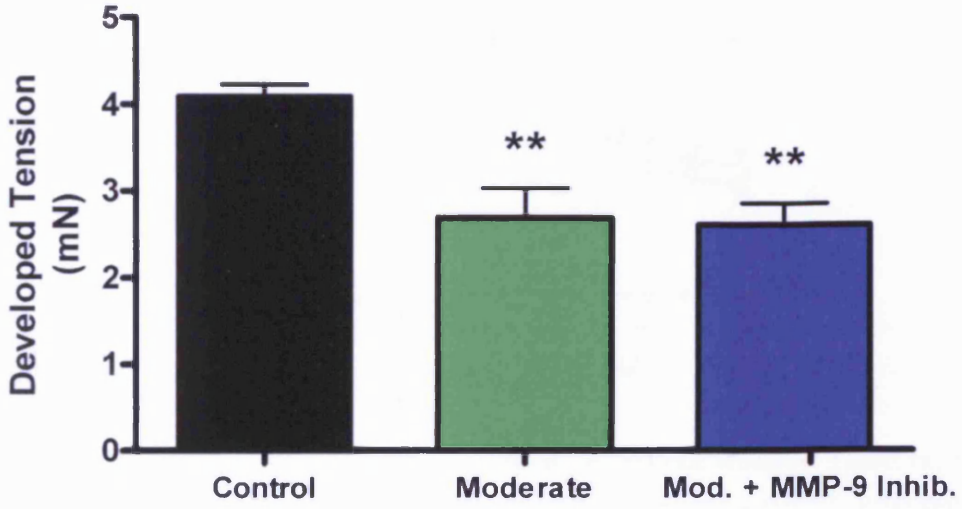

Figure 6.34. Graphs Showing Constriction Responses to K+ (6x10-2M) Following Twenty Four Hour (TC) Incubation from Control and Moderate tissue, the latter in the Absence and Presence of an MMP-9 Inhibitor. **$p<0.01$ determined by one-way ANOVA followed by Newman-Keuls test, Control n=5, moderate n=8, moderate and MMP-9 inhibitor n=8.

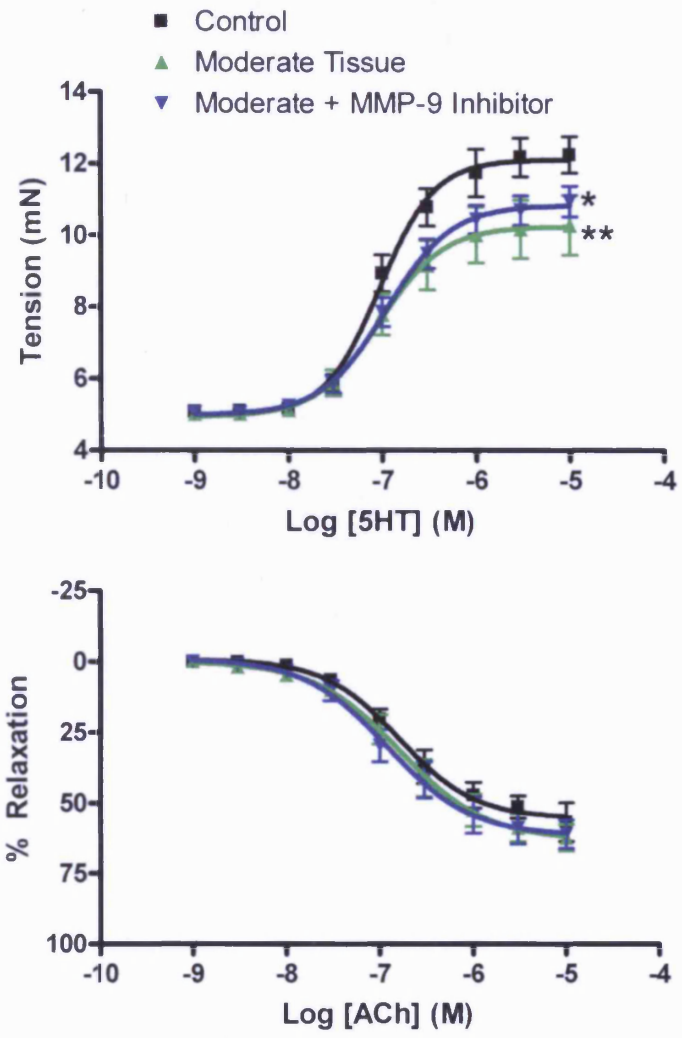

Figure 6.35. Graphs Showing Vessel Responses from Control and Moderate Tissue, the latter in the Absence and Presence of a MMP-9 Inhibitor. A. Constrictions responses. B. Relaxation responses. Control n=5, moderate n=8, moderate and MMP-9 inhibitor n=8. *$p<0.05$, **$p<0.01$ compared to control.

	Developed Tension Rmax (Mean ± SEM) (mN)	Level of Significance
Control	7.12 ± 0.26	-
Moderate	5.26 ± 0.38	***
Moderate + MMP-9 Inhibitor	5.86 ± 0.22	**

	Relaxation Rmax (Mean ± SEM) (%)	Level of Significance
Control	55.43 ± 0.96	-
Moderate	63.11 ± 4.23	-
Moderate + MMP-9 Inhibitor	61.58 ± 4.12	-

	Constriction EC50 (M)	Level of Significance
Control	9.52×10^{-8}	-
Moderate	9.43×10^{-8}	-
Moderate + MMP-9 Inhibitor	1.1×10^{-7}	-

	Relaxation EC50 (M)	Level of Significance
Control	1.62×10^{-7}	-
Moderate	1.64×10^{-7}	-
Moderate + MMP-9 Inhibitor	1.21×10^{-7}	-

Table 6.14. Rmax and EC50 Values for Constriction Responses in Control and Moderate Vessels Incubated for Twenty Four Hours (TC), the Latter in the Presence and Absence of a MMP-9 Inhibitor.

6.4.6 Immunohistochemistry: Localisation and Cellular Sources of MMP-9 in mCIA joints

6.4.6.1 Localisation of MMP-9 staining

Paws were removed as appropriate from naïve animals (and represent normal anatomy) and those with mild, moderate and severe scores for mCIA. Sections of joints were stained for MMP-9 (total) to observe the change in expression of this enzyme with the progression of arthritis. To demonstrate antibody specificity a negative control was used; briefly a serial section from each sample measured was incubated with an isotype control immunoglobulin at the same concentration as the primary antibody in place of the primary antibody. Representative staining for MMP-9 is shown in figure 6.36. As indicated (figure 6.37) MMP-9 expression is present in the joint proximal to bone areas and in the cellular infiltrate. Residing in this infiltrate will be immune cells such as DCs, T-cells, B-cells, mast cells, neutrophils, monocytes macrophages and others, all of which contribute to inflammation and bone destruction (for an overview of the inflammatory process in the rheumatoid joint see Chapter 1, section 1.2.2). Figure 6.38 shows an example of MMP-9 staining in a normal joint and joints taken from mCIA animals.

MMP-9 was observed and measured within the infiltrate in the joint space and levels of this enzyme were observed to increase with increasing arthritic severity. Results are shown for both these areas in figure 6.38. Statistical analyses showed no significant difference between the means for any groups although an obvious trend is observed.

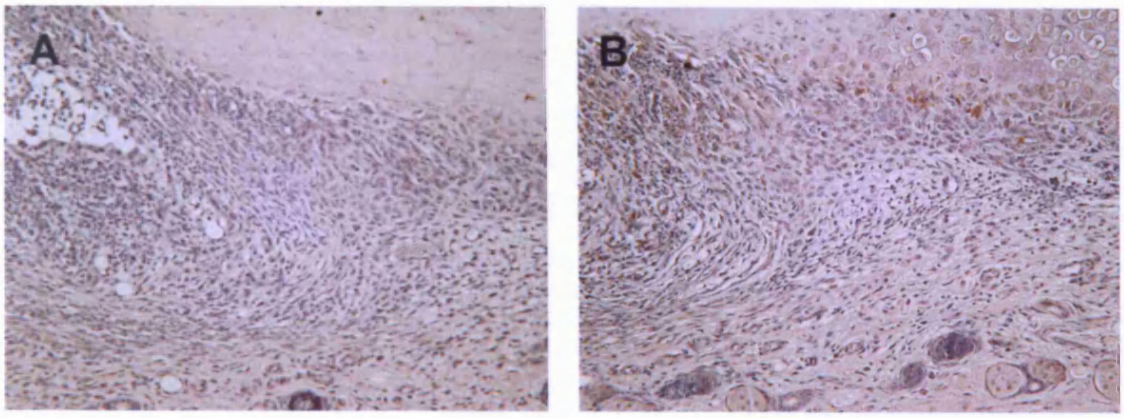

Figure 6.36. Positive and Negative Staining for MMP-9. A. Shows negative staining following incubation with an IgG isotype control. B. Positive staining with the MMP-9 antibody.

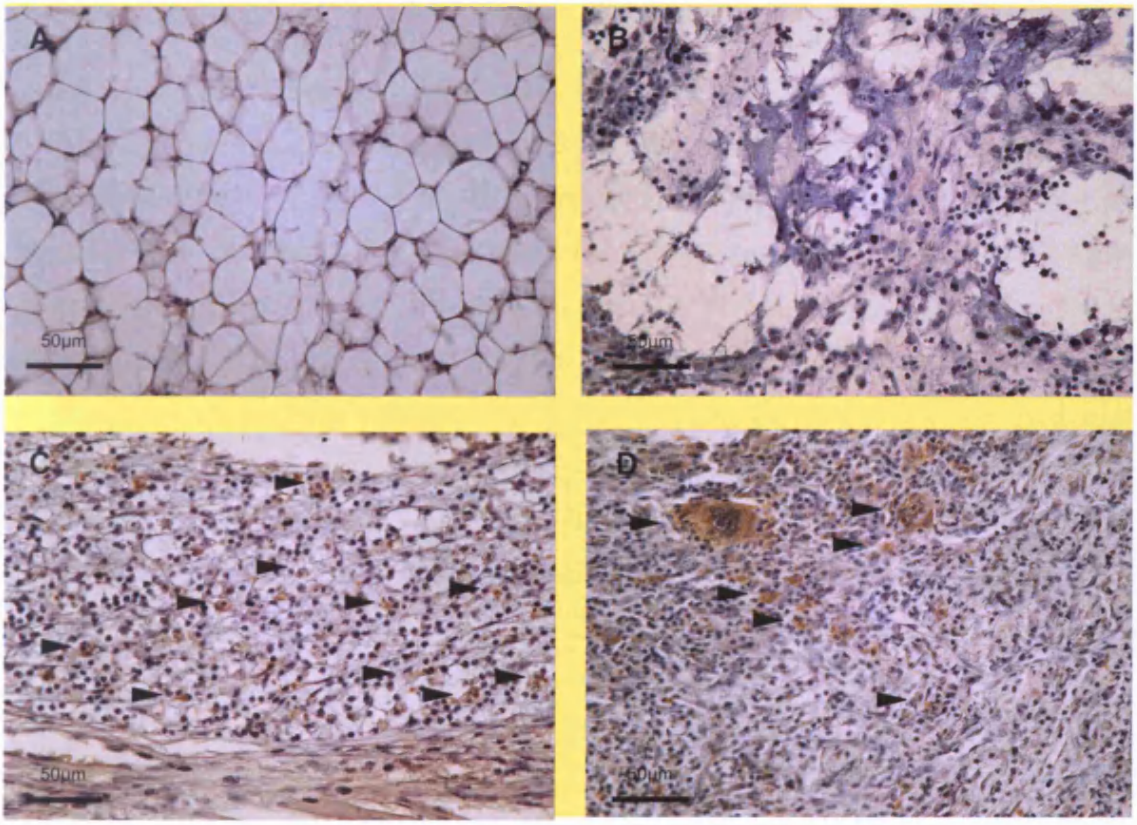

Figure 6.37. Example of MMP-9 Staining. MMP-9 is indicated by the presence of brown around the purple nuclei shown here by black arrow heads. MMP-9 staining in the joint space in A. a normal joint, B. a mild joint, C. a moderate joint and D a severely arthritic joint (at X 40 magnification).

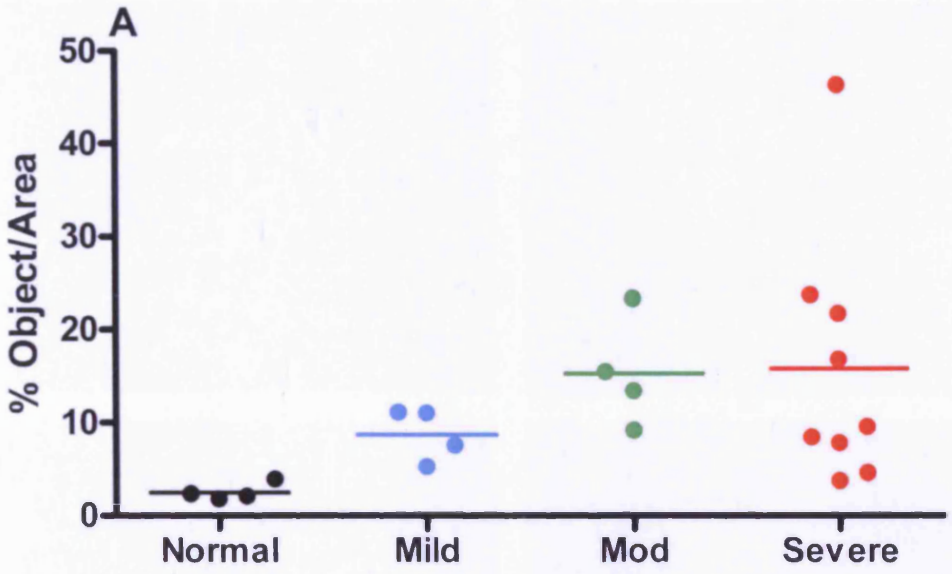

Figure 6.38. Percentage of MMP-9 Staining in Normal and mCIA Joints. A. MMP-9 staining in the cellular infiltrate of normal, mild, moderate and severe joints. For definition of y-axis see section 6.3.9.4.

6.4.6.2 Staining for Macrophages in the mCIA Joint

In these experiments appropriate paw sections (as above) were stained for F4/80, the macrophage antigen. Antibody specificity was demonstrated by using a negative control; a serial section from each sample was incubated with an isotype control immunoglobulin. Representative staining for F4/80 is shown in figure 6.39. Macrophages were observed in the infiltrate (figure 6.40) and near the bone surfaces (figure 6.41) indicating a role for them in bone destruction. The numbers of macrophages present also increased with arthritic severity (see figure 6.42). In serial sections, the production of MMP-9 could be localised to macrophages (see figure 6.43). On occasion macrophages could be observed in the hyperplastic synovial membrane, an occurrence which was associated with MMP-9 production (see figure 6.44). This was a rare occurrence and as such was not quantified.

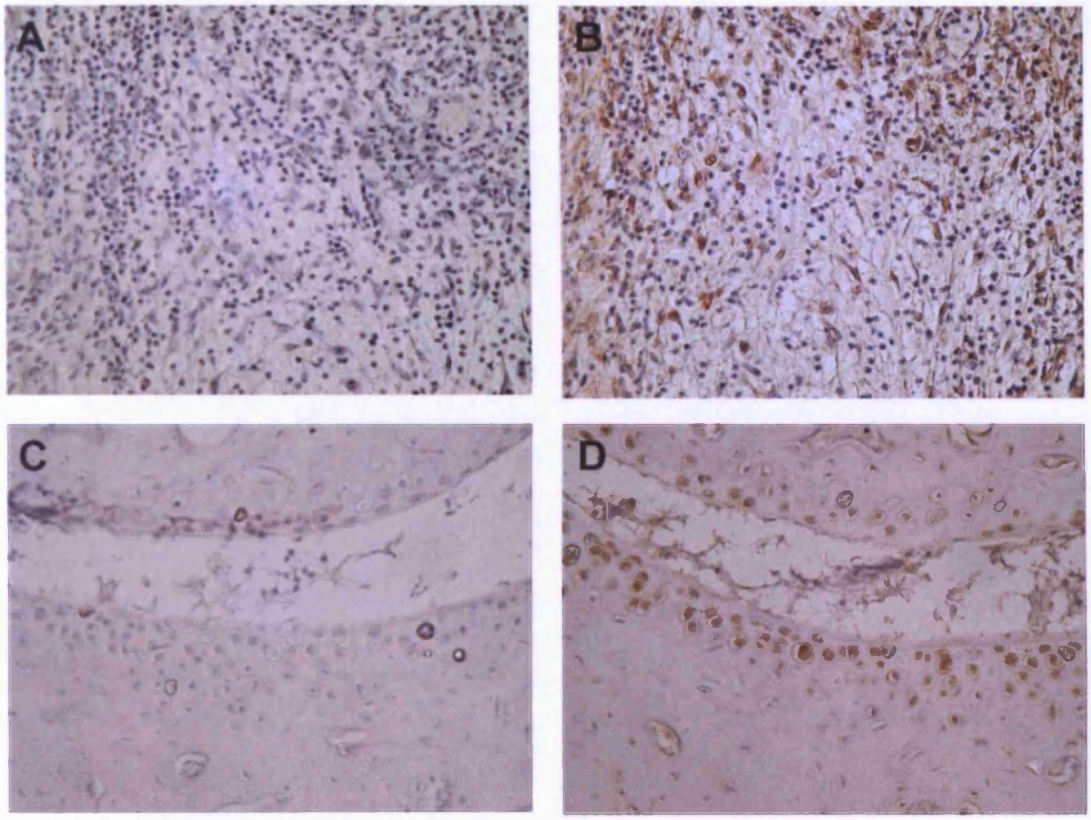

Figure 6.39 Negative and Positive Staining for F4/80 A. Negative staining following incubation with an IgG isotype control and B. Positive staining with the F4/80 antibody in a serial section shown in the infiltrate. C. Negative staining using an isotpye control and D. Positive staining using the F4/80 antibody in serial sections of the talus and tibia.

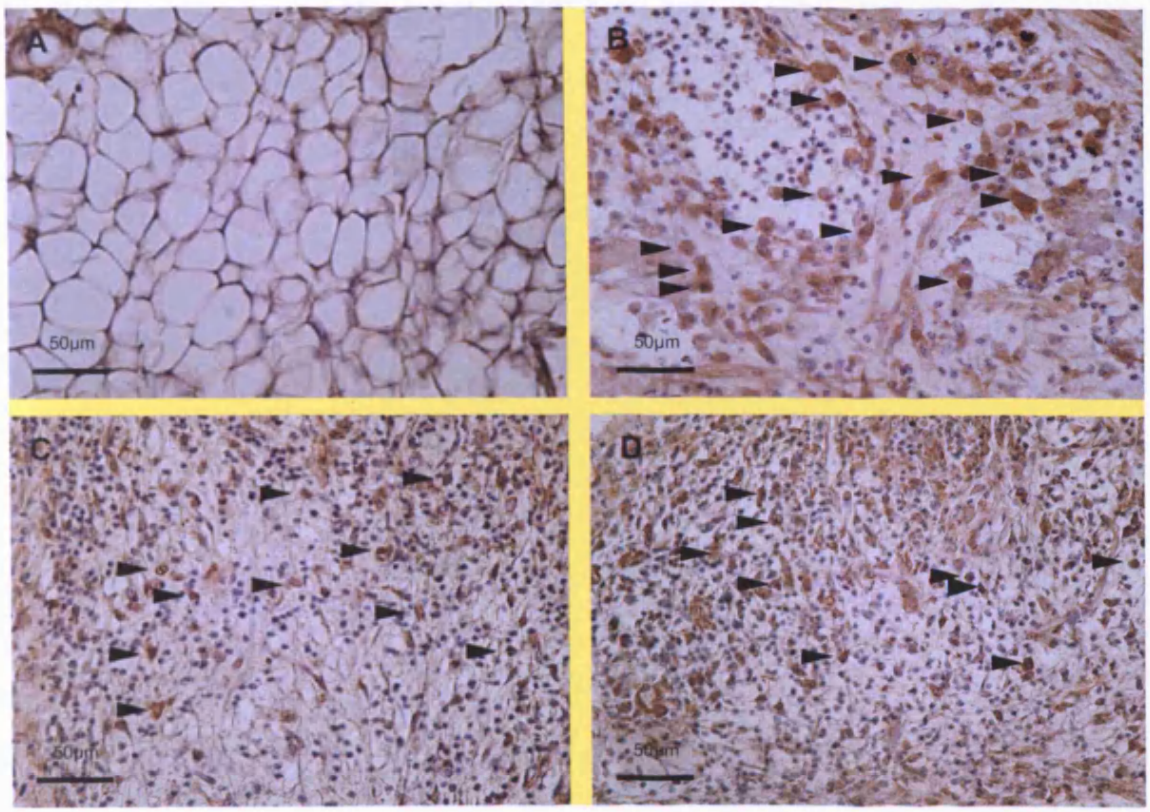

Figure 6.40. Macrophage Staining in Normal and mCIA Joints. Macrophages are indicated by the presence of large brown blobs surrounding the purple nuclei shown here by black arrow heads. Macrophage staining in the joint space in A. a normal joint, B. a mild joint, C. a moderate joint and D a severely arthritic joint (at X40 magnification).

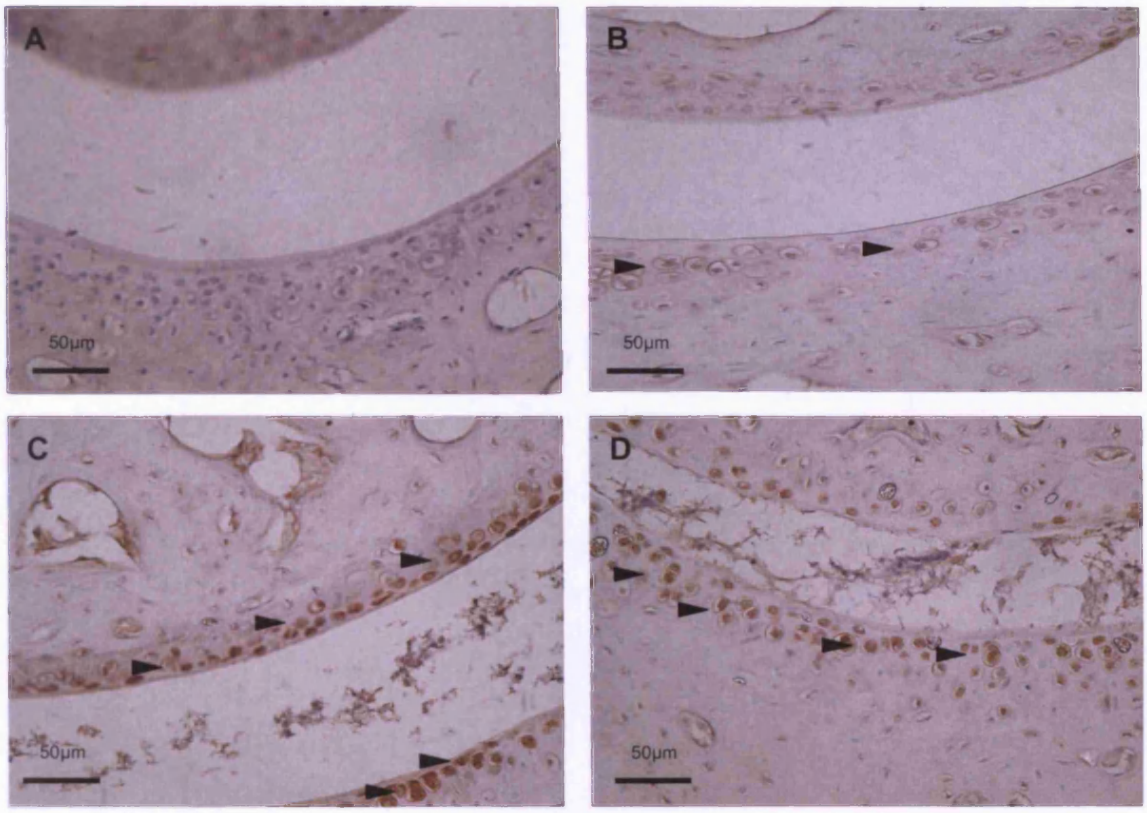

Figure 6.41. Macrophage Staining in the Talus/Tibia Area. Macrophages are indicated by the presence of large brown blobs surrounding the purple nuclei shown here by black arrow heads. Macrophage staining at the talus tibia joint in A. a normal joint, B. a mild joint, C. a moderate joint and D a severely arthritic joint (at X 40 magnification).

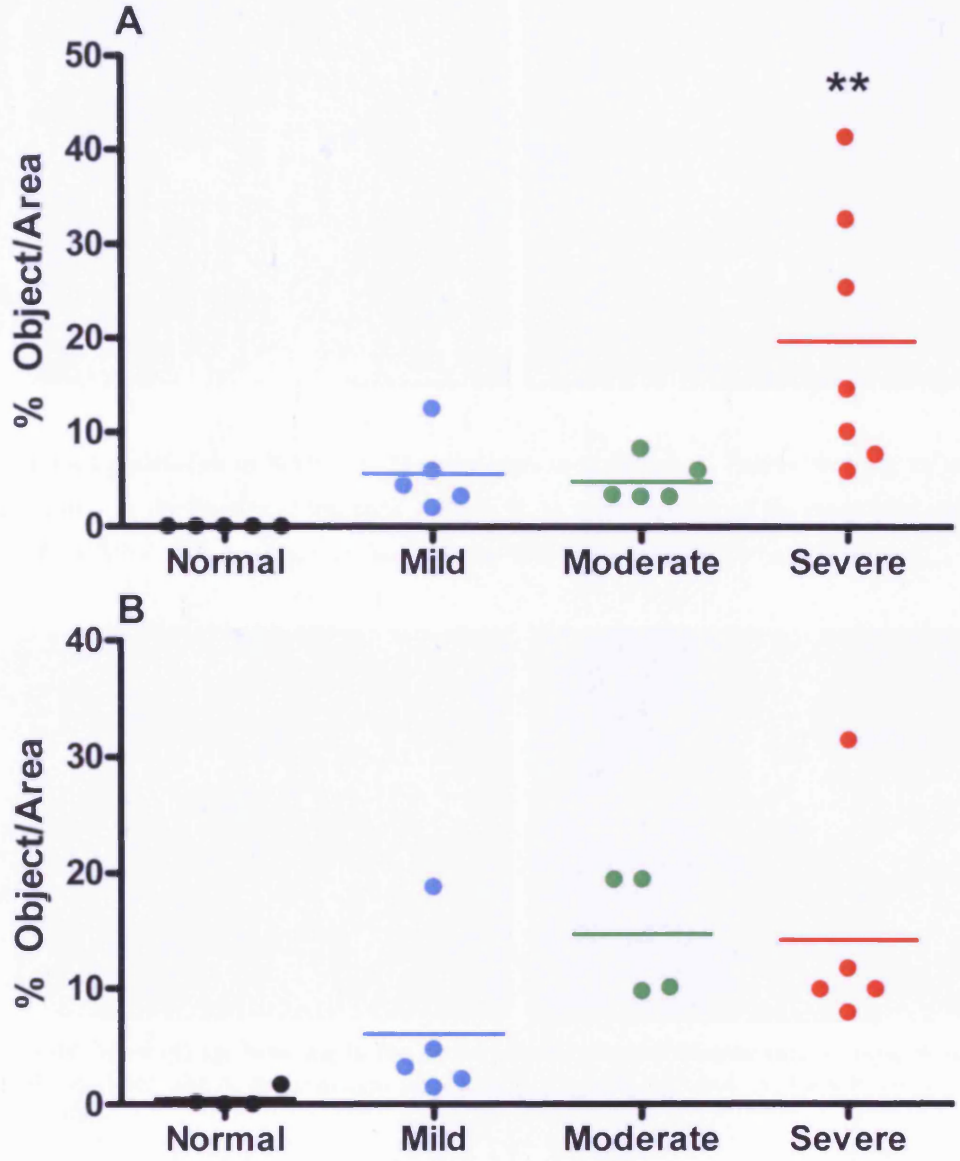

Figure 6.42. Macrophage Staining in the Arthritic Joints. A, Percentage of macrophages in the cellular infiltrate. B. Macrophages present in the talus/tibia joint. **$p<0.01$ compared to normal. For definition of y-axis see section 6.3.9.4

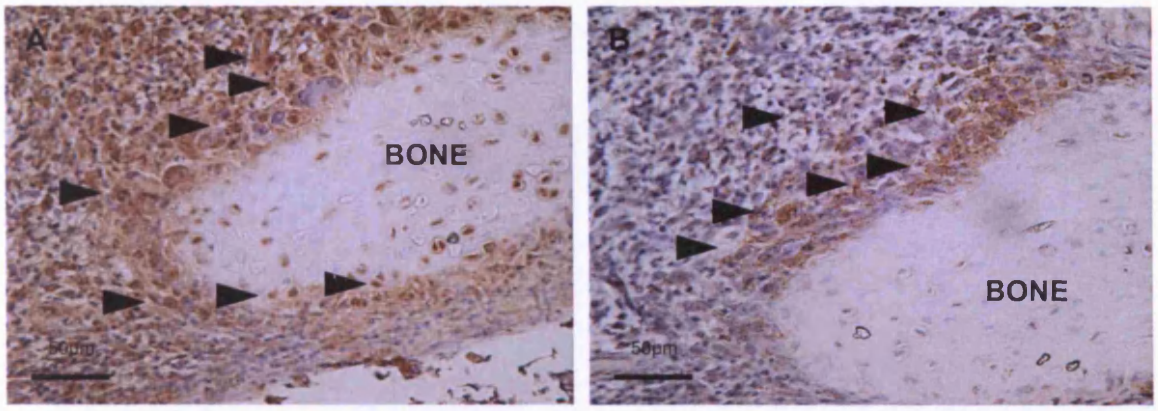

Figure 6.43. Localisation of MMP-9 to Macrophages in the Joint. A. Positive staining for macrophages (black arrows) in the joint near the bone surface. B. A serial section of the same joint showing areas positive for MMP-9 staining (black arrows) near the bone in the joint (at X40 magnification).

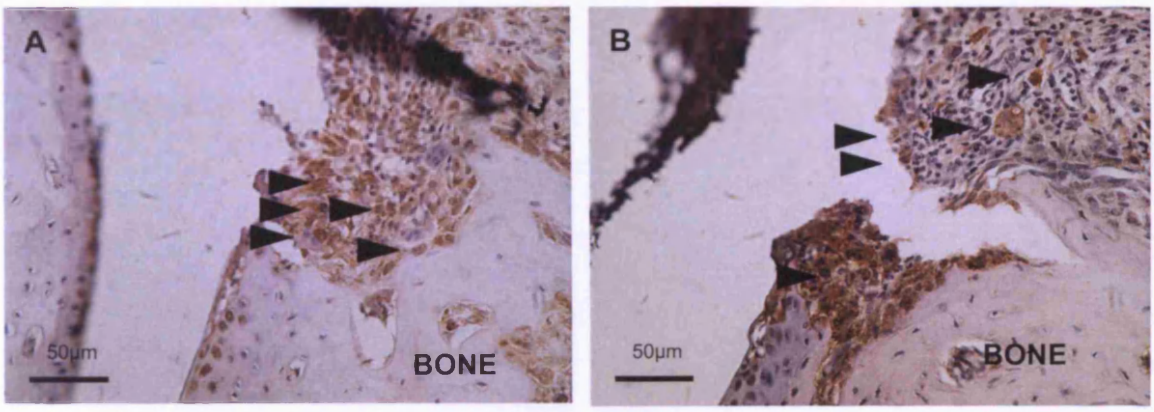

Figure 6.44. Macrophage Staining in the Hyperplastic Synovial Membrane. Staining in the talus/tibia in an arthritic joint for A. macrophages and B. MMP-9, both indicated by black arrow heads (at X 40 magnification).

6.4.6.3 Staining for Neutrophils in the mCIA Joint.

In these experiments appropriate paw sections (as above) were stained for the presence of Ly6G, a neutrophil marker. Again, in order too demonstrate antibody specificity a negative control was used at the same concentration as the primary antibody. Representative staining for Ly6G is shown in figure 6.45. On analysis neutrophils were found to be present in the cellular infiltrate and, contrasting to the location of MMP-9 and macrophages, the bone marrow shown by figures 6.46 and 6.47 respectively. The number of neutrophils in the joint was seen to increase from normal to mild and continue throughout the progression of arthritis (see figure 6.48). In serial sections the production

of MMP-9 appeared to be more closely associated with the presence of macrophages than neutrophils (see figure 6.49).

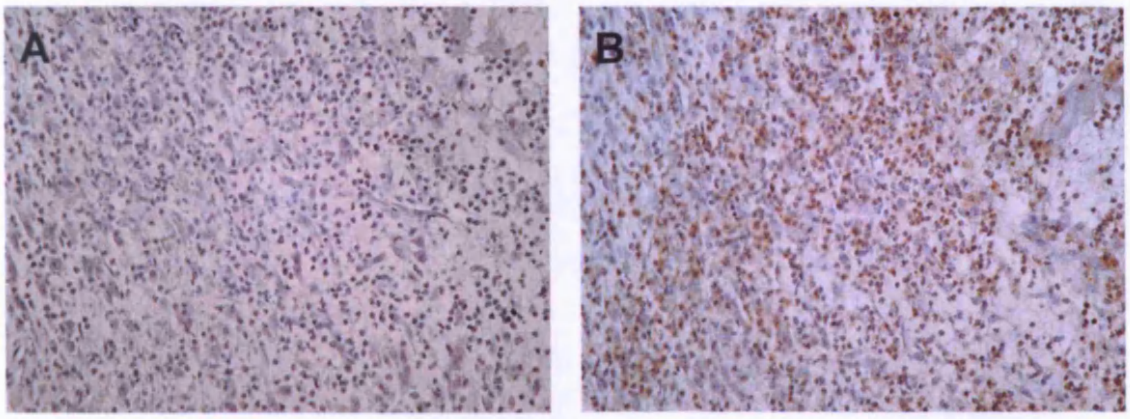

Figure 6.45. Negative and Positive Staining for Ly6G. A. Negative staining following incubation with an IgG isotype control and B. Positive staining with the Ly6G antibody in a serial section shown in the infiltrate

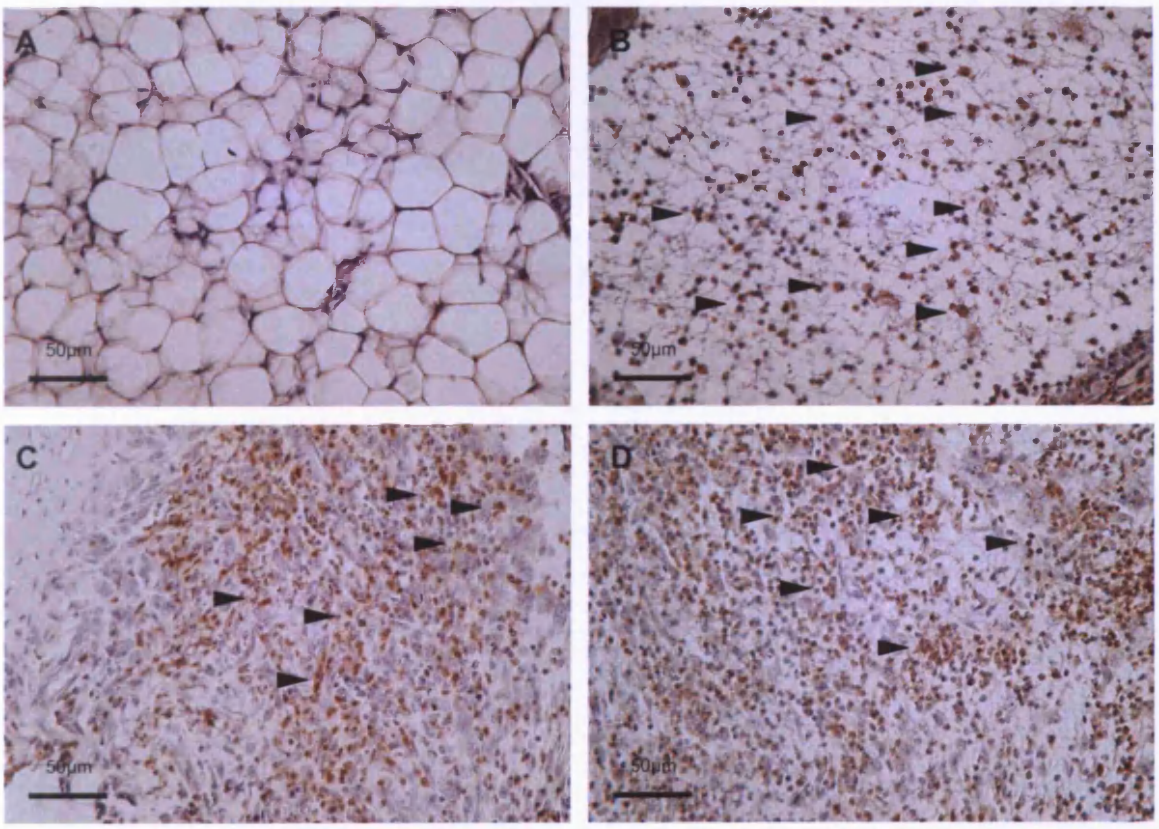

Figure 6.46. Neutrophil Staining in the Normal and mCIA Joints. Neutrophils are indicated by the presence of large brown blobs surrounding the purple nuclei shown here by black arrow heads. Neutrophil staining in the joint space in A. a normal joint, B. a mild joint, C. a moderate joint and D a severely arthritic joint, (all at X40 magnification).

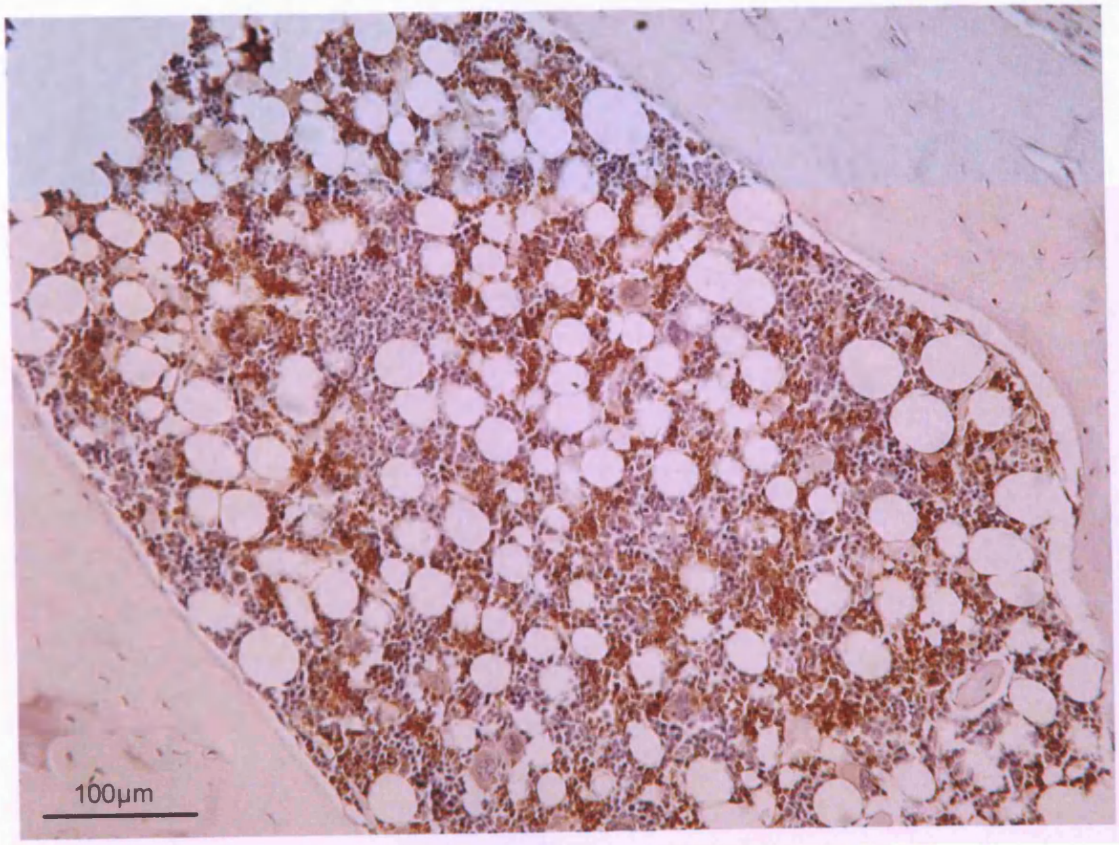

Figure 6.47. Neutrophil Staining in the Bone Marrow. At X20 magnification.

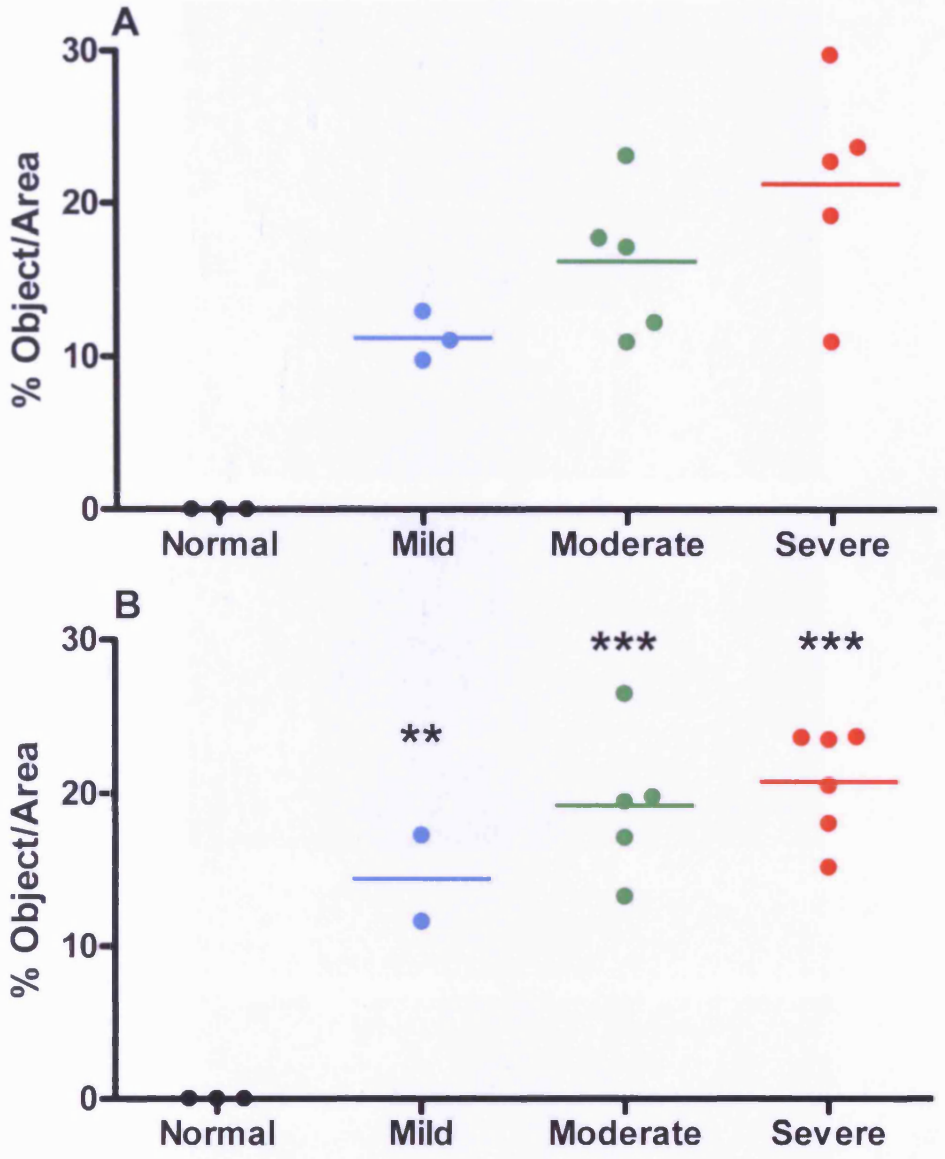

Figure 6.48 Neutrophil Staining in the Joints. A. Percentage of neutrophil staining in the joint infiltrate. B. Percentage of neutrophil staining in the bone marrow. **p<0.01, ***p<0.001 compared to normal. For definition of y-axis see section 6.3.9.4

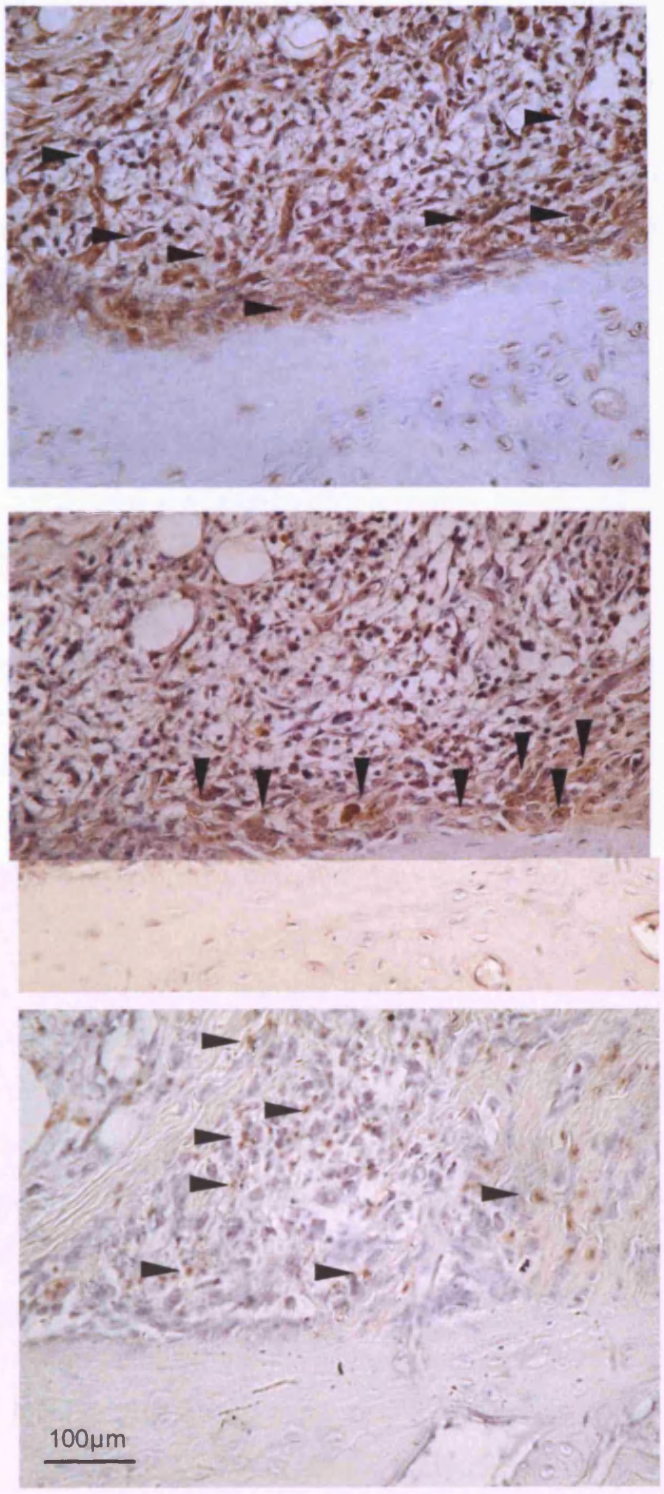

Figure 6.49. Localisation of MMP-9, Macrophage and Neutrophil Staining. Serial sections of a moderately arthritic joint staining for MMP-9 (top), macrophages (middle) and neutrophil (bottom) as indicated by arrowheads (at X40 magnification).

6.5 Discussion

6.5.1 Overview

To investigate the effects of mCIA on blood pressure, non-invasive tail-cuff photoplethysmography was utilised. Data collected over the time course of the experiment indicated that following the onset, and during the progression of mCIA there was no measurable change in blood pressure.

To assess the hypothesis that MMP-9 may be responsible for the observed reduction in vessel contractility aorta, paw and blood serum samples were taken from DBA/1 normal animals, and those with mCIA at appropriate time points. Following homogenisation of aortae and paws, levels of total MMP-9 in both the resulting homogenate and blood serum were assessed. The data showed that levels of MMP-9 increased over the course of mCIA in each case, although these changes did not necessarily reflect changes in vascular contractility. Importantly the pattern of contractile dysfunction was more closely mirrored by aortic rather than serum MMP-9 changes, indicating perhaps that the detrimental effect was due to local as opposed to systemic MMP-9 production.

As IL-1β has been reported to have a positive effect on MMP-9 production (Roh, Oh et al. 2000; Gurjar, DeLeon et al. 2001; Gurjar, Deleon et al. 2001) (see section 6.1.2), the effect of this cytokine on vascular function was investigated. In the presence of IL-1β (70 or 700 pg/ml for twenty four hours) contractile responses to 5HT in tissues from naïve animals were significantly depressed, thus resembling the responses observed in the mCIA model and indicating similarities between the effect of IL-1β and mCIA on vessel contractility. However, unlike the mCIA model, exposure to IL-1β also produced significant impairment of endothelium-dependent relaxation. For further clarification of the mechanism(s) involved the above experiments were repeated as appropriate in the presence of either an eNOS, iNOS or COX inhibitor. Following eNOS or iNOS inhibition contraction responses were normalised, indicating a possible role for eNOS/iNOS-derived NO in the initial IL-1β-mediated decrease in vessel constriction. On the other hand inhibition of COX was without effect discounting a role for prostacyclin.

To further investigate a possible role for MMP-9 in this IL-1β–induced dysfunction, vessels that had been incubated with IL-1β for twenty four hours were homogenised and MMP-9 levels measured by ELISA. Importantly no change in expression of MMP-9 was observed.

Given the changes in MMP-9 levels described above, subsequently the direct effect of MMP-9 on vessel responses was measured. As with IL-1β, vessels from naïve control animals were removed, incubated in the absence and presence of MMP-9 and vessel contractility measured. A concentration of MMP-9 seen in "severe" animals had a detrimental effect on vessel contractility as observed in the mCIA model. The use of a MMP-9 inhibitor subsequently prevented the development of this dysfunction indicating the potential for MMP-9 to compromise the integrity of the vessel. Importantly, such incubations were largely without negative effect on endothelial function.

The reversibility of damage hypothesised to be caused by MMP-9 in the mCIA model was assessed using a MMP-9 inhibitor and aortic tissue taken from moderately diseased mCIA animals. Inhibition of MMP-9 *ex-vivo* showed no change to impaired vessel function.

Staining for the presence of MMP-9, macrophages and neutrophils in the joints indicated an upregulation of all three following the onset and duration of arthritis. MMP-9 and macrophages were located in similar areas indicating that macrophages could be the primary producers of articular MMP-9 in mCIA. This association was seen near bone within the joint emphasising the role of these cells and this protease in bone degradation.

The main findings of this Chapter are discussed in more detail below.

6.5.2 Blood pressure

Although no such reports of BP measurement in the mCIA model have been published previously, similar measurements have been carried out in an experimental rat AIA model. Indeed analogous observations were made, with AIA having no effect on BP over

the time course of the experiment ((Sakuta, Morita et al.). Interestingly in this model it was observed that infusion of AngII (see Chapter 1, section1.4.2.3 for description) over the disease period resulted in increased sensitivity for development of hypertension. Moreover an increase in the expression of AT_1, the angiotensin receptor was subsequently observed (Sakuta, Morita et al.). These findings may indicate that increased expression of this receptor in human RA may be a risk factor for the development of such RA-associated pathologies and could explain the increased incidence of hypertension in human disease. No such reports regarding this hypothesis exist in the literature, however an increased production of angiotensin converting enzyme (ACE) has been reported in the synovial fluid from RA patients (Veale, Yanni et al. 1992). This enzyme is responsible for the conversion of inert AngI to the potent vasoconstrictor/growth promoter AngII. If this increase in ACE was associated with a similar increase in AngII, the rise in circulating levels could certainly contribute to the observed hypertension in human RA. Interestingly administration of ACE inhibitors to sufferers of RA improves endothelial function, and furthermore is hypothesised to potentially reduce the risk of cardiovascular events in these patients (Flammer, Sudano et al. 2008).

As discussed in the introduction to this Chapter (see section 6.1) arterial stiffness and increased systolic hypertension are pathologies which have been described extensively in human RA (Panoulas, Douglas et al. 2007; Bazzichi, Ghiadoni et al. 2009; Galarraga, Khan et al. 2009). As such the development of hypertension in mCIA would not have been an unexpected observation. Reasons for the negative result here could be due simply to an absence of this pathology in this model. Since this experimental arthritis only progresses for a period of 2 to 14 days, it may be too short for measurable hypertension to develop. Alternatively, early adaptive compensatory mechanisms (for example increased antioxidant/anti-inflammatory defences) could initially mask the pathological changes and result in no "net change" in blood pressure. Such suggestions are merely speculative and investigations of such mechanisms were well outside the scope of the current thesis. Alternatively however, problems encountered during both experimental work and data collection highlighted that the tail-cuff photoplethysmography technique may not be completely reliable.

One issue could arise from the fact that interpretation of the data was largely subjective. As can be seen from figure 6.1, the exact point at which the pulse is detectable is not overtly clear from the graph, indeed there are several points at which this could be taken. To remove this variability, criteria regarding the time point at which the reading was taken was pre-decided, as described in the graph. Consequently readings taken by the blinded analysers were generally consistent and variation between blinded assessments was minimal. On reflection a way to avoid this variability would be to set criteria which automatically discarded anomalous data. For example excluding data which was greater than two standard deviations away from the mean (Feng, Deerhake et al. 2009). However, if the method produced consistent results this would be an unnecessary step and as such there should be no need for such intervention.

Criticisms of the method also stem from problems encountered when executing experimental work. Due to the small size of the DBA/1 mice used, animals fell into the lower weight threshold recommended for the restraining device (weight range was ~18-24g, the smallest cage obtainable was suitable for mice 20-40g). Consequently, animals were often too small for complete prevention of movement, problematic for both obtaining and maintaining the signals. Additionally, the tail length of the mice was only just long enough to be accommodated in the smallest of occlusion and sensory cuffs, causing further difficulty when obtaining readings. An accumulation of these factors could result in inaccurate measurements, loss of signal and undue stress to the animals, further affecting precision.

Manufacturers Kent Scientific suggest that light-based blood pressure analysis is not the most accurate technique; the light signal can be over-saturated by external sources of light, pressure signals can vary in rodents with dark skin and the extreme motion sensitivity makes accurate readings difficult. Moreover, the occlusion cuff length is inversely associated with the accuracy of the blood pressure; longer cuffs produce lower blood pressure readings, whilst shorter cuffs give higher pressure readings (Bunag 1973). In DBA/1 animals, naïve or with mCIA, the average blood pressure ranged between 105 and 120mm/Hg. Previous studies in other murine strains suggest an average blood pressure of around 120mm/Hg, and this was shown to correlate with blood pressure

measured intra-arterially (Krege, Hodgin et al. 1995; Tilley, Audoly et al. 1999). No such information exists in the literature for the DBA/1 strain.

To achieve accurate blood pressure measurements, various techniques could be utilised. For instance anaesthetising animals would eliminate variation caused by motion sensitivity, although such an action in itself could influence blood pressure. On the other hand further non-invasive methods exist with greater sensitivity than the tail-cuff photoplethysmography used here. For example a technique using piezoelectric ceramic crystals (piezoplethysmography), that works in a similar way to photoplethysmography, detects a change in pulse via a cuff and is able to detect at a higher sensitivity (Bunag 1973) both systolic and diastolic pressures (Reddy, Taffet et al. 2003). Similarly volume pressure recording could also be used to measure the blood flow and volume in the tail, and since it is not disrupted by movement or pigmentation, has increased reliability (Bunag 1973) and has been proven to be an accurate method for this measurement (Feng, Whitesall et al. 2008). Invasive techniques, while more complex, would perhaps provide more reliable readings. Suitable examples are the use of an in-dwelling intra-arterial catheter to record changes via a pressure transducer (Hatton, Qi et al. 2000), highly sensitive but requires surgery or alternatively radiotelemetry, where a very small radio-transmitter is implanted in the body of the mouse, a method that has been used and is widely regarded as highly sensitive (Feng, Whitesall et al. 2008) and is now the gold standard for measuring rodent blood pressure (Plehm, Barbosa et al. 2006). Unfortunately use of these techniques did not comply with the project licence and as such could not be executed during this work.

Despite the issues encountered with tail-cuff photoplethysmography in the DBA/1 strain, the technique has been used reliably and successfully by others in this institution (Anning, Coles et al. 2005; Coles, Lewis et al. 2007). However, in this work mice were a different strain (12/15-LOX knockout mice and C57/BL6), older and weighing on average 25-30g, indicating that perhaps the size of the animals was the limiting factor in obtaining reproducible results in the mCIA model.

While the chosen method for blood pressure measurement presented an unsatisfactory degree of variability and difficulty , if 'real' changes in blood pressure occurred with arthritis progression then our equipment would have been sufficiently sensitive to pick up these differences. Further detailed studies are obviously required.

6.5.3 MMP-9 Levels in the mCIA Model.

Varying levels of total (pro- and active) MMP-9 were detected in serum and aortic and paw homogenates. In normal animals there was a low level of total MMP-9 detected in all three samples tested. Following the onset of arthritis the levels were seen to increase with arthritis severity. In aortic, paw and serum samples the increase in levels of total MMP-9 was associated with arthritis progression. Interestingly levels of MMP-9 present in the serum failed to reach significance compared to normal levels at the same time point as vascular dysfunction was demonstrated in this model. This could signify that vascular dysfunction is not dependent on serum levels of MMP-9 but instead on local production within the vessel wall.

Large differences were observed between the amount of MMP-9 present in paw and aortic samples (200pg/mg protein compared to 100ng/mg protein respectively). At the paw damage is being driven by a wide range of cells, cytokines and deleterious enzymes, with MMP-9 playing an important role in bone and cartilage destruction (Yoshihara, Nakamura et al. 2000). The observation of MMP-9 in the vessel wall is a novel finding in this model and provides credence to the notion that impaired constriction may be a result of MMP-9 activity; however the pathway of events leading to this upregulation remains unknown.

Inflammatory cytokines such as IL-1β and TNFα are known to be upregulated in inflammatory situations and have on occasion been linked with increased MMP-9 production (see section 6.1.3). As such this pathway could potentially be involved in the observed increase in vascular MMP-9. That IL-1β levels had been measured and characterised in the mCIA model (see section 6.1.3) lead to the investigation of the role of this cytokine in the upregulation of MMP-9.

6.5.4 IL-1β Incubations

While the effect of IL-1β on vessel function and the role MMP-9 plays in any subsequent changes has not been previously investigated in the DBA/1 animal, similar work on vessel tension studies has been performed in rats. Following constriction with PE, IL-1β-mediated relaxation was largely inhibited by the presence of the MMP inhibitor doxycyclin, indicating a role for MMPs in this process (Lalu, Cena et al. 2006). In addition to this there are several conflicting reports regarding the effects of IL-1β on vessel function. Firstly with respect to contractility, incubation with IL-1β has been observed to have a direct effect on VSMC function, enhancing contractile responses to PE in endothelium-denuded vessels from hypertensive rats (Dorrance 2007). On the other hand decreased vessel sensitivity to PE has also been reported, as demonstrated by reduced aortic constriction following incubation with IL-1β, and subsequently attributed to increased production of both COX and NOS products (Soler, Camacho et al. 2003). In order to clarify the action of IL-1β on vessel function, and to relate this to MMP-9 production, incubations of naïve DBA/1 aortae with this cytokine were performed.

An initial IL-1β concentration of 70pg/ml was chosen as a representative level of IL-1β in mCIA (as measured on day 35 MD thesis, Cardiff University, "STAT-1 and STAT-3 signalling in Collagen Induced Arthritis: Towards New Therapeutic Targets for Rheumatoid Arthritis" Dr Shaun Smale 2010). Subsequently, since local tissue levels of this cytokine are likely to be very much higher, experiments were repeated with a ten-fold excess concentration (700pg/ml). In both cases no significant change was observed in the developed tension achieved after exposure to K^+, which conflicts with other studies (Lalu, Cena et al. 2006), and indicates that IL-1β had no lasting effect on VSMC depolarisation/calcium influx into the cells. As already outlined above, in the same tissues 5HT-induced constrictions were impaired. Moreover similar results were observed for relaxation responses; following twenty four hour incubation the ability of the tissue to relax was significantly decreased compared to controls. This echoes the findings of Jiminez-Altayo et al (2006), who demonstrated impaired relaxation responses after a similar fourteen hour incubation (Jimenez-Altayo, Briones et al. 2006). That such an action was not seen following a shorter incubation period of thirty minutes (Wimalasundera, Fexby et al. 2003) indicates the need for a prolonged exposure, and the

possibility of differential regulation of downstream effectors following stimulation with IL-1β. However despite the initial decrease in relaxation function, following a twenty four hour exposure to a higher concentration of IL-1β, no change was observed in the relaxation response (Wimalasundera, Fexby et al. 2003). This could be indicative of the vessels switching to a protective state and masking the initially observed deleterious effect of the IL-1β. Unfortunately these investigation were not continued and as such this aberrant result remains unexplained.

The initial observations of the present studies that in the presence of IL-1β responses to 5HT are compromised, yet responses to K^+ in the same tissue are unchanged is somewhat surprising. However that the observed difference is related to the mechanism via which contraction is elicited is a possibility. For instance K^+ induces contraction by depolarising the plasma membrane and activation of Ca^{2+} influx via voltage-gated calcium channels. The absence of an effect of IL-1β on these channels would explain its lack of effect on K^+-induced contraction. On the other hand 5HT-induced constriction is mediated via interactions with the agonist and the $5HT_{2A}$ receptor on the plasma membrane. This triggers a downstream cascade of events ultimately resulting in Ca^{2+} release from the intracellular stores and subsequent constriction. Therefore the dampening effect of IL-1β on 5HT-induced tone may be due to a detrimental effect on intracellular signalling rather than affecting extracellular Ca^{2+} influx or alternatively compromised receptor/agonist interactions. Interestingly, Soler et al (2003) showed decreased contractility following IL-1β challenge in rat aortae and increased K^+ channel activation in the vessel wall. Subsequent blocking of these K^+ channels restored vessel contractility (Soler, Camacho et al. 2003) indicating their activation played a role in the decreased contractile function. Therefore it may be of interest to investigate changes Ca^{2+} signalling in these conditions to see whether a similar effect on ion channels could be occurring and as such contribute to the different responses observed between stimulations with K^+ and 5HT.

As a result of data in the literature regarding increased the blood vessel expression of NOS and COX isoforms following IL-1β exposure (Soler, Camacho et al. 2003), the

effect of such experimental conditions was investigated in this thesis. This was achieved utilising the inhibitors of NOS, iNOS and COX; L-NAME, 1400W and indomethacin respectively. Responses to 5HT in IL-1β-incubated tissues in the presence of L-NAME or 1400W were not statistically different from the control responses, thus indicating a role for increased NO bioavailability in the dampening effect of IL-1β on contraction. On the other hand in the presence of IL-1β and indomethacin 5HT-induced responses were still impaired suggesting that COX-derived products do not contribute directly to the observed decrease in vessel function. This agrees with the observations of Soler et al, (2003); in IL-1β-induced vessel dysfunction, the role of NO plays a more prominent role in the development of dysfunction than COX-related products (Soler, Camacho et al. 2003).

In these three experimental conditions relaxations responses were unchanged compared to normal indicating that the addition of IL-1β and 1400W or indomethacin did not affect endothelial function. An important observation from these prolonged incubation experiments is that relaxation responses in normal vessels following twenty four hour incubation in tissue culture conditions failed to reach that achieved in previous "freshly-isolated" normal tissue. Similar observations have been reported previously (Jimenez-Altayo, Briones et al. 2006), and suggests that overnight incubation can damage the endothelium *per se*, resulting in endothelial dysfunction (Manoury, Etheridge et al. 2009) and reduced relaxation. The cause of this damage has been attributed to the possible hypoxic nature of the TC environment, and additionally raised secretion of $endothelin_{1A}$ (Manoury, Etheridge et al. 2009) which may result in a constant level of basal constriction preventing complete vessel relaxation. In this thesis the manual pre-setting of baseline tension negates the latter possibility since the minimum set baseline would be higher than the resting tension. Constrictions and relaxation responses varied in these experiments despite identical experimental conditions. The unfavourable conditions of the TC environment coupled with biological variation mean that these changes may manifest themselves in slightly altered responses between animals. Despite this, the trends observed here between experimental conditions still ultimately showed the same changes.

The data above did not provide any explanation for the role of MMP-9 in IL-1β-mediated effects on vessel function, indeed a role for increased NOS activity was more likely. To confirm the former, tissue incubated with IL-1β was homogenised and levels of MMP-9 assessed by ELISA. There was negligible change in MMP-9 levels between tissues indicating MMP-9 production is not induced via IL-1β in these experiments. Interestingly it has been observed in the literature that exogenous NO can inhibit the production of MMP-9 from IL-1β stimulated VSMCs in isolated rat aorta (Gurjar, DeLeon et al. 2001). Therefore if IL-1β stimulates NOS isoforms to produce excess NO, resulting in dampened contractile responses, it may also be inhibiting the production of MMP-9. However, this is not necessarily an accurate representation of the underlying pathway of events in mCIA; it must be taken into consideration that mCIA is a multifactorial disease and that many other inflammatory cytokines may be involved in the observed vessel dysfunction. That MMP-9 does not play a role in the effect of IL-1β in normal control tissue does not necessarily mean that it is not involved in the mCIA model.

Alternative cytokines have been implicated in the production of MMP-9 in RA and these may also be involved in producing the changes in vessel function described above. For instance TNFα, a key inflammatory cytokine in the progression of disease is described not only in the pathogenesis of inflammatory arthritis (Marinova-Mutafchieva, Williams et al. 1997) but furthermore, has been associated with the production of MMP-9 from both human (Lee and Moon 2005) and rat (Lee, Kim et al. 2009) VSMCs experimentally. In hindsight, it may have been of interest to measure TNFα in the mCIA model, however, that IL-1β levels were already characterised lead to the studies carried out here.

6.5.5 Incubations with MMP-9

Primary cellular sources of MMP-9 in human RA are macrophages, osteoclasts, synovial fibroblasts and neutrophils (Van den Steen, Dubois et al. 2002; Tchetverikov, Ronday et al. 2004; Chia, Chen et al. 2008; Garvin, Nilsson et al. 2008). The hypothesis that MMP-9 may be causing detrimental effects on vessel function in the mCIA model is supported by the wealth of information in the literature surrounding its activity in inflammatory

diseases. To elucidate this further, the direct effect of MMP-9 on vessel function was assessed by exposing tissues to concentrations of MMP-9 that were observed in the serum of the mCIA model for varying periods of time before measuring constriction and relaxation responses to K^+, 5HT and ACh respectively.

Bolus addition of MMP-9 following peak 5HT-induced constriction saw no change in maintained constriction compared to normal, contradicting published observations in the rat (Chew, Conte et al. 2004; Raffetto, Qiao et al. 2008). This could be due to the difference in MMP-9 incubation periods; Chew, Conte et al (2004) incubating for one hour, Raffetto, Qiao et al (2008) for 30 minutes compared to the twenty minutes here. Alternatively the difference could be due to the agonist used to elicit the constriction, with both methods in the literature utilising PE. This would indicate interference between MMP-9 and the agonist/receptor occurring more readily in the case of PE, therefore dampening constriction. Alternatively, species variation between rat and mouse could account for this difference. As receptor/agonist function in DBA/1 mice has not been characterised this is merely speculation and thus it would be unreliable to draw conclusions from this.

Responses to K^+ in the presence of MMP-9 were not different compared to normal vessels, indicating the changes observed in these conditions are not identical to changes occurring in mCIA. Interestingly MMP-9 has previously been associated with reduced K^+-induced contractile function and reduced Ca^{2+} influx into VSMCs (Chew, Conte et al. 2004). Moreover Chew, Conte et al (2004) observed that incubation of rat aortae with MMP-9 resulted in the inability of the vessel to attain maximal PE-induced constriction. Such differences to the data presented in this thesis could again be due to a disparity in the methodology; in the study of Chew et al (2004), MMP-9 was present in the bath with the vessel throughout the constriction responses while in this thesis it was washed out prior to K^+ or 5HT exposure. It is possible therefore that the presence of MMP-9 may be necessary for a change in K^+-induced contractility to occur. These observations do not eliminate a role for MMP-9 in the development of vascular dysfunction, in fact that a decrease in K^+ constriction in the mCIA model is observed supports the theory that vessel

dysfunction may be associated with local rather that systemic levels of MMP-9, as hypothesised following elucidation of tissue MMP-9 levels.

No change in vessel constriction was observed following a one-hour incubation with a "severe" concentration of MMP-9. However a three hour incubation had a detrimental effect on vessel contractility. It remains to be seen whether this three hour incubation would be of sufficient duration to alter the ECM structure, or indeed mechanistically alter contractile mechanisms. Instead MMP-9 may be interacting directly with the 5HT receptors altering downstream signalling and decreasing the maximal constriction attainable. As no other studies have investigated the effects of MMP-9 on 5HT-induced constrictions this is merely speculation. Interestingly relaxation function in these studies showed no change compared to control vessels indicating no detrimental effect on endothelial function.

Exposure to low "normal" levels of MMP-9 also resulted in contractile dysfunction following a three hour incubation. This was an unexpected result; basal levels of expression seen *in-vivo* in non-diseased control animals should not affect vessel integrity. However the *ex-vivo* conditions to which the vessel was subjected could well change the vessel sensitivity resulting in an aberrant response. Moreover incubation in culture medium could impose hypoxic conditions and may not be conducive to fully functioning vessels (Manoury, Etheridge et al. 2009). Reversal of hypoxia may be achieved by increasing the oxygenation state of the chamber the tissue was maintained in (Manoury, Etheridge et al. 2009), however at the time of experimentation this was not known. Alternatively the low levels of MMP-9 in this condition may enhance local production of MMP-9 *in-situ* causing altered vessel contractility.

Interestingly in subsequent experiments vessels exposed to low "normal" MMP-9 for twenty four hours exhibited no change in contractile function compared to controls. The difference in these results could be due to one of several reasons. For instance the initial insult to the vessel wall by MMP-9 could be reversed after a longer incubation due to the increased expression of protective factors, thus masking the initial damage. Alternatively the enhanced sensitivity proposed above may be a transient effect with vessels

equilibrating in the new environment, becoming less sensitive following the initial first few hours. Lastly, the apparent dysfunction observed after three hours could be an experimental anomaly. Interestingly the vessels in these experiments displayed signs of endothelial dysfunction, failing to relax to the level achieved by the normal vessels indicating the incubation period has compromised endothelial function.

Incubation with a high "severe" level of MMP-9 for twenty four hours had a detrimental effect on 5HT-induced vessel constriction akin to that observed in mCIA. However, a somewhat confusing observation of these experiments is that relaxation responses were far greater in vessels incubated with MMP-9 contradicting that observed following incubation with a low concentration of MMP-9 for the same duration (see figure 6.39 and 6.42). Importantly a large level of variability was demonstrated between normal responses in this group of experiments, even though tissues were isolated from the same batch of animals and measurements made under identical conditions. Whether the latter can be attributed to a direct effect of the tissue culture environment on the endothelium is a matter for speculation. At the very least it emphasises that care must be taken when interpreting data collected under such conditions.

Incubating the vessel with MMP-9 in the presence of a MMP-9 inhibitor removed the detrimental effect on vessel constriction, proving the deleterious effect of MMP-9. Overall the data presented here indicates that "severe" concentrations of MMP-9 result in diminished vessel contractile function in naïve vessels following a twenty four hour incubation period. Although the changes demonstrated do not directly mimic those seen in the mCIA aorta, it does not discount MMP-9 in the development of this pathology. The detrimental effect of MMP-9 on vessel function has been previously documented (Chew, Conte et al. 2004; Chung, Au Yeung et al. 2007), and has subsequently been attributed to fragmentation of elastin and loss of elastic integrity (Chung, Au Yeung et al. 2007). However, that K^+ responses were not impaired following conditions imposed here indicate that perhaps the detrimental effect of MMP-9 incubation is not due entirely to the development of a faulty contractile mechanism. Indeed MMP-9 may interfere with receptor/agonist interactions or perhaps cause damage via another unexplored pathway.

The observations described here do not eliminate a role for MMP-9 in the development of this pathology in mCIA and indeed it is likely that other inflammatory mediators play a role in this disease, although to date such underlying mechanisms remain unclear

6.5.6 Incubation of mCIA tissue with a MMP-9 inhibitor.

Following the observation that impaired constriction due to MMP-9 activity is reversible (Chew, Conte et al. 2004) the effect of a MMP-9 inhibitor on diseased tissue was investigated. Vessels from moderately diseased mCIA animals were incubated for twenty four hours in the presence and absence of a MMP-9 inhibitor. Subsequent vessel responses to K^+ and 5HT were measured and remained impaired as described previously in this thesis. It is likely therefore that damage inflicted to the vessels via the chronic inflammatory state posed by mCIA is irreversible and cannot be altered by *ex vivo* MMP-9 inhibition. Possible structural changes to the wall, for example the induction of calcium deposition following damage to elastin fragments (Basalyga, Simionescu et al. 2004), could contribute to a pathology that is resistant to subsequent interventions. As such this may indicate that the earliest possible treatment to prevent such vascular damage in human RA is essential. Once established it may only be possible to moderate the pathology. Therefore a full understanding of the changes in the vasculature in RA is paramount if appropriate treatment regimes, and indeed new drug targets are to be established. An alternative approach to assess the impact of MMP-9 on the development of this pathology could be to administer the inhibitor systemically as a therapy, or alternatively attempt to develop mCIA in a MMP-9 null mouse. This would give an indication of how detrimental MMP-9 alone is at the vessel wall. Unfortunately due to time constraints, to undertake either of these was not feasable.

6.5.7 Localisation of MMP-9 in the joint.

To investigate production and localisation of MMP-9 in the joints, paw sections from mCIA animals were stained for MMP-9 and the presence of macrophages and neutrophils These cells were chosen with respect to MMP-9 production since both neutrophils (Van

den Steen, Proost et al. 2002) and macrophages (Tetlow, Lees et al. 1993; Dreier, Grassel et al. 2004; Kim, Kim et al. 2005) are known producers of MMP-9 in the arthritic environment.. Subsequently all three antigens were upregulated following induction of arthritis, with levels continuing to rise with increasing severity. Further investigation saw that MMP-9 and macrophages were largely present in the infiltrating cell mass, with levels of both prominent in areas adjacent to bone tissue. Contrastingly, neutrophils were observed to a lesser extent in the infiltration in the joint space, and more predominantly in the bone marrow. While MMP-9 production could be visually localised to macrophages in serial sections from the paws, the same could not be achieved for neutrophils indicating that macrophages may be the primary producers of MMP-9 and together these could be major contributors to bone destruction. However, it is important to note that these are not the sole producers of MMP-9, with synovial fibroblasts, and osteoclasts also observed to contribute throughout this pathology (Van den Steen, Dubois et al. 2002; Tchetverikov, Ronday et al. 2004; Chia, Chen et al. 2008).

It is unclear how the production of MMP-9 in the joints, may translate to the vessels. The work in this chapter has lead to the hypothesis that local production of MMP-9 at the vessel site is likely to be the causative factor in the development of contractile dysfunction. It seems unlikely that vessel production is mediated by macrophages, as infiltration of these into the vessel wall is typical following physical injury to the vessel (Hanke, Hassenstein et al. 1994) or during the development of atheroscleoritc lesions (Bui, Prempeh et al. 2009) neither of which occur during mCIA. As mCIA progresses for a relatively short time span, it neither seems likely that the initial insult to the vessel wall will have developed enough to allow for macrophages to infiltrate. Alternatively the production of MMP-9 may be due to VSMCs following the cytokine activity at the vessel wall. Indeed VSMC production of MMP-9 has been observed in different pathologies; in a mouse model of Kawasaki disease (vasculitis commonly leading to coronary artery aneurysm) following TNFα stimulation, addition of doxycyclin (a MMP-9 inhibitor) reduced VSMC production of MMP-9 and inhibited MMP-9 activity (Lau, Duong et al. 2009). As previously discussed both of these cytokines are upregulated in mCIA and thus could potentially play a pivotal role regarding MMP-9 production from VSMCs.

To confirm this vessel segments could be stained for MMP-9 and an attempt at localising the production sites could be made. Furthermore elastin fragments could be stained for in the vessel wall. Both of these were attempted in aortic segments however problems with tissue orientation and maintaining tissue integrity throughout cutting and staining was compromised, resulting in unreliable data. Time constraints on the project hindered the attempted staining in the vasculature and optimising such proved impossible.

Additionally the activity of MMP-9 could be assessed in the vasculature. This would perhaps give an estimation of potential damage that might be caused at the vessel site. A method considered for this was zymography, however there are limitations of this technique, and it was not clear whether bands would be detected for the picomolar concentrations present in the aortic samples. Additionally as mentioned previously an abundance of sample volume was not available and as such an attempt was made to investigate the mechanism underlying vascular dysfunction. Measuring the activity could have been achieved by pooling samples, however this did not seem an appropriate way to measure this and ultimately the lack of tissue resulted in zymography not being completed.

6.6 Scope for Further Work

6.6.1 Arterial Stiffening, Hypertension and Vascular Calcification

There are a multitude of factors which could affect vessel function throughout the progression of mCIA. Arterial stiffness, hypertension and vascular calcification have all been associated with human RA (Panoulas, Douglas et al. 2007; Panoulas, Metsios et al. 2008; Wang, Yiu et al. 2009), and moreover, MMP-9 has been implicated in the development of all three pathologies.

Early onset vascular calcification has been reported in the aorta of RA-afflicted patients (Wang, Yiu et al. 2009). Interestingly, calcium deposition occurs proximal to elastin fragments in the vessel, and in a destructive feedback loop, secretion of elastin fragments following ECM remodelling can induce calcium deposition (Basalyga, Simionescu et al.

2004). That MMP-9 has been implicated in elastin degradation (Chung, Au Yeung et al. 2007) indicates there may be a role for the gelatinases in calcification. This proposal has been substantiated by work investigating the systemic effects of chronic kidney disease (CKD), which manifest as degeneration of elastic fibres, arterial stiffening and calcification, the development of which has been associated with gelatinase activity (Chung, Yang et al. 2009).

As discussed previously the activity of this gelatinase has also been described in the inhibition of PE-induced vascular constriction (Chew, Conte et al. 2004; Chung, Au Yeung et al. 2007; Raffetto, Ross et al. 2007). Reduced constriction has been demonstrated in patients with renal disease who also exhibit a decreased responsiveness to NA contributing to hypertension (Hand, Haynes et al. 1995). Relating to this is the observation that in the spontaneously hypertensive rat (SHR) model of hypertension, a specific role for MMP-9 activity has emerged; there is an increase in production and enzymatic activity of MMP-9 in cultured VSMCs obtained from the model following stimulation with TNFα, suggesting that MMP-9 could be involved in the vascular remodelling associated with hypertension (Lee, Kim et al. 2009). This data supports the theory that gelatinases are associated with diminished constriction and subsequent development of hypertension, a pathology that although not measurable after the two week period of disease development could present if disease were allowed to progress.

The evidence presented here outlines the importance of gelatinases in the production of aortic stiffening and, following observations in the mCIA model, it may be speculated that calcification could ensue in this scenario. However it is not known how early this might present itself in the mCIA model. To investigate this further it may be of interest to perform histology using the von Kossa staining in the aorta for the deposition of calcium. If the early stages of aortic calcification were observed it could be of benefit to intervene therapeutically to prevent this progression. One way of doing this would be to adopt the use of MMP-9 inhibitors *in vivo*. Alternatively, novel therapies have emerged utilising hyaluronic acid (HA) oligomers and TGFβ. These used in combination attenuate TNFα-induced VSMC matrix calcification and gelatinase activity, and enhance elastin and collagen production, elastin cross linking and promoted elastin fiber formation in smooth

muscle cell culture (Kothapalli and Ramamurthi). If further investigations saw the development of aortic calcification, this novel therapy may be utilised in an attempt to prevent this.

Additional pathways which may cause the development of arterial calcification involve mediators of inflammation specifically involved in dysregulation at the RA joint site. For example Osteopontin (OPN) is a glycoprotein secreted by activated immune cells (eg T-cells, macrophages) at inflammatory sites. It mediates interactions between bones and osteoclasts and has a dual role in cell signalling. Evidence exists for the involvement of OPN in RA progression following discovery of OPN in the synovial fluid, the pannus (Gravallese 2003), and plasma (Bazzichi, Ghiadoni et al. 2009). Furthermore OPN-deficient animals are protected from joint destruction post-development of experimental arthritis (Yumoto, Ishijima et al. 2002). In addition to a role in RA, OPN has been implicated in arterial stiffness, and it has been suggested that OPN could be the bridge between the crucial point of contact in the vascular bed, and the vascular damage that subsequently develops there, resulting in CVD (Bazzichi, Ghiadoni et al. 2009). An association between OPN and vascular calcification has also been described (Uz, Kardesoglu et al. 2009), and is prevalent in calcified atherosclerotic plaques (Ohmori, Momiyama et al. 2003). The production of OPN at these damage sites comes from the VSMCs, and larger volumes are synthesised by macrophages following infiltration of the vessel wall (O'Brien, Garvin et al. 1994), a pathology that, although not present in mCIA, could well develop if the disease was allowed to progress. Additionally some studies have shown that OPN can have a positive effect on VSMC proliferation (Gadeau, Campan et al. 1993). That OPN has been implicated in the development of vascular calcification, and is known to be a key molecule in RA progression, it may be speculated that higher systemic levels of this protein could be a factor in the vascular damage developed in the mCIA. Investigating this in current model could again use the Von Kossa staining for calcification, or alternatively blood or vessel homogenates could be assessed for the production of OPN via western blot or ELISA.

Another candidate that may play a part in vascular dysfunction is RANKL. There are three molecules that control osteoclast function and thus bone resorption; the receptor

activator of NFκB (RANK), its ligand (RANKL) and the natural decoy receptor for RANKL, osteoprotegerin (OPG) (reviewed in (Leibbrandt and Penninger 2008)). RANKL, discussed in the Introduction to this thesis, is required for osteoclast development, as demsonstrated in RANK/RANKL knock out animals by the absence of fully differentiated osteoclasts (Dougall, Glaccum et al. 1999). RANKL is also responsible for bone destruction during the development of RA (Drexler, Kong et al. 2008) due to the production of bone-resorptive osteoclasts (Collin-Osdoby 2004), increased levels of which are observed in mCIA (Juarranz, Abad et al. 2005). OPG, RANKL and RANK have been implicated in vascular calcification following the observation that this pathology is associated with osteoporosis (Collin-Osdoby 2004). Furthermore experimental evidence implicates a protective role for OPG in preventing the development of this pathology (reviewed in (Collin-Osdoby 2004). As such, dysregulation of these factors resulting in an imbalance could potentially be responsible for the development of vascular calcification in the mCIA model of RA.

The pathways and pathologies listed above are speculation as to how vascular dysfunction might arise in the mCIA model, and there are several other mechanisms via which this could occur. Discussed below is one of these pathways which was chosen to be investigated in more detail; phenotypic changes to the VSMCs.

6.6.2 VSMC Hyperplasia

Many vascular diseases are characterised by intimal hyperplasia occurring via cytoskeleton breakdown and reorganisation allowing for cell movement and proliferation. MMP-9 produced by the VSMCs (Cho and Reidy 2002) has been implicated in this process; an MMP-9 deficiency has been observed to reduce VSMC proliferation and migration (Galis, Johnson et al. 2002) as it is this enzyme which is able to disrupt the ECM via their basement-membrane and elastin degrading capabilities (Senior, Griffin et al. 1991). It has been suggested that MMP-9 activity is necessary for this VSMC migration following arterial injury (Cho and Reidy 2002) and notion that is substantiated by the observation that MMP inhibition prevents VSMC proliferation (Bendeck, Conte et

al. 2002). As MMP-9 is reported to play such a prominent role in VSMC physiology and subsequent development of vascular disease it is of importance to investigate pathways via which this could occur in the mCIA model.

The mediators and pathologies discussed above are just a few of the mechanisms via which vessel function may be compromised in this model of mCIA. Investigating VSMC calcification in this model was not viable due to the earlier problems encountered whilst attempting to stain for both MMP-9 and elastin. As such investigations focussed on the contribution phenotypic changes to VSMCs may play in the development of vascular dysfunction, and the role for MMP-9 therein. Possible mechanisms and subsequent results are discussed in more detail in Chapter 7.

CHAPTER 7

N-CADHERIN, B-CATENIN AND CD9 -POSSIBLE CONTRIBUTORS TO VASCULAR DYSREGULATION IN INFLAMMATORY ARTHRITIS

7.1 Introduction

Data in this thesis has shown that contraction of isolated aortic rings is compromised following the onset of experimentally-induced arthritis; a role for excess vasodilation in this pathology via NO/prostacyclin has subsequently been discounted. Interestingly a role for the gelatinase MMP-9 has been established with increases in this enzyme being associated with increasing arthritic severity. Importantly in complimentary experiments incubation of naïve vessels with MMP-9 caused similar vascular dysfunction to that observed in the mCIA model. Upregulation of MMP-9 directly by IL-1β was discounted. The role of IL-1β in modulating MMP-9 cannot be entirely discounted in RA; the multifactorial nature of the disease and complex cytokine milieu within the joint results in a myriad of events which could elicit changes driven indirectly by IL-1β and/or other inflammatory mediators.

MMP-9 has been associated with vascular dysfunction in other animal models of disease and several underlying mechanisms have now been established (see Chapter 1, section 1.6.3). Intercellular adhesion via N-cadherin and CD9 may be relevant to the dysregulation of vascular smooth muscle contraction.

7.1.1 N-Cadherin

Cadherins are calcium dependent cell-cell adhesion molecules, mediating homophillic extracellular interactions. As such, cells expressing certain cadherins aggregate according to cell type (George and Beeching 2006). The cadherin superfamily is divided into several smaller families, the classical and best characterised consists of E-cadherin, VE-

cadherin and N-cadherin (Takeichi 1990). These cadherins are transmembrane glycoproteins with three distinct domains; an extracellular domain (mediates cell-cell contacts), a transmembrane domain, and a cytoplasmic domain (Wheelock and Johnson 2003) (see figure 7.1 for structure). Extracellular cadherin domains interact in a zipper-like fashion. The presence of calcium confers rigidity to the structure, ensures correct folding (Koch, Bozic et al. 1999) and provides protection against proteolytic digestion (Hyafil, Babinet et al. 1981). In the cytoplasm, the intracellular domain is attached to cytoskeletal components such as actin, via a protein called β-catenin (George and Dwivedi 2004), and this forms the cytoplasmic cell-adhesion complex (CCC). β-catenin is also a plasma-associated protein with a dual function; governing cell contact and additionally partaking in cellular signalling (George and Dwivedi 2004; Gosens, Meurs et al. 2008). The localisation of β-catenin is controlled by a cytoplasmic multi-protein complex consisting of adenomatosis polyposis coli (APC), glycogen synthase kinase-3β (GSK3β) and axin/conductin which controls cytoplasmic levels of β-catenin. Attachment of β-catenin to the CCC is critical for N-cadherin to function correctly as an extracellular adhesion molecule (George and Dwivedi 2004).

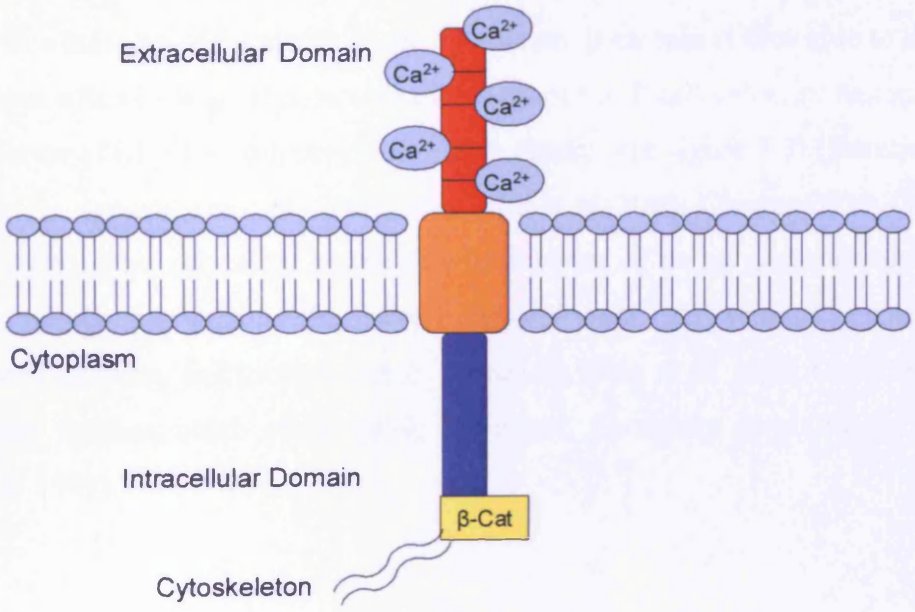

Figure 7.1. Structure of N-Cadherin. Calcium molecules help to stabilise the external domain. Calcium, and cadherin together with β-catenin form the CCC .

The dual functionality of β-catenin results in its localisation, either membrane-associated or in the cytoplasmic/nuclear pool (George and Dwivedi 2004), being tightly regulated. When β-catenin is membrane-associated any free β-catenin is phosphorylated by the APC/GSK3β/axin complex and directed for ubiquitination and subsequent degradation by the proteasome (see figure 7.2) (Behrens, Jerchow et al. 1998; Brantjes, Barker et al. 2002; George and Dwivedi 2004). This action occurs when the cells are in their adherent state and in the absence of Wnt signalling.

The Wnt family are secreted glycoproteins which have been grouped into the canonical and non-canonical Wnts. Canonical Wnts stabilise cytoplasmic β-catenin resulting in transcription of TCF/LEF target genes (Kawano and Kypta 2003) The receptor which activates this pathway contains two components: a member of the frizzled (Fz) family and either one of two single-span transmembrane proteins, low-density-lipoprotein-receptor-related proteins (LRP-5 and LRP-6) (Pinson, Brennan et al. 2000; Tamai, Semenov et al. 2000). When upregulated, Wnt binds to Fz/LRP and, via the protein dishevelled (Dsh), inhibits the GSK-3β component of the CCC (Shin, Her et al. 2005). This prevents β-catenin phosphorylation and subsequent ubiquitination and degradation, resulting ultimately in a build up of β-catenin in the cytoplasm. β-catenin is now able to translocate to the nucleus whereby it associates with members of the T-cell enhancer factor/lymphoid enhancer factor (TCF/LEF) transcription factor family (see figure 7.3) (Brantjes, Barker et al. 2002; George and Dwivedi 2004; Shin, Her et al. 2005; Clevers 2006; George and Beeching 2006). This promotes expression of a series of target genes involved in cell proliferation/regulation such as the mitotic factor Cyclin D1, protease expression, pro-inflammatory enzymes and growth factors (Brabletz, Jung et al. 1999; Gradl, Kuhl et al. 1999; Howe, Subbaramaiah et al. 1999; Shtutman, Zhurinsky et al. 1999; Tetsu and McCormick 1999).

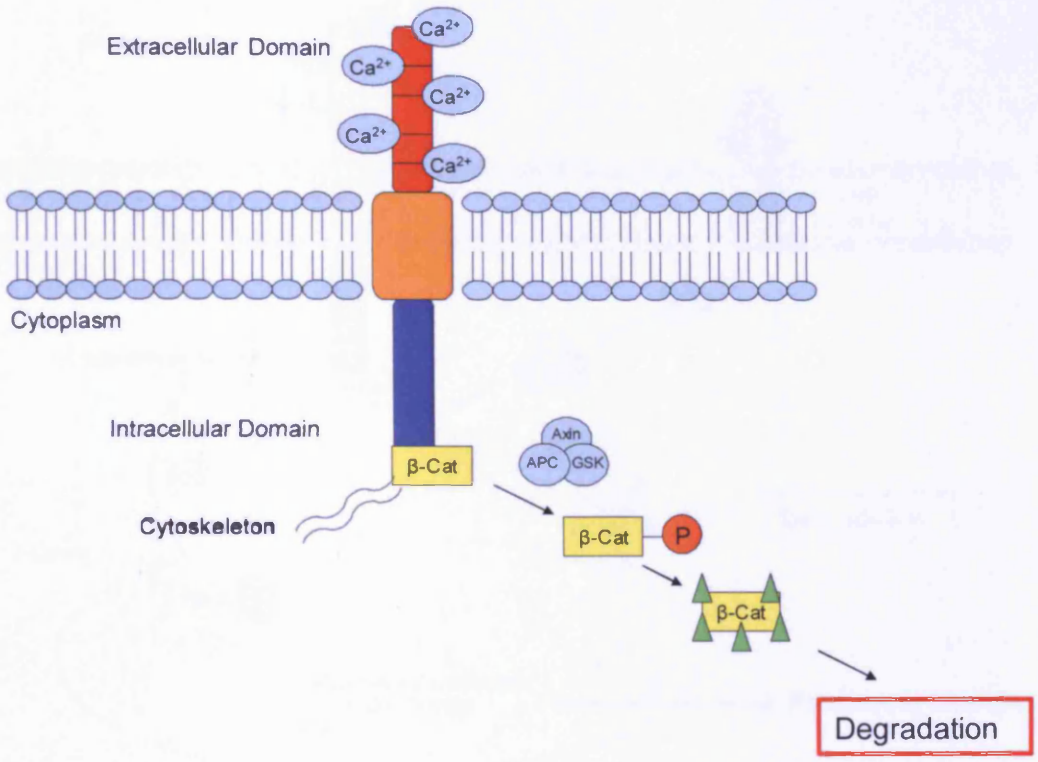

Figure 7.2. Controlled Localisation of β-catenin. When β-catenin is membrane associated, any free β-catenin is directed for ubiquitination (green triangles) and subsequent degradation.

Altered gene expression induced by Wnt signalling results in phenotypic changes to the VSMC. Cadherins have long been understood to play a role in the development of cancer (Agrez 1996), but recent evidence suggests that (loss of) cadherin-mediated cell-cell adhesion may play a part in the development of vascular disease. N-cadherin is expressed primarily on VSMCs (Moiseeva 2001; Jones, Sabatini et al. 2002), mediating cell-cell contacts between these cells. Disruption of this contact results in phenotypic changes such as switching to a proliferating state subsequently leading to intimal hyperplasia. It is not difficult to see how this could contribute to vascular contractile dysfunction

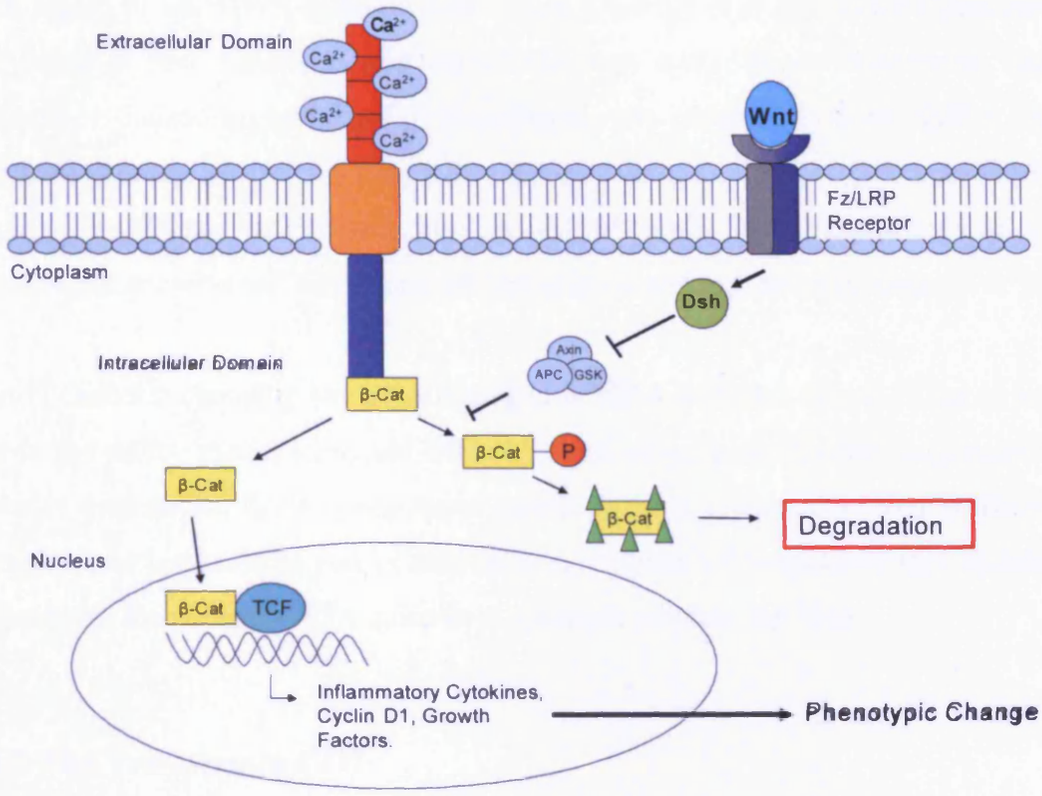

Figure 7.3. Changes in Gene Expression Following Wnt Upregulation. Wnt binds to the Fz/LRP receptor activating Dsh, resulting in inhibition of GSK3β; subsequently β-catenin accumulates in the cytoplasm. Free β-catenin translocates to the nucleus whereby it associates with TCF and promotes gene expression.

Uglow et al investigated the hypothesis that constraints on proliferation were reliant on cells and their extracellular matrices being intact (Uglow, Slater et al. 2003). Interestingly a decrease in N-cadherin was observed in cultured VSMCs following stimulation with platelet derived growth factor-BB (PDGF-BB). This increase was associated with a translocation of β-catenin to the nucleus and furthermore, was apparently inhibited by TIMP overexpression, indicating a role for MMPs in this pathology. Additionally expression of a truncated form of N-cadherin inhibited cell-cell contacts subsequently enhancing cell proliferation (Uglow, Slater et al. 2003). Further studies have demonstrated an upregulation of N-cadherin (Jones, Sabatini et al. 2002), β-catenin (Wang, Xiao et al. 2002) and cyclin d1 (Slater, Koutsouki et al. 2004), a cell cycle regulator (Tetsu and McCormick 1999; Kim and Diehl 2009), following balloon injury to vessels. As such this indicates a role for N-cadherin in VSMC phenotypic changes.

With regard to a MMP/N-cadherin connection, Dwivedi et al (2008) have demonstrated that MMP-9 and MMP-12 (the metalloelastase) have direct N-cadherin cleaving capabilities. Indeed higher levels of N-cadherin were observed in both MMP-9 and -12 knockout animals, accompanied by reduced β-catenin and cyclin D1 following PDGF-BB stimulation. This data therefore implicates MMP-9/-12 in the breakdown of VSMC extracellular contacts and subsequent phenotypic switching (Dwivedi, Slater et al. 2009).

That N-cadherin shedding has been linked to MMP-9 activity has lead to the hypothesis that in the mCIA model increased MMP-9 levels may cause this shedding, resulting in vascular dysfunction due to phenotypic switching from a contractile to a synthetic one. Levels of the intracellular and extracellular component of N-cadherin will therefore be measured in the aorta of mCIA animals to ascertain whether this is so.

7.1.2 The Tetraspanin CD9

Tetraspanins form a large family of proteins collectively known as TM4SF, the primary role of which is membrane organisation (Kotha, Zhang et al. 2009). These proteins have four conserved membrane-spanning hydrophobic regions and possess two extracellular loops (Scherberich, Moog et al. 1998; Hemler 2001), enabling interaction with other tetraspanins, integrins, Ig superfamilies, growth factors, glycoproteins and intracellular signalling molecules (Hemler 2001; Kotha, Zhang et al. 2009; Suzuki, Tachibana et al. 2009). Of primary relevance to this thesis is the interaction with integrins, receptors that mediate both cell-cell and cell-ECM protein attachment. Integrins and their ligands also play key roles in cell signalling, regulation of the cell cycle and help to maintain cell homeostasis (Hynes 2002). In forming these multi-protein interactions, tetraspanins develop transmembrane networks regulating cell motility, aggregation, fusion and signalling (Hemler 2001). Recent studies have suggested that changes to these molecular complexes could participate in the pathway of changes involved in VSMC proliferation (Scherberich, Moog et al. 1998) and therefore could perhaps play a role in the development of vascular dysfunction observed in this model.

Heparin binding epidermal-like growth factor (HB-EGF) is a potent mitogen for VSMCs and can be expressed in a membrane-anchored form (proHB-EGF) that acts via cell-cell contact in a juxtacrine manner (Nishida, Miyagawa et al. 2000). Moreover, it can also be cleaved to form a stable auto- and paracrine growth factor (Nishida, Miyagawa et al. 2000). CD9, a 24 KDa member of the tetraspanin family has been shown to uniquely interact with proHB-EGF and has been described as an activity enhancer of HB-EGF. While CD9 alone fails to induce growth factor activity (Higashiyama, Iwamoto et al. 1995), when co-expressed CD9 and HB-EGF markedly stimulate juxtacrine growth (Nishida, Miyagawa et al. 2000). Interestingly tetraspanins have been detected in atherosclerotic aorta, implicating CD9 in atherogenesis (Nishida, Miyagawa et al. 2000). Additionally SMCs expression of CD9 is increased 2 fold in cells of the synthetic phenotype compared to those in the contractile state (Scherberich, Moog et al. 1998) providing support for the role for CD9 in cell proliferation.

CD9 can also form associations with β_1 integrins on VSMCs (Kotha, Zhang et al. 2009). An abundance of CD9 has been described in the endothelium and smooth muscle of the vessel wall and an association of CD9 with the fibronectin integrin $\alpha_5\beta_1$ has been demonstrated (Kotha, Zhang et al. 2009). This has subsequently been associated with the PI3/Akt pathway which in VSMCs, plays a critical role in proliferation; Akt activity is important in the downstream down-regulation of contractile proteins (Kaplan-Albuquerque, Garat et al. 2003). CD9 blockade showed inhibition of Akt phosphorylation, a product of the Akt/PIP3 pathway, and a subsequent reduction in formation of neointima following injury (Kotha, Zhang et al. 2009). Significantly CD9 KOs have a diminished injury response and decreased intima formation compared to their wild type counterparts (Kotha, Zhang et al. 2009), further implicating a role for CD9 in vascular dysregulation and a proliferative phenotype.

As a consequence of the observations above CD9 levels will be assessed in the mCIA model with a view to investigating the hypothesis that CD9 contributes to the RA-associated vascular dysfunction.

7.2 Aims

To determine levels of N-cadherin, β-catenin and CD9 in tissues from normal and arthritic animals.

To assess VSMC hyperplasia in aortic segments by histological staining.

7.3 Methods

7.3.1 Mice

DBA/1 male mice aged 8-10 weeks were purchased, housed and euthanised as appropriate according to section 2.1.

7.3.2 Induction of mCIA

Experimental arthritis was induced as described in section 2.2.

7.3.3 Collection of experimental Tissue

Following induction of mCIA, at appropriate time points, aortae were collected from normal and mCIA animals post-euthanasia as described in section 2.3.2i.

Brain tissue was also collected from normal DBA/1 animals for use as a positive control since N-cadherin is known to be expressed here (Hatta, Nose et al. 1988; Walsh, Barton et al. 1990). Similarly testes were removed from DBA/1 normal animals for use as a positive control since CD9 is essential for sperm and oocyte fusion during fertilisation and has been detected in both human (Nakamura, Handa et al. 2001) and mouse (Kanatsu-Shinohara, Toyokuni et al. 2004) tissues.

7.3.4 Protein Homogenisation

Aortae were homogenised as described in section 2.5.1i. Brain and testicle tissue were homogenised as aorta, using RIPA buffer and a glass homogeniser.

7.3.5 Protein Assay

All extracts were assayed for protein content using the Bradford protein assay as described in section 2.7.1.

7.3.6 Western Blot

This method is a modified version of one developed by Renart et al (Renart, Reiser et al. 1979). Western Blots were run using the Mini-protean 3 Cell (165-3301, 165-3302, Bio-Rad) kit. 0.75mm glass plates were cleaned with methanol, assembled with running apparatus according to the Bio-Rad Mini-PROTEAN 3 Cell Instruction Manual. A 7.5% or 10% (depending on protein of interest, see tables 7.1 and 7.2) v/v acrylamide SDS polyacrylaminde gel was made, allowed to set, then a 5% (v/v acrylamide) (see table 7.1) stacking gel poured on top with lanes inserted. 15μg protein sample (appropriate volume determined by Bradford assay) was added to an equal volume of Laemmli sample buffer (S3401, Sigma Aldrich) in a 1.5ml Eppendorf tube and heated for 5 minutes at 95°C. Samples were spun at 16464g for 30 seconds at 4°C before being loaded on to the gel alongside precision plus protein dual colour molecular weight standards (161-0374, Bio-Rad).

The gel was run at 200V for 1 hour in running buffer (13mM tris, 0.1% SDS, 944 mM glycine) after which the gel was removed from the glass plates and laid flat on a nitrocellulose membrane (RPN303F, GE Healthcare), which was sandwiched between two filter papers, and then two fiber pads. This was then immersed in transfer buffer (25mM tris, 192mM glycine, 20% methanol) and transferred for 2 hours at 100V. To ensure correct transfer, equipment was assembled according to manufacturer's guidelines. Membranes were removed and checked for viable transfer (indicated by transfer of colour from the gel to the membrane) and placed in a universal container.

These were then blocked in milk protein (for concentration see table 8.1) to reduce non-specific binding.

Post-blocking membranes were probed with the appropriate primary antibody at a suitable concentration (see table 7.2). Following this, membranes were washed in milk protein made in wash buffer (0.02M tris, 0.15M NaCl (pH7.5) 0.1% v/v tween) (for concentration see table 7.1) for 2x5 minutes and 3x15 minutes before probing with the appropriate secondary antibody again at a suitable concentration (see table 7.2). Washing occurred as before but with TBS wash buffer, before exposure to luminol reagent (sc-2048 Santa Cruz) for 1 minute and development on to Hyperbond film (28-9068-37 GE Healthcare) and an X-omatic developer.

	Percentage Constituents	
Gel Percentage	7.5% Gel	10% Gel
dH20	47.75	40
30% Acrylamide (A3449 Sigma Aldrich)	25.25	33
1.5M Tris pH 8.8	25	25
10% SDS (L4390, Sigma Aldrich)	0.1	0.1
10% Ammonium Persulfate (APS) (A3678, Sigma Aldrich)	0.1	0.1
Tetramethylethylenediamine (TEMED) (T9281, Sigma Adlrich)	0.08	0.04

	Percentage Constituents
	Stacking Gel 5%
dH20	68
30% Acrylamide	17
1M Tris pH 6.8	12.5
10% SDS	0.1
10% (APS)	0.1
TEMED	0.01

Table 7.1. SDS Gel Constituents.

Antibody	Block	Primary	Wash	Secondary
Extracellular N-Cadherin (ab76011, Abcam)	5% Milk One Hour	1/200 Overnight	5% Milk	Goat Anti-Rabbit IgG (Santa Cruz sc-2004)
Intracellular N-Cadherin (ab76057, Abcam)	5% Milk One Hour	1/500 Overnight	5% Milk	Goat Anti-Rabbit IgG (Santa Cruz sc-2004)
GAPDH (ab ab9485, Abcam)	5% Milk One Hour	1/2000 Overnight	5% Milk	Goat Anti-Rabbit IgG (Santa Cruz sc-2004)
β-Catenin (ab3602, Abcam)	6% Milk Overnight	1/1000 One Hour	6% Milk	Goat Anti-Rabbit IgG (Santa Cruz sc-2004)
CD9 (sc-9148, Santa Cruz)	6% Milk One Hour	1/200 Overnight 10% Gel**	6% Milk	Goat Anti-Rabbit IgG (Santa Cruz sc-2004)

Table 7.2. Antibody Concentration and Incubation Times. All gels were made at 7.5% unless otherwise stated.

For all proteins results were normalised to GAPDH levels. Protein levels were subsequently expressed as a ratio of the control sample; relative optical density units (relative ODu). Quantification was achieved using a GS700 densitometer (Biorad) using Quantity One software (Biorad).

7.3.7 H and E Staining for Assessment of VSMC Hyperplasia.

Aortae were removed from mCIA-diseased animals as described in section 2.3.2i before being embedded in OCT (see section 2.5.2i). Following this aortic sections were stained using H and E as described in section 2.6.1. As aortae were not embedded in paraffin the initial xylene incubations were excluded from the protocol and aortic sections were fixed by immersion in acetone, following which they were treated in increasing concentrations of ethanol. From herein the protocol was followed as described in 2.6.1. Care was taken at all times to maintain the integrity of the vessel wall.

7.4 Results

7.4.1 Levels of N-cadherin

Levels of N-cadherin were assessed by western blot probing for the appropriate extra- and intra-cellular components. These antibodies detect the whole of the N-cadherin molecule, and the intracellular component only, respectively. This was a direct measure of cadherin cleavage; if intracellular cadherin was present but extracellular levels could not be detected this would be indicative of shedding of the extracellular component. Extracellular N-cadherin could not be detected in any experimental sample, whilst the positive control did produce bands (see figure 7.4). Intracellular N-cadherin was not detectable in normal tissues. Brain samples produced bands, as did aortic samples from mCIA animals. The latter produced variable bands throughout the progression of arthritis (see figure 7.5). Results were quantified and expressed as relative optical density (ODu) (see figure 7.6).

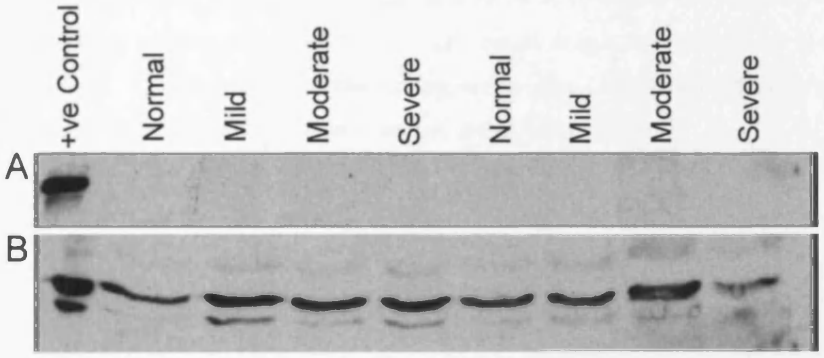

Figure 7.4. Representative Western Blot for Detection of Extracellular N-Cadherin. A. Extracellular N-cadherin (Ab 76011) expression in aortic homogenates from naïve (normal) and arthritic mice of varying severity (as labelled). Bands for N-cadherin were detectable at ~100kDa. Each severity refers to an individual animal. B. Housekeeping gene GAPDH expression in the same blot (~40kDa). +ve control refers to relevant expression in mouse brain homogenate.

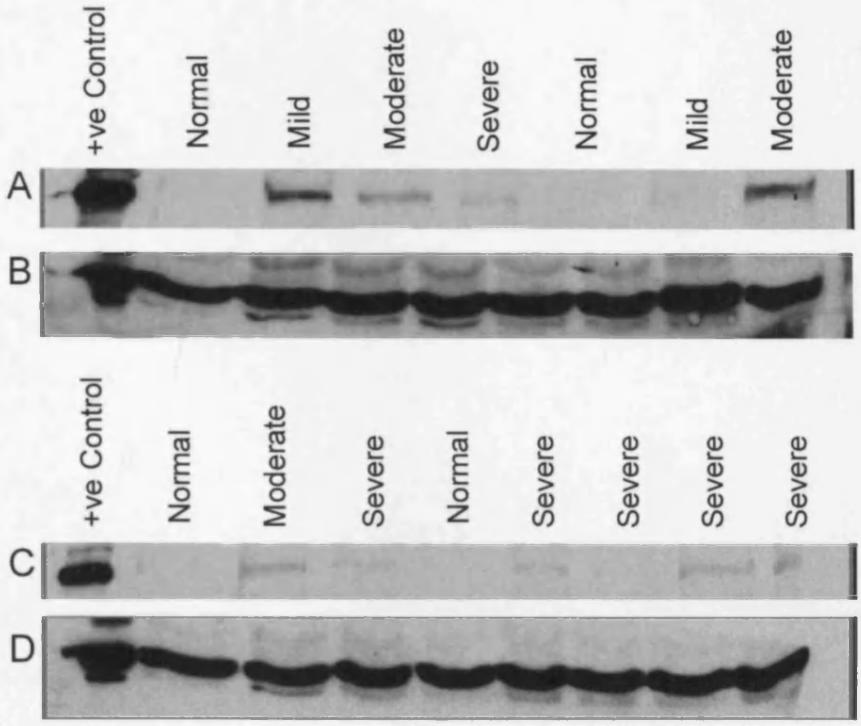

Figure 7.5. Representative Western Blot for Detection of Intracellular N-Cadherin. A, C. Intracellular N-cadherin (ab 76057) expression in aortic homogenates from naïve (Normal) and arthritic mice of varying severity (as labelled). Each severity refers to an individual animal. Bands for intracellular N-cadherin were detectable at ~100kDa B, D. Expression of the housekeeping gene GAPDH in the same blot (~40kDa). +ve control refers to relevant protein expression in mouse brain homogenate.

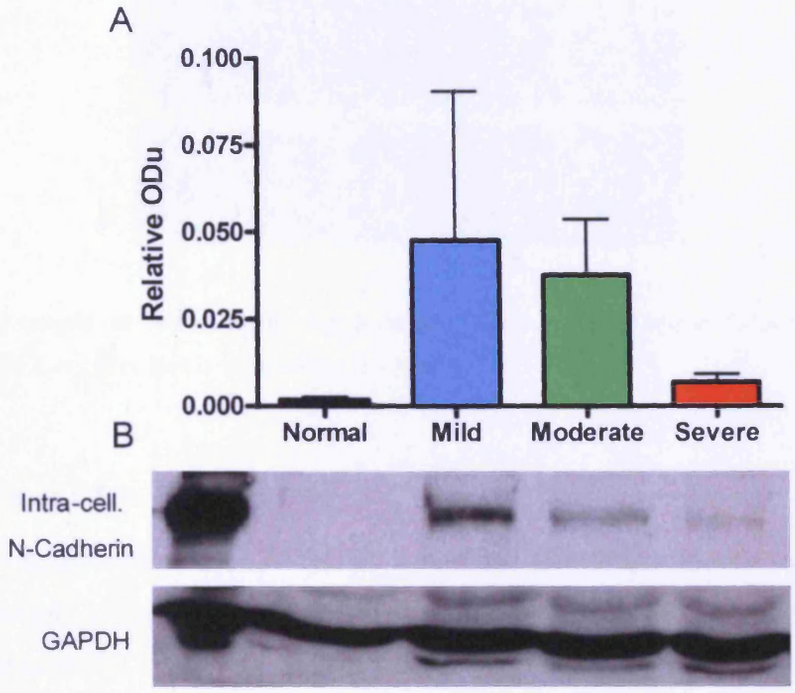

Figure 7.6. Graph Showing Expression of Intracellular N-cadherin in mCIA Aortic Homogenates. A. Relative optical density of N-cadherin from normal, mild, moderate and severe artic homogenates. Results were normalised to GAPDH. n≥2. (No statistics were performed given the low "n" values for "mild"). B. Representative blot for N-cadherin and GAPDH bands are shown at ~100kDa, and ~40kDa respectively).

7.4.2 Levels of β-catenin

β-catenin levels proved very difficult to both measure and quantify. Blots obtained were messy and showed non-specific binding and were therefore unfit for quantification. Figure 7.7 shows an example of some of the blots obtained for this antibody. Here blots were blocked overnight with 6% milk, and exposed for one second on the x-ray film, however background staining remained high. The large amount of staining here could be due to non-specific binding, or too large a quantity of protein may have been loaded onto the gel.

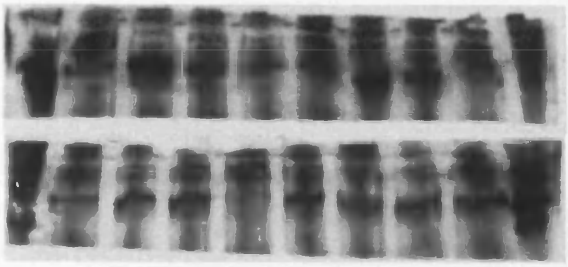

Figure 7.7. Example of Western Blot for β-catenin. Blotting for β-Catenin following one second exposure on the X-ray film. Bands were visible at ~94 kDa.

7.4.4 Levels of CD9

Since it was hypothesised that CD9 levels would increase with arthritic severity, and due to limited sample availability, CD9 was measured only in severe aorta and mouse testicle as a positive control. Levels were not detectable in this aorta (see figure 7.8)

Figure 7.8. Representative Western Blot for CD9. Western blot for CD9 in samples taken from a severe aorta and a mouse testicle as a positive control at ~24kDa. No band was visible for the severe aorta.

7.4.5 Assessing VSMC Hyperplasia.

Examples of sections cut from aortic segments are shown below, both taken from normal animals. As shown here sections varied in depth, a trait which can not be attributed to disease severity. As the minority of sections cut resembled 7.8A and D achieving

accurate measurement of vessel wall depth was difficult for comparison to normal vessels.

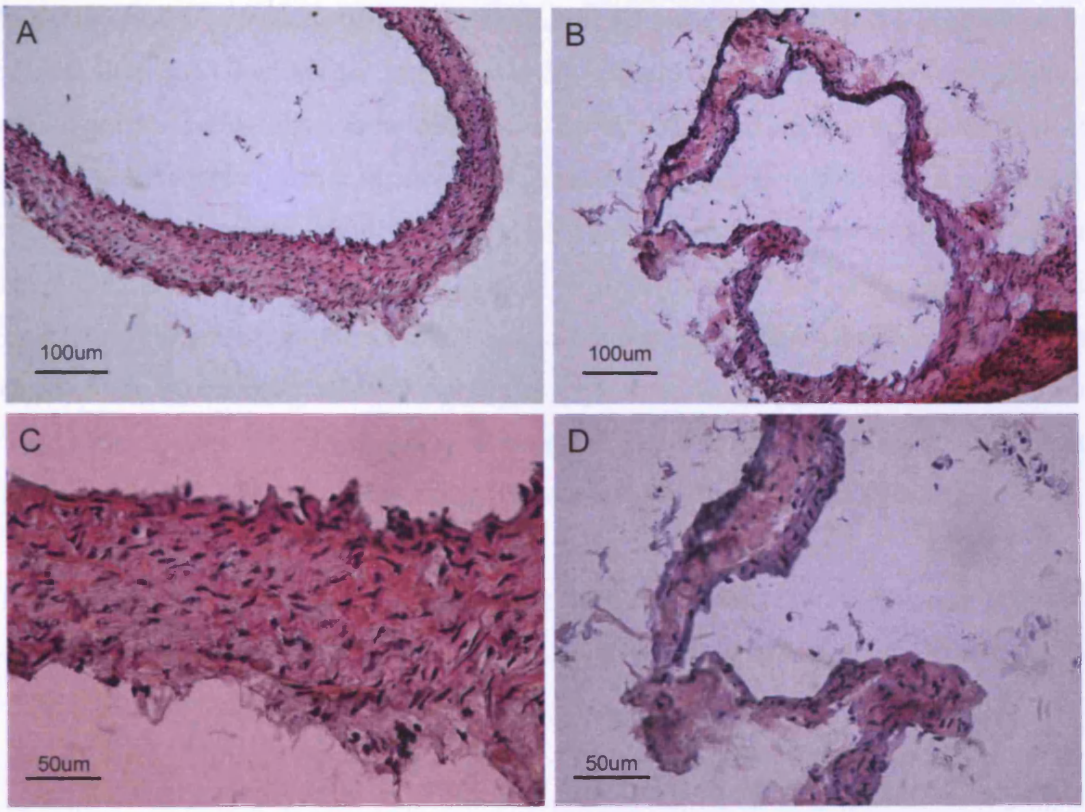

Figure 7.9. Examples of Aortic Sections. Sections cut from OCT-embedded aortic sections from normal control animals. A. An aortic section representing the smooth muscle of the aorta (X20). B. A section which has collapsed following the motion of the cryostat blade (X20). C. A at X40. D. B at X40.

7.5 Discussion

7.5.1 N-cadherin/β-catenin

Levels of N-cadherin were assessed in normal and mCIA aortae to investigate whether alterations to these and subsequent changes in phenotype may be a precursor to vessel

dysfunction. Neither intracellular nor extracellular N-cadherin could be detected in normal aorta implying this protein is not present in this tissue. In mCIA aorta extracellular N-cadherin was not detected, however an increase was observed in levels of intracellular N-cadherin presenting evidence for increased expression of N-cadherin, with shedding of the extracellular component present. Hovever, this increase was irregular throughout mCIA severity bands, showing no real association with the progression of arthritis, and that neither the intra- or extra- cellular components were detectable in normal aortae is confusing. In addition, the irregular levels found in this tissue indicate that this area requires further investigation. Previous studies have shown a decrease in N-cadherin following stimulation with growth factors (Uglow, Slater et al. 2003), a change that was later attributed to MMP activity (Dwivedi, Slater et al. 2009). It was on these observations that the hypothesis was based; a decrease in extracellular N-cadherin will be observed as a result of MMP-9 upregulation during the progression of mCIA. The consequences of the experimental data presented here imply that alternative processes may be occurring; but does not entirely rule out a role for N-cadherin shedding.

Experiments to measure levels of β-catenin were inconclusive. Expression in the tissue was high; however quantification was impossible due to the large level of non specific binding. Due to time constraints antibody conditions were not optimized to produce viable results. Time permitting it would be of interest to optimize conditions or find alternative antibodies in order to fully investigate levels of this protein in the mCIA model. Investigations localizing β-catenin to the membrane or nucleus may also provide important information regarding the activity of this protein during the development of vascular dysfunction.

That extracellular N-cadherin could not be detected at all is somewhat confusing. In normal animals, where cadherin shedding should be absent, the presence of intracellular N-cadherin should be accompanied by the extracellular component. The faint band obtained for intracellular N-cadherin in mCIA implies this protein is not present in abundance although upregulation in mCIA is indicated. That the band was just detectable signifies a scarcity of this protein, and as such, detection limits of the antibody may be to

blame for the lack of bands for the extracellular component. However using a positive control should in theory eliminate this possibility.

While the present evidence may still indicate a role for the upregulation of N-cadherin in changes to vessel function, the causes and consequences of this remain open to speculation. Previous cases of N-cadherin upregulation have been reported; in particular in cancer biology the process is associated with subsequent alterations in cell growth behaviors resulting in invasive and motile cells (Tran, Nagle et al. 1999; Bussemakers, Van Bokhoven et al. 2000; Ho, Voura et al. 2001). However, reports of this nature in VSMC are less readily available. In the carotid artery an increase in N-cadherin and β-catenin is observed following injury and associated with healing and cell migration (Jones, Sabatini et al. 2002), however separate levels of intra-and extra-cellular N-cadherin have not been assessed.

7.5.1.1 Scope for Further Work

N-cadherin signaling has been reported to occur via three signaling pathways; the previously discussed β-catenin pathway, via receptor tyrosine kinases and lastly via Rho GTPases. Rho GTPases have been shown to regulate cellular signaling both from outside-in, and inside-out. These involve members of the small GTPase family cdc42, rac1 and RhoA, that have been observed to be upregulated in myoblasts following cell-cell N-cadherin contact and ultimately resulting in myogenesis (Wheelock and Johnson 2003). Further investigation may be of interest to investigate this signaling pathway in VSMCs and any potential disruption to cell function/phenotype it may cause.

Additionally with regard to the small GTPases is an association with the juxtamembrane domain (JMD) in the cadherin molecule, a site that has been identified as a regulator of cell migration and invasion (Noren, Liu et al. 2000). Interactions between the JMD and binding partners can influence the activity of small GTPases and cytoskeletal dynamics (Piccoli, Rutishauser et al. 2004). Studies carried out by Piccoli et al 2004 demonstrated that in chick ciliary cells (of the ciliary body in the eye) the presence of the JMD resulted in a decrease in the calcium current thought to reflect the number of open voltage-gated N-type calcium channels (Piccoli, Rutishauser et al. 2004). This was subsequently

attributed to small GTPase signalling although other unknown mediators could not be ruled out. The conclusion of this work was that voltage-gated calcium channel modulation by JMDs could be achieved via the action of ROCK and a change in the actin-myosin skeleton (Piccoli, Rutishauser et al. 2004) Although the N-type calcium channels are neuronal (Dolphin 1998) and it is the L-type channel that is predominantly found in VSMCs (Webb 2003) these channels are major regulators of calcium in their respective cells. Given that N-cadherin is found on VSMCs (Moiseeva 2001; Jones, Sabatini et al. 2002) it may be possible that changes to the cell-cell contacts via N-cadherin causes alterations to downstream signalling which may potentially cause contractile changes within the cell. However due to lack of information with regard to this process in VSMCs this is merely speculation and would require much further investigation.

7.5.2 CD9

While CD9 was observed in positive control testicular tissue, it was not detectable in aortic tissue of the mCIA model, possibly indicating that alterations to levels of this protein do not play a role in decreased vessel function. However due to animal number limitations only severe tissues were available. These experiments were performed prior to the N-cadherin work, and in hindsight it may have been of more value to measure levels in all disease severity cohorts. Since previous studies described higher levels of CD9 in dysfunctional compared to normal tissues (Scherberich, Moog et al. 1998; Nishida, Miyagawa et al. 2000) this course of action was deemed appropriate at the time.

Interestingly RANKL (Receptor Activator for Nuclear Factor κ B Ligand) has a positive post-translational effect on CD9 expression in macrophages (Ishii, Iwai et al. 2006). RANKL a member of the TNFα superfamily and a key molecule key involved in osteoclast differentiation is upregulated during human RA, pushing osteoclast function towards degradation (Drexler, Kong et al. 2008) (see chapter one, section 1.2.2). It is known that levels of RANKL are increased in early stages of experimental arthritis(Stolina, Adamu et al. 2005); as such changes in CD9 levels could be attributed to changes in systemic levels of RANKL. Further work in this area is therefore essential to

gain a better understanding of the role of tetraspanins in arthritis-associated vascular dysfunction.

7.5.3 Assessing VSMC Hyperplasia

It became apparent that staining aortic segments was problematic due to problems associated with cutting the sections and subsequent staining. Often the action of the blade sweeping over the section caused damage and resulted in tearing or folding of the sample. Following this often during staining procedures sections became unstuck and float off in the media incubated in. As such it became difficult to obtain reproducible results regarding smooth muscle hyperplasia.

Although these final studies proved largely inconclusive, that changes in expression were seen indicate that further investigation into changes in the ECM in this tissue would be of interest to further elucidate the mechanism behind vascular dysfunction. Additionally in depth investigation of extracellular receptors and indeed cell-cell interactions may prove invaluable to further understanding disease pathology in this model.

CHAPTER 8

GENERAL DISCUSSION

The original hypothesis stated that "Due to the highly inflammatory nature of RA, and similarities of this exhibited in the murine model of RA, endothelial dysfunction will ensue following the onset of arthritis". Indeed it was proposed that such dysfunction would "be characterised by a decrease in bioavailable NO both in the vessel and circulation" and that "plasma levels of inflammatory mediators will be increased and thus contribute to the detrimental effect on the vasculature".

However to quote Thomas Huxley "the great tragedy of science - the slaying of a beautiful hypothesis by an ugly fact". To this end primary observations indicated that the presence of mCIA was not associated with endothelial dysfunction. Indeed following the onset of arthritis an unexpected contractile dysfunction was observed. Given the possible influence of inflammatory mediators it was logically presumed that in mCIA irregular activity of NOS isoforms may have produced uncharacteristically large amounts of NO, thus impairing vasoconstriction. Subsequent experiments again rejected this hypothesis. Experiments using inhibitors of both eNOS and iNOS failed to correct the contractile dysfunction, furthermore, total plasma NOx was not altered in mCIA over age-matched non-arthritic mice. COX inhibition using indomethacin also failed to restore contractile responses in arthritic mice which also rules out a role for vasodilators such as prostacyclin.

Contractile dysfunction in blood vessels has been characterised in a model of Marfan syndrome and subsequently an association was observed between the development of this pathology and MMP-9. We therefore investigated whether there was indeed a link between MMP-9 and attenuated contractile responses in mCIA. Levels of MMP-9 were quantified using ELISA and immunohistochemistry and found to be elevated in the joints, plasma and aorta of mCIA animals. MMP-9 concentrations in the joints and plasma did indeed increase as arthritis progressively increased in severity. Next we

postulated that IL-1β, a potent pro-inflammatory cytokine which elicits catabolic responses within the joint via the induction of MMPs, could be responsible for the raised MMP-9 expression we detected in mCIA. Whilst an *in vivo* role for IL-1β in the upregulation of MMP-9 could not be ruled out, the results of subsequent *ex vivo* experiments would argue against this possibility. Following this, *ex vivo* studies cemented belief that direct exposure of the aorta to MMP-9 is responsible for the contractile dysfunction seen in the mCIA model. The mechanism by which MMP-9 expression is regulated within the vasculature requires further investigation. These data implicate MMP-9 in a distinct role during the development of vascular dysfunction associated with inflammatory arthritis; for example during RA.

Concrete conclusions regarding the mechanism by which MMP-9 may act on the vessel wall to affect contractile function cannot be drawn from this thesis. The cellular source of the enzyme within the vessel or indeed surrounding the vessel is unlikely to be restricted to a single cell type. Given that the pathological changes and pathways initiated during the development of mCIA are diverse and diffuse it is highly likely that multiple factors are involved. MMP-9 may prove to be an early defining marker for unwanted pathological changes in the vasculature. MMP-9 is perceived to play a minor role in the perpetuation of chronic joint pathology (when compared with other MMPs such as MMP-1 and MMP-3). However MMP-9s true role may as yet be unrecognised in the complex sequence of events which lead to both joint destruction and vascular dysfunction in RA. Further investigation is warranted.

Phenotypic switching of VSMCs from contractile to synthetic/proliferative functionality may also contribute to the defective contractile responses noted in the vasculature during inflammatory arthritis. N-cadherin has previously been linked to this VSMCs functional switch. Subsequent studies focussed upon establishing whether N-cadherin was indeed important in controlling vascular contractile responses in mCIA. In the first instance it was crucial to determine whether N-cadherin was indeed expressed in the vasculature of mice with CIA. Subsequent experimental findings eliminated extracellular N-cadherin shedding as a direct cause of VSMC phenotypic shedding. The exact activity of N-cadherin in this model remains to be seen.

The research presented in this thesis goes in the face of the vast majority of published data regarding vascular dysfunction in RA. As discussed in Chapter One, in many cases it has been suggested that inflammatory cytokines characteristic of RA become systemic and induce damage to the endothelium causing the initial insult that gradually progresses to endothelial dysfunction. That this pathology is not apparent in the mCIA model may be attributed to the duration of the disease. Indeed in this model of arthritis the early upregulation of other factors such as the antioxidants superoxide dismutase and glutathione reductase may protect the endothelium and prevent the development of overt endothelial damage, allowing VSMC dysfunction to present itself. In fact if mCIA was allowed to progress further endothelial dysfunction may well ensue if such initial mechanisms became overwhelmed by the inflammatory milieu presented in RA. That human RA is normally only diagnosed following the initial symptoms of disease, at which point approximately 30% of patients have visible bone erosion (van der Heijde 1995), indicates that they may have been subjected to the systemic effects of RA for some time. Additionally it has been reported that many patients fail to realise the significance of their symptoms and will delay on average for three months before visiting their general practitioner (Kumar, Daley et al. 2007). As such, any contractile dysfunction may go unnoticed and subsequently only endothelial dysfunction is observed; the latter being the major vascular pathology detected during human disease duration. The consequences of ignoring contractile dysfunction by simply looking for the development of endothelial dysfunction could be dire with regards to vascular pathology. Figure 8.1. summarises the detrimental effect that vessel stiffening, as a consequence contractile dysfunction, may have on the cardiovascular system, all of which may be initially attributed to dysregulation of VSMC function.

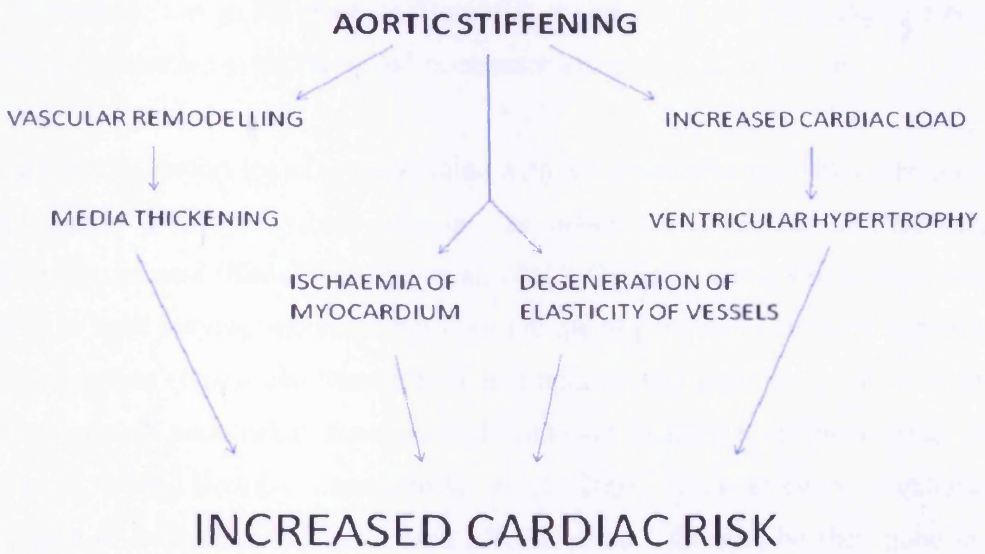

Figure 8.1. Flow Diagram Showing the Potential Consequences of Aortic Stiffening

A factor that may play a part in the development of vascular pathology in human disease, in addition to the systemic inflammation, is the use of various treatment therapies. For instance the switch from commonly used NSAIDs to more recent selective COX-2 inhibitors may be implicated. While such interventions were introduced to prevent the gastric toxicity side-effects of the broad spectrum COX inhibitors, elimination of COX-2 activity results in a pro-thrombotic environment for the vessel due to the removal of protective PGI_2 without an associated change in thromboxane expression (Funk and FitzGerald 2007). This itself may produce an environment favouring the development of endothelial dysfunction and could explain the high incidence of this pathology reported within the RA population.

Another possible damaging intervention in RA is the commonly used antifolate agent methotrexate. As a result of its mechanism of action it is known to increase plasma levels of homocysteine, the latter widely described as an independent risk factor for CVD and endothelial dysfunction (Desouza, Keebler et al. 2002). Consequently folic acid is often prescribed for use in combination with methotrexate (Visser, Katchamart et al. 2009) to lower homocysteine and reduce the risk of associated vascular toxicity. While the jury is still out as to the role of homocysteine in vascular disease risk *per se* a recent study suggests that high plasma homocysteine is indeed associated with increased

atherothrombotic risk in RA patients (Berglund, Sodergren et al. 2009). Again a possible role for homocysteine in mCIA would be an interesting topic to follow up.

In an attempt to abolish toxicities associated with RA drugs alternative RA therapies have recently been developed which rely on the action of antibodies to neutralise the inflammation present (Nam, Winthrop et al. 2010). Of these, anti-TNFα therapy has been reported to have varying successes between groups of patients in terms of improvement of RA symptoms (Olsen and Stein 2004), and interestingly has also shown concomitant improvements in endothelial function and reduction in arterial stiffness (Maki-Petaja, Hall et al. 2006; Bosello, Santoliquido et al. 2008). This evidence highlights the importance of evaluating the associated effects of each therapy, be they good or bad; those that are beneficial with respect to RA symptoms may be causing unseen damage elsewhere in the body. However, vascular damage may well be present before the RA intervention is initiated and the slightest risk from a therapy might contribute further to further CVD. In this case it may be beneficial to determine cardiovascular risk at the initial RA diagnosis, for example by utilising measurements of vascular stiffening such as augmentation index or flow-mediated dilation and so establish the overall disease risk for each patient. Unfortunately, the latter techniques are really research tools only at present. Improvements in technology may lead to such tailored individual diagnosis becoming a reality in the clinic and therefore provide significant health benefits.

It may well be of interest to investigate mechanisms involved in the potential "reversibility" of the vascular pathology in RA following remission. Currently remission classification is vague; although the physician and patient agree they are in remission, there may still be residual RA activity present (Wolfe, Boers et al. 2009). As such this would complicate the identification of vascular pathology for although the risk of this developing may be reduced, the initial inflammatory-disease associated insult could have initiated a cascade of damage that might be irreversible despite the amelioration of joint symptoms.

8.1 Endothelial Progenitor Cells

Interestingly an additional reason why endothelial dysfunction is not observed in the mCIA model may be attributed to increased production of MMP-9 itself. Endothelial progenitor cells (EPCs) reside in the bone marrow before differentiating into cells bearing endothelial characteristics (van Zonneveld, de Boer et al. 2010). A role for these cells in re-endothelialisation has been described and evidence is accumulating in support of their function in endothelial repair (van Zonneveld, de Boer et al. 2010). Furthermore their role in the development of atherosclerosis has been demonstrated by studies showing the larger the risk of event, the smaller the number of circulating EPCs present (Hirata, Nagata et al. 2010). These cells normally reside in a quiescent state in the bone marrow, but stimulation by growth factors, namely VEGF (Asahara, Takahashi et al. 1999), or via injury (Kawabe, Ushikubi et al. 2010) causes migration into the peripheral blood where they are able to proliferate and differentiate contributing to re-endothelialization (Padfield, Newby et al. 2010). Importantly this process has been observed to be dependent on the secretion of MMP-9, which in the bone marrow stimulates release of the stem-cell active cytokine soluble kit-ligand, increasing motility of the bone marrow stem cells. The latter then translocate from their quiescent niche in the bone to the vasculature for repair (Heissig, Hattori et al. 2002). That increased levels of MMP-9 have been demonstrated in the mCIA model both systemically and at the arthritic joint suggests that it may produce stimulated release of EPCs. Initiation of such repair processes could prevent endothelial dysfunction and subsequent damage to the vascular wall. As such, upregulation of MMP-9 may be both beneficial and detrimental to vessel function, repairing the endothelium whilst causing underlying damage to VSMC function. However, this theory is questionable given the duration of disease and extent of vascular damage in the mCIA model, and such is rather speculative.

FINAL THOUGHTS

Underlying damage to the VSMCs in mCIA may precede damage to the endothelium implying that this pathology may play a greater role in the development of RA-associated cardiovascular co-morbidities than is currently recognised. Investigating these changes in patients with early RA and developing suitable therapies to target this could prove invaluable in preventing vascular disease and providing a better quality of life for the long-suffering RA cohort.

REFERENCES

Abeles, A. M. and M. H. Pillinger (2006). "The role of the synovial fibroblast in rheumatoid arthritis: cartilage destruction and the regulation of matrix metalloproteinases." Bull NYU Hosp Jt Dis **64**(1-2): 20-4.

Agrez, M. V. (1996). "Cell adhesion molecules and colon cancer." Aust N Z J Surg **66**(12): 791-8.

Alvarez, Y., A. M. Briones, et al. (2008). "Role of NADPH oxidase and iNOS in vasoconstrictor responses of vessels from hypertensive and normotensive rats." Br J Pharmacol **153**(5): 926-35.

Andreakos, E., U. Rauchhaus, et al. (2009). "Amphoteric liposomes enable systemic antigen-presenting cell-directed delivery of CD40 antisense and are therapeutically effective in experimental arthritis." Arthritis Rheum **60**(4): 994-1005.

Anning, P. B., B. Coles, et al. (2005). "Elevated endothelial nitric oxide bioactivity and resistance to angiotensin-dependent hypertension in 12/15-lipoxygenase knockout mice." Am J Pathol **166**(3): 653-62.

Asahara, T., T. Takahashi, et al. (1999). "VEGF contributes to postnatal neovascularization by mobilizing bone marrow-derived endothelial progenitor cells." Embo J **18**(14): 3964-72.

Assoian, R. K., B. E. Fleurdelys, et al. (1987). "Expression and secretion of type beta transforming growth factor by activated human macrophages." Proc Natl Acad Sci U S A **84**(17): 6020-4.

Bacon, P. A., R. J. Stevens, et al. (2002). "Accelerated atherogenesis in autoimmune rheumatic diseases." Autoimmun Rev **1**(6): 338-47.

Basalyga, D. M., D. T. Simionescu, et al. (2004). "Elastin degradation and calcification in an abdominal aorta injury model: role of matrix metalloproteinases." Circulation **110**(22): 3480-7.

Bayes-Genis, A., J. H. Campbell, et al. (2002). "Macrophages, myofibroblasts and neointimal hyperplasia after coronary artery injury and repair." Atherosclerosis **163**(1): 89-98.

Bazzichi, L., L. Ghiadoni, et al. (2009). "Osteopontin is associated with increased arterial stiffness in Rheumatoid Arthritis." Mol Med.

Bazzichi, L., L. Ghiadoni, et al. (2009). "Osteopontin is associated with increased arterial stiffness in rheumatoid arthritis." Mol Med **15**(11-12): 402-6.

Beckman, J. S. (1996). "Oxidative damage and tyrosine nitration from peroxynitrite." Chem Res Toxicol **9**(5): 836-44.

Behrens, J., B. A. Jerchow, et al. (1998). "Functional interaction of an axin homolog, conductin, with beta-catenin, APC, and GSK3beta." Science **280**(5363): 596-9.

Bell, D. M., T. E. Johns, et al. (1998). "Endothelial dysfunction: implications for therapy of cardiovascular diseases." Ann Pharmacother **32**(4): 459-70.

Bendeck, M. P., M. Conte, et al. (2002). "Doxycycline modulates smooth muscle cell growth, migration, and matrix remodeling after arterial injury." Am J Pathol **160**(3): 1089-95.

Berglund, S., A. Sodergren, et al. (2009). "Atherothrombotic events in rheumatoid arthritis are predicted by homocysteine - a six-year follow-up study." Clin Exp Rheumatol **27**(5): 822-5.

Bijl, M. (2003). "Endothelial activation, endothelial dysfunction and premature atherosclerosis in systemic autoimmune diseases." Neth J Med **61**(9): 273-7.

Birschmann, I. and U. Walter (2004). "Physiology and pathophysiology of vascular signaling controlled by guanosine 3',5'-cyclic monophosphate-dependent protein kinase." Acta Biochim Pol **51**(2): 397-404.

Bocker, J. M., F. J. Miller, et al. (2001). "Calcium-activated potassium channels mask vascular dysfunction associated with oxidized LDL exposure in rabbit aorta." Jpn Heart J **42**(3): 317-26.

Boer, R., W. R. Ulrich, et al. (2000). "The inhibitory potency and selectivity of arginine substrate site nitric-oxide synthase inhibitors is solely determined by their affinity toward the different isoenzymes." Mol Pharmacol **58**(5): 1026-34.

Bohme, E., H. Graf, et al. (1978). "Effects of sodium nitroprusside and other smooth muscle relaxants on cyclic GMP formation in smooth muscle and platelets." Adv Cyclic Nucleotide Res **9**: 131-43.

Bond, M., R. P. Fabunmi, et al. (1998). "Synergistic upregulation of metalloproteinase-9 by growth factors and inflammatory cytokines: an absolute requirement for transcription factor NF-kappa B." FEBS Lett **435**(1): 29-34.

Bosello, S., A. Santoliquido, et al. (2008). "TNF-alpha blockade induces a reversible but transient effect on endothelial dysfunction in patients with long-standing severe rheumatoid arthritis." Clin Rheumatol **27**(7): 833-9.

Brabletz, T., A. Jung, et al. (1999). "beta-catenin regulates the expression of the matrix metalloproteinase-7 in human colorectal cancer." Am J Pathol **155**(4): 1033-8.

Bradford, M. M. (1976). "A rapid and sensitive method for the quantitation of microgram quantities of protein utilizing the principle of protein-dye binding." Anal Biochem **72**: 248-54.

Brantjes, H., N. Barker, et al. (2002). "TCF: Lady Justice casting the final verdict on the outcome of Wnt signalling." Biol Chem **383**(2): 255-61.

Bratt, J. and J. Palmblad (1997). "Cytokine-induced neutrophil-mediated injury of human endothelial cells." J Immunol **159**(2): 912-8.

Braun, J. and R. Rau (2009). "An update on methotrexate." Curr Opin Rheumatol **21**(3): 216-23.

Brew, K., D. Dinakarpandian, et al. (2000). "Tissue inhibitors of metalloproteinases: evolution, structure and function." Biochim Biophys Acta **1477**(1-2): 267-83.

Bruhl, H., J. Cihak, et al. (2009). "Important role of interleukin-3 in the early phase of collagen-induced arthritis." Arthritis Rheum **60**(5): 1352-61.

Bryant, C. E., I. Appleton, et al. (1998). "Vascular endothelial growth factor upregulates constitutive cyclooxygenase 1 in primary bovine and human endothelial cells." Life Sci **62**(24): 2195-201.

Bui, Q. T., M. Prempeh, et al. (2009). "Atherosclerotic plaque development." Int J Biochem Cell Biol **41**(11): 2109-13.

Bull, M. J., A. S. Williams, et al. (2008). "The Death Receptor 3-TNF-like protein 1A pathway drives adverse bone pathology in inflammatory arthritis." J Exp Med **205**(11): 2457-64.

Bunag, R. D. (1973). "Validation in awake rats of a tail-cuff method for measuring systolic pressure." J Appl Physiol **34**(2): 279-82.

Bussemakers, M. J., A. Van Bokhoven, et al. (2000). "Complex cadherin expression in human prostate cancer cells." Int J Cancer **85**(3): 446-50.

Cai, S., J. Khoo, et al. (2005). "Endothelial nitric oxide synthase dysfunction in diabetic mice: importance of tetrahydrobiopterin in eNOS dimerisation." Diabetologia **48**(9): 1933-40.

Can, C., M. G. Cinar, et al. (2002). "Vascular endothelial dysfunction associated with elevated serum homocysteine levels in rat adjuvant arthritis: effect of vitamin E administration." Life Sci **71**(4): 401-10.

Capone, M. L., S. Tacconelli, et al. (2003). "Clinical pharmacology of selective COX-2 inhibitors." Int J Immunopathol Pharmacol **16**(2 Suppl): 49-58.

Carter, A. M. (2005). "Inflammation, thrombosis and acute coronary syndromes." Diab Vasc Dis Res **2**(3): 113-21.

Catterall, W. A., E. Perez-Reyes, et al. (2005). "International Union of Pharmacology. XLVIII. Nomenclature and structure-function relationships of voltage-gated calcium channels." Pharmacol Rev **57**(4): 411-25.

Chakraborti, S., M. Mandal, et al. (2003). "Regulation of matrix metalloproteinases: an overview." Mol Cell Biochem **253**(1-2): 269-85.

Chang, Y. H., I. L. Lin, et al. (2008). "Elevated circulatory MMP-2 and MMP-9 levels and activities in patients with rheumatoid arthritis and systemic lupus erythematosus." Clin Biochem.

Chew, D. K., M. S. Conte, et al. (2004). "Matrix metalloproteinase-specific inhibition of Ca2+ entry mechanisms of vascular contraction." J Vasc Surg **40**(5): 1001-10.

Chia, W. T., Y. W. Chen, et al. (2008). "MMP-9 mRNA as a therapeutic marker in acute and chronic stages of arthritis induced by type II collagen antibody." J Formos Med Assoc **107**(3): 245-52.

Cho, A. and M. A. Reidy (2002). "Matrix metalloproteinase-9 is necessary for the regulation of smooth muscle cell replication and migration after arterial injury." Circ Res **91**(9): 845-51.

Cho, Y. G., M. L. Cho, et al. (2007). "Type II collagen autoimmunity in a mouse model of human rheumatoid arthritis." Autoimmun Rev **7**(1): 65-70.

Choi, H. K., M. A. Hernan, et al. (2002). "Methotrexate and mortality in patients with rheumatoid arthritis: a prospective study." Lancet **359**(9313): 1173-7.

Choi, S. T., J. H. Kim, et al. (2009). "Therapeutic effect of anti-vascular endothelial growth factor receptor I antibody in the established collagen-induced arthritis mouse model." Clin Rheumatol **28**(3): 333-7.

Chow, A. K., J. Cena, et al. (2007). "Acute actions and novel targets of matrix metalloproteinases in the heart and vasculature." Br J Pharmacol **152**(2): 189-205.

Chung, A. W., K. Au Yeung, et al. (2007). "Loss of elastic fiber integrity and reduction of vascular smooth muscle contraction resulting from the upregulated activities of matrix metalloproteinase-2 and -9 in the thoracic aortic aneurysm in Marfan syndrome." Circ Res **101**(5): 512-22.

Chung, A. W., H. H. Yang, et al. (2009). "Upregulation of matrix metalloproteinase-2 in the arterial vasculature contributes to stiffening and vasomotor dysfunction in patients with chronic kidney disease." Circulation **120**(9): 792-801.

Chung, A. W., H. H. Yang, et al. (2008). "Long-term doxycycline is more effective than atenolol to prevent thoracic aortic aneurysm in marfan syndrome through the inhibition of matrix metalloproteinase-2 and -9." Circ Res **102**(8): e73-85.

Chung, C. P., A. Oeser, et al. (2005). "Increased coronary-artery atherosclerosis in rheumatoid arthritis: relationship to disease duration and cardiovascular risk factors." Arthritis Rheum **52**(10): 3045-53.

Clevers, H. (2006). "Wnt/beta-catenin signaling in development and disease." Cell **127**(3): 469-80.

Cohen, R. A., R. M. Weisbrod, et al. (1999). "Mechanism of nitric oxide-induced vasodilatation: refilling of intracellular stores by sarcoplasmic reticulum Ca2+ ATPase and inhibition of store-operated Ca2+ influx." Circ Res **84**(2): 210-9.

Coles, B., R. Lewis, et al. (2007). "CD59 or C3 are not requred for angiotensin II-dependent hypertension or hypertrophy in mice." Immunology **121**(4): 518-25.

Collin-Osdoby, P. (2004). "Regulation of vascular calcification by osteoclast regulatory factors RANKL and osteoprotegerin." Circ Res **95**(11): 1046-57.

Courtenay, J. S., M. J. Dallman, et al. (1980). "Immunisation against heterologous type II collagen induces arthritis in mice." Nature **283**(5748): 666-8.

Csiszar, A., N. Labinskyy, et al. (2007). "Vascular superoxide and hydrogen peroxide production and oxidative stress resistance in two closely related rodent species with disparate longevity." Aging Cell **6**(6): 783-97.

Cuchacovich, R. and L. R. Espinoza (2009). "Does TNF-alpha blockade play any role in cardiovascular risk among rheumatoid arthritis (RA) patients?" Clin Rheumatol **28**(10): 1217-20.

Cuzzocrea, S. (2006). "Role of nitric oxide and reactive oxygen species in arthritis." Curr Pharm Des **12**(27): 3551-70.

Dale M. M, H. D. G. (2004). Pharmacology

Condensed, Churchill Livingstone. **1**.

Dashwood, M. R. and J. C. Tsui (2002). "Endothelin-1 and atherosclerosis: potential complications associated with endothelin-receptor blockade." Atherosclerosis **160**(2): 297-304.

Day, R. (2002). "Adverse reactions to TNF-alpha inhibitors in rheumatoid arthritis." Lancet **359**(9306): 540-1.

de Gasparo, M., K. J. Catt, et al. (2000). "International union of pharmacology. XXIII. The angiotensin II receptors." Pharmacol Rev **52**(3): 415-72.

Dejam, A., C. J. Hunter, et al. (2005). "Erythrocytes are the major intravascular storage sites of nitrite in human blood." Blood **106**(2): 734-9.

DeMaria, A. N. (2002). "Relative risk of cardiovascular events in patients with rheumatoid arthritis." Am J Cardiol **89**(6A): 33D-38D.

Desouza, C., M. Keebler, et al. (2002). "Drugs affecting homocysteine metabolism: impact on cardiovascular risk." Drugs **62**(4): 605-16.

Dinarello, C. A. (2002). "The IL-1 family and inflammatory diseases." Clin Exp Rheumatol **20**(5 Suppl 27): S1-13.

Do, K. H., M. S. Kim, et al. (2009). "Angiotensin II-induced aortic ring constriction is mediated by phosphatidylinositol 3-kinase/L-type calcium channel signaling pathway." Exp Mol Med **41**(8): 569-76.

Dolphin, A. C. (1998). "Mechanisms of modulation of voltage-dependent calcium channels by G proteins." J Physiol **506 (Pt 1)**: 3-11.

Dorrance, A. M. (2007). "Interleukin 1-beta (IL-1beta) enhances contractile responses in endothelium-denuded aorta from hypertensive, but not normotensive, rats." Vascul Pharmacol **47**(2-3): 160-5.

Dougall, W. C., M. Glaccum, et al. (1999). "RANK is essential for osteoclast and lymph node development." Genes Dev **13**(18): 2412-24.

Dreier, R., S. Grassel, et al. (2004). "Pro-MMP-9 is a specific macrophage product and is activated by osteoarthritic chondrocytes via MMP-3 or a MT1-MMP/MMP-13 cascade." Exp Cell Res **297**(2): 303-12.

Drexler, S. K., P. L. Kong, et al. (2008). "Cell signalling in macrophages, the principal innate immune effector cells of rheumatoid arthritis." Arthritis Res Ther **10**(5): 216.

Dwivedi, A., S. C. Slater, et al. (2009). "MMP-9 and -12 cause N-cadherin shedding and thereby beta-catenin signalling and vascular smooth muscle cell proliferation." Cardiovasc Res **81**(1): 178-86.
Eklund, K. K. (2007). "Mast cells in the pathogenesis of rheumatic diseases and as potential targets for anti-rheumatic therapy." Immunol Rev **217**: 38-52.
El-Hamamsy, I. and M. H. Yacoub (2009). "Cellular and molecular mechanisms of thoracic aortic aneurysms." Nat Rev Cardiol **6**(12): 771-86.
Ersoy, S., I. Orhan, et al. (2008). "Endothelium-dependent induction of vasorelaxation by Melissa officinalis L. ssp. officinalis in rat isolated thoracic aorta." Phytomedicine **15**(12): 1087-92.
Fabunmi, R. P., A. H. Baker, et al. (1996). "Divergent regulation by growth factors and cytokines of 95 kDa and 72 kDa gelatinases and tissue inhibitors or metalloproteinases-1, -2, and -3 in rabbit aortic smooth muscle cells." Biochem J **315 (Pt 1)**: 335-42.
Feng, M., M. E. Deerhake, et al. (2009). "Genetic analysis of blood pressure in 8 mouse intercross populations." Hypertension **54**(4): 802-9.
Feng, M., S. Whitesall, et al. (2008). "Validation of volume-pressure recording tail-cuff blood pressure measurements." Am J Hypertens **21**(12): 1288-91.
Filippin, L. I., R. Vercelino, et al. (2008). "Redox signalling and the inflammatory response in rheumatoid arthritis." Clin Exp Immunol **152**(3): 415-22.
Flamant, M., S. Placier, et al. (2007). "Role of matrix metalloproteinases in early hypertensive vascular remodeling." Hypertension **50**(1): 212-8.
Flammer, A. J., I. Sudano, et al. (2008). "Angiotensin-converting enzyme inhibition improves vascular function in rheumatoid arthritis." Circulation **117**(17): 2262-9.
Fleming, S. D. and G. C. Tsokos (2006). "Complement, natural antibodies, autoantibodies and tissue injury." Autoimmun Rev **5**(2): 89-92.
Fontaine, J., A. Herchuelz, et al. (1984). "A pharmacological analysis of the responses of isolated aorta from rats with adjuvant arthritis." Agents Actions **14**(5-6): 684-7.
Forstermann, U. (2006). "Endothelial NO synthase as a source of NO and superoxide." Eur J Clin Pharmacol **62 Suppl 13**: 5-12.
Forstermann, U. (2008). "Oxidative stress in vascular disease: causes, defense mechanisms and potential therapies." Nat Clin Pract Cardiovasc Med **5**(6): 338-49.
Forstermann, U. and T. Munzel (2006). "Endothelial nitric oxide synthase in vascular disease: from marvel to menace." Circulation **113**(13): 1708-14.
Foster, R. W. (1986). Basic Pharmacology, Butterworths.
Foudi, N., L. Louedec, et al. (2009). "Selective cyclooxygenase-2 inhibition directly increases human vascular reactivity to norepinephrine during acute inflammation." Cardiovasc Res **81**(2): 269-77.
Fujisaki, K., N. Tanabe, et al. (2007). "Receptor activator of NF-kappaB ligand induces the expression of carbonic anhydrase II, cathepsin K, and matrix metalloproteinase-9 in osteoclast precursor RAW264.7 cells." Life Sci **80**(14): 1311-8.
Funk, C. D. and G. A. FitzGerald (2007). "COX-2 inhibitors and cardiovascular risk." J Cardiovasc Pharmacol **50**(5): 470-9.
Furchgott, R. F. and J. V. Zawadzki (1980). "The obligatory role of endothelial cells in the relaxation of arterial smooth muscle by acetylcholine." Nature **288**(5789): 373-6.
Gabriel, S. E. (2001). "The epidemiology of rheumatoid arthritis." Rheum Dis Clin North Am **27**(2): 269-81.
Gadeau, A. P., M. Campan, et al. (1993). "Osteopontin overexpression is associated with arterial smooth muscle cell proliferation in vitro." Arterioscler Thromb **13**(1): 120-5.
Galarraga, B., F. Khan, et al. (2009). "Etanercept improves inflammation-associated arterial stiffness in rheumatoid arthritis." Rheumatology (Oxford) **48**(11): 1418-23.
Galis, Z. S., C. Johnson, et al. (2002). "Targeted disruption of the matrix metalloproteinase-9 gene impairs smooth muscle cell migration and geometrical arterial remodeling." Circ Res **91**(9): 852-9.
Gamble, J. B. M. (2008). Theory and Practice of Histological Techniques.
Ganea, E., M. Trifan, et al. (2007). "Matrix metalloproteinases: useful and deleterious." Biochem Soc Trans **35**(Pt 4): 689-91.
Gao, Y., A. D. Portugal, et al. (2007). "Role of Rho kinases in PKG-mediated relaxation of pulmonary arteries of fetal lambs exposed to chronic high altitude hypoxia." Am J Physiol Lung Cell Mol Physiol **292**(3): L678-84.
Garvey, E. P., J. A. Oplinger, et al. (1997). "1400W is a slow, tight binding, and highly selective inhibitor of inducible nitric-oxide synthase in vitro and in vivo." J Biol Chem **272**(8): 4959-63.

Garvin, P., L. Nilsson, et al. (2008). "Circulating matrix metalloproteinase-9 is associated with cardiovascular risk factors in a middle-aged normal population." PLoS ONE **3**(3): e1774.
George, S. J. and C. A. Beeching (2006). "Cadherin:catenin complex: a novel regulator of vascular smooth muscle cell behaviour." Atherosclerosis **188**(1): 1-11.
George, S. J. and A. Dwivedi (2004). "MMPs, cadherins, and cell proliferation." Trends Cardiovasc Med **14**(3): 100-5.
Gibson, C. L., D. Constantin, et al. (2005). "Progesterone suppresses the inflammatory response and nitric oxide synthase-2 expression following cerebral ischemia." Exp Neurol **193**(2): 522-30.
Gielen, S., M. Sandri, et al. (2009). "Risk factor management: antiatherogenic therapies." Eur J Cardiovasc Prev Rehabil **16 Suppl 1**: S29-36.
Gluszko, P. and A. Bielinska (2009). "Non-steroidal anti-inflammatory drugs and the risk of cardiovascular diseases: are we going to see the revival of cyclooxygenase-2 selective inhibitors?" Pol Arch Med Wewn **119**(4): 231-5.
Godecke, A., U. K. Decking, et al. (1998). "Coronary hemodynamics in endothelial NO synthase knockout mice." Circ Res **82**(2): 186-94.
Goodson, N. (2002). "Coronary artery disease and rheumatoid arthritis." Curr Opin Rheumatol **14**(2): 115-20.
Gorman, C. L. and A. P. Cope (2008). "Immune-mediated pathways in chronic inflammatory arthritis." Best Pract Res Clin Rheumatol **22**(2): 221-38.
Goronzy, J. J. and C. M. Weyand (2005). "Rheumatoid arthritis." Immunol Rev **204**: 55-73.
Gorska, A., O. Kowal-Bielecka, et al. (2008). "Impairment of microcirculation in juvenile idiopathic arthritis - studies by nailfold videocapillaroscopy and correlation with serum levels of sICAM and VEGF." Folia Histochem Cytobiol **46**(4): 443-7.
Gosens, R., H. Meurs, et al. (2008). "The GSK-3/beta-catenin-signalling axis in smooth muscle and its relationship with remodelling." Naunyn Schmiedebergs Arch Pharmacol **378**(2): 185-91.
Gradl, D., M. Kuhl, et al. (1999). "The Wnt/Wg signal transducer beta-catenin controls fibronectin expression." Mol Cell Biol **19**(8): 5576-87.
Gravallese, E. M. (2003). "Osteopontin: a bridge between bone and the immune system." J Clin Invest **112**(2): 147-9.
Green, G. A. (2001). "Understanding NSAIDs: from aspirin to COX-2." Clin Cornerstone **3**(5): 50-60.
Gregersen, P. K., J. Silver, et al. (1987). "The shared epitope hypothesis. An approach to understanding the molecular genetics of susceptibility to rheumatoid arthritis." Arthritis Rheum **30**(11): 1205-13.
Gross, S. S. and R. Levi (1992). "Tetrahydrobiopterin synthesis. An absolute requirement for cytokine-induced nitric oxide generation by vascular smooth muscle." J Biol Chem **267**(36): 25722-9.
Grosser, T., S. Fries, et al. (2006). "Biological basis for the cardiovascular consequences of COX-2 inhibition: therapeutic challenges and opportunities." J Clin Invest **116**(1): 4-15.
Gruber, B. L., D. Sorbi, et al. (1996). "Markedly elevated serum MMP-9 (gelatinase B) levels in rheumatoid arthritis: a potentially useful laboratory marker." Clin Immunol Immunopathol **78**(2): 161-71.
Gurjar, M. V., J. DeLeon, et al. (2001). "Mechanism of inhibition of matrix metalloproteinase-9 induction by NO in vascular smooth muscle cells." J Appl Physiol **91**(3): 1380-6.
Gurjar, M. V., J. Deleon, et al. (2001). "Role of reactive oxygen species in IL-1 beta-stimulated sustained ERK activation and MMP-9 induction." Am J Physiol Heart Circ Physiol **281**(6): H2568-74.
Hall, F. C. and N. Dalbeth (2005). "Disease modification and cardiovascular risk reduction: two sides of the same coin?" Rheumatology (Oxford) **44**(12): 1473-82.
Halpern, W., M. J. Mulvany, et al. (1978). "Mechanical properties of smooth muscle cells in the walls of arterial resistance vessels." J Physiol **275**: 85-101.
Hanke, H., S. Hassenstein, et al. (1994). "Accumulation of macrophages in the arterial vessel wall following experimental balloon angioplasty." Eur Heart J **15**(5): 691-8.
Hart, F. D. and P. L. Boardman (1963). "Indomethacin: a New Non-Steroid Anti-Inflammatory Agent." Br Med J **2**(5363): 965-70.
Hartog, A., J. Hulsman, et al. (2009). "Locomotion and muscle mass measures in a murine model of collagen-induced arthritis." BMC Musculoskelet Disord **10**: 59.
Haruna, Y., Y. Morita, et al. (2006). "Endothelial dysfunction in rat adjuvant-induced arthritis: vascular superoxide production by NAD(P)H oxidase and uncoupled endothelial nitric oxide synthase." Arthritis Rheum **54**(6): 1847-55.
Haruna, Y., Y. Morita, et al. (2007). "Fluvastatin reverses endothelial dysfunction and increased vascular oxidative stress in rat adjuvant-induced arthritis." Arthritis Rheum **56**(6): 1827-35.

Hatta, K., A. Nose, et al. (1988). "Cloning and expression of cDNA encoding a neural calcium-dependent cell adhesion molecule: its identity in the cadherin gene family." J Cell Biol **106**(3): 873-81.

Hatton, D. C., Y. Qi, et al. (2000). "Heritability of the blood pressure response to acute ethanol exposure in five inbred strains of mice." Alcohol Clin Exp Res **24**(10): 1483-7.

Haynes, D. R. (2007). "Inflammatory cells and bone loss in rheumatoid arthritis." Arthritis Res Ther **9**(3): 104.

Hayward, K. and C. A. Wallace (2009). "Recent developments in anti-rheumatic drugs in pediatrics: treatment of juvenile idiopathic arthritis." Arthritis Res Ther **11**(1): 216.

Hegen, M., J. C. Keith, Jr., et al. (2008). "Utility of animal models for identification of potential therapeutics for rheumatoid arthritis." Ann Rheum Dis **67**(11): 1505-15.

Heissig, B., K. Hattori, et al. (2002). "Recruitment of stem and progenitor cells from the bone marrow niche requires MMP-9 mediated release of kit-ligand." Cell **109**(5): 625-37.

Hemler, M. E. (2001). "Specific tetraspanin functions." J Cell Biol **155**(7): 1103-7.

Henderson B, E. J., Pettipher ER (1995). Mechanisms and Models in Rheumatoid Arthritis, Academic Press.

Hetzel, J., B. Balletshofer, et al. (2005). "Rapid effects of rosiglitazone treatment on endothelial function and inflammatory biomarkers." Arterioscler Thromb Vasc Biol **25**(9): 1804-9.

Higashiyama, S., R. Iwamoto, et al. (1995). "The membrane protein CD9/DRAP 27 potentiates the juxtacrine growth factor activity of the membrane-anchored heparin-binding EGF-like growth factor." J Cell Biol **128**(5): 929-38.

Hink, U., H. Li, et al. (2001). "Mechanisms underlying endothelial dysfunction in diabetes mellitus." Circ Res **88**(2): E14-22.

Hirano, K. (2007). "Current topics in the regulatory mechanism underlying the Ca2+ sensitization of the contractile apparatus in vascular smooth muscle." J Pharmacol Sci **104**(2): 109-15.

Hirata, Y., D. Nagata, et al. (2010). "Diagnosis and treatment of endothelial dysfunction in cardiovascular disease." Int Heart J **51**(1): 1-6.

Hishinuma, T., H. Nakamura, et al. (2001). "Analysis of urinary prostacyclin and thromboxane/prostacyclin ratio in patients with rheumatoid arthritis using gas chromatography/selected ion monitoring." Prostaglandins Leukot Essent Fatty Acids **65**(2): 85-90.

Ho, A. T., E. B. Voura, et al. (2001). "MMP inhibitors augment fibroblast adhesion through stabilization of focal adhesion contacts and up-regulation of cadherin function." J Biol Chem **276**(43): 40215-24.

Hoge, M. and S. Amar (2006). "Role of interleukin-1 in bacterial atherogenesis." Drugs Today (Barc) **42**(10): 683-8.

Holmdahl, R., L. Jansson, et al. (1986). "Female sex hormones suppress development of collagen-induced arthritis in mice." Arthritis Rheum **29**(12): 1501-9.

Holmdahl, R., M. Karlsson, et al. (1989). "Localization of a critical restriction site on the I-A beta chain that determines susceptibility to collagen-induced arthritis in mice." Proc Natl Acad Sci U S A **86**(23): 9475-9.

Honda, T., E. Segi-Nishida, et al. (2006). "Prostacyclin-IP signaling and prostaglandin E2-EP2/EP4 signaling both mediate joint inflammation in mouse collagen-induced arthritis." J Exp Med **203**(2): 325-35.

Horowitz, M. C., Y. Xi, et al. (2001). "Control of osteoclastogenesis and bone resorption by members of the TNF family of receptors and ligands." Cytokine Growth Factor Rev **12**(1): 9-18.

Horvath, B., P. Orsy, et al. (2005). "Endothelial NOS-mediated relaxations of isolated thoracic aorta of the C57BL/6J mouse: a methodological study." J Cardiovasc Pharmacol **45**(3): 225-31.

Howe, L. R., K. Subbaramaiah, et al. (1999). "Transcriptional activation of cyclooxygenase-2 in Wnt-1-transformed mouse mammary epithelial cells." Cancer Res **59**(7): 1572-7.

Huang, A., D. Sun, et al. (1998). "Gender difference in flow-induced dilation and regulation of shear stress: role of estrogen and nitric oxide." Am J Physiol **275**(5 Pt 2): R1571-7.

Hyafil, F., C. Babinet, et al. (1981). "Cell-cell interactions in early embryogenesis: a molecular approach to the role of calcium." Cell **26**(3 Pt 1): 447-54.

Hynes, R. O. (2002). "Integrins: bidirectional, allosteric signaling machines." Cell **110**(6): 673-87.

Ignarro, L. J. and C. Napoli (2004). "Novel features of nitric oxide, endothelial nitric oxide synthase, and atherosclerosis." Curr Atheroscler Rep **6**(4): 281-7.

Ikonomidis, J. S., J. R. Barbour, et al. (2005). "Effects of deletion of the matrix metalloproteinase 9 gene on development of murine thoracic aortic aneurysms." Circulation **112**(9 Suppl): I242-8.

Inglis, J. J., C. A. Notley, et al. (2007). "Collagen-induced arthritis as a model of hyperalgesia: functional and cellular analysis of the analgesic actions of tumor necrosis factor blockade." Arthritis Rheum **56**(12): 4015-23.

Ishii, M., K. Iwai, et al. (2006). "RANKL-induced expression of tetraspanin CD9 in lipid raft membrane microdomain is essential for cell fusion during osteoclastogenesis." J Bone Miner Res **21**(6): 965-76.

Itoh, T., H. Matsuda, et al. (2002). "The role of matrix metalloproteinase-2 and matrix metalloproteinase-9 in antibody-induced arthritis." J Immunol **169**(5): 2643-7.

Jackson, C. J., J. Arkell, et al. (1998). "Rheumatoid synovial endothelial cells secrete decreased levels of tissue inhibitor of MMP (TIMP1)." Ann Rheum Dis **57**(3): 158-61.

Jantzen, F., S. Konemann, et al. (2007). "Isoprenoid depletion by statins antagonizes cytokine-induced down-regulation of endothelial nitric oxide expression and increases NO synthase activity in human umbilical vein endothelial cells." J Physiol Pharmacol **58**(3): 503-14.

Jimenez-Altayo, F., A. M. Briones, et al. (2006). "Increased superoxide anion production by interleukin-1beta impairs nitric oxide-mediated relaxation in resistance arteries." J Pharmacol Exp Ther **316**(1): 42-52.

Jones, M., P. J. Sabatini, et al. (2002). "N-cadherin upregulation and function in response of smooth muscle cells to arterial injury." Arterioscler Thromb Vasc Biol **22**(12): 1972-7.

Juarranz, Y., C. Abad, et al. (2005). "Protective effect of vasoactive intestinal peptide on bone destruction in the collagen-induced arthritis model of rheumatoid arthritis." Arthritis Res Ther **7**(5): R1034-45.

Judkins, C. P., C. G. Sobey, et al. (2006). "NADPH-induced contractions of mouse aorta do not involve NADPH oxidase: a role for P2X receptors." J Pharmacol Exp Ther **317**(2): 644-50.

Kanatsu-Shinohara, M., S. Toyokuni, et al. (2004). "CD9 is a surface marker on mouse and rat male germline stem cells." Biol Reprod **70**(1): 70-5.

Kaplan-Albuquerque, N., C. Garat, et al. (2003). "Platelet-derived growth factor-BB-mediated activation of Akt suppresses smooth muscle-specific gene expression through inhibition of mitogen-activated protein kinase and redistribution of serum response factor." J Biol Chem **278**(41): 39830-8.

Kaplan, M. J. (2006). "Cardiovascular disease in rheumatoid arthritis." Curr Opin Rheumatol **18**(3): 289-97.

Karanian, J. W. and P. W. Ramwell (1996). "Effect of gender and sex steroids on the contractile response of canine coronary and renal blood vessels." J Cardiovasc Pharmacol **27**(3): 312-9.

Kasapis, C. and P. D. Thompson (2005). "The effects of physical activity on serum C-reactive protein and inflammatory markers: a systematic review." J Am Coll Cardiol **45**(10): 1563-9.

Kauser, K. and G. M. Rubanyi (1994). "Gender difference in bioassayable endothelium-derived nitric oxide from isolated rat aortae." Am J Physiol **267**(6 Pt 2): H2311-7.

Kawabe, J., F. Ushikubi, et al. (2010). "Prostacyclin in vascular diseases. - Recent insights and future perspectives." Circ J **74**(5): 836-43.

Kawano, Y. and R. Kypta (2003). "Secreted antagonists of the Wnt signalling pathway." J Cell Sci **116**(Pt 13): 2627-34.

Kawashima, S. and M. Yokoyama (2004). "Dysfunction of endothelial nitric oxide synthase and atherosclerosis." Arterioscler Thromb Vasc Biol **24**(6): 998-1005.

Kelm, M., S. Schafer, et al. (1997). "Nitric oxide induced contractile dysfunction is related to a reduction in myocardial energy generation." Cardiovasc Res **36**(2): 185-94.

Kim, H., W. J. Kim, et al. (2005). "Cyclophilin A may contribute to the inflammatory processes in rheumatoid arthritis through induction of matrix degrading enzymes and inflammatory cytokines from macrophages." Clin Immunol **116**(3): 217-24.

Kim, J. K. and J. A. Diehl (2009). "Nuclear cyclin D1: an oncogenic driver in human cancer." J Cell Physiol **220**(2): 292-6.

Kirkpatrick, C. J., M. Wagner, et al. (1997). "Physiology and cell biology of the endothelium: a dynamic interface for cell communication." Int J Microcirc Clin Exp **17**(5): 231-40.

Kiviranta, I., J. Jurvelin, et al. (1985). "Microspectrophotometric quantitation of glycosaminoglycans in articular cartilage sections stained with Safranin O." Histochemistry **82**(3): 249-55.

Knedla, A., E. Neumann, et al. (2007). "Developments in the synovial biology field 2006." Arthritis Res Ther **9**(2): 209.

Kobayashi, Y. and H. Okunishi (2002). "Mast cells as a target of rheumatoid arthritis treatment." Jpn J Pharmacol **90**(1): 7-11.

Koch, A. W., D. Bozic, et al. (1999). "Homophilic adhesion by cadherins." Curr Opin Struct Biol **9**(2): 275-81.

Kotha, J., C. Zhang, et al. (2009). "Functional relevance of tetraspanin CD9 in vascular smooth muscle cell injury phenotypes: a novel target for the prevention of neointimal hyperplasia." Atherosclerosis **203**(2): 377-86.

Kothapalli, C. R. and A. Ramamurthi "Induced elastin regeneration by chronically activated smooth muscle cells for targeted aneurysm repair." Acta Biomater **6**(1): 170-8.

Krege, J. H., J. B. Hodgin, et al. (1995). "A noninvasive computerized tail-cuff system for measuring blood pressure in mice." Hypertension **25**(5): 1111-5.

Kroll, J. and J. Waltenberger (1998). "VEGF-A induces expression of eNOS and iNOS in endothelial cells via VEGF receptor-2 (KDR)." Biochem Biophys Res Commun **252**(3): 743-6.

Ku, I. A., J. B. Imboden, et al. (2009). "Rheumatoid arthritis: model of systemic inflammation driving atherosclerosis." Circ J **73**(6): 977-85.

Kumar, K., E. Daley, et al. (2007). "Delay in presentation to primary care physicians is the main reason why patients with rheumatoid arthritis are seen late by rheumatologists." Rheumatology (Oxford) **46**(9): 1438-40.

Kwon, H. J., T. R. Cote, et al. (2003). "Case reports of heart failure after therapy with a tumor necrosis factor antagonist." Ann Intern Med **138**(10): 807-11.

Labinskyy, N., P. Mukhopadhyay, et al. (2009). "Longevity is associated with increased vascular resistance to high glucose-induced oxidative stress and inflammatory gene expression in Peromyscus leucopus." Am J Physiol Heart Circ Physiol **296**(4): H946-56.

Lalu, M. M., J. Cena, et al. (2006). "Matrix metalloproteinases contribute to endotoxin and interleukin-1beta induced vascular dysfunction." Br J Pharmacol **149**(1): 31-42.

Lamping, K. G. and F. M. Faraci (2001). "Role of sex differences and effects of endothelial NO synthase deficiency in responses of carotid arteries to serotonin." Arterioscler Thromb Vasc Biol **21**(4): 523-8.

Lau, A. C., T. T. Duong, et al. (2009). "Inhibition of matrix metalloproteinase-9 activity improves coronary outcome in an animal model of Kawasaki disease." Clin Exp Immunol **157**(2): 300-9.

Lau, A. C., T. T. Duong, et al. (2008). "Matrix metalloproteinase 9 activity leads to elastin breakdown in an animal model of Kawasaki disease." Arthritis Rheum **58**(3): 854-63.

Lauer, T., M. Preik, et al. (2001). "Plasma nitrite rather than nitrate reflects regional endothelial nitric oxide synthase activity but lacks intrinsic vasodilator action." Proc Natl Acad Sci U S A **98**(22): 12814-9.

Lebre, M. C. and P. P. Tak (2008). "Dendritic cell subsets: their roles in rheumatoid arthritis." Acta Reumatol Port **33**(1): 35-45.

Lebre, M. C. and P. P. Tak (2009). "Dendritic cells in rheumatoid arthritis: Which subset should be used as a tool to induce tolerance?" Hum Immunol **70**(5): 321-4.

Lee, B. and S. K. Moon (2005). "Resveratrol inhibits TNF-alpha-induced proliferation and matrix metalloproteinase expression in human vascular smooth muscle cells." J Nutr **135**(12): 2767-73.

Lee, M. Y., H. F. Tse, et al. (2007). "Genomic changes in regenerated porcine coronary arterial endothelial cells." Arterioscler Thromb Vasc Biol **27**(11): 2443-9.

Lee, S. J., W. J. Kim, et al. (2009). "TNF-alpha regulates vascular smooth muscle cell responses in genetic hypertension." Int Immunopharmacol **9**(7-8): 837-43.

Leibbrandt, A. and J. M. Penninger (2008). "RANK/RANKL: regulators of immune responses and bone physiology." Ann N Y Acad Sci **1143**: 123-50.

Lerman, A. and A. M. Zeiher (2005). "Endothelial function: cardiac events." Circulation **111**(3): 363-8.

Libby, P. (2008). "Role of inflammation in atherosclerosis associated with rheumatoid arthritis." Am J Med **121**(10 Suppl 1): S21-31.

Libby, P., S. J. Warner, et al. (1988). "Interleukin 1: a mitogen for human vascular smooth muscle cells that induces the release of growth-inhibitory prostanoids." J Clin Invest **81**(2): 487-98.

Lincoln, T. M., N. Dey, et al. (2001). "Invited review: cGMP-dependent protein kinase signaling mechanisms in smooth muscle: from the regulation of tone to gene expression." J Appl Physiol **91**(3): 1421-30.

Lindblad, S. S., P. Mydel, et al. (2009). "Smoking and nicotine exposure delay development of collagen-induced arthritis in mice." Arthritis Res Ther **11**(3): R88.

Liu, X., M. J. Miller, et al. (1998). "Diffusion-limited reaction of free nitric oxide with erythrocytes." J Biol Chem **273**(30): 18709-13.

Lonn, E., S. Yusuf, et al. (2006). "Homocysteine lowering with folic acid and B vitamins in vascular disease." N Engl J Med **354**(15): 1567-77.

Lu, J., T. Kasama, et al. (2000). "Vascular endothelial growth factor expression and regulation of murine collagen-induced arthritis." J Immunol **164**(11): 5922-7.

Luross, J. A. and N. A. Williams (2001). "The genetic and immunopathological processes underlying collagen-induced arthritis." Immunology **103**(4): 407-16.

MacArthur, P. H., S. Shiva, et al. (2007). "Measurement of circulating nitrite and S-nitrosothiols by reductive chemiluminescence." J Chromatogr B Analyt Technol Biomed Life Sci **851**(1-2): 93-105.

MacNaul, K. L. and N. I. Hutchinson (1993). "Differential expression of iNOS and cNOS mRNA in human vascular smooth muscle cells and endothelial cells under normal and inflammatory conditions." Biochem Biophys Res Commun **196**(3): 1330-4.

Maharaj, D. (1986). "Autoimmune haemolytic anaemia associated with rheumatoid arthritis and paroxysmal nocturnal haemoglobinuria." Acta Haematol **75**(4): 241.

Makelainen, P., K. Vehvilainen-Julkunen, et al. (2008). "Rheumatoid arthritis patients' knowledge of the disease and its treatments: A descriptive study." Musculoskeletal Care.

Maki-Petaja, K. M., F. C. Hall, et al. (2006). "Rheumatoid arthritis is associated with increased aortic pulse-wave velocity, which is reduced by anti-tumor necrosis factor-alpha therapy." Circulation **114**(11): 1185-92.

Manoury, B., S. L. Etheridge, et al. (2009). "Organ culture mimics the effects of hypoxia on membrane potential, K(+) channels and vessel tone in pulmonary artery." Br J Pharmacol **158**(3): 848-61.

Marinova-Mutafchieva, L., R. O. Williams, et al. (1997). "Dynamics of proinflammatory cytokine expression in the joints of mice with collagen-induced arthritis (CIA)." Clin Exp Immunol **107**(3): 507-12.

Marnett, L. J. and A. S. Kalgutkar (1999). "Cyclooxygenase 2 inhibitors: discovery, selectivity and the future." Trends Pharmacol Sci **20**(11): 465-9.

Metsios, G. S., A. Stavropoulos-Kalinoglou, et al. (2008). "Rheumatoid arthritis, cardiovascular disease and physical exercise: a systematic review." Rheumatology (Oxford) **47**(3): 239-48.

Mikuls, T. R. (2003). "Co-morbidity in rheumatoid arthritis." Best Pract Res Clin Rheumatol **17**(5): 729-52.

Miller, V. M. and S. P. Duckles (2008). "Vascular actions of estrogens: functional implications." Pharmacol Rev **60**(2): 210-41.

Miossec, P. (2008). "Dynamic interactions between T cells and dendritic cells and their derived cytokines/chemokines in the rheumatoid synovium." Arthritis Res Ther **10 Suppl 1**: S2.

Mitchell, J. A. and T. D. Warner (1999). "Cyclo-oxygenase-2: pharmacology, physiology, biochemistry and relevance to NSAID therapy." Br J Pharmacol **128**(6): 1121-32.

Moiseeva, E. P. (2001). "Adhesion receptors of vascular smooth muscle cells and their functions." Cardiovasc Res **52**(3): 372-86.

Montecucco, F. and F. Mach (2009). "Common inflammatory mediators orchestrate pathophysiological processes in rheumatoid arthritis and atherosclerosis." Rheumatology (Oxford) **48**(1): 11-22.

Moodley, I. (2008). "Review of the cardiovascular safety of COXIBs compared to NSAIDS." Cardiovasc J Afr **19**(2): 102-7.

Mor, A., S. B. Abramson, et al. (2005). "The fibroblast-like synovial cell in rheumatoid arthritis: a key player in inflammation and joint destruction." Clin Immunol **115**(2): 118-28.

Moscana A, M. A. (2003). Cell Surface Proteases: Vol 54 (Current Topics in Developmental Biology). San Diego, Academic Press.

Munzel, T., A. Daiber, et al. (2005). "Vascular consequences of endothelial nitric oxide synthase uncoupling for the activity and expression of the soluble guanylyl cyclase and the cGMP-dependent protein kinase." Arterioscler Thromb Vasc Biol **25**(8): 1551-7.

Myers, L. K., E. F. Rosloniec, et al. (1997). "Collagen-induced arthritis, an animal model of autoimmunity." Life Sci **61**(19): 1861-78.

Myllykangas-Luosujarvi, R., K. Aho, et al. (1995). "Shortening of life span and causes of excess mortality in a population-based series of subjects with rheumatoid arthritis." Clin Exp Rheumatol **13**(2): 149-53.

Nakamura, Y., K. Handa, et al. (2001). "Immunohistochemical distribution of CD9, heparin binding epidermal growth factor-like growth factor, and integrin alpha3beta1 in normal human tissues." J Histochem Cytochem **49**(4): 439-44.

Nam, J. L., K. L. Winthrop, et al. (2010). "Current evidence for the management of rheumatoid arthritis with biological disease-modifying antirheumatic drugs: a systematic literature review informing the EULAR recommendations for the management of RA." Ann Rheum Dis.

Newby, A. C. and A. B. Zaltsman (2000). "Molecular mechanisms in intimal hyperplasia." J Pathol **190**(3): 300-9.

Nishida, M., J. Miyagawa, et al. (2000). "Localization of CD9, an enhancer protein for proheparin-binding epidermal growth factor-like growth factor, in human atherosclerotic plaques: possible involvement of juxtacrine growth mechanism on smooth muscle cell proliferation." Arterioscler Thromb Vasc Biol **20**(5): 1236-43.

Noren, N. K., B. P. Liu, et al. (2000). "p120 catenin regulates the actin cytoskeleton via Rho family GTPases." J Cell Biol **150**(3): 567-80.

Nowell, M. A., A. S. Williams, et al. (2009). "Therapeutic targeting of IL-6 trans signaling counteracts STAT3 control of experimental inflammatory arthritis." J Immunol **182**(1): 613-22.

Nozaki, K., H. Goto, et al. (2007). "Effects of keishibukuryogan on vascular function in adjuvant-induced arthritis rats." Biol Pharm Bull **30**(6): 1042-7.

O'Brien, E. R., M. R. Garvin, et al. (1994). "Osteopontin is synthesized by macrophage, smooth muscle, and endothelial cells in primary and restenotic human coronary atherosclerotic plaques." Arterioscler Thromb **14**(10): 1648-56.

O'Shaughnessy, M. C., E. K. Vetsika, et al. (2006). "The effect of substance P on nitric oxide release in a rheumatoid arthritis model." Inflamm Res **55**(6): 236-40.

Ohmori, R., Y. Momiyama, et al. (2003). "Plasma osteopontin levels are associated with the presence and extent of coronary artery disease." Atherosclerosis **170**(2): 333-7.

Olsen, N. J. and C. M. Stein (2004). "New drugs for rheumatoid arthritis." N Engl J Med **350**(21): 2167-79.

Otero, M. and M. B. Goldring (2007). "Cells of the synovium in rheumatoid arthritis. Chondrocytes." Arthritis Res Ther **9**(5): 220.

Owens, G. K. (1995). "Regulation of differentiation of vascular smooth muscle cells." Physiol Rev **75**(3): 487-517.

Owens, G. K., M. S. Kumar, et al. (2004). "Molecular regulation of vascular smooth muscle cell differentiation in development and disease." Physiol Rev **84**(3): 767-801.

Padfield, G. J., D. E. Newby, et al. (2010). "Understanding the role of endothelial progenitor cells in percutaneous coronary intervention." J Am Coll Cardiol **55**(15): 1553-65.

Palframan, R., M. Airey, et al. (2009). "Use of biofluorescence imaging to compare the distribution of certolizumab pegol, adalimumab, and infliximab in the inflamed paws of mice with collagen-induced arthritis." J Immunol Methods.

Panoulas, V. F., K. M. Douglas, et al. (2007). "Prevalence and associations of hypertension and its control in patients with rheumatoid arthritis." Rheumatology (Oxford) **46**(9): 1477-82.

Panoulas, V. F., G. S. Metsios, et al. (2008). "Hypertension in rheumatoid arthritis." Rheumatology (Oxford) **47**(9): 1286-98.

Park, Y. B., H. K. Choi, et al. (2002). "Effects of antirheumatic therapy on serum lipid levels in patients with rheumatoid arthritis: a prospective study." Am J Med **113**(3): 188-93.

Pasceri, V. and E. T. Yeh (1999). "A tale of two diseases: atherosclerosis and rheumatoid arthritis." Circulation **100**(21): 2124-6.

Peri, G., F. Chiaffarino, et al. (1990). "Cytotoxicity of activated monocytes on endothelial cells." J Immunol **144**(4): 1444-8.

Piccoli, G., U. Rutishauser, et al. (2004). "N-cadherin juxtamembrane domain modulates voltage-gated Ca2+ current via RhoA GTPase and Rho-associated kinase." J Neurosci **24**(48): 10918-23.

Pinder, A. G., S. C. Rogers, et al. (2009). "The measurement of nitric oxide and its metabolites in biological samples by ozone-based chemiluminescence." Methods Mol Biol **476**: 10-27.

Pinson, K. I., J. Brennan, et al. (2000). "An LDL-receptor-related protein mediates Wnt signalling in mice." Nature **407**(6803): 535-8.

Plehm, R., M. E. Barbosa, et al. (2006). "Animal models for hypertension/blood pressure recording." Methods Mol Med **129**: 115-26.

Pollock, D. M., T. L. Keith, et al. (1995). "Endothelin receptors and calcium signaling." Faseb J **9**(12): 1196-204.

Prusakiewicz, J. J., A. S. Felts, et al. (2004). "Molecular basis of the time-dependent inhibition of cyclooxygenases by indomethacin." Biochemistry **43**(49): 15439-45.

Pulichino, A. M., S. Rowland, et al. (2006). "Prostacyclin antagonism reduces pain and inflammation in rodent models of hyperalgesia and chronic arthritis." J Pharmacol Exp Ther **319**(3): 1043-50.

Quinn, S., C. O'Brien, et al. (2003). "Role of cyclooxygenase and haemoxygenase products in nitric oxide-independent vasodilatation in the porcine ciliary artery." Eye **17**(5): 628-36.

Quinones, M. P., C. A. Estrada, et al. (2005). "The complex role of the chemokine receptor CCR2 in collagen-induced arthritis: implications for therapeutic targeting of CCR2 in rheumatoid arthritis." J Mol Med **83**(9): 672-81.

Rabelink, T. J. and T. F. Luscher (2006). "Endothelial nitric oxide synthase: host defense enzyme of the endothelium?" Arterioscler Thromb Vasc Biol **26**(2): 267-71.

Raffetto, J. D. and R. A. Khalil (2008). "Matrix metalloproteinases and their inhibitors in vascular remodeling and vascular disease." Biochem Pharmacol **75**(2): 346-59.

Raffetto, J. D., X. Qiao, et al. (2008). "Prolonged increases in vein wall tension increase matrix metalloproteinases and decrease constriction in rat vena cava: Potential implications in varicose veins." J Vasc Surg **48**(2): 447-56.

Raffetto, J. D., R. L. Ross, et al. (2007). "Matrix metalloproteinase 2-induced venous dilation via hyperpolarization and activation of K+ channels: relevance to varicose vein formation." J Vasc Surg **45**(2): 373-80.

Ram, M., Y. Sherer, et al. (2006). "Matrix metalloproteinase-9 and autoimmune diseases." J Clin Immunol **26**(4): 299-307.

Rang H.P, D. M. M., Ritter J. M, Moore P.K (2003). Pharmacology, Churchill Livingstone.

Rannou, F., M. Francois, et al. (2006). "Cartilage breakdown in rheumatoid arthritis." Joint Bone Spine **73**(1): 29-36.

Rao, J. V., A. N. Swamy, et al. (1991). "In vitro brain acetylcholinesterase response among three inbred strains of mice to monocrotophos." J Environ Sci Health B **26**(4): 449-58.

Ratcliffe, A. (2000). "Tissue engineering of vascular grafts." Matrix Biol **19**(4): 353-7.

Ray, K. K. and C. P. Cannon (2004). "Intensive statin therapy in acute coronary syndromes: clinical benefits and vascular biology." Curr Opin Lipidol **15**(6): 637-43.

Rectenwald, J. E., L. L. Moldawer, et al. (2000). "Direct evidence for cytokine involvement in neointimal hyperplasia." Circulation **102**(14): 1697-702.

Reddy, A. K., G. E. Taffet, et al. (2003). "Noninvasive blood pressure measurement in mice using pulsed Doppler ultrasound." Ultrasound Med Biol **29**(3): 379-85.

Reilly, P. A., J. A. Cosh, et al. (1990). "Mortality and survival in rheumatoid arthritis: a 25 year prospective study of 100 patients." Ann Rheum Dis **49**(6): 363-9.

Renart, J., J. Reiser, et al. (1979). "Transfer of proteins from gels to diazobenzyloxymethyl-paper and detection with antisera: a method for studying antibody specificity and antigen structure." Proc Natl Acad Sci U S A **76**(7): 3116-20.

Rodriguez, J. A., J. Orbe, et al. (2007). "[Metalloproteases, vascular remodeling and atherothrombotic syndromes]." Rev Esp Cardiol **60**(9): 959-67.

Rogers, S. C., A. Khalatbari, et al. (2005). "Detection of human red blood cell-bound nitric oxide." J Biol Chem **280**(29): 26720-8.

Roh, C. R., W. J. Oh, et al. (2000). "Up-regulation of matrix metalloproteinase-9 in human myometrium during labour: a cytokine-mediated process in uterine smooth muscle cells." Mol Hum Reprod **6**(1): 96-102.

Ronday, H. K., W. H. van der Laan, et al. (2001). "Human granzyme B mediates cartilage proteoglycan degradation and is expressed at the invasive front of the synovium in rheumatoid arthritis." Rheumatology (Oxford) **40**(1): 55-61.

Rosenberg, L. (1971). "Chemical basis for the histological use of safranin O in the study of articular cartilage." J Bone Joint Surg Am **53**(1): 69-82.

Ross, R. (1999). "Atherosclerosis--an inflammatory disease." N Engl J Med **340**(2): 115-26.

Rubanyi, G. M., A. D. Freay, et al. (1997). "Vascular estrogen receptors and endothelium-derived nitric oxide production in the mouse aorta. Gender difference and effect of estrogen receptor gene disruption." J Clin Invest **99**(10): 2429-37.

Sakurada, S., N. Takuwa, et al. (2003). "Ca2+-dependent activation of Rho and Rho kinase in membrane depolarization-induced and receptor stimulation-induced vascular smooth muscle contraction." Circ Res **93**(6): 548-56.

Sakuta, T., Y. Morita, et al. "Involvement of the renin-angiotensin system in the development of vascular damage in a rat arthritis model: Efect of angiotensin receptor blockers." Arthritis Rheum.

Salliot, C. and D. van der Heijde (2009). "Long-term safety of methotrexate monotherapy in patients with rheumatoid arthritis: a systematic literature research." Ann Rheum Dis **68**(7): 1100-4.

Salo, T., J. G. Lyons, et al. (1991). "Transforming growth factor-beta 1 up-regulates type IV collagenase expression in cultured human keratinocytes." J Biol Chem **266**(18): 11436-41.
Sattar, N., D. W. McCarey, et al. (2003). "Explaining how "high-grade" systemic inflammation accelerates vascular risk in rheumatoid arthritis." Circulation **108**(24): 2957-63.
Sattar, N. and I. B. McInnes (2005). "Vascular comorbidity in rheumatoid arthritis: potential mechanisms and solutions." Curr Opin Rheumatol **17**(3): 286-92.
Sauzeau, V., H. Le Jeune, et al. (2000). "Cyclic GMP-dependent protein kinase signaling pathway inhibits RhoA-induced Ca2+ sensitization of contraction in vascular smooth muscle." J Biol Chem **275**(28): 21722-9.
Scherberich, A., S. Moog, et al. (1998). "Tetraspanin CD9 is associated with very late-acting integrins in human vascular smooth muscle cells and modulates collagen matrix reorganization." Arterioscler Thromb Vasc Biol **18**(11): 1691-7.
Schwab, C., G. Bruckner, et al. (1990). "Different levels of acetylcholinesterase and choline acetyltransferase activities in C57Bl/6 and DBA/2 mice are not accompanied with different density of cortical acetylcholinesterase reactive fibers." Neurochem Res **15**(11): 1127-33.
Seasholtz, T. M., H. Gurdal, et al. (1997). "Desensitization of norepinephrine receptor function is associated with G protein uncoupling in the rat aorta." Am J Physiol **273**(1 Pt 2): H279-85.
Senior, R. M., G. L. Griffin, et al. (1991). "Human 92- and 72-kilodalton type IV collagenases are elastases." J Biol Chem **266**(12): 7870-5.
Shin, C. S., S. J. Her, et al. (2005). "Dominant negative N-cadherin inhibits osteoclast differentiation by interfering with beta-catenin regulation of RANKL, independent of cell-cell adhesion." J Bone Miner Res **20**(12): 2200-12.
Shiva, S., X. Wang, et al. (2006). "Ceruloplasmin is a NO oxidase and nitrite synthase that determines endocrine NO homeostasis." Nat Chem Biol **2**(9): 486-93.
Shore, A., S. Jaglal, et al. (1986). "Enhanced interleukin 1 generation by monocytes in vitro is temporally linked to an early event in the onset or exacerbation of rheumatoid arthritis." Clin Exp Immunol **65**(2): 293-302.
Shtutman, M., J. Zhurinsky, et al. (1999). "The cyclin D1 gene is a target of the beta-catenin/LEF-1 pathway." Proc Natl Acad Sci U S A **96**(10): 5522-7.
Shyu, K. G. (2009). "Cellular and molecular effects of mechanical stretch on vascular cells and cardiac myocytes." Clin Sci (Lond) **116**(5): 377-89.
Siddhanta, U., A. Presta, et al. (1998). "Domain swapping in inducible nitric-oxide synthase. Electron transfer occurs between flavin and heme groups located on adjacent subunits in the dimer." J Biol Chem **273**(30): 18950-8.
Silman, A. J. and J. E. Pearson (2002). "Epidemiology and genetics of rheumatoid arthritis." Arthritis Res **4 Suppl 3**: S265-72.
Simionescu, M. (2007). "Implications of early structural-functional changes in the endothelium for vascular disease." Arterioscler Thromb Vasc Biol **27**(2): 266-74.
Singer, C. A., S. Salinthone, et al. (2004). "Synthesis of immune modulators by smooth muscles." Bioessays **26**(6): 646-55.
Slater, S. C., E. Koutsouki, et al. (2004). "R-cadherin:beta-catenin complex and its association with vascular smooth muscle cell proliferation." Arterioscler Thromb Vasc Biol **24**(7): 1204-10.
Soler, M., M. Camacho, et al. (2003). "Imidazolineoxyl N-oxide prevents the impairment of vascular contraction caused by interleukin-1beta through several mechanisms." J Infect Dis **188**(6): 927-37.
Somlyo, A. P. and A. V. Somlyo (1994). "Signal transduction and regulation in smooth muscle." Nature **372**(6503): 231-6.
Staines, N. A. and P. H. Wooley (1994). "Collagen arthritis--what can it teach us?" Br J Rheumatol **33**(9): 798-807.
Stolina, M., S. Adamu, et al. (2005). "RANKL is a marker and mediator of local and systemic bone loss in two rat models of inflammatory arthritis." J Bone Miner Res **20**(10): 1756-65.
Stolina, M., B. Bolon, et al. (2008). "The evolving systemic and local biomarker milieu at different stages of disease progression in rat collagen-induced arthritis." Biomarkers **13**(7): 692-712.
Storer, J. B. (1966). "Longevity and gross pathology at death in 22 inbred mouse strains." J Gerontol **21**(3): 404-9.
Streichert, L. C. and P. B. Sargent (1992). "The role of acetylcholinesterase in denervation supersensitivity in the frog cardiac ganglion." J Physiol **445**: 249-60.
Stuart-Smith, K. (2002). "Demystified. Nitric oxide." Mol Pathol **55**(6): 360-6.

Suleyman, H., B. Demircan, et al. (2007). "Anti-inflammatory and side effects of cyclooxygenase inhibitors." Pharmacol Rep **59**(3): 247-58.

Sullivan, J. C. and J. S. Pollock (2006). "Coupled and uncoupled NOS: separate but equal? Uncoupled NOS in endothelial cells is a critical pathway for intracellular signaling." Circ Res **98**(6): 717-9.

Sussman, J. L., M. Harel, et al. (1991). "Atomic structure of acetylcholinesterase from Torpedo californica: a prototypic acetylcholine-binding protein." Science **253**(5022): 872-9.

Suzuki, M., I. Tachibana, et al. (2009). "Tetraspanin CD9 negatively regulates lipopolysaccharide-induced macrophage activation and lung inflammation." J Immunol **182**(10): 6485-93.

Svelander, L., H. Erlandsson-Harris, et al. (2009). "Inhibition of cathepsin K reduces bone erosion, cartilage degradation and inflammation evoked by collagen-induced arthritis in mice." Eur J Pharmacol **613**(1-3): 155-62.

Tak, P. P. and B. Bresnihan (2000). "The pathogenesis and prevention of joint damage in rheumatoid arthritis: advances from synovial biopsy and tissue analysis." Arthritis Rheum **43**(12): 2619-33.

Takeichi, M. (1990). "Cadherins: a molecular family important in selective cell-cell adhesion." Annu Rev Biochem **59**: 237-52.

Tallant, C., A. Marrero, et al. (2009). "Matrix metalloproteinases: Fold and function of their catalytic domains." Biochim Biophys Acta.

Tamai, K., M. Semenov, et al. (2000). "LDL-receptor-related proteins in Wnt signal transduction." Nature **407**(6803): 530-5.

Tanasescu, C., C. Jurcut, et al. (2009). "Vascular disease in rheumatoid arthritis: from subclinical lesions to cardiovascular risk." Eur J Intern Med **20**(4): 348-54.

Tchetverikov, I., H. K. Ronday, et al. (2004). "MMP profile in paired serum and synovial fluid samples of patients with rheumatoid arthritis." Ann Rheum Dis **63**(7): 881-3.

Tetlow, L. C., M. Lees, et al. (1993). "Differential expression of gelatinase B (MMP-9) and stromelysin-1 (MMP-3) by rheumatoid synovial cells in vitro and in vivo." Rheumatol Int **13**(2): 53-9.

Tetsu, O. and F. McCormick (1999). "Beta-catenin regulates expression of cyclin D1 in colon carcinoma cells." Nature **398**(6726): 422-6.

Thyberg, J., K. Blomgren, et al. (1997). "Phenotypic modulation of smooth muscle cells after arterial injury is associated with changes in the distribution of laminin and fibronectin." J Histochem Cytochem **45**(6): 837-46.

Tilley, S. L., L. P. Audoly, et al. (1999). "Reproductive failure and reduced blood pressure in mice lacking the EP2 prostaglandin E2 receptor." J Clin Invest **103**(11): 1539-45.

Todd, J. A., H. Acha-Orbea, et al. (1988). "A molecular basis for MHC class II--associated autoimmunity." Science **240**(4855): 1003-9.

Tran, N. L., R. B. Nagle, et al. (1999). "N-Cadherin expression in human prostate carcinoma cell lines. An epithelial-mesenchymal transformation mediating adhesion withStromal cells." Am J Pathol **155**(3): 787-98.

Trentham, D. E., A. S. Townes, et al. (1977). "Autoimmunity to type II collagen an experimental model of arthritis." J Exp Med **146**(3): 857-68.

Tsioufis, C., K. Dimitriadis, et al. (2007). "Low-grade inflammation and hypoadiponectinaemia have an additive detrimental effect on aortic stiffness in essential hypertensive patients." Eur Heart J **28**(9): 1162-9.

Turesson, C., L. T. Jacobsson, et al. (2008). "Cardiovascular co-morbidity in rheumatic diseases." Vasc Health Risk Manag **4**(3): 605-14.

Turesson, C. and E. L. Matteson (2007). "Cardiovascular risk factors, fitness and physical activity in rheumatic diseases." Curr Opin Rheumatol **19**(2): 190-6.

Uglow, E. B., S. Slater, et al. (2003). "Dismantling of cadherin-mediated cell-cell contacts modulates smooth muscle cell proliferation." Circ Res **92**(12): 1314-21.

Urbina, E. M., R. V. Williams, et al. (2009). "Noninvasive assessment of subclinical atherosclerosis in children and adolescents: recommendations for standard assessment for clinical research: a scientific statement from the American Heart Association." Hypertension **54**(5): 919-50.

Uz, O., E. Kardesoglu, et al. (2009). "The relationship between coronary calcification and the metabolic markers of osteopontin, fetuin-A, and visfatin." Turk Kardiyol Dern Ars **37**(6): 397-402.

van den Berg, W. B. (2001). "Anti-cytokine therapy in chronic destructive arthritis." Arthritis Res **3**(1): 18-26.

van den Berg, W. B., P. L. van Lent, et al. (2007). "Amplifying elements of arthritis and joint destruction." Ann Rheum Dis **66 Suppl 3**: iii45-8.

Van den Steen, P. E., B. Dubois, et al. (2002). "Biochemistry and molecular biology of gelatinase B or matrix metalloproteinase-9 (MMP-9)." Crit Rev Biochem Mol Biol **37**(6): 375-536.
Van den Steen, P. E., P. Proost, et al. (2002). "Cleavage of denatured natural collagen type II by neutrophil gelatinase B reveals enzyme specificity, post-translational modifications in the substrate, and the formation of remnant epitopes in rheumatoid arthritis." Faseb J **16**(3): 379-89.
van der Heijde, D. M. (1995). "Joint erosions and patients with early rheumatoid arthritis." Br J Rheumatol **34 Suppl 2**: 74-8.
Van Wart, H. E. and H. Birkedal-Hansen (1990). "The cysteine switch: a principle of regulation of metalloproteinase activity with potential applicability to the entire matrix metalloproteinase gene family." Proc Natl Acad Sci U S A **87**(14): 5578-82.
van Zonneveld, A. J., H. C. de Boer, et al. (2010). "Inflammation, vascular injury and repair in rheumatoid arthritis." Ann Rheum Dis **69 Suppl 1**: i57-60.
Vane, J. R. and R. M. Botting (1995). "Pharmacodynamic profile of prostacyclin." Am J Cardiol **75**(3): 3A-10A.
Vanhoutte, P. M. (1998). "Vascular biology. Old-timer makes a comeback." Nature **396**(6708): 213, 215-6.
Vanhoutte, P. M. (2009). "COX-1 and vascular disease." Clin Pharmacol Ther **86**(2): 212-5.
Vaziri, N. D., Z. Ni, et al. (1998). "Upregulation of renal and vascular nitric oxide synthase in young spontaneously hypertensive rats." Hypertension **31**(6): 1248-54.
Veale, D., G. Yanni, et al. (1992). "Production of angiotensin converting enzyme by rheumatoid synovial membrane." Ann Rheum Dis **51**(4): 476-80.
Villar, I. C., A. J. Hobbs, et al. (2008). "Sex differences in vascular function: implication of endothelium-derived hyperpolarizing factor." J Endocrinol **197**(3): 447-62.
Visse, R. and H. Nagase (2003). "Matrix metalloproteinases and tissue inhibitors of metalloproteinases: structure, function, and biochemistry." Circ Res **92**(8): 827-39.
Visser, K., W. Katchamart, et al. (2009). "Multinational evidence-based recommendations for the use of methotrexate in rheumatic disorders with a focus on rheumatoid arthritis: integrating systematic literature research and expert opinion of a broad international panel of rheumatologists in the 3E Initiative." Ann Rheum Dis **68**(7): 1086-93.
Voskuyl, A. E. (2006). "The heart and cardiovascular manifestations in rheumatoid arthritis." Rheumatology (Oxford) **45 Suppl 4**: iv4-7.
Wahl, S. M., N. McCartney-Francis, et al. (2003). "Nitric oxide in experimental joint inflammation. Benefit or detriment?" Cells Tissues Organs **174**(1-2): 26-33.
Waites, G. T. and A. Whyte (1987). "Effect of pregnancy on collagen-induced arthritis in mice." Clin Exp Immunol **67**(3): 467-76.
Walch, L., C. Taisne, et al. (1997). "Cholinesterase activity in human pulmonary arteries and veins." Br J Pharmacol **121**(5): 986-90.
Walsh, F. S., C. H. Barton, et al. (1990). "N-cadherin gene maps to human chromosome 18 and is not linked to the E-cadherin gene." J Neurochem **55**(3): 805-12.
Wang, S., K. H. Yiu, et al. (2009). "Prevalence and extent of calcification over aorta, coronary and carotid arteries in patients with rheumatoid arthritis." J Intern Med **266**(5): 445-52.
Wang, X., Y. Xiao, et al. (2002). "A role for the beta-catenin/T-cell factor signaling cascade in vascular remodeling." Circ Res **90**(3): 340-7.
Wang, Y., X. R. Zheng, et al. (2009). "ROCK isoform regulation of myosin phosphatase and contractility in vascular smooth muscle cells." Circ Res **104**(4): 531-40.
Webb, R. C. (2003). "Smooth muscle contraction and relaxation." Adv Physiol Educ **27**(1-4): 201-6.
Welch, G. N. and J. Loscalzo (1998). "Homocysteine and atherothrombosis." N Engl J Med **338**(15): 1042-50.
Welland, A., P. E. Garnaud, et al. (2008). "Importance of the domain-domain interface to the catalytic action of the NO synthase reductase domain." Biochemistry **47**(37): 9771-80.
Wessels, J. A., T. W. Huizinga, et al. (2008). "Recent insights in the pharmacological actions of methotrexate in the treatment of rheumatoid arthritis." Rheumatology (Oxford) **47**(3): 249-55.
Wheelock, M. J. and K. R. Johnson (2003). "Cadherin-mediated cellular signaling." Curr Opin Cell Biol **15**(5): 509-14.
Wheelock, M. J. and K. R. Johnson (2003). "Cadherins as modulators of cellular phenotype." Annu Rev Cell Dev Biol **19**: 207-35.
Williams, R. O., J. J. Inglis, et al. (2005). "Analysing the effect of novel therapies on cytokine expression in experimental arthritis." Int J Exp Pathol **86**(5): 267-78.

Wills, A., M. M. Thompson, et al. (1996). "Pathogenesis of abdominal aortic aneurysms--cellular and biochemical mechanisms." Eur J Vasc Endovasc Surg **12**(4): 391-400.

Wimalasundera, R., S. Fexby, et al. (2003). "Effect of tumour necrosis factor-alpha and interleukin 1beta on endothelium-dependent relaxation in rat mesenteric resistance arteries in vitro." Br J Pharmacol **138**(7): 1285-94.

Wolfe, F., M. Boers, et al. (2009). "Remission in rheumatoid arthritis: physician and patient perspectives." J Rheumatol **36**(5): 930-3.

Wooley, P. H., H. S. Luthra, et al. (1981). "Type II collagen-induced arthritis in mice. I. Major histocompatibility complex (I region) linkage and antibody correlates." J Exp Med **154**(3): 688-700.

Xia, C., I. Misra, et al. (2009). "Regulation of interdomain interactions by calmodulin in inducible nitric oxide synthase." J Biol Chem.

Yasmin, C. M. McEniery, et al. (2005). "Matrix metalloproteinase-9 (MMP-9), MMP-2, and serum elastase activity are associated with systolic hypertension and arterial stiffness." Arterioscler Thromb Vasc Biol **25**(2): 372.

Yki-Jarvinen, H., R. Bergholm, et al. (2003). "Increased inflammatory activity parallels increased basal nitric oxide production and blunted response to nitric oxide in vivo in rheumatoid arthritis." Ann Rheum Dis **62**(7): 630-4.

Yoshihara, Y., H. Nakamura, et al. (2000). "Matrix metalloproteinases and tissue inhibitors of metalloproteinases in synovial fluids from patients with rheumatoid arthritis or osteoarthritis." Ann Rheum Dis **59**(6): 455-61.

Young, A. and G. Koduri (2007). "Extra-articular manifestations and complications of rheumatoid arthritis." Best Pract Res Clin Rheumatol **21**(5): 907-27.

Yumoto, K., M. Ishijima, et al. (2002). "Osteopontin deficiency protects joints against destruction in anti-type II collagen antibody-induced arthritis in mice." Proc Natl Acad Sci U S A **99**(7): 4556-61.

Zemse, S. M., R. H. Hilgers, et al. (2007). "Interleukin-10 counteracts impaired endothelium-dependent relaxation induced by ANG II in murine aortic rings." Am J Physiol Heart Circ Physiol **292**(6): H3103-8.

Zieman, S. J., V. Melenovsky, et al. (2005). "Mechanisms, pathophysiology, and therapy of arterial stiffness." Arterioscler Thromb Vasc Biol **25**(5): 932-43.

Zou, M. H. and V. Ullrich (1996). "Peroxynitrite formed by simultaneous generation of nitric oxide and superoxide selectively inhibits bovine aortic prostacyclin synthase." FEBS Lett **382**(1-2): 101-4.